Bioremediation of Persistent Contaminants of Concern in the Petroleum Industry

by

Amy-lynne Balaberda

A thesis submitted in partial fulfillment of the requirements for the degree of

Doctor of Philosophy

in

Environmental Engineering

Department of Civil and Environmental Engineering
University of Alberta

Abstract

The petroleum industry is a major economic driver in Canada; however, toxic and persistent contaminants such as Naphthenic Acid Fraction Compounds (NAFCs) and benzene can be generated during upstream and downstream operations. NAFCs are acutely toxic organics which are solubilized and concentrated during bitumen extraction from Alberta's oil sands. Coupling chemical oxidation with biodegradation may be a feasible remediation method that requires further investigation. This research utilized persulfate as a stable, persistent, and effective oxidant that has not previously been coupled with biodegradation for NAFCs. An initial oxidation phase was followed by a coupled treatment phase consisting of the residual persulfate with biodegradation by *Pseudomonas fluorescens*. The first project used unactivated persulfate and commercial Merichem NAs (100 mg/L), while the second project used an initial heat activated persulfate phase followed by continued reaction at room temperature for oil sands process-affected water (OSPW) NAFCs (61 mg/L). Using 100-1000 mg/L of unactivated persulfate, 30-99% of Merichem NAs were removed and toxicity towards *Vibrio fischeri* was reduced by 75-100% over 317 days. Coupled treatments improved Merichem NA and chemical oxygen demand (COD) removals by up to 1.8- and 6.7-fold, respectively, compared to oxidation alone, and cell counts were higher in bottles with 100-500 mg/L persulfate compared to bottles without persulfate. Activating 250-1000 mg/L of persulfate at 60ºC for 8 hours decreased OSPW NAFCs by 45-89%, significantly reducing the acutely toxic O_2 group and shifting to more oxidized (O_{3+}) NAFCs. Toxicity towards *V. fischeri* increased from 18% to 28-61% inhibition effect after activated persulfate oxidation but was reduced to non-toxic with continued oxidation at room temperature. Recalcitrant NAFCs such as those with higher molecular weight (n>16) and unsaturation (DBE>6) were oxidized, highlighting the potential

to be combined with biodegradation. However, the addition of *P. fluorescens* with the residual persulfate did not improve the treatment over 150 days but increased the toxicity up to 40%. The bacteria appeared to experience considerable stress, with cell counts decreasing over 3 orders of magnitude. This research demonstrated that persulfate oxidation is promising to reduce NAFC concentrations and coupling with biodegradation can increase mineralization and lower costs, however improving microbial viability is imperative for success.

Accidental spills and releases at downstream facilities such as refineries and underground storage tanks is an additional concern for the oil and gas industry, with benzene often driving remediation efforts due to its carcinogenicity. Sites with anaerobic conditions are particularly challenging as benzene contamination persists, and thus may require specialized bioaugmentation cultures to treat. Salt co-contamination can also occur at these sites, however the impact of salinity on in situ anaerobic biodegradation is largely unknown. A highly enriched methanogenic benzene-degrading consortium (DGG-B) was tested under sudden osmotic stress by adding 2.5-100 g/L NaCl and by gradual acclimation to NaCl. The impact of salinity on benzene fermenting bacteria (ORM2) and methanogenic archaea was differentiated by feeding DGG-B benzene, acetate or H_2/CO_2(g). Benzene degradation rates were inhibited at 5 and 10 g/L NaCl, decreasing from 20 µM/day in control bottles to 6 µM/day. Benzene degradation stalled at 15 g/L NaCl and ORM2 cells exhibited predominately decay. Slowly acclimating DGG-B to salinity increased the benzene degradation rate to 29.5 µM/day at 10.5 g/L NaCl. Methanogenesis occurred at 25 g/L NaCl however shifted from *Methanosaeta* and *Methanoregula* to *Methanosarcina* and *Methanobacterium*. This is one of the first studies to show that methanogenic benzene biodegradation is sensitive to salt, however strategies such as a gradual acclimation process can improve bioaugmentation success at impacted sites.

Preface

This thesis is an original work by Amy-lynne Balaberda under the supervision of Dr. Ania Ulrich. A version of Chapter 3 has been published as Balaberda, A., and Ulrich, A.C. 2021. Persulfate oxidation coupled with biodegradation by *Pseudomonas fluorescens* enhances naphthenic acid remediation and toxicity reduction. Microorganisms, MDPI AG, 9(7): 1502. Dr. Ania Ulrich and I contributed to the conceptualization and design of the research project, while I conducted the experiments, data collection, analysis, and visualization.

Preliminary research results in Chapter 4 were published in conference proceedings as Balaberda, A., and Ulrich, A.C. 2022. Remediation of oil sands naphthenic acids by activated persulfate oxidation and biodegradation. In Mine Closure 2022: 15th International Conference on Mine Closure, Australian Centre for Geomechanics, Perth, pp. 479-486. Research completed in Chapter 4 was conceptualized, designed, and executed by me under the supervision of Dr. Ania Ulrich. Ian Vander Meulen and Dr. John Headley (Environment and Climate Change Canada, National Hydrology Research Centre, SK) contributed to the Orbitrap-MS analysis and preliminary data compiling. I completed all other data collection, analysis and visualization.

Research conduced in Chapter 5 was part of a collaborative project funded by Alberta Innovates and Genomic Applications Partnership Program (GAPP), led by Dr. Elizabeth Edwards at the University of Toronto, with Dr. Ania Ulrich being the lead collaborator at the University of Alberta. Experiment conception and design were completed by Dr. Ania Ulrich, Dr. Elizabeth Edwards and I. Data analysis of 16S rRNA amplicon sequencing was conducted by Courtney Toth at University of Toronto. I implemented and executed laboratory experiments and completed all other data collection, analysis and visualization.

Acknowledgements

First and foremost, I want to express my heartfelt gratitude to my supervisor, Dr. Ania Ulrich, for her unwavering support and invaluable guidance throughout both my undergraduate and graduate degrees. I feel incredibly lucky to have her as my mentor and friend as she inspires me to always lead with kindness and compassion. She has been an integral part of my growth on many levels, personally and professionally, and there is no one else I would have wanted on this journey with me.

I am extremely grateful to my committee members, Dr. Tariq Siddique and Dr. Yang Liu, who have provided me with vital knowledge and feedback throughout my program, along with the support from my examining committee: Dr. Won Jae Chang, Dr. Dominic Sauvageau, Dr. Jeffrey Farner, and Dr. Victor Liu. I am also thankful to the National Sciences and Engineering Research Council for providing funding throughout my degree (Postgraduate Doctoral Research Scholarship). I truly appreciate the advice from the various technicians, research assistants and post doctoral fellows over the years. In particular, I am thankful for the guidance of the benzene team at University of Toronto, most notably Dr. Elizabeth Edwards, Dr. Courtney Toth and Shen Guo. Thank you to all my colleagues from the Ulrich lab over the years: Kelvin Chan, Luke Gjini, Nesma Allam, Korris Lee, and Anya Batycky. Special thanks to Petr Kuznetsov for being a fierce champion for everyone in the Ulrich lab and keeping everything running smoothly; to Dena Cologgi for her mentorship when I first started in research; and especially to Sarah Miles for her constant grounding presence and always being available to chat. I am extremely thankful to have gone through this experience with Heidi Cossey who not only provided support and friendship, but also became my favourite travel buddy.

I am also thankful for the ongoing support from my friends and family over the years, in particular, Stephanie Florence, Shelley Wells, my sisters (Shaelyn and Nicole), and my dad, Daryl Balaberda, all who offered up a listening ear whenever I needed it and reminded me to keep everything in perspective. Of course, I am always grateful for my cats, Luna and Asha, who show me unconditional love and frequently demand I take breaks to give them the attention they deserve. Most importantly, I want to thank my mom, Tracey Christiansen. Words cannot express how grateful I feel to have her unfailing support and continuous encouragement. She is the most thoughtful, steadfast, and loyal person I know. Throughout all my schooling she has always been there to help however she can, all while keeping me grounded. She is my biggest cheerleader and for that I am eternally grateful.

Table of Contents

List of Tables

List of Figures

List of Abbreviations

Glossary of Terms

ADA: adamantane carboxylic acid
AOPs: advanced oxidation processes
BOD: biochemical oxygen demand
BTEX: benzene, toluene, ethylbenzene, xylene
BH: Bushnell Haas mineral media
CFU: colony forming units
COD: chemical oxygen demand
CHCA: cyclohexane carboxylic acid
DBE: double bond equivalence
DNT: dinitrotoluene
DOC: dissolved organic carbon
DOM: dissolved organic matter
EPL: end pit lake
EPS: extracellular polymeric substances
FTIR: Fourier transform infrared spectroscopy
GAC: granular activated carbon
IC50: inhibitory concentration that reduces biological response/function by 50%
ISCO: in situ chemical oxidation
NAs: classically defined naphthenic acids with only the O_2 group ($C_nH_{2n+z}O_2$)
NAFCs: naphthenic acid fraction compounds/acid extractable organics ($C_nH_{2n+z}O_xN_\alpha S_\beta$)
NOM: natural organic matter
OSPW: oil sands process affected water
PAH: polyaromatic hydrocarbons
PHC: petroleum hydrocarbons
PMS: peroxymonosulfate
PS: persulfate ($S_2O_8^{2-}$)
qPCR: real time quantitative polymerase chain reaction
ROS: reactive oxygen species
SVE: soil vapour extraction
TEA: terminal electron acceptor
TOC: total organic carbon
TU: toxicity unit
TPH: total petroleum hydrocarbons
UV: ultraviolet light
ZVI: zero valent iron

Experimental Treatment Abbreviations

PS: persulfate oxidation treatments
CPS: coupled persulfate with biodegradation by *Pseudomonas fluorescence*
APS: activated persulfate treatment
CAPS: coupled activated persulfate with biodegradation by *Pseudomonas fluorescence*
NC: negative control (NA/NAFCs without persulfate or bacteria)
NCC: no carbon control (persulfate without NA/NAFCs)
KC: killed control (heat killed *Pseudomonas fluorescence*)

Chapter 1

Introduction

1.1 Introduction

Canada is the world's fifth largest producer of oil in the world, with production growing by 3 million barrels per day over the last 30 years, securing Canada's importance in the global petroleum industry (NRCan 2020, CER 2022). Petroleum can be extracted by various methods depending on the type (conventional crude oil or bitumen) and the site geology, before being sent to refineries and processing plants to create gasoline, diesel and other consumer products (CAPP 2013). A key issue with both upstream and downstream petroleum facilities are the impacts to the water matrix. Bitumen extraction requires large volumes of water that become contaminated and cannot be released back into the environment (Allen 2008a), and groundwater contamination is common at downstream sites such as petroleum storage facilities (U.S. EPA 2008). Further issues arise as contaminants at these sites can be persistent and current remediation technologies are intrusive and expensive.

1.2 Background

1.2.1 Upstream Petroleum Processes

Canada has the third largest oil reserves in the world which can be classified as either conventional or unconventional oil (CAPP 2013, NRCan 2020). Conventional oil is extracted using traditional drilling and pumping methods which are easier, less expensive, and require less processing, yet contributes to less than 30% of total oil production in Canada (ECCC 2022). Unconventional oil is too heavy and does not flow on its own, instead requiring advanced extraction techniques such as oil sands mining. The oil sands have been the main contributor to Canadian oil production since 2009, representing over 70% of oil production as of 2020 (CAPP 2022, CER 2022). Out of the approximately 168 billion barrels of proven oil reserves in Canada, 164 billion barrels exist as bitumen in the Alberta oil sands, with deposits

located in Athabasca, Cold Lake and Peace River (NRCan 2020). There are two main methods for extracting bitumen from the oil sands: in situ and surface mining. Deposits that are located deep underground require in situ extraction, most commonly using steam assisted gravity drainage (SAGD) during which bitumen is heated with steam making it fluid enough to pump. In suit extraction is energy intensive, however it has a smaller environmental footprint compared to surface mining and most emissions are to the air (ECCC 2022).

Approximately 20% of oil sands deposits are shallow (<75 m) and can be surface mined, occurring north of Fort McMurray near the Athabasca River (ACR 2004). Surface mined oil sands use a caustic hot water extraction process to separate the bitumen from sand, clay and water (Allen 2008a). To produce 1 barrel of oil, approximately 3 barrels of non-saline water are required (AER 2016). Leftover sand, clay and water (collectively termed "tailings") are stored long term in tailings ponds, creating a large inventory of waste that cannot be discharged into the environment (Allen 2008a). In 2017, there was an estimated 1 billion m^3 of tailings stored in tailings ponds, covering an area of approximately 220 km^2 (Foght et al. 2017, NRCan 2019). Total reported tailings from oil sands surface mining have increased by 56% between 2010 and 2019 (ECCC 2022). While much of the process-affected water in tailings can be recycled after the sand and clay have settled, this creates an increasingly contaminated waste stream and may reduce the recovery rate of bitumen (Allen 2008a).

There are numerous contaminants present in oil sands process-affected water (OSPW) such as salts, minerals, heavy metals, bitumen, polyaromatic hydrocarbons (PAHs), benzene, toluene, ethylbenzene, xylenes (BTEX), and naphthenic acid fraction compounds (NAFCs) (Allen 2008a, Li et al. 2017a). NAFCs are organic compounds in bitumen that are solubilized and concentrated during the extraction process and are considered the primary cause of OSPW

toxicity (Allen 2008a, Morandi et al. 2017, Scott et al. 2005). In general, NAFC concentrations range from 20 – 80 mg/L in fresh settling basins and 5 – 40 mg/L in reclamation ponds (Li et al. 2017a). The National Pollutant Release Inventory (NPRI) began tracking NAFC disposal and release in 2020. Between 2020 and 2021, three oil sands facilities reported 34,369 tonnes of NAFC waste disposed of in tailings ponds, along with approximately 26 tonnes unintentionally released to surrounding water (NPRI 2023).

Remediation of NAFCs is imperative to allow OSPW to be safely reintroduced into the watershed. Treatments can be physical (adsorption, filtration), chemical (advanced oxidation processes, AOPs), or biological (bioreactors, in situ bioremediation) (Allen 2008b, Quinlan and Tam 2015). The lack of harmful by-products and low cost compared to other options make bioremediation a desirable choice for the large volumes of OSPW that requires treatment. However, the more complex NAFCs, particularly those with higher cyclicity or unsaturation, are resistant to biodegradation even under aerobic conditions (Quagraine et al. 2005a, Scott et al. 2005). In order to address the recalcitrant nature of NAFCs, more sophisticated remediation options are needed that can produce bioavailable compounds. To date, coupled remediation techniques have focused on pre-treatment with ozone generated hydroxyl radicals (OH•) followed by a biological polishing step, which has shown improved removal of organics and toxicity compared to ozonation alone (Martin et al. 2010, Brown et al. 2013, Dong et al. 2015, Zhang et al. 2018a, 2018b). However, issues with ozonation include its high cost, short lifespan (seconds to minutes) and the non-selective nature of OH• (Li et al. 2017b, Ganiyu et al. 2022b). Persulfate is another effective oxidant that is commonly used in coupling strategies for petroleum contaminated sites as it is cheaper, more persistent, and less aggressive than ozone (Tsitonaki et al. 2008, 2010, Cassidy et al. 2009, Yen et al. 2011, Liao et al. 2018).

Furthermore, it can be activated to produce both sulfate and hydroxyl radicals which can provide more comprehensive removals (Lee et al. 2020). The potential for coupling persulfate oxidation (unactivated or activated) with in situ biodegradation for OSPW has not yet been studied.

1.2.2 Downstream Petroleum Processes

After bitumen is extracted, some undergoes upgrading to create synthetic crude oil at which point it is then further refined along with conventional crude oil to make products such as gasoline, diesel, jet fuel, kerosene, and naphtha (CAPP 2013). Refined petroleum products are then sent to storage tanks and eventually to distribution terminals. More than 30% of Canadian oil production is refined in Canada (CAPP 2013), with 18 refineries located mainly in Alberta and Ontario along major waterways (NEB 2018, Oil Sands Magazine 2023). Gasoline is the largest output from refineries, representing 47% of finished consumer products (NEB 2018).

A range of organic and inorganic contaminants can exist at downstream petroleum sites, including petroleum hydrocarbon (PHC) fractions (F1, F2, F3, F4), sodium, chloride, arsenic, barium, boron, cadmium, chromium and lead (Thiessen and Achari 2017). The aromatic BTEX hydrocarbons exist within F1 PHCs (C_6-C_{10}). Benzene is classified as a Group 1 carcinogen and is one of the most problematic contaminants due to its recalcitrant and mobile nature (Bennett 1999, ATSDR 2007, Toth et al. 2021). Benzene is a natural constituent of petroleum and thus is a by-product of the oil refining process, and is commonly used to manufacture other chemicals and pharmaceuticals (CCME 2004, ATSDR 2007). In gasoline, benzene is added as an octane-enhancer and antiknock agent. Previously benzene accounted for up to 4% of gasoline, but regulations under the Canadian Environmental Protection Act

1999 prohibited the supply of gasoline with a benzene content exceeding 1% (CCME 2004, Government of Canada 2020). Main sources of benzene contamination to the subsurface are from industrial discharge, or accidental leaks and spills at downstream oil operations such as upgrading facilities, refineries, storage facilities, and gas plants (CCME 2004, NPRI 2023).

Since 2017 there was an average yearly disposal of 1650 tonnes of industrial benzene waste in Canada as reported to the NPRI, with an average of 97 tonnes per year inadvertently released to nearby water and soil (NPRI 2023). The concentration of benzene in the groundwater at oil and gas impacted sites can vary widely (<1 – 100 mg/L) depending on the contents, amount, depth and age of the spill, along with the site geology and groundwater velocity (Toth, C. 2020. Personal communication). Groundwater near underground storage tanks containing gasoline in Canada have been found to range from below detection limit (BDL) up to 15 mg/L of benzene (Government of Canada 1993). In the US, groundwater plumes from fuel spills at a gasoline station were found to have benzene levels as high as 1.2 – 19 mg/L, while one bulk storage facility had a benzene concentration of 45 mg/L (ATSDR 2007). In Alberta, the Tier 1 remediation guideline for benzene in groundwater is 0.005 mg/L (Government of Alberta 2022).

The most commonly used remediation strategy for benzene is excavation and disposal of impacted soils, or pump and treat for groundwater. While this approach is simple and time efficient, it is also more costly and disruptive. Bioremediation offers a low cost and non-intrusive method; however, requires longer timelines and an appropriate benzene-degrading microbial community (Anderson et al. 1998, Luo et al. 2016). Benzene can be biodegraded relatively easy aerobically, often on a timescale of days or weeks, but anaerobic conditions quickly develop as aerobic microorganisms utilize the oxygen in the subsurface, at which point

benzene contamination persists over many years (Paustenbach et al. 1993, Lovley 2000). Recently, microbial communities capable of anaerobic benzene biodegradation have been identified (Ulrich and Edwards 2003, Luo et al. 2016), suggesting bioaugmentation may be an effective treatment strategy at petroleum impacted sites.

In Alberta, soil and groundwater can have increased salinity due to both natural and anthropogenic factors, but is particularly relevant for both upstream and downstream oil facilities due to the release of produced waters (AENV 2001). At high concentrations (> 10 g/L) salinity can be acutely toxic; however, even lower concentrations salinity can influence biological productivity, change microbial community composition and act as a stressor that increases the toxicity of other contaminants (Yan et al. 2015). Salts can also influence the properties of the contaminant, making them less soluble and accessible for microbes (Nicholson and Fathepure 2005, De Visscher 2018). For aerobic hydrocarbon biodegradation, increasing salinity leads to increased lag times and decreased degradation (Amatya et al. 2002, Børresen and Rike 2007, De Carvalho and Da Fonseca 2005, Ulrich et al. 2009). The impact of salt on anaerobic hydrocarbon biodegradation in a naturally non-saline environments has not been well studied (Chen et al. 2022a, Jiang et al. 2023). Benzene in particular is already challenging to degrade anaerobically, and the impact of salinity is unknown.

1.3 Research Questions

The oil and gas industry is a key economic driver in Canada that has been expanding at a rapid pace, producing a large inventory of waste that requires remediation. Common environmental remediation methods such as excavation, pump-and-treat and chemical oxidation are costly and intrusive which has led to a transition to methods such as bioremediation. However, issues such as complex contaminants that are recalcitrant and salt

co-contamination hinder the success and large-scale implementation of bioremediation as a remediation strategy. Therefore, the overall objective of this research is to address these knowledge gaps for NAFCs and benzene, two main contaminations of concern in the Canadian oil industry. NAFCs do not currently have a standard remediation protocol and a combination of techniques will likely be required. Coupling chemical oxidation with biodegradation may be a viable solution, however operational parameters such as the ideal oxidant of choice, dose, and biological treatment configurations require investigation. Anaerobic benzene bioremediation offers many challenges for practical application in the field. The identification of bioaugmentation cultures is promising, however it is still unknown how anaerobic benzene biodegradation will be impacted by other environmentally relevant factors such as salinity. The specific research questions and hypotheses are as follows:

Research Question 1: Does coupling unactivated persulfate oxidation and biodegradation using *Pseudomonas fluorescens* decrease Merichem Naphthenic Acid (NA) concentration, overall organics (Chemical Oxygen Demand, COD) and toxicity of the water? Is the rate of removal of Merichem NAs improved by increasing the temperature to 30ºC? Does persulfate effect the number of viable bacteria cells?

Hypothesis: Unactivated persulfate has been shown to be reactive with OSPW NAFCs, however long timelines are required (Sohrabi et al. 2013). *P. fluorescens* is a well-known hydrocarbon degrader that is present in OSPW and many oil and gas contaminated sites worldwide (Whitby 2010, Imron et al. 2020), therefore it is expected to be capable of degrading by-products produced from persulfate oxidation of NAs. Persulfate is considered a less aggressive oxidant and while microbial populations have been shown to decline after addition of persulfate, they withstand oxidative stress and bounce back (Sutton et al. 2014b). Therefore, it is hypothesized that

persulfate will oxidize Merichem NAs, creating more bioavailable organics for the *P. fluorescens* to degrade, thus leading to more complete overall removals. *P. fluorescens* has an optimal growth temperature of 25-30^{o}C (Moore et al. 2006) so increasing the temperature to 30^{o}C is expected to improve bacteria growth. Heat can also activate persulfate, creating more sulfate/hydroxyl radicals which will improve reactivity with Merichem NAs, but may add stress to the bacteria.

Research Question 2: Does an initial heat activated persulfate oxidation phase followed by unactivated persulfate oxidation coupled to biodegradation using *P. fluorescens* decrease Merichem NA and OSPW NAFC concentration and reduce toxicity of process water? How does the NAFC distribution shift with each treatment phase? Is the coupled treatment more effective at NAFC and toxicity reduction compared to oxidation or bioremediation alone? How is the growth of bacteria impacted by oxidative stress and OSPW toxicity in the coupled treatment?

Hypothesis: Activated persulfate has been shown to effectively oxidize OSPW NAFCs and model NAs using heat, ultraviolet (UV), solar and iron as activation methods at much faster rates than unactivated persulfate (Aher et al. 2017, Drzewicz et al. 2012, Fang et al. 2018, Liang et al. 2011, Xu et al. 2016b). Therefore, an initial heat activated persulfate phase is expected to be effective in considerably reducing NAFC concentrations. Advanced oxidation processes (AOPs) such as ozonation have been shown to preferentially oxidize the more biopersistent NAFCs (cyclic and highly unsaturated) (Xu et al. 2017). Augmenting persulfate treated-OSPW with bacteria after bulk NAFC removal during persulfate activation is hypothesized to lead to more complete mineralization than oxidation alone. Studies using ozone pre-treatment followed by biodegradation for NAFCs have shown success in higher rates of NAFC removal than ozonation alone (Brown et al. 2013, Martin et al. 2010). Microbes

exposed to ozone were able to re-establish (Brown et al. 2013), and since persulfate is a less aggressive oxidant the bacteria are expected to have some hindered growth but ultimately not impede their biodegradation capabilities.

Research Question 3: What impact does salt (NaCl) have on anaerobic benzene biodegradation of a highly enriched benzene-degrading methanogenic culture? Is there a difference in benzene degradation rate when microorganisms have been slowly adapted to high salt conditions compared to sudden salt shock? How is the microbial community composition impacted by salt?

Hypothesis: Salt has been shown to negatively impact aerobic biodegradation of hydrocarbons (Ulrich et al. 2009, Chang et al. 2018). Concentrations that are relevant to produced water (10-50 g/L NaCl) are hypothesized to decrease the extent and the rate of the degradation. Microorganisms can enhance their stress tolerance by gradual modifications of their stress response and substrate utilization techniques while in a stressful environment. Gradual adaptation to stressful environments is commonly used to improve performance of microbes in bioengineered strains (Tan et al. 2022). Therefore, slowly adapting the benzene-degrading microbial communities to salt is expected to increase benzene degradation rates at high NaCl concentrations compared to cultures not acclimated to salt. Different microorganisms have different salt tolerance levels (Yan et al. 2015), so the addition of salt is expected to shift the community, particularly in slowly acclimated cultures.

1.4 Thesis Organization

Chapter 1 provides a brief introduction to the topic of research, objectives and hypotheses. Chapter 2 reviews relevant literature in support of this research, including a review on the properties and toxicity of each contaminant of concern (NAFCs and benzene), along with relevant remediation options. Chapter 3, 4, and 5 address research questions 1, 2, and 3, respectively, as highlighted above. Chapter 6 provides a summary of the findings of this research and recommendations for future work.

Chapter 2

Literature Review

2.1 Introduction

The petroleum industry is a major economic driver in Canada but contributes to significant contamination. The development of effective remediation strategies is increasingly important for providing environmental protection, supporting human health and lowering public costs. This chapter presents a literature review on persistent contaminants of concern for the petroleum industry, including NAFCs for upstream oil sands operations and anaerobic benzene for downstream petroleum refineries.

2.2 Naphthenic Acid Fraction Compounds

Oil sands process affected water (OSPW) contains naphthenic acids (NAs) which are organic compounds in bitumen that are solubilized during the extraction process and considered the primary cause of toxicity (Allen 2008a, Morandi et al. 2017, Scott et al. 2005). Large volumes of OSPW are currently stored in tailings ponds, and the remediation of NAs is a main concern prior to potential discharge into the watershed. This section provides a literature review of NA contamination as it relates to the oil sands industry. The properties and toxicity of NAs will be reviewed, along with remediation methods currently being studied. Biodegradation, chemical oxidation and combined remediation strategies will be explored in depth.

2.2.1 Properties and Toxicity of NAFCs

NAs are classically defined as a complex mixture of cyclic and acyclic alkanes possessing a single carboxylated side chain, with the general formula $C_nH_{2n+z}O_2$, where 'n' represents the carbon number, and 'z' represents the hydrogen loss due to ring and double bond formation (Brient et al. 2000, Headley et al. 2002). The term naphthenic acid fraction compounds (NAFCs) describe a broader class of acid extractable organics that includes the

classically defined NAs (O_2 group), along with a complex mixture of oxidized compounds (3 or more oxygen atoms) and compounds containing sulphur and nitrogen (Grewer et al. 2010, Headley et al. 2011, Bauer et al. 2015). NAFCs can be described by the formula $C_nH_{2n+z}O_xN_\alpha S_\beta$, with X, α, and β describing the number of oxygen, nitrogen and sulfur atoms, respectively (Vander Meulen et al. 2021). OSPW contains NAFCs with carbon numbers (n) ranging from 6 to 50 and z from 0 to -24 (Kannel and Gan 2012). Fresh OSPW is dominated by z=0 family while aged OSPW contains predominately z= -4 and -6 compounds, describing a higher level of cyclicity and unsaturation (Grewer et al. 2010). The degree of unsaturation and cyclicity can also be discussed in terms of double bond equivalence (DBE) where the number of rings is the DBE subtracted by 1 (DBE=1 or z=0 indicates no rings). Commercial NA compounds are commonly used to determine mechanisms of toxicity and potential biodegradation pathways, and are much simpler than OSPW NAFCs, consisting of only the classical O_2 group with more straight chained saturated NAs (Barrow et al. 2004). Examples of NAFCs found in OSPW are shown in Figure 2-1 below.

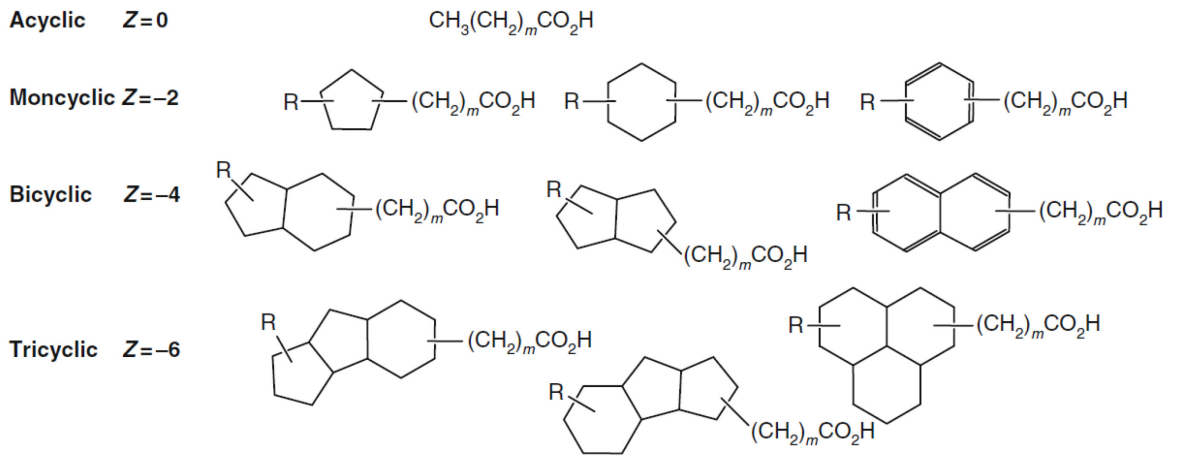

Figure 2-1. Examples of aromatic and nonaromatic NAFC structures. R represents aliphatic groups and m is the number if CH2 units (from Whitby 2010).

The properties of NAFCs will vary with their chemical composition and molecular structure. However, in general they are chemically stable, with low volatility, sorption and bioaccumulation potential. NAFCs are amphiphilic with a hydrophilic carboxyl functional group and hydrophobic alicyclic end, making them surfactants that concentrate at aqueous-nonaqueous interfaces (Brown and Ulrich 2015). NAFCs are weak acids with a pKa of 5-6, and therefore exist in their ionized (anionic) form in OSPW (pH>8) and river water (Brient et al. 2000). Sorption to clays is unlikely due to electrostatic repulsion when they exist in their anionic form (Marsh 2006). Table 2-1 outlines the range of properties for NAFCs.

Table 2-1: Physical and Chemical Properties of OSPW NAFCs at pH 7. Data taken from: Kannel and Gan 2012. **BCF*: bioconcentration factor, Scott et al. 2020.

Parameter	Value	Units
Molecular Weight	140-450	g/mol
Density	0.97-0.99	g/cm^3
Water Solubility	< 50	mg/L
Vapour Pressure	2.35×10^{-6}	atm
Henry's Law Constant	8.56×10^{-6}	$amt\bullet m^3/mol$
log K_{ow}	2.4	unitless
K_d	0.2-2.5	L/kg
BCF*	0.24 - 53	L/kg

Exposure to OPSW can cause compromised immune function, developmental delays, impaired reproduction, disrupted endocrine system, and tissue specific symptoms to a variety of organisms (Li et al. 2017a). In vitro toxicity towards *Vibrio fischeri* (now *Aliivibrio fischeri*) gives IC_{50} values of 25-67% for fresh OSPW and 65-100% for aged OSPW (Li et al. 2017a). OSPW is a complex mixture which makes it difficult to determine the exact cause of toxicity. However, research has consistently suggested that the acidic fraction (NAFCs) are likely the

principal toxicants (Frank et al. 2008, Headley and McMartin 2004, Hughes et al. 2017). NAFCs have exhibited toxicity towards invertebrates, fish, amphibians, birds, and mammals (reviewed in: Li et al. 2017a). The mechanism of toxicity for NAFCs is not yet fully established, but narcosis is considered the main driver due to the surfactant properties of NAFCs, allowing them to penetrate and disrupt the cell membrane (Frank et al. 2008, Kannel and Gan 2012, Klopman et al. 1999, Quagraine et al. 2005b, Rogers et al. 2002b). Other modes of action such as endocrine disruption, oxidative stress, electrophilic reactivity and enzyme inhibition have also been suggested (Bauer et al. 2017, Li et al. 2017a).

The toxicity of NAFCs will depend on their structure and composition, with the classical O_2 group demonstrating the highest toxicity. Bartlett et al. (2017) found that commercial NAs, which contain only the O_2 group, were more toxic than OSPW. Furthermore, aged OSPW was less toxic than fresh OPSW which contains more O_2 compounds. Lower molecular weight NAFCs have generally shown greater toxicity, likely due to the decreased carboxylic acid groups which increases hydrophobicity (Frank et al. 2009). Conversely, increased molecular weight for NAFCs is often due to increased oxygenated groups and aromaticity, which can increase aqueous solubility and thus decreases toxicity (Morandi et al. 2015, Bauer et al. 2017). However, some studies have found that higher molecular weight NAFCs were more toxic, suggesting that toxicity is not only driven by molecular weight but by aromaticity and heteroatom content (Bauer et al. 2017, Hughes et al. 2017). The increased presence of aromatic rings and double bond equivalence has increased toxicity towards fish (Scarlett et al. 2013, Morandi et al. 2015). Therefore, it appears that the structure-toxicity relationship for NAFCs depends on many complex factors.

2.2.2 Remediation Techniques

The goal of remediation is to eliminate toxicity and allow OSPW to be safely reintroduced into the watershed. Due to the large volumes of OSPW, any treatment option needs to have considerable scale-up capacity. There are many physical, chemical and biological remediation techniques currently being investigated, however the lack of remediation guidelines makes implementation difficult. The complex water chemistry of OPSW impacts removals rates and costs of potential treatments, which is further complicated as different sources of OSPW have different chemistry (Allen 2008b).

Physical treatments such as granular activated carbon (GAC) adsorption and membrane filtration make use of adsorption, electrostatic attraction or size exclusion to remove NAFCs from the water stream (Quinlan and Tam 2015). Coagulation and flocculation are commonly studied for settling fines in OSPW, but some research has shown that the positive surface charge from alum precipitates attract the negatively charged NAFCs (Pourrezaei et al. 2011). Physical treatments are simple but often do not lead to complete removal of NAFCs (Allen 2008b). One of the most significant disadvantages of physical treatments is that they require treatment of a secondary waste stream, such as used sorbent during GAC adsorption, retentate/brine from membrane filtration and sludge in coagulation and flocculation (Allen 2008b, Quinlan and Tam 2015).

Chemical oxidation describes processes where NAFCs are partially or completely degraded through oxidation reactions. While oxidation reactions are fast and effective for NAFC removal, there are various considerations. For example, oxidants can be scavenged by other organics or inorganics in OSPW, and reaction intermediates may be more resistant to oxidation, requiring greater amounts of energy and chemical reagents to achieve adequate

removals (Allen 2008b, Brown and Ulrich 2015). The main limitation of chemical oxidation is the cost and possible by-products.

Conversely, biological treatments that utilize microorganisms to metabolize the NAFCs are low cost and produce negligible by-products. Biological treatment is often enhanced through the addition of nitrogen and phosphorous (biostimulation) and can be done via in situ biodegradation in tailings ponds or ex situ treatment in bioreactors. However, a portion of NAFCs are recalcitrant and persist regardless of nutrient addition and incubation time, limiting their remediation potential (Han et al. 2008, Toor et al. 2013, Yue et al. 2016, Xue et al. 2018). Constructed wetlands and end pit lakes (EPLs) where a freshwater cap is applied over tailings is another technique currently being investigated by industry. These wet landscape methods utilize natural detoxification processes and are advantageous for large scale application. However, there is the potential for NAFCs and other contaminants to diffuse from tailings into the freshwater cap, and relying on natural attenuation is not recommended for OSPW due to the long timelines involved and persistence of NAFCs (Allen 2008b, Brown and Ulrich 2015, White and Liber 2020, Kuznetsov et al. 2023).

Given the limitations of each individual remediation method, emerging research has focused on using a combination of techniques, primarily by combining physical or chemical treatment with biodegradation. Examples include using GAC-bioreactors or membrane-bioreactors and ozone pre-treatment followed by biological polishing (Allen 2008b, Brown and Ulrich 2015, Quinlan and Tam 2015).

2.2.3 Biodegradation of NAFCs

Biodegradation is the most cost-effective remediation technique for the large volumes of OSPW that require treatment. Unfortunately, a portion of NAFCs are recalcitrant even under

aerobic conditions, and the practical limit for in situ biodegradation of NAFCs was estimated to be 18 mg/L with a half life up to 14 years (Han et al. 2009, Quagraine et al. 2005b). Biodegradation in OSPW has been found to be nitrogen and phosphorous limited (Herman et al. 1994); the biodegradation of model NAs has been improved 2-fold by addition of N and P (Lai et al. 1996). However, even the addition of nitrogen and phosphorous does not appear to facilitate the complete degradation of NAFCs in situ (Toor et al. 2013), and despite decades long residence times aged OSPW still exhibits toxic effects (Anderson et al. 2012a).

There has been extensive research done on the biodegradation potential of NAFCs. Early work done by Herman et al. (1994) showed 50% removal of commercial Kodak NAs and only 20% removal of OSPW NAFCs in 24 days. Similarly, Scott et al. (2005) observed 77-93% removal of various commercial NAs in 10 days compared to 25% NAFC removal in OSPW after 49 days; while Han et al. (2008) found that over half of OSPW NAFCs remained after 98 days of incubation. Commercial NAs have consistently been shown to be more biodegradable than NAFCs from OSPW (Clemente et al. 2004, Del Rio et al. 2006, Han et al. 2008, Headley et al. 2010, Herman et al. 1994, Scott et al. 2005, Toor et al. 2013). OSPW NAFCs have undergone extensive biodegradation in tailings ponds and oil deposits, leaving behind more recalcitrant NAFCs, while commercial NAs come from petroleum sources that have not yet been subject to significant biodegradation (Quinlan and Tam 2015). Bioreactors are often utilized to improve degradation of recalcitrant organics as they can better tolerate stressful conditions due to the help of a protective extracellular polymeric substance (EPS) barrier (Xue et al. 2018). However, even the more resilient bioreactors still cannot fully degrade NAFCs and classical O_2-NAs. A moving bed biofilm reactor removed 18% and 35%

of NAFCs and O_2-NAs, respectively (Shi et al. 2015), while an integrated fixed film activated sludge reactor degraded 12% and 43% of NAFCs and O_2-NAs (Huang et al. 2015).

The dominant factors that have been shown to impact OSPW NAFC biodegradability include the molecular weight, chain length, number of carbon atoms in the alkyl chain, the number of cyclic rings and the number and position of alkyl groups (Quagraine et al. 2005a, 2005b). There have been some inconsistencies in correlation between carbon numbers and biodegradability as it appears to also depend on other structural components (Han et al. 2008). In general, lower molecular weight NAFCs are preferentially degraded, leaving behind a larger fraction of $n > 22$ compounds that are mostly comprised of O_{3+} NAFCs in aged ponds (Holowenko et al. 2002, Bataineh et al. 2006, Han et al. 2009). Increasing cyclicity increases bio-persistence, with linear and monocyclic NAFCs more degradable than bicyclic NAFCs (Lai et al. 1996, Del Rio et al. 2006, Quesnel et al. 2011, D'Souza et al. 2014). The amount and location of alkyl side branching also plays a vital role, with increasing branching increasing persistence. For example, Smith et al. (2008) found that over 97% of less branched model NAs were degraded compared to only 2.5% of highly branched NAs. Overall, lower molecular weight, acyclic NAFCs are the most labile, and those with a higher degree of branching and cyclization persist (Clemente et al. 2004, Han et al. 2008). This further explains why commercial NAs are more readily biodegradable, as they consist of more structurally simple compounds with lower molecular weights (Scott et al., 2005).

Microorganisms capable of partial degradation of recalcitrant model NA compounds have been identified (Demeter et al. 2015, Paulssen and Gieg 2019, Miles et al. 2020). Significantly, an algal-bacteria community isolated from an oil sands tailings pond was able to biodegrade up to 80% of 1-adamantane carboxylic acid (ADA) over 90 days (Paulssen and

Gieg 2019). ADA is a diamondoid NA compound that is known to be recalcitrant and toxic in OSPW. However, model NA compounds may not behave the same as OSPW NAFCs and there is still significant research needed in improving biodegradability of NAFCs. Techniques such as bioaugmentation with microbes capable of degrading refractory NAFCs, use of bioreactors optimized for NAFC degraders, and biostimulation have been suggested to improve biodegradation, but have not demonstrated success for completely removing OSPW toxicity (Whitby 2010, Xue et al. 2018). Therefore, the long timelines and bio-persistence of NAFCs imply that bioremediation will need to be supplemented with more powerful remediation methods to be viable (Foght et al. 2017, Scott et al. 2005).

2.2.4 Chemical Oxidation of NAFCs

Oxidizing agents that have been studied for NAFC remediation in OSPW include ozone (O_3), hydrogen peroxide (H_2O_2), chlorine (Cl), and persulfate ($S_2O_8^{2-}$) (Xu et al. 2017, Ganiyu et al. 2022b). While these have varying abilities to oxidize organics on their own, they are often activated to form powerful reactive oxygen species (ROS) which are referred to as advanced oxidation processes (AOPs). The oxidation of NAFCs during AOPs involves a complex series of propagation reactions where ROS are formed from the oxidizing agent, the NAFCs, and intermediates in the reaction pathway (Xu et al. 2017). Activation of oxidants to form ROS can occur by the addition of catalysts such as iron, alkaline conditions, and ultraviolet (UV) radiation. ROS can also be formed by electrochemical oxidation, photocatalysis of TiO_2 and gamma-ray irradiation. Hydroxyl radicals (OH•) are the most common ROS utilized for NAFC oxidation. Oxidants, ROS, and their oxidation potentials, E^o, are listed below in Table 2-2.

Table 2-2. Oxidation potentials, E^o (v), for common oxidizing agents and ROS (Ganiyu et al. 2022b) *Lenntech 2023.

Oxidants	E^o (v)
Cl^*	1.4
$H_2O_2{}^*$	1.8
O_3	2.1
$S_2O_8{}^{2-}$	2.1
Cl•	2.4
OH•	2.8
$SO_4{}^{\bullet-}$	2.5-3.1

Oxidation of NAFCs using hydrogen peroxide and ozone has been well reviewed (Brown and Ulrich 2015, Xu et al. 2017, Ganiyu et al. 2022b). For oxidation of organic contaminants, H_2O_2 is often catalyzed with Fe^{2+} (Fenton's reaction) at low pH (~3) to form OH•. However, this is not relevant for alkaline OSPW (pH~8), so iron chelates (Zhang et al. 2016c, 2016b, 2016a) and UV light (Afzal et al. 2012a, 2012b, Drzewicz et al. 2010, Liang et al. 2011, Wang et al. 2016) have been used instead. Ozone is commonly studied for NAFC removal both academically and by industry (Scott et al. 2008, Gamal El-Din et al. 2011, Garcia-Garcia et al. 2011, Pérez-Estrada et al. 2011, Anderson et al. 2012b, Wang et al. 2013b, 2016, Pereira et al. 2013, Islam et al. 2014, Klamerth et al. 2015). Ozone is an electrophilic oxidant with selective reactivity towards electron rich moieties in organics and can react directly or indirectly to form OH•. Ozone and hydroxyl radicals oxidize NAFCs by hydrogen abstraction, selectively attacking hydrogen atoms attached to tertiary carbons that exist in more complex structural elements, preferentially oxidizing NAFCs with higher carbon number and cyclicity (Scott et al. 2008, Gamal El-Din et al. 2011, Pérez-Estrada et al. 2011, Wang et al. 2013b, Pereira et al. 2013, Islam et al. 2014).

There are several drawbacks that have limited the industrial application of ozonation for NAFC remediation. Complete mineralization with ozone is challenging due to the creation of less reactive intermediate species, and increased exposure to ozone does not proportionally increase NAFC degradation (Gamal El-Din et al. 2011, Pérez-Estrada et al. 2011, Wang et al. 2013b). There is also concern over reaction intermediates and oxidation by-products having toxic effects (Garcia-Garcia et al. 2011). Ozone treatment has a high initial investment and an extremely short lifespan once added to OSPW (Ganiyu et al. 2022b). Therefore, the large amount of energy and high ozone dose needed to achieve complete mineralization of NFACs may be cost prohibitive (Brown and Ulrich 2015).

Recently, persulfate has been gaining interest as an alternative to ozone as it is a powerful oxidant, economical, simple to utilize and versatile. In addition, persulfate has a high water solubility, no odour, is persistent and is effective over a wide range of pH (Liang et al. 2006, Drzewicz et al. 2012, Wacławek et al. 2017). Persulfate can be used either unactivated or activated. Unactivated persulfate reacts directly with the compound, taking two electrons to form two sulfate anions (Eq 1) (Tsitonaki et al. 2010). Activation aims to create sulfate radicals by either imparting energy (heat or UV light) to cleave the peroxide bond (Eq 2) or undergoing a redox reaction with an electron donor (transition metals) (Eq 3) (Matzek and Carter 2016). The sulfate radicals can then also react with water to create hydroxyl radicals (Eq 4).

$$S_2O_8^{2-} + 2\,e^- \rightarrow 2\,SO_4^{2-} \qquad (Eq\ 1)$$

$$S_2O_8^{2-} \rightarrow 2\,SO_4^{\bullet -} \qquad (Eq\ 2)$$

$$S_2O_8^{2-} + M^{n+} \rightarrow SO_4^{\bullet -} + SO_4^{2-} + M^{n+1} \qquad (Eq\ 3)$$

$$SO_4^{\bullet -} + H_2O \rightarrow OH^{\bullet} + SO_4^{2-} + H^+ \qquad (Eq\ 4)$$

Despite a lower redox potential, unactivated persulfate can be useful in situ because it does not require a catalyst thus lowering costs and increasing the lifespan (Tsitonaki et al. 2010, Sohrabi et al. 2013). However, some studies have suggested that a degree of thermal activation occurs at ambient temperatures, and that some activation can occur in situ due to naturally occurring minerals (Liang et al. 2008a). This may provide a balance between utilizing the advantages of both activated and unactivated persulfate. The main concerns when using persulfate are acidification and increased electrical conductivity due to the production of sulfate ions (Tsitonaki et al. 2010).

For OSPW, unactivated persulfate along with UV, heat and iron activated persulfate has been studied for NAFC remediation, summarized in Table 2-3. Activated persulfate has been shown to be more effective than other commonly used oxidants such as hydrogen peroxide. Liang et al. (2011) compared UV activated TiO_2, periodate, hydrogen peroxide and persulfate for commercial NA (Sigma) degradation. UV activated persulfate gave the fastest degradation with half lives of 18-28 min for 10-20 mM persulfate, while higher concentrations of hydrogen peroxide (50 mM) were required to reach a similar degradation rate. Similarly, Fang et al. (2020) compared UV activated chlorine, hydrogen peroxide and persulfate for OSPW NAFC removal. Activated persulfate exhibited higher removals of classical (O_2) NAs at 81-95%, compared to 71-84% for hydrogen peroxide and chlorine. The authors attributed the improved degradation to the combination of sulfate and hydroxyl radicals; sulfate radicals are more effective than hydroxyl radicals for aliphatic acid oxidation, thus each radical removed different groups of NAFCs. Similar to ozonation, persulfate oxidation appears to be highly reactive with higher carbon and z number NAFCs (Fang et al. 2019). To-date, only one study focused on unactivated persulfate oxidation (Sohrabi et al. 2013). The authors found that

10 g/L of persulfate was able to reduce the OSPW NAFC concentration from 57 mg/L to <1 mg/L over 111 days, demonstrating that the unactivated persulfate ion can react with NAFCs, albeit at much slower timeframes. Furthermore, only 20% of the persulfate was consumed over the experiment timeframe, indicating that much smaller doses of persulfate can be used, lowering treatment costs.

Most AOPs for treatment of produced waters, including OSPW, are still in lab and pilot scale and there are very few used in industrial applications. The main limiting factor is their cost, as large quantities of reagent are required to achieve adequate removals of recalcitrant NAFCs. Sulfate radical based AOPs such as persulfate may be more cost effective but are still being validated at the lab scale and require more research on fundamentals, cost, and efficiency (Ganiyu et al. 2022b).

Table 2-3. Summary of Studies Utilizing Persulfate Oxidation for Oil Sands NAFCs

Reference	NA Type & Concentration	Persulfate Dose	Activation Method	Timeline	Results
(Liang et al. 2011)	Sigma NA: 100 mg/L	3800 mg/L	UV	6 hours	• 95% degradation with UV activation • No removal without activation
(Drzewicz et al. 2012)	Model NA (CHCA): 50 mg/L OSPW: 35 mg/L	100-2000 mg/L	Heat (20-80°C) + ZVI	6 days	• 90% NAFC removal at 20°C in 6 days • 20, 45, 90% CHCA removal at 40, 60, 80°C in 2 hours • ZVI improved PS reaction at low temperatures only
(Sohrabi et al. 2013)	OSPW: 57 mg/L	10,000 mg/L	N/A	111 days	• 98% degradation O2-NAs • 20% persulfate consumed
(Xu et al. 2016b)	Model NA (CHCA, CHBA, 2-NA, 1234-T-2): 50 mg/L	10-100% stoichiometric dose	Heat (40-97°C)	1 day	• 100% degradation at 80°C, >40% stoichiometric dose • Chloride (10 - 50 g/L) had negative effect • Bicarbonate (0.5, 10g/L) had negligible effect
(Aher et al. 2017)	OSPW: 34 mg/L Sigma NA: 38 mg/L	5000 mg/L	Iron	10 min	• OSPW: 95% degradation • Sigma NA: 46% degradation
(Xu et al. 2018a)	Model NA (CHCA): 50 mg/L	20% stoichiometric dose	Heat (Followed by H_2O_2)	6 hours	• 40% mineralization by heat activated PS • 80% mineralization by heat activated PS-H_2O_2 system

Table 2-3 (cont'). Summary of Studies Utilizing Persulfate Oxidation for Oil Sands NAFCs

Reference	NA Type & Concentration	Persulfate Dose	Activation Method	Timeline	Results
(Fang et al. 2018)	Model NA (CHCA, PVA, CHPA, HPA, ADA): 0.39 mM	2 mM	UV	30 min	• 100% degradation • Chloride (824 mg/L) significantly decreased removal
(Xu et al. 2019b)	Model NA (CHCA, CHBA, 2-NA, 1234-T-2): 50 mg/L	5, 20% stoichiometric dose	Heat (80°C)	2-4 hours	• Decarboxylation is initial step in PS oxidation • Oxygen plays important role
(Fang et al. 2019)	OSPW: 40.8 mg/L	0.5, 2, 4 mM	UV	40 min	• 59, 84, 92% removal O2-NAs for 0.5, 2 and 4 mM PS • Higher carbon and z numbers have higher reactivity
(Fang et al. 2020)	OSPW: 40.8 mg/L	0.5, 2, 4 mM	UV	40 min	• 81-94% removal classical NAs • Toxicity reduced from 31% to 2% • Formed chlorinated byproducts
(Ganiyu et al. 2022a)	Model NA (PVA): 50 mg/L OSPW: 35.9 mg/L	0.5, 2, 5, 10 mM	Solar	6 hours	• 39-100% PVA removal for 0.5-10mM PS • 96-99% OSPW NA removal for 5-10 mM PS

CHCA: cyclohexane carboxylic acid; CHBA: cyclohexanebutyric acid; 2-NA: 2-napthoic acid; 1234-T-2: 1,2,3,4-tetrahydro-2-napthoix acid; PVA:5-phenylvaleric acid; CHPA: cyclohexanepentanoic acid; HPA: heptanoic acid; ADA: 1-adamantane carboxylic acid; UV: ultraviolet light; ZVI: zero valent iron; PS: persulfate

2.2.5 Coupling Chemical Oxidation and Biodegradation for NAFC Remediation

Chemical oxidation can be used to enhance bioremediation by transforming recalcitrant NAFCs into more bioavailable compounds for the microbes to degrade into non-toxic end products, which would otherwise require substantial volumes of chemical oxidation to accomplish. The combined remediation method has higher cleanup efficiency, shorter duration and moderate costs (Michael-Igolima et al. 2022).

There has been significant research into using ozone as a pre-treatment to make NAFCs more bioavailable. Ozone is highly reactive with cyclic and alkyl-branched NAFCs which are considered the most bio-persistent fractions (Martin et al. 2010, Hwang et al. 2013, Wang et al. 2013b, Islam et al. 2014). After ozonation, there is a shift in composition to simpler, lower molecular weight NAFCs that may be more susceptible to biodegradation, as seen by increased BOD/COD ratios (Gamal El-Din et al. 2011, Wang et al. 2013b, Brown and Ulrich 2015, Zhang et al. 2018a, 2018b, Al Jibouri et al. 2018).

For OSPW, most studies that combine oxidation and biodegradation have been applied using various ex situ bioreactor configurations (Huang et al. 2015, Hwang et al. 2013, Islam et al. 2014, Shi et al. 2015, Zhang et al. 2016d, 2018a, 2018b, 2019), or with batch suspended growth microcosm systems (Brown et al. 2013, Dong et al. 2015, Martin et al. 2010, Vaiopoulou et al. 2015, Wang et al. 2013b, Xue et al. 2016a, 2016b). These studies have consistently demonstrated higher biomass in reactors utilizing ozonated-OSPW and improved removals of classical NAs. Martin et al. (2010) found that microbes grew more rapidly in ozonated-OSPW due to the formation of labile intermediated products such as hydroxylated NAFCs and short chains acids. Mineralization was significantly improved in a combined

ozonation-fluidized bed biofilm reactor system, increasing from 33% after ozonation to 62% after combined ozonation-biodegradation (Islam et al. 2014). Furthermore, while ozonation alone often does not significantly improve toxicity of OSPW due to incomplete mineralization (Meshref et al. 2017), combined treatments have shown complete removals in toxicity to *V. fischeri* (Dong et al. 2015, Wang et al. 2013b).

Overall, ozonation coupled with biodegradation appears to provide greater rates and extent of NAFC removal than biodegradation or ozonation alone (Martin et al. 2010, Brown et al. 2013, Hwang et al. 2013, Wang et al. 2013b). The main concern when developing a coupling treatment is how the chemical oxidant will impact the microbial population, which can occur through oxidative stress, changes in pH and changes in redox conditions (Sutton et al. 2011). To-date, most studies on coupling oxidation and biodegradation apply pre-ozonated OSPW to an ex situ bioreactor with an active microbial population, or will inoculate a batch system with unstressed indigenous microbes after ozonation. While this could simulate ozonated-OSPW entering a tailings pond with an established microbial community, it is also important to understand how native communities are affected during ozonation, for which there has only been one study. Brown et al. (2013) utilized a coupled system and found that indigenous OSPW microbes were not eliminated after ozonation and could re-establish. In addition, the microbes exposed to ozone could perform as well as those not exposed. Ozonation improved biodegradability of organic fraction of aged OPSW by 20% over 12 weeks incubation, however microbial degradation stagnated after 35 days. As ozone is an expensive, aggressive and short-lived oxidant, the coupled treatment may be improved by exploring other oxidants.

Persulfate oxidation has been successfully coupled with bioremediation for various petroleum contaminants (Bumbac and Diacu 2012, Mora et al. 2014, Bajagain et al. 2018, Liao

et al. 2018, Medina et al. 2018, Gou et al. 2020b, 2020a, Xia et al. 2020). Furthermore, many studies have suggested it may be more effective than other oxidants in coupled systems and has less impact on microbial populations. Cassidy et al. (2009) compared coupling ozone, Fenton's reagent, and iron activated persulfate with indigenous soil microbes for dinitrotoluene (DNT) removal. While activated persulfate less effectively oxidized DNT, overall remediation occurred within 14 days, as opposed to 30-90 days for Fenton's reagent and ozonation. Persulfate showed a minimal impact on microbial numbers and time for rebound, suggesting that using a less aggressive oxidant minimizes microbial stress and thus enhances overall remediation. Permanganate is another common oxidant combined with biodegradation for in situ treatment of hydrocarbon contaminated soils. There have been limited studies to-date on permanganate use for OSPW NAFC remediation, however results suggest that persulfate leads to more mineralization of NAFCs than permanganate (Sohrabi et al. 2013). Conversely, iron activated persulfate oxidation alone was less effective than permanganate and Fenton's reagent for PAH removal, but the coupled persulfate-biodegradation treatment gave the highest overall removal efficiency and increase in microbial plate counts following oxidation (Liao et al. 2018, 2019). Heat activated persulfate was found to be less damaging to indigenous soil microbes when compared with Fenton's reagent, hydrogen peroxide and permanganate (Tsitonaki et al. 2008). Persulfate concentrations ≤10g/L did not impact cell density but hindered acetate consumption at 10g/L, indicating membrane integrity does not always relate to metabolic activity.

The studies above suggest that persulfate is less damaging to microbial populations than other commonly used oxidants; however, the impact depends on site specific factors, oxidant dose and activation conditions (Kakosová et al. 2017). Higher doses of persulfate

(>10g/L) lead to more effective short-term removal from the oxidant but have been shown to hinder biological activity, leading to 1-3 order magnitude decreases in bacterial abundance, largely due to oxidative stress and decrease in pH (Gou et al. 2020b, Mora et al. 2014, Richardson et al. 2011, Sutton et al. 2015). While microbial abundance is often restored to initial levels after oxidation, there can be considerable lag phases ranging from 30 to 200 days (Chen et al. 2016, Medina et al. 2018, Richardson et al. 2011, Sutton et al. 2015). As discussed above, more aggressive oxidation does not improve overall removal efficiency in a treatment coupled with biodegradation and therefore lower oxidant doses are recommended. Using lower persulfate doses can have a biostimulatory effect and shorten lag phases without negative impacts on soil properties (Mora et al. 2014, Sutton et al. 2015). For example, Xu et al. (2019a) found that 2.7-5.4 g/L persulfate promoted microbial viability and facilitated the occurrence of more PAH degrading microbes. Further increasing the persulfate dose made the coupled treatment system ineffective and only the oxidant removed PAHs.

Persulfate is not as well studied for oxidation of NAFCs and only two studies have looked at coupling it with biodegradation. Balaberda and Ulrich (2021) utilized unactivated persulfate coupled to biodegradation for commercial Merichem NAs with results presented in Chapter 3 of this thesis. Ganiyu et al. (2022a) examined two sulfate radical based AOPs, persulfate and peroxymonosulfate, and found that biofiltration following oxidation led to 60% dissolved organic carbon (DOC) and 40% COD reduction, which is a greater extent of mineralization than most studies in coupled ozone-biodegradation systems. Persulfate is emerging as a promising oxidant for NAFC remediation that may be less harmful than ozone to microbial populations, making it an ideal choice in a combined oxidation-biodegradation treatment. Utilizing lower doses of less aggressive oxidants can lead to more efficient overall

remediation of contaminants, as seen in studies with other petroleum contaminants. The potential for coupling persulfate oxidation with biodegradation for NAFC remediation is an area that requires more research.

2.3 Benzene Contamination at Petroleum Sites

Benzene is a natural constituent of crude oil and gasoline. Accidental spills and releases, particularly from underground storage tanks, make benzene a widespread contaminant at petroleum sites (Paustenbach et al. 1993, Lovley 2000). However, benzene contamination can occur anywhere during the production, transport and use of crude oil, gasoline and isolated benzene (Health Canada 2009). Benzene is classified as a Group 1 carcinogen, with blood forming organs exhibiting the most sensitivity, potentially leading to leukemia after long-term exposure. Acute benzene exposure affects the central nervous system, causing drowsiness, dizziness, headaches, tremors, confusion, and unconsciousness at lower levels, and death at high levels (Health Canada 2009).

This section provides a literature review of benzene contamination as it relates to downstream petroleum sites. The properties of benzene and its fate and transport in the subsurface will be reviewed, along with commonly used remediation strategies. Anaerobic benzene biodegradation and the impact of salt co-contamination will be explored in depth.

2.3.1 Benzene Properties, Fate and Transport

Benzene is one of the simplest aromatic hydrocarbons with the molecular formula C_6H_6, with the 6 carbon atoms arranged in a hexagon as a stable ring without any side chains (Health Canada 2009). The physical and chemical properties of benzene that impact its fate and transport through the environment are listed in Table 2.4 below.

Table 2-4: Physical and Chemical Properties of Benzene at 25ºC. Data taken from: ATSDR 2007. "BCF" bioconcentration factor.

Parameter	Value	Units
Molecular Weight	78.11	g/mol
Density	0.88	g/cm^3
Water Solubility	1.8	g/L
Vapour Pressure	12.7	kPA
Henry's Law Constant	0.23	unitless
	5.5×10^{-3}	$amt\bullet m^3/mol$
log K_{ow}	2.13-2.15	unitless
log K_{oc}	1.78-1.92	unitless
BCF	4.27	unitless

When benzene enters the environment, it will preferentially distribute to the atmosphere as it is highly volatile ($H > 10^{-3}$ $atm\bullet m^3/mol$) (Katyal and Morrison 2007). Issues of benzene persistence arise when benzene is released deeper underground (e.g., from leaking underground storage tanks) where volatilization to the atmosphere is not possible. Benzene is considered mobile, with little sorption to soil particles occurring, as can be seen by the low soil adsorption coefficient (log $K_{oc} < 2$) (McCall et al. 1980). Therefore, while some residual benzene may be left in soil pores, the bulk will continue to flow downward through the unsaturated subsurface via gravity. Benzene is relatively soluble in water, so once it reaches the groundwater the contamination is easily spread via advection and dispersion. Alternatively, if benzene encounters an impermeable layer, the bulk mass can pool as a light non-aqueous phase liquid (LNAP) as it is slightly lighter than water (density < 1 g/cm^3). The low bioconcentration factor (BCF < 1000) and octanol-water partition coefficient (log $K_{ow} < 4$) of benzene indicates that it will not bioaccumulate in fatty tissue of organisms (Paustenbach et al.

1993, CCME 1999). Overall, benzene is a problematic contaminant at petroleum impacted sites due to its carcinogenicity and highly mobile nature in the subsurface.

2.3.2. Benzene Remediation Options

A variety of in situ and ex situ remediation technologies exist for aromatic hydrocarbons such as benzene. Common remediation methods utilized include pump-and-treat, excavation/removal (dig-and-dump), soil vapour extraction (SVE), in situ chemical oxidation, monitored natural attenuation and in situ bioremediation (U.S. EPA 2018). The choice of remediation technology depends on several factors such as the depth and extent of the contamination, soil permeability and heterogeneity, along with financial constraints (FRTR 2023).

Ex situ methods such as physical excavation of contaminated soil and pump-and-treat for contaminated groundwater are the most traditional remediation techniques. Contaminated soil that is excavated and removed from the site can be treated by incineration or stored in landfills. Excavation is easily implemented for more shallow spills; however, is very disruptive to the site and involves health risks from removing contaminated material (Sutton et al. 2011). Contaminated water that is pumped out can be treated with activated carbon which would require periodic replacement and disposal as it becomes saturated. Pump-and-treat is simple to implement but is higher cost than other methods (FRTR 2023). Since these ex situ methods are often expensive, energy intensive and intrusive, there has been a transition towards utilizing in situ remediation methods (Sutton et al. 2011). In particular, in situ methods are preferred for deeper or more widespread contamination, along with sites below existing infrastructure, where contamination is more difficult to treat (Toth et al. 2021).

SVE is a common remediation method for benzene contamination in the unsaturated vadose zone. In this technique, a vacuum is applied to create a controlled flow of air and induce the transfer of benzene to the airstream, which is collected and treated above ground (FRTR 2023). SVE is very effective for volatile contaminants but only works for non-saturated soils with high permeability; additional disadvantages are that SVE has a diminished rate of contaminant removal over time and the high energy requirements can be economically prohibitive (Aparicio et al. 2022, FRTR 2023). In situ chemical oxidation (ISCO) is an effective choice for benzene contamination since oxidants such as hydrogen peroxide, ozone and persulfate are very reactive with benzene (FRTR 2023). Chemical oxidation is fast, ideal for high concentrations of contaminants and does not generate a secondary waste stream; however, it can create toxic intermediates and require large volumes of chemicals. Furthermore, despite fast removals initially, chemical oxidation often reaches a point of diminishing return where the amount of oxidant required for complete removal is not viable (Aparicio et al. 2022, FRTR 2023).

In situ bioremediation makes use of the reduction-oxidation (redox) reactions occurring during microbial metabolism. For benzene biodegradation, microorganisms use benzene as an electron donor and commonly used terminal electron acceptors (TEA) include oxygen, iron, nitrate, sulfate, and CO_2 (methanogenic). Depending on site conditions, biodegradation may require biostimulation (addition of nutrients/TEA) or bioaugmentation (addition of specialized microbes). Bioremediation has many advantages over other remediation technologies: it is simple with minimal site disruption, has low installation and operating costs, is effective for low concentrations that SVE and ISCO cannot efficiently treat, can be applied for widespread contamination, and has high public acceptance (Aparicio et al. 2022, Michael-Igolima et al.

2022). While benzene degrades easily aerobically, under anaerobic conditions benzene biodegradation has drawbacks such as long timelines, low predictability, and persistence (Michael-Igolima et al. 2022).

2.3.3 Benzene Biodegradation

Aerobic benzene biodegradation occurs relatively quickly with a half-life ranging between 6 hours and 28 days, and thus is the preferred in situ remediation strategy for contamination in the shallow subsurface (CCME 1999, Lovley 2000). However, oxygen is quickly depleted by aerobic benzene-degrading microorganisms, leading to the development of anaerobic conditions. Anaerobic benzene biodegradation was not thought to be possible until the late 1980s, when Wilson et al. (1986) reported the first disappearance of benzene in methanogenic aquifer materials after a lag period of 20 weeks. To-date, anaerobic benzene biodegradation remains inconsistent and is characterized by considerable lag phases (>100 days) and low degradation rates, with a half life ranging from 28-720 days (CCME 2004, Foght 2008, Vogt et al. 2011).

Due to the persistence of benzene in anaerobic conditions, injecting air into the subsurface (biosparging) to stimulate aerobic biodegradation is sometimes recommended (Michael-Igolima et al. 2022). However, maintaining aerobic conditions can be technically difficult and expensive, particularly for deep, widespread contamination. Furthermore, oxygen may not be distributed equally at heterogenous sites or those with fine textured soils (Aparicio et al. 2022, FRTR 2023). Therefore, utilizing anaerobic bioremediation would be ideal. Researchers now believe that benzene persistence may be due to a low abundance of intrinsic benzene-degrading microbes (Anderson et al. 1998, Luo et al. 2016). Bioaugmentation with a commercially developed benzene-degrading consortium may be useful as it can take a long

time for native microbial communities to reach levels needed to degrade benzene, or they may not be capable.

Laboratory enriched cultures capable of anaerobic benzene biodegradation have been established under various TEAs, such as iron (Lovley et al. 1996, Nales et al. 1998, Weiner and Lovley 1998, Kunapuli et al. 2007, Zhang et al. 2012, Lee and Ulrich 2021), nitrate (Burland and Edwards 1999, Ulrich and Edwards 2003, van der Zaan et al. 2012), sulfate (Edwards and Grbic-Galic 1992, Phelps et al. 1996, 1998, Nales et al. 1998, Caldwell and Suflita 2000, Kleinsteuber et al. 2008, Abu Laban et al. 2009), and carbon dioxide (Grbić-Galić and Vogel 1987, Kazumi et al. 1997, Ulrich and Edwards 2003, Sakai et al. 2009, Noguchi et al. 2014, Lee and Ulrich 2021). The amount of energy released from the oxidation of benzene and potentially available for microbial growth under different electron-accepting conditions is shown below (Table 2-5).

Table 2-5: Stoichiometric equations and standard free energy changes (ΔG°) for benzene oxidation. Modified from Vogt et al. 2011.

Electron Acceptors (oxidized/reduced)	**Stoichiometric Equation**	**ΔG° (kJ/mol)**
O_2 / H_2O	$C_6H_6 + \mathbf{7.5\ O_2} + 3\ H_2O \rightarrow 6\ HCO_3^- + 6H^+$	-3,173
Fe^{3+} / Fe^{2+}	$C_6H_6 + 18\ H_2O + \mathbf{30\ Fe^{3+}} \rightarrow 6\ HCO_3^- + 30\ Fe^{2+} + 36\ H^+$	-3,070
NO_3^- / N_2	$C_6H_6 + \mathbf{6\ NO_3^-} \rightarrow 6\ HCO_3^- + 3\ N_2$	-2,978
NO_3^- / NO_2^-	$C_6H_6 + \mathbf{15\ NO_3^-} + 3\ H_2O \rightarrow 6\ HCO_3^- + 15\ NO_2^- + 6\ H^+$	-2,061
SO_4^{2-} / H_2S	$C_6H_6 + 3\ H_2O + \mathbf{3.75\ SO_4^{2-}} \rightarrow 6\ HCO_3^- + 1.875\ H_2S + 1.875\ HS^- + 0.375\ H^+$	-185
CO_2 / CH_4	$C_6H_6 + 6.75\ H_2O \rightarrow 2.25\ HCO_3^- + 3.75\ CH_4 + 2.25\ H^+$	-116

During biodegradation, the more energetically favorable electron acceptors are quickly depleted, leading to the development of methanogenic conditions in the regions closest to the contaminant source. Methanogenic benzene degrading cultures are of particular interest for bioremediation as the microbes are not limited by an exogenous electron acceptor and there is no need to inject nutrients into the subsurface (Luo et al. 2016). Ulrich and Edwards (2003) studied benzene degrading cultures under nitrate, sulfate and methanogenic conditions, and found that the methanogenic cultures utilized the highest substrate concentration and gave the maximum benzene degradation rates, highlighting the potential for methanogenic application. The slow growth of microorganisms under methanogenic conditions makes it challenging to create large volumes needed for a bioaugmentation culture, and there are currently very few long-term methanogenic enrichment cultures successfully maintained (Luo et al. 2016, Phan et al. 2021).

While some benzene-degrading isolates have been identified for nitrate- and iron-reducing conditions (Coates et al. 2001, Kasai et al. 2006, Dou et al. 2010, Holmes et al. 2011, Zhang et al. 2012), no isolate has been found to degrade benzene under sulfate-reducing or methanogenic conditions. During methanogenesis, benzene is degraded by a microbial consortium, and microbial community structure remains highly complex even after decades long enrichment (Ulrich and Edwards 2003, Noguchi et al. 2014, Luo et al. 2016). Sequencing confirms the abundance of fermentative bacteria, acetoclastic methanogens and hydrogenotrophic methanogens in enrichment cultures (Sakai et al. 2009, Noguchi et al. 2014, Luo et al. 2016).

To-date, microbes identified in benzene-degrading cultures belong to a few clades, primarily in the class *Deltaproteobacteria* (now proposed to be *Desulfobacterota*) (Toth et al.

2021). Luo et al. (2016) examined 16 methanogenic benzene-degrading enrichment cultures from soils at an oil refinery and former gas station. The authors found that an operational taxonomic unit (OTU) from *Deltaproteobacteria*, *Deltaproteobacteria* candidate Sva0485 (ORM2), was consistently identified in all the cultures and typically comprised of at least half of the bacterial sequence. Subsequent microcosm studies verified that ORM2 abundance increased only when benzene was present. Similarly, a research group in Japan identified a putative benzene-degrader in enriched methanogenic cultures (Hasda-A) that has a nearly identical 16S rRNA sequence to ORM2 (Sakai et al. 2009, Masumoto et al. 2012, Noguchi et al. 2014, Phan et al. 2021). Qiao et al. (2018) also recently showed field and microcosm evidence that anaerobic benzene bioremediation at a contaminated site in China was attributed to enrichment of *Deltaproteobacteria* Sva0485. This suggests that bioaugmentation with enrichment cultures that have a high abundance of Sva0485 shows promise as a bioremediation strategy. Toth et al. (2021) demonstrated that inoculating PHC contaminated aquifer materials with 2.5% of an enriched methanogenic consortium containing ORM2 led to benzene biodegradation in only 34 days. Conversely, natural attenuation and sulfate biostimulation did not degrade any benzene after 1-2 years of incubation.

Methanogenic benzene biodegradation is most likely initiated by fermentative bacteria (eg. ORM2) that convert benzene to benzoyl-CoA, which is eventually transformed to hydrogen, formate and acetate to be mineralized by methanogenic archaea (Toth et al. 2021). However, the lack of a methanogenic benzene degrading isolate makes it difficult to determine the benzene activation mechanism. Benzene is persistent due to the thermodynamic stability of the aromatic ring without any reactive substituents (Foght 2008). The detection of toluene (Ulrich and Edwards 2003), phenol (Caldwell and Suflita 2000), and benzoate (Caldwell and

Suflita 2000, Ulrich et al. 2005) during anaerobic benzene biodegradation has led to three pathways being proposed for benzene activation: methylation, hydroxylation and carboxylation.

2.3.4 Impact of Salt on Benzene Biodegradation

High salinity at a contaminated site can complicate biological remediation methods as salt is acutely toxic to microorganisms at high concentrations; however, even at lower concentrations salt can lower microbial activity due to osmotic stress (Yan et al. 2015). Cells act under positive turgor pressure, and the maintenance of this outward-directed pressure is essential as the driving force for cell division and growth. Therefore, for proper cell function, the osmotic pressure of the cytoplasm must exceed that of the outside medium (Martin et al. 1999, Gunde-Cimerman et al. 2018). High concentrations of soluble salts in the medium will increase the osmotic potential, drawing water out of the cell, resulting in dehydration and cell lysis (Singh 2016, Yan et al. 2015). Salts can also influence the properties of the contaminant by acting as a stressor that increases contaminant toxicity and by decreasing contaminant solubility, making it less accessible for microbes (Nicholson and Fathepure 2005, Yan et al. 2015). Lozupone and Knight (2007) found that salt was a greater factor in shaping microbial communities compared to temperature or pH. These microbial community changes occur as different microorganisms have different tolerances toward osmotic stress (de Souza Silva and Fay 2012). Depending on their salt tolerance, microbes can be classified as non-halophiles (<1% NaCl), slightly halophilic (1-3% NaCl), moderately halophilic (3-15% NaCl) and extremely halophilic (15-32% NaCl) (Fathepure 2014, Ahmadi et al. 2017).

There are two approaches that microbes use to cope with osmotic stress from high salinity: the salt-in strategy and the compatible solute strategy. The salt-in strategy achieves

osmotic balance between the high salt medium and the cell by accumulating high concentrations of salts (normally KCl) in the cytoplasm (Oren 2002, Gunde-Cimerman et al. 2018). In this strategy, intracellular enzymes have adapted to high levels of internal salts, making the metabolic and regulatory cell functions extremely halotolerant. These cells may require high levels of salt for their growth and thus are less flexible to changing salt concentrations in the environment. This method is mainly used by aerobic halophilic bacteria and archaea that thrive when salinity levels are >20% (Oren 2002).

The second method, known as the compatible solute or low salt-in strategy, is where microbes avoid the high concentrations of salts in the medium from reaching the cytoplasm. Unlike the salt-in strategy, cellular enzymes are not adapted to the presence of high salt and microbes protect the cell using organic solutes that are either synthesized by the cell or accumulated from the medium (Oren 2002). These solutes accumulate at intracellular regions and enhance the production of EPS, thus forming a protective layer (Hu et al. 2020). This strategy is more flexible and can be rapidly adjusted based on external salt concentrations. However, the synthesis of compatible solutes is energetically expensive which reduces the energy available for microbial growth and activity (Gunde-Cimerman et al. 2018, Hoehler et al. 2010, Yan et al. 2015). This method is widely used by halotolerant bacteria and methanogenic archaea (Oren 2002).

Anthropogenic salinity sources have been found to cause a more drastic impact to microorganisms than natural salinity sources (de Souza Silva and Fay 2012). In Alberta, salt affected soils are becoming more widespread due to increasing oil and gas sites and related produced water spills (AENV 2001). While both sodium chloride (NaCl) and sodium sulfate (Na_2SO_4) are common salts in Alberta, chloride is more toxic and abundant in produced waters

(AENV 2001, Rath et al. 2016). Saline water is commonly described in terms of the concentration of total dissolved salts (TDS; most commonly NaCl) or the electrical conductivity (EC, dS/m). Freshwater is defined as having less than 1000 mg/L of dissolved salts, while seawater is 35,000 mg/L TDS (AENV 2001). Brackish water refers to salt concentrations between freshwater and seawater, while brine water is when the salinity is higher than that of seawater. In Alberta, groundwater with > 4000 mg/L of dissolved salts or soil with EC > 2 dS/m is classified as saline (Water Act, RSA 2000, c W-3; AENV 2001). Table 2-6 lists common salt concentrations in Alberta from both natural and anthropogenic sources.

Table 2-6: Salinity concentrations relevant to Alberta (data from AENV 2001 unless otherwise stated).

	Sample Type	**EC** (dS/m)	**Na^+** (mg/kg soil; mg/L water)	**Cl^-** (mg/kg soil; mg/L water)	**SO_4^{2-}** (mg/kg soil; mg/L water)
Soils	Non-Saline Soils	0.5	6	6	0.3
	Solonetzic Soils (Csk horizon)	7.2	161	0.1	1,537
	Solonetzic Soils (Bnt horizon)	1.9	185	trace	432
	Solonetzic Soils (Bntks horizon)	7.8	1,425	71	3,459
	Brine Contaminated Soils	25.3	2,580	4,270	10
Water	River Water	<1	7	8	31
	Seawater	30-60**	10,800	19,500	2,700
	Alberta Basin Formation Water	N/A	390 - 100,800	305 - 199,510	1 - 6,444
	Western Canadian Basin Formation Water	N/A	14,340	26,920	350
	Viking Formation - Swan Hills	19.6	15,000	24,800	150
	Gilwood Formation – Swan Hills	N/A	62,800	132,000	500
	Oil Battery Brine Water	187	47,250	125,000	<3
	Oil Sands Process Affected Water*	1-4	381 - 950	44 - 57	85 - 536

** (Mahaffey and Dube 2016)* ***(Zheng et al. 2018)* *N/A: Not available*

Halophilic microorganisms isolated from hypersaline environments that are capable of hydrocarbon degradation have been well-studied (Riis et al. 2003, Kleinsteuber et al. 2006, Abed et al. 2006, Minai-Tehrani et al. 2009, Bonfá et al. 2011, Liang et al. 2014, Shetaia et al. 2016). For benzene contamination, aerobic halophilic benzene-degrading microorganisms such as *Marinobacter* spp. have been isolated from saline environments including brine soils near an oil production facility (Nicholson and Fathepure 2004), Utah's Great Salt Lake region (Nicholson and Fathepure 2005, Sei and Fathepure 2009), seawater near a petroleum refinery (Berlendis et al. 2010), oil contaminated harbour sediments (Lee and Lin 2006), a saline lake in Egypt (Hassan et al. 2012), and hypersaline coastal regions (Al-Mailem et al. 2013). Under anaerobic sulfate-reducing conditions, benzene-degrading cultures have been identified from marine sediments (Lovley et al. 1995, Coates et al. 1996, Phelps et al. 1996) and salt marsh sediment (Yu et al. 2012).

Bioaugmentation with halophilic hydrocarbon-degrading microorganisms isolated from hypersaline environments is one proposed remediation strategy for petroleum sites with salt co-contamination (Fathepure 2014, Khoshkholgh Sima et al. 2019). A potential drawback to this strategy is that these microbes may be less flexible to varying levels of salinity at contaminated sites depending on how they adapt to salt stress. Furthermore, benzene is already difficult to degrade anaerobically, particularly in methanogenic conditions, and finding specialized microbes that can do so in high salinity is a challenge (Fathepure 2014). Therefore, understanding the impact of produced water spills on microorganisms from naturally non-saline environments is important. Currently, there are limited studies examining the impacts of salt co-contamination on hydrocarbon degradation in naturally non-saline environments, and even less so under anaerobic conditions, summarized in Table 2-7.

Table 2-7: Summary of studies on impact of salinity for hydrocarbon biodegradation in naturally non-saline environments.

Reference	Contaminant	Microbial Source	Aerobic/ Anaerobic	Salt Concentration	Degradation Results
(Rhykerd et al. 1995)	Motor oil	Uncontaminated soil	Aerobic	0, 0.4, 1.2, 2 % w/w NaCl	• Inhibited mineralization by 10% (0.4% NaCl) to 44% (2% NaCl)
(Amatya et al. 2002)	Flare pit hydrocarbons	PHC contaminated soil	Aerobic	0, 20, 40 dS/m	• 8% less oil and grease reduction in soil treatments with EC 40 dS/m
(De Carvalho and Da Fonseca 2005)	Methanol, ethanol, n-Hexane, Iso-octane, n-Octane	Rhodococcus erythropolis DCL14 (isolated from uncontaminated sediment)	Aerobic	1, 2, 2.5% w/v NaCl	• Increased lag phases from 50 - 200 hrs with 1 - 2.5% NaCl • Cell size decreased 30% at 2.5% NaCl
(Lee and Liu 2006)	Toluene and trichloroethane (TCE)	Uncontaminated sediments with freshwater or saline water	Aerobic	0, 2, 3.5 % w/v NaCl	• Toluene removal time increased from 2 hrs to 13 hrs at 3.5% NaCl • Long term salt exposure caused loss of TCE degradation ability
(Lee and Lin 2006)	***Benzene***, toluene, xylene	Oil contaminated sediment	Aerobic	0.1, 1, 2, 3, 4, 5 % w/v NaCl	• Benzene removal time increased from 21 hrs to 30-40 hrs at 2% NaCl • Incomplete benzene removal in 120 hrs at 4% NaCl
(Børresen and Rike 2007)	Hexadecane	PHC contaminated arctic soils	Aerobic	0, 0.02, 0.04, 0.08, 0.17, 0.25, 0.42% w/w NaCl	• Increased initial lag phase, but similar final degradation extent • Low levels (<0.3% w/w) slightly stimulated rates
(Ulrich et al. 2009)	Hexadecane, phenanthrene, decane, toluene	PHC contaminated soils	Aerobic	0, 0.5, 1.0, 2.5, 5% w/v NaCl	• Increased lag time and decreased degradation rates with increasing salinity • NaCl < 1% slightly stimulated mineralization for phenanthrene

Table 2-7 (cont'd): Summary of studies on impact of salinity for hydrocarbon biodegradation in naturally non-saline environments.

Reference	Contaminant	Microbial Source	Aerobic/ Anaerobic	Salt Concentration	Degradation Results
(Hua and Wang 2014)	Crude oil	Pseudomonas sp. DG17 (isolated from PHC contaminated soil)	Aerobic	0.5, 1, 2, 3, 5 % w/v NaCl	• Removal increased 45-55% when salinity increased from 0.5-1% NaCl • Removal deceased to <30-10% for 2-5% NaCl
(Chang et al. 2017)	Diesel fuel, hexadecane	Dietzia maris (isolated from PHC contaminated sub-arctic soil)	Aerobic	0, 2.5, 5, 7.5, 10, 12.5 % NaCl	• Cold tolerant bacteria can exhibit dual tolerance to salinity: best growth was achieved at 2.5 – 10% NaCl • Growth was slightly hindered at 0 and 12.5 % NaCl
(Feizi et al. 2020)	Phenanthrene	Bacillus kochii AHV-KH14 (isolated from compost)	Aerobic	0.5, 1, 1.5, 2 % w/v NaCl	• Similar removals (63-65%) up to 1.5% NaCl • Decreased removal to 32% at 2% NaCl
(Hu et al. 2020)	Diesel oil	Rhodococcus sp. HX-2 (isolated from an oil field)	Aerobic	0, 1, 2, 3, 4, 5, 6, 7, 8, 9, 10 % w/v NaCl	• Similar removals (>80%) up to 2% NaCl • Decreased removal (<50-10%) at 6-10% NaCl
(Akbari et al. 2021)	Hexadecane	Weathered PHC contaminated soils	Aerobic	0, 2.5, 5 % w/v NaCl	• Without nutrients, salinity improved mineralization from 19-44% with 0-5% NaCl • With nutrients, salinity decreased mineralization from 53-37 % at 0-5% NaCl

Table 2-7 (cont'd): Summary of studies on impact of salinity for hydrocarbon biodegradation in naturally non-saline environments.

Reference	Contaminant	Microbial Source	Aerobic/ Anaerobic	Salt Concentration	Degradation Results
(Zhang et al. 2021)	n-decane, n-dodecane, n-hexadecane	Enriched culture from crude oil contaminated soil	Aerobic	0.5, 1, 2, 3 % w/v NaCl	• Salinity up to 2% NaCl inhibited overall bacteria growth but similar degradation extent • No growth or degradation at 3% NaCl
(Li et al. 2022)	Phenanthrene, pyrene	Crude oil contaminated soil	Aerobic	0, 1, 3 % w/v NaCl	• Removal increased from 65-82% with 0-1% NaCl • Removal decreased to 40% at 3% NaCl
(Chen et al. 2022a)	***Benzene***, toluene, ethylbenzene, xylene	BTEX/salt co-contaminated oil field	***Anaerobic*** and Aerobic (6 well sites)	0.08 - 3.7 g/L Cl^-	• Archaea was more susceptible to elevated BTEX and salinity • Produced water enriched salt-tolerant microbes
(Jiang et al. 2023)	Toluene	PHC contaminated soil	***Anaerobic***	0.1, 1, 2 % w/v NaCl	• Removal decreased with salinity, from 100, 60 and 25% at 0.1, 1, and 2 % NaCl

"PHC": Petroleum hydrocarbon; "BTEX": Benzene, toluene, ethylbenzene, xylenes.

Overall, microcosm studies have shown increased lag times and decreased hydrocarbon degradation when salt is applied to microorganisms sourced from non-saline environments (Amatya et al. 2002, Børresen and Rike 2007, De Carvalho and Da Fonseca 2005, Ulrich et al. 2009). In general, some salt is helpful as it provides a more ionically balanced medium, while zero salinity can destabilize intracellular pressure and cause cell lysis (Martin et al. 1999, Ulrich et al. 2009, Imron et al. 2020). Increasing NaCl concentrations up to 1% (10 g/L) stimulated aerobic mineralization of hexadecane, phenanthrene, pyrene and crude oil, while further increasing NaCl led to decreased rates of degradation (Ulrich et al. 2009, Hua and Wang 2014, Li et al. 2022). Rhykerd et al. (1995) found that the addition of 0.4% and 2% NaCl inhibited aerobic biodegradation of motor oil by 10% and 44%, respectively, compared to microcosms without additional NaCl. Similarly, an anaerobic toluene degrading consortia using humin as a TEA showed a decrease in toluene removals from 100% to 60% and 25% when salt was increased from 0.1% to 1% and 2.5% NaCl, respectively (Jiang et al. 2023).

The impact of salt on a microbial consortium will vary depending on which hydrocarbon is added as a substrate (Ulrich et al. 2009, Zhang et al. 2021). For example, degradation of n-decane and n-dodecane were not impacted at salt levels up to 2% NaCl, while n-hexadecane degradation was improved with salinity (Zhang et al. 2021). However, despite the improved degradation there was a significant decrease in optical density, indicating hindered microbial growth. Akbari et al. (2021) found that aerobic mineralization of hexadecane was enhanced by salinity in the absence of nutrients. The authors noted a 5.2× decrease in overall microbial population size, but a 4.8× increase of halotolerant hydrocarbon degrading bacteria. However, in the presence of nutrients salinity decreased the extent of mineralization (Akbari et al. 2021).

To-date, few studies have examined the impact of salt on benzene biodegradation. Aerobic benzene biodegradation in water samples taken from Utah's Great Salt Lake varied from 100% removal when salt levels were 16% but was reduced to 60% removal in areas of the lake containing 34% salt (Prince and Prince 2022). Similarly, a trickle bed bioreactor was no longer able to fully degrade benzene after the addition of 4% NaCl (Lee and Lin 2006). Currently, most studies have looked at the impact of salt on aerobic biodegradation (Table 2-7). However, anaerobic conditions can quickly develop at sites with subsurface petroleum contamination, as discussed earlier. Salt itself can also cause anaerobic conditions to develop as it affects the structure of the soil and reduces soil pore oxygen levels (Khoshkholgh Sima et al. 2019). Therefore, it is vital to understand how anaerobic microbial communities are impacted by salt. Anaerobic benzene degradation was found to be inversely related to sediment salinity with freshwater sediments (0.17 g/L Cl) providing the highest degradation rates compared to brackish (4.5 g/L Cl) and saltwater (7.9 g/L Cl) sediments (Tao and Yu 2013). This suggests that degradation by anaerobic microbes is negatively impacted by increasing salinity, similar to the trends noted for aerobic studies above. Under salt stress, non-halophilic microorganisms need to redirect energy for cell growth towards stress adaptation. Therefore, the impact of salt may be more notable for anaerobes, particularly methanogens, which already have less energy available for their growth compared to aerobic microbes. For example, Chen et al. (2022a) found that methanogenic archaea were the most susceptible to elevated levels of salinity at a BTEX and salt co-contaminated oil field site.

The mobility, persistence and carcinogenicity of benzene make it a primary contaminant of concern for the petroleum industry. Anaerobic bioremediation of benzene is emerging as a promising, cost-effective remediation method for the many petroleum impacted

sites in Alberta. Salt co-contamination due to the release of produced water at these sites complicates remediation efforts. While the impact of salt on aerobic biodegradation of hydrocarbons has been explored, there are limited studies for anaerobic biodegradation of hydrocarbons, highlighting a critical research need.

Effective and economical remediation methods are required to manage the petroleum industry in an environmentally sustainable manner and restore the land to a usable state. In situ bioremediation is advantageous as it is less intrusive and often lower cost than other commonly used remediation methods, however issues can arise that hinder large-scale implementation. For upstream bitumen extraction in the oil sands, acutely toxic NAFCs have a recalcitrant portion that persists over decades and will likely require a combination of remediation techniques, however still requires research development and validation. For downstream petroleum facilities, the impact of salt co-contamination on persistent contaminants such as benzene in anaerobic environments is unknown. This research aimed to address these key knowledge gaps for NAFCs and benzene, two contaminants of concern in the Canadian petroleum industry.

Chapter 3

Persulfate Oxidation Coupled with Biodegradation by *Pseudomonas fluorescens* Enhances Merichem Naphthenic Acid Remediation and Toxicity Reduction

3.1 Introduction

The extraction of surface mined bitumen produces large volumes of OSPW containing acutely toxic NAFCs, which operate under a zero-discharge policy and are stored in tailings ponds (Allen 2008a, Brown and Ulrich 2015, Finkel 2018, Morandi et al. 2017, Scott et al. 2005). With the large footprint currently required to store tailings and concerns of subsurface contamination, effective water management and remediation methods is an ever-increasing concern. Chemical oxidation and biodegradation have been extensively reviewed for NAFC remediation (Ganiyu et al. 2022b, Whitby 2010, Xu et al. 2017, Xue et al. 2018). However, the cost needed for oxidants to mineralize NAFCs can become prohibitive (Brown and Ulrich 2015), and a portion of NAFCs are resistant to biodegradation by indigenous tailings microorganisms (Foght et al. 2017, Quagraine et al. 2005a, Scott et al. 2005). Therefore, a combined treatment may be more effective, where chemical oxidant is used to breakdown recalcitrant NAFCs into more bioavailable compounds for microorganisms to further degrade.

Ozone is highly reactive with the most bio-persistent NAFCs, such as those with higher cyclicity, and therefore has been studied as a pre-treatment for biodegradation (Hwang et al. 2013, Islam et al. 2014, Martin et al. 2010, Wang et al. 2013b). The use of lower doses of less aggressive oxidants has been shown to improve remediation for creosote (Valderrama et al. 2009), jet fuel hydrocarbons (Xie and Barcelona 2003), dinitrotoluene (DNT) (Cassidy et al. 2009) and diesel (Jung et al. 2005). As ozone is an expensive and aggressive oxidant, the coupled treatments for OSPW may be improved by exploring alternative oxidants, such as persulfate, which may be less harmful towards soil microbes than ozone (Cassidy et al., 2009). Persulfate oxidation has been coupled with bioremediation for petroleum contaminants such as total petroleum hydrocarbons (TPHs) in diesel (Bajagain et al. 2018, Chen et al. 2016, Sutton

et al. 2014a, 2014b), PAHs (Mora et al. 2014, Xu et al. 2016a, Medina et al. 2018, Liao et al. 2019), and BTEX (Xiong et al. 2012, Shayan et al. 2018, Bartlett et al. 2019). Persulfate oxidation has demonstrated >90% removals for OSPW NAFCs and model NAs using activation methods such as UV (Liang et al. 2011, Fang et al. 2018, 2019, 2020), heat (Xu et al., 2016b, 2018b, 2019b), and iron (Drzewicz et al. 2012, Aher et al. 2017). In addition, activated persulfate was more effective than hydrogen peroxide and chlorine commercial NAs and OSPW NAFCs (Liang et al. 2011, Fang et al. 2020). Some studies have suggested that unactivated persulfate is not reactive with NAFCs (Liang et al. 2011, Fang et al. 2018). However, the short time frame of these studies (minutes-hours) would be insufficient for an unactivated persulfate reaction, which requires anywhere from days to months (Drzewicz et al. 2012, Sohrabi et al. 2013). Despite the longer timeframes involved, unactivated persulfate has the advantage of being more economical, having fewer scavenging reactions and being less harmful to microbial populations. Furthermore, longer timelines are ideal for oil sands in situ applications such as end pit lakes and groundwater systems.

To date, no studies have examined the potential for coupling unactivated persulfate oxidation and biodegradation for NA removal and toxicity reduction, and thus was a primary focus for this research project. The objectives of this study were to: **1)** compare persulfate oxidation alone with persulfate oxidation coupled to biodegradation for Merichem NA, COD and toxicity reduction; **2)** investigate the performance of unactivated (21^{o}C) persulfate compared to heat activated (30^{o}C) persulfate; and **3)** determine the concentration of persulfate that improves biodegradation potential with the least detrimental effect on microbial viability.

3.2 Materials and Methods

3.2.1. Source of NAs and Bacteria

Commercial NAs were gifted from Merichem Chemicals and Refinery Services LLC (Houston, TX). Merichem NAs are known to only have O_2^- species and are the closest match to NAFCs in OSPW (Bartlett et al. 2017) and thus were used to create a controlled system focused on the most toxic NA fraction.

Pseudomonas fluorescens was chosen to study biodegradation potential as it is a well-known hydrocarbon degrader that is native to OSPW and has previously shown potential to degrade NAs (Del Rio et al. 2006, Herman et al. 1994). *P. fluorescens* LP6a was previously obtained from Dr. Julia Foght and had been isolated from an enrichment culture derived from petroleum condensate-contaminated soil and has demonstrated potential to utilize various PAHs as the sole carbon and energy source (Foght and Westlake 1991, 1996). Preliminary unpublished work in our lab verified that *P. fluorescens* LP6a is capable of degrading BTEX compounds and grows in the presence of both Merichem NAs and OSPW NAFCs.

3.2.2. Experimental Setup

Unless otherwise stated, all materials were purchased from Thermo Fisher Scientific (Waltham, MA). Microcosms were created using 1L Fisherbrand™ glass media bottles, filled aseptically with 500 mL of Bushnell Haas (BH) media (per L: 1 g K_2HPO_4; 1 g KH_2PO_4; 0.2 g $MgSO_4.7H_2O$; 0.02 g $CaCl_2.2H_2O$; 0.05 g $FeCl_3$; 1 g NH_4NO_3, pH adjusted to 8.2), 100 mg/L Merichem NAs, and either 0 (biological treatment), 100, 250, 500, or 1000 mg/L of sodium persulfate (> 98%, Sigma Aldrich). Bottles were shaken at 150 rpm. For the first stage of the experiment, bottles were loosely topped with aluminum foil to prevent bacterial contamination while allowing for the release of carbon dioxide produced from the persulfate reaction.

Unactivated persulfate (PS) refers to conditions where there was no intention activation and was tested at room temperature (21ºC), and heat activated persulfate (APS) was done at 30ºC.

The chemical reaction between Merichem NAs and persulfate was left for approximately 2 months (68 days for unactivated persulfate, 52 days for activated persulfate) to provide time for the persulfate to oxidize NAs into more bioavailable carbon sources before the *P. fluorescens* (CPS, CAPS) was inoculated. *P. fluorescens* was grown in Luria-Bertani (LB) media (per L: 10 g peptone; 5 g yeast extract; 5 g sodium chloride) to exponential phase (optical density, OD ~ 0.9), cells were then washed 3× by centrifuging at 4000 rpm for 4 min, discarding the supernatant and resuspending in phosphate buffer solution. Cells were inoculated into microcosms to an initial starting concentration of approximately $6.0x10^5$ colony forming units (CFU) per mL. The persulfate reaction was not quenched to better mimic in situ conditions and examine any stress effects on the bacteria from the combination of oxidant and contaminant, creating the coupled treatment bottles (100CPS-1000CPS, 500CAPS-1000CAPS; Table 3-1, Figure 3-1). Fisherbrand™ caps, modified with 20 mm blue butyl septa, were added at the same time *as P. fluorescens* to allow for measurement of headspace carbon dioxide ($CO_2(g)$). pH was routinely monitored and adjusted to 8.2 by the addition of 1.5 mL of 1 N NaOH when required.

Negative controls contained only 100 mg/L of Merichem NAs (0NC), biological treatment bottles did not have persulfate added (0CPS, 0CAPS) and chemical treatment bottles were not inoculated with bacteria (100PS-1000PS, 500APS-1000APS) in order to differentiate the chemical and biological contribution in the coupled bottles. No carbon controls (NCC) were created containing 1000 mg/L of persulfate without Merichem NAs to determine the

decomposition of persulfate in the absence of NAs. Treatments containing *P. fluorescens* were set up in triplicate and chemical treatments were set up in duplicate (Table 3-1).

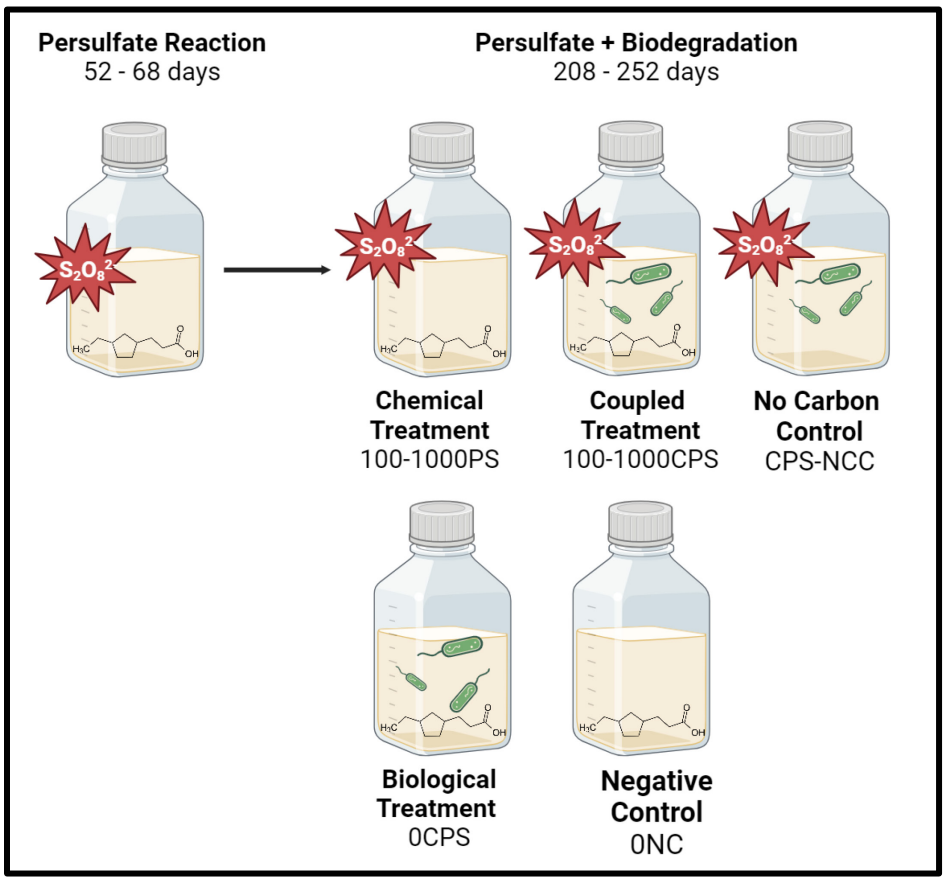

Figure 3-1. Illustration of experimental set-up. Unactivated Persulfate ($S_2O_8^{2-}$) experiments were completed at 21°C and activated experiments were done at 30°C. *P. fluorescens* was inoculated into select treatment bottles after 68 days (unactivated) or 52 days (activated). Created in BioRender.

Table 3-1. Summary of persulfate oxidation and biodegradation experimental bottles. Note: "PS": persulfate concentration, "CPS": coupled treatment bottles, "APS": activated persulfate, "CAPS": coupled activated persulfate treatment bottles, "NCC": no carbon controls, *P. fluorescens* was added after 2 months (*).

Identification Label		Persulfate (mg/L)	*Pseudomonas fluorescens**	Merichem NAs (mg/L)	Temperature (°C)	Replicates
		Unactivated Persulfate				
Negative Control	0NC	0	No	100	21	2
Chemical Treatment	100PS	100	No	100	21	2
	250PS	250	No	100	21	2
	500PS	500	No	100	21	2
	1000PS	1000	No	100	21	2
Biological Treatment	0CPS	0	Yes	100	21	3
Coupled Treatment	100CPS	100	Yes	100	21	3
	250CPS	250	Yes	100	21	3
	500CPS	500	Yes	100	21	3
	1000CPS	1000	Yes	100	21	3
No Carbon Control	1000CPS-NCC	1000	Yes	0	21	3
		Activated Persulfate				
Chemical Treatment	1000APS	1000	No	100	30	3
Biological Treatment	0CAPS	0	Yes	100	30	3
Coupled Treatment	500CAPS	500	Yes	100	30	3
	1000CAPS	1000	Yes	100	30	3
No Carbon Control	1000CAPS-NCC	1000	Yes	0	30	3

3.2.3 Chemical Analyses

Merichem NAs

The persulfate reaction was quenched with excess sodium thiosulfate, filtered with 0.22 µm nylon filters and stored at 4°C until analysis. Merichem NA content in samples was then determined using Fourier transform infrared (FTIR) spectroscopy (Jivraj et al. 1995, Scott et al. 2008, Brown et al. 2013). Briefly, 8mL of filtered samples were acidified to pH 2.0 by

adding concentrated HCl, exchanged three times with approximately 5-6 mL of HPLC grade dichloromethane (DCM), passed through a sodium sulfate column to remove trace water, and then dried overnight. The dried Merichem NAs were then reconstituted in a known amount of DCM and measurement was completed on a Spectrum 100 FTIR (Perkin Elmer, Waltham, MA) using a 3 mm-spaced, potassium bromide window cell (International Crystal, Garfield, NJ). Data was collected with Spectrum software (V10, Perkin Elmer, Waltham, MA) using 32 scans with a spectral resolution of 4 cm^{-1}. Absorbance at 1743 cm^{-1} (for monomers) and 1706 cm^{-1} (for hydrogen-bonded dimers) were summed to calculate total Merichem NAs concentration. Standard solutions were prepared using known concentrations of Merichem NAs (Merichem Chemicals and Refinery Services, Houston, TX) in DCM.

Chemical Oxygen Demand

Chemical oxygen demand (COD) was measured with HACH COD Low Range (LR; limits of 3 - 150 mg/L) digestion solution vials (product 2125815, Fisher Scientific, Fair Lawn, NJ) following method 8000, using a HACH digestor reactor and UV-Vis Hach DR/4000 spectrophotometer (Hach, Loveland, CO). COD was measured immediately after sampling, without filtering or quenching samples as sodium thiosulfate interferes with the COD digestion solution.

Carbon Dioxide

Headspace CO_2(g) was measured with an Agilent 7890A gas chromatograph equipped with a thermal conductivity detector (GC-TCD) (Agilent HP-PLOT/Q column: 30 m x 320 µm x 0.2 µm) using an injection volume of 100 µL. The oven temperature gradient was as follows: 50°C for 2 min, then increased at a rate of 30°C min^{-1} to 150°C which was maintained for 2 min. Helium was used as carrier gas with the following flow program: 8.83 mL min^{-1} for

2 min, decreasing to 5.67 mL min^{-1} until the end of the separation. Total run time was 7.33 min. The detector was maintained at 200°C, and the injection port at 300°C. The makeup gas (helium) was set to 5 mL min^{-1}. The injector split ratio was set to 5:1 (no gas saver), with a column flow of 8.89 mL min^{-1}, split vent flow of 44.4 mL min^{-1}, and a septum purge flow of 58.3 mL min^{-1} under a pressure of 30 pounds per square inch (psi). Standards were created using various concentrations of CO_2 and N_2 gas mixes in Tedlar gas sampling bags.

Persulfate

The persulfate ($S_2O_8^{2-}$) concentration in solution was determined based on a rapid spectrophotometric method developed by Liang et al. (2008b). In this method, 500 µL of sample was added to a 40 mL EPL glass vial containing 0.2 g of $NaHCO_3$, 4 g of KI, and 40 mL of Milli-Q water. The resulting solution was hand shaken and allowed to equilibrate at room temperature for 15 min. The absorbance of 1 mL of solution at 352 nm was then measured on a UV-Vis spectrophotometer (Nano Drop 2000c Spectrophotometer, Thermo Fisher Scientific, Waltham, MA).

3.2.4 Bacterial Enumeration

Viable bacterial cell counts were obtained using the drop plate method (Zelver et al. 1999). A series of 10-fold dilutions were performed to obtain the dilution that would provide 30-300 colonies per plate. 100 µL of each dilution was plated on LB agar plates (per L: 10 g peptone; 5 g yeast extract; 5 g sodium chloride; 12 g agar) in triplicate. Plates were incubated at 28°C for 24 hours before counting.

3.2.5 Microtox Assay

Acute toxicity was measured immediately after sampling (samples were not filtered or quenched) at the beginning and end of the experiment, via a Microtox assay with a Model 500

Analyzer (Modern Water, New Castle, DE) and Microtox Omni 4.3 (Modern Water, New Castle, DE) software. The 81.9% basic toxicity method was employed with four 2:1 dilutions and incubation times of 5 min and 15 min. There was no significant difference between incubation times, therefore only the 5 min data was used to estimate the IC_{50} toxicity, which represents the percent volume of sample required to reduce the bioluminescence of the test specimen (*Vibrio fischeri,* now *Aliivibrio fischeri*) by 50%. Toxicity units (TU) were then derived from IC_{50} ($TU=100/IC_{50}$). Phenol (100 mg/L) and deionized water were used as positive and negative controls, respectively, according to the manufacturer instructions (data not shown).

3.2.6 Statistical Analysis

Welch's t-tests (two independent samples, normal distribution, unequal variance) were performed in Microsoft Excel 2014 to examine the statistical significance of the chemical treatments compared to coupled treatments; while paired t-tests were used to determine significance over time in individual treatments. p values less than 0.05 were used to indicate a statistically significant difference.

3.3 Results and Discussion

To determine the efficacy of coupling persulfate oxidation and biodegradation for commercial Merichem NA remediation, the degradation of organics, including both Merichem NAs and by-products, was first investigated; second, the impact of the coupled treatment system on the bacteria and subsequent toxicity reduction was examined. For each result, the coupled treatment was compared to the chemical and biological treatments, and the effect of temperature and persulfate concentration was studied.

3.3.1 Degradation of Organics

Merichem NA and COD Removal

NAFCs represent a major toxic fraction in OSPW; in particular, the classical O_2^- species are considered main contributors to acute toxicity (Hughes et al. 2017, Morandi et al. 2017). Therefore, the use of commercial NA mixtures such as Merichem NAs, which are comprised solely of O_2^- species, creates a controlled system to study the most toxic fraction directly, while also accounting for the complexity of a mixture of compounds (Miles et al. 2020). Since quantifying classical NAs requires methods with high resolving power, using FTIR spectroscopy to measure the acid extractable NAFCs is commonly done in the oil sands industry (Dong et al. 2015, Ripmeester and Duford 2019). Figure 3-2 displays the results of Merichem NA degradation for the unactivated (21°C) and activated (30°C) persulfate experiments. Chemical oxygen demand is also commonly used to determine the amount of oxidizable organics, including potential by-products without carboxyl groups that are not captured by FTIR (Figure 3-3).

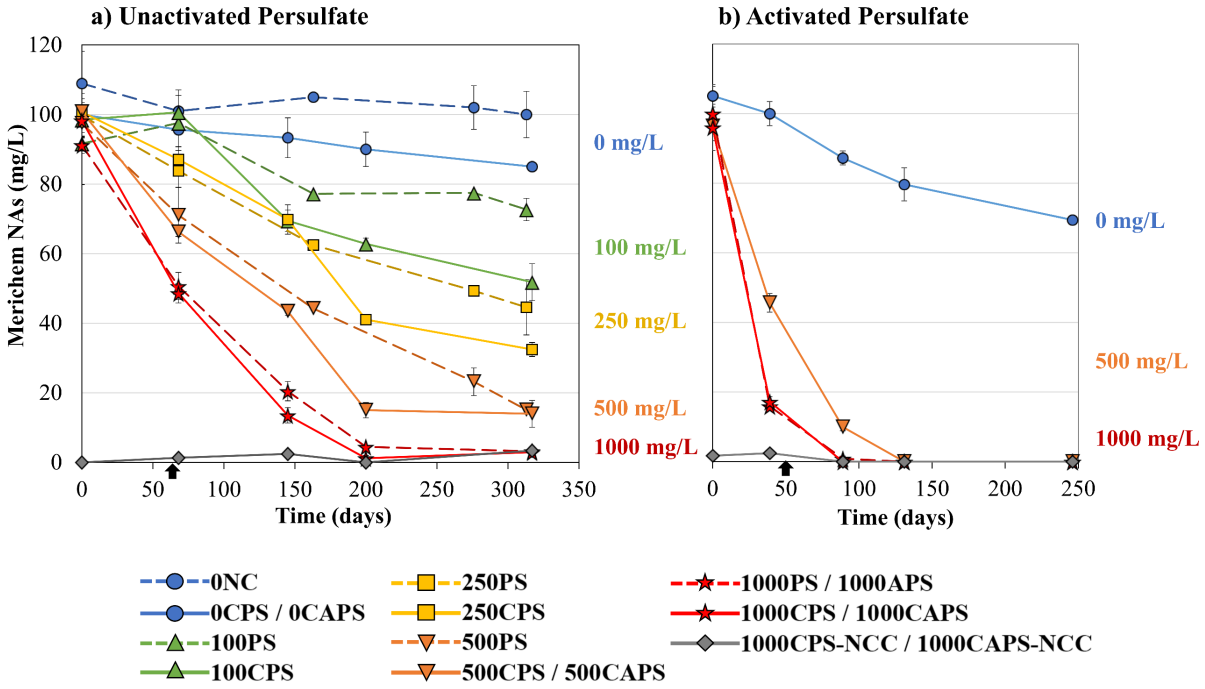

Figure 3-2. Merichem NA concentration for (a) unactivated persulfate bottles at 21ºC, and (b) and activated persulfate bottles at 30ºC. Note: "PS": unactivated persulfate, "CPS": coupled unactivated persulfate with *P. fluorescens*, "APS": activated persulfate, "CAPS": coupled activated persulfate with *P. fluorescens,* "NC": negative controls, "NCC": no carbon controls, *P. fluorescens* was added after 2 months (⬆), dashed lines represent chemical treatments. All data points are an average of duplicate or triplicate bottles. Error bars represent one standard error of the averaged value.

At 21ºC, negative control bottles without persulfate or *P. fluorescens* (0NC) showed no significant Merichem NA or COD removal over the course of the experiment ($p>0.05$; paired t-test), indicating that degradation in experimental bottles occurred only due to persulfate oxidation and/or microbial degradation. Biological treatment bottles were used to demonstrate the capacity of the isolate to biodegrade Merichem NAs, and thus contained *P. fluorescens* without persulfate (0CPS). Results showed that *P. fluorescens* alone at 21ºC removed 15.9% of Merichem NAs by day 313 (Figure 3-2a) and 11.5% of COD by day 310 (Figure 3-3a). Similarly, *P. fluorescens* (LD2) isolated from wetland sediments exposed to OSPW degraded 15% of commercial Kodak NAs, however a mixture of *P. fluorescens* and *P. putida* improved degradation to >95% (Del Rio et al. 2006). Microbial isolates commonly do

not perform as well as a microbial community where synergistic relationships exist among microorganisms (Demeter et al. 2015). In this study, an isolate was used to create a controlled system for proof of concept, and it is important to note that the treatment will likely improve when using an indigenous microbial consortium, which should be investigated in the future. However, microbial degradation in nutrient limited OSPW may be hindered and require biostimulation (Herman et al. 1993, Lai et al. 1996, Kinley et al. 2016). BH media was used in this study to examine the potential of Merichem NAs to act as a carbon source without nitrogen and phosphorous as confounding variables. In addition, Merichem NAs generally contain linear, lower molecular weight compounds with 7-17 carbon atoms (n), which are considered more biodegradable than the complex mixture of NAFCs found in OSPW including higher molecular weight (n=7-28) compounds (Han et al. 2009, Scott et al. 2005). At 30ºC, the bacteria performed significantly better compared to biological treatments at 21ºC ($p<0.05$), removing 33.9% of Merichem NAs over a slightly shorter period of 246 days (0CAPS). This is expected as *P. fluorescens* is a mesophilic microorganism with optimal growth temperatures between 25-30ºC (Moore et al. 2006).

Chemical treatment bottles (PS) were used to determine the capability of persulfate alone to oxidize Merichem NAs. As expected, increasing the concentration of persulfate led to increased Merichem NA removal. For unactivated persulfate (21ºC), Merichem NA removals were 30.2%, 53.9%, 84.5% and 95.1% for 100PS, 250PS, 500PS and 1000PS, respectively, by day 317 (Figure 3-2a). Persulfate concentrations of 250-1000 mg/L exhibited a linear degradation trend; however, microcosms with 100 mg/L exhibited no significant Merichem NA removal in the first 68 days, followed by a large reduction at day 163 and then no further significant removal for the remainder of the experiment ($p>0.05$; paired t-test). Removal of

COD was also found to increase with increasing persulfate concentration, with 4.6%, 23.1%, 29.2%, and 71.9% COD removed for 100PS, 250PS, 500PS and 1000PS, respectively, by day 310 (Figure 3-3a). The incomplete COD removals suggest that the persulfate alone was not completely mineralizing Merichem NAs. In particular, the lower persulfate concentrations tested (100-500 mg/L) showed very little COD removal, despite 30-85% Merichem NAs degradation.

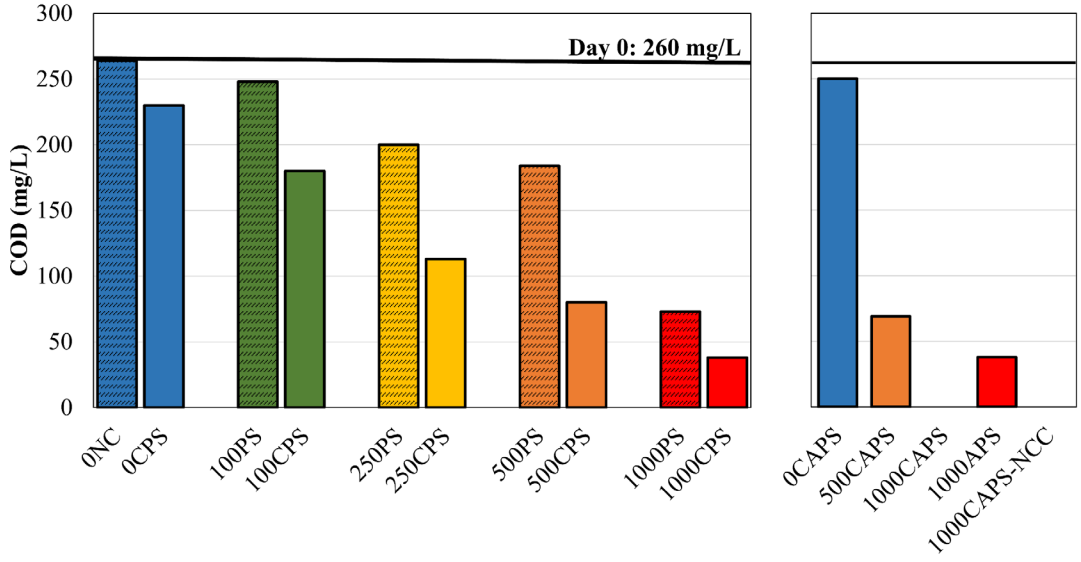

Figure 3-3. Chemical oxygen demand for (a) unactivated persulfate bottles at 21°C on day 310, and (b) and activated persulfate bottles at 30°C on day 240. Dashed pattern indicates chemical treatments and solid pattern indicates coupled treatments. Note: "PS": unactivated persulfate, "CPS": coupled unactivated persulfate with *P. fluorescens*, "APS": activated persulfate, "CAPS": coupled activated persulfate with *P. fluorescens*, "NC" negative control. Data points represent a single microcosm for each condition.

Overall, all chemical treatments showed removal of organics over the course of the experiment, demonstrating that lower concentrations of unactivated persulfate than previously studied (2-10 g/L) can degrade Merichem NAs. Current literature on NA oxidation using unactivated persulfate is lacking and provides inconsistent results regarding the reaction timeframe. Sohrabi et al. (2013) utilized a much higher dose of 10 g/L of unactivated persulfate

and found OSPW NAFCs were removed to <1 mg/L by day 111, with the majority removed by day 60. Conversely, Drzewicz et al. (2012) found that only 2000 mg/L of unactivated persulfate was needed to remove >95% of classical NAs after only 6 days. Regardless, these studies verify that unactivated persulfate can degrade OSPW NAFCs and therefore should be considered as a treatment option for OSPW.

At 30ºC, 1000 mg/L of activated persulfate (1000APS) led to improved Merichem NA removals, in terms of both quantity and rate, with 99.2% Merichem NA removal by day 89 and 100% removal by day 131 (Figure 3-2b). Activating persulfate is well known to increase removal efficiency. For various model NA compounds, temperatures as high as 80ºC were required to achieve complete mineralization in 4 hours, compared to less than 10% TOC (total organic carbon) removal over 24 hours at 40ºC (Xu et al. 2016b). For OSPW NAFCs, increasing the activation temperature to 80ºC led to >90% removal in 2 hours compared to 6 days required at 20ºC; activating persulfate using zero valent iron significantly improved NAFC removal at lower temperatures (Drzewicz et al. 2012). Likewise, 95% NAFC degradation occurred in only 10 minutes in produced water samples using 5000 mg/L of iron activated persulfate at 23ºC (Aher et al. 2017). Commercial Sigma NAs were found to be less reactive and only 46% were removed, indicating activated persulfate may be more reactive towards OSPW NAFC compared to commercial NA mixtures (Aher et al. 2017). Ozonation also appears to be more effective for OSPW NAFCs compared to commercial Merichem NAs (Martin et al. 2010). How this applies to unactivated persulfate reactivity with OSPW NAFC is uncertain. Unactivated persulfate has been shown to preferentially react with n=12-14 and O_2^- species in OSPW NAFCs (Sohrabi et al. 2013) which are present in Merichem NAs,

compared to activated persulfate which is more reactive towards higher carbon numbers and ring containing NAFCs not found in commercial NA mixtures (Fang et al. 2018, 2020).

It is important to note that the controlled system utilized in this study (BH media and commercial Merichem NAs) may impact the persulfate oxidation kinetics compared to OSPW NAFCs. The high concentration of bicarbonate ions in OSPW have the potential to act as oxidant scavengers by forming relatively non-reactive free radical sinks, or positively contribute to degradation by propagating free radical chain reactions (Petri et al. 2011). Xu et al. (2016b) found that 0.5-10 g/L of bicarbonate had a negligible effect on model NA degradation by heat activated persulfate. However, chloride ions can also act as oxidant scavengers and have been shown to negatively impact model NA degradation by persulfate in concentrations ranging from 0.8-50 g/L (Xu et al. 2016b, Fang et al. 2018). BH media contains only 300 mg/L of chloride while OSPW commonly contains up to 600 mg/L (Allen 2008a) which may affect persulfate oxidation.

Coupled treatment bottles (CPS) where *P. fluorescens* was inoculated into persulfate bottles were used to determine if the combined strategy would improve removals compared to the biological and chemical treatments alone. At 21^{o}C, unactivated persulfate coupled with *P. fluorescens* removed 52.8%, 65.1%, 85.1% and 98.9% for 100CPS, 250CPS, 500CPS and 1000CPS, respectively, by day 317 (Figure 3-2a). As described in Section 3.2.2, *P. fluorescens* was inoculated at day 68 to allow time for the persulfate to create more bioavailable carbon sources and thus shorten the lag phase. At all concentrations of persulfate tested, there was increased removal in the coupled treatments compared to the chemical treatment bottles. However, only 100CPS exhibited significantly improved Merichem NA degradation, removing 1.8× more Merichem NAs than persulfate oxidation alone ($p<0.05$).

An interesting trend was noted for 250CPS and 500CPS, where the coupled treatment bottles followed the same linear trend as the chemical treatments until day 200, at which point the coupled treatments exhibited a sharp increase in Merichem NA removal. Therefore, while the final Merichem NA removals were not significantly different between coupled and chemical treatments ($p>0.05$), the coupled bottles achieved the final removals more quickly.

As the concentration of persulfate was increased, the difference between chemical and coupled treatments decreased, suggesting that the persulfate was primarily responsible for the Merichem NA degradation. However, more notable differences can be seen when comparing the COD removals. At day 310, 30.8%, 56.5%, 69.2% and 85.4% of COD was removed, for 100CPS, 250CPS, 500CPS and 1000CPS, respectively (Figure 3-3a), which is 1.2-6.7× more than the chemical treatments. This indicates that while the persulfate may have been primarily responsible for degrading the Merichem NAs, the *P. fluorescens* assisted in the removal of the oxidation by-products, leading to more complete mineralization. Similar to Merichem NA removals, the greatest difference in COD removal between the chemical and coupled treatments bottles (6.7×) was seen at the lowest concentration of persulfate tested (100 mg/L).

The coupled system at 30ºC (CAPS) removed more Merichem NAs at a faster rate compared to at 21ºC, with 99.7% removed by day 131 for 500CAPS, and 99.4% removed by day 89 for 1000CAPS. Even with the improved Merichem NA degradation at 30ºC, 500APF removed 73.5% of COD, which is only 1.1× more compared to 21ºC (500CPS). 1000CAPS was the only treatment that resulted in 100% removal of COD, possibly due to the sulfate radicals assisting the *P. fluorescens* with degrading by-products.

Biodegradation enhancing mineralization by assisting with by-product degradation is commonly noted in studies that have coupled ozonation with biodegradation. Brown et al.

(2013) found that ozonation removed OSPW NAFCs but did not decrease DOC and instead doubled the labile fraction of DOC, allowing for more complete mineralization by microorganisms. Dong et al. (2015) also noted that ozonation alone and combined with biodegradation removed similar amounts of OSPW NAFCs (33.6-41.5%); however, there was a significant difference in COD, with ozone alone removing only 13.5% while the combined system with biodegradation removed 62.5%. Ozonation appears to remove more COD for commercial NA mixtures, as Vaiopoulou et al. (2015) found 50% COD removal of NAs obtained from Tokyo Chemical Industry Co. (TCI); however, the removal further increased to 89% removal after biodegradation.

Coupling unactivated persulfate oxidation and biodegradation has not previously been studied for OSPW remediation but has shown positive results for other common environmental contaminants. For diesel contaminated soil, Bajagain et al. (2018) found that application of a 50 mN persulfate foam followed by 1 month of bioaugmentation removed 1.2× more TPHs than the persulfate foam alone, and 1.5× more than when only bioaugmented. Some studies have suggested persulfate provides a biostimulatory effect by releasing nutrients. In particular, lower persulfate concentrations have been recommended to enhance removals without the negative effects on physicochemical and biological soil properties (Mora et al. 2014). Medina et al. (2018) found that persulfate (33 g/kg) removed a significant amount of PAHs and created more bioavailable daughter compounds, while also oxidizing and mobilizing organic matter from the soil matrix, promoting cometabolic degradation. This coupled system saw a substantial increase in aliphatic hydrocarbon removal to 66%, compared to negligible removal for persulfate or biodegradation alone, and improved PAH removal by 1.6× compared to persulfate oxidation alone.

This is the first study to couple persulfate oxidation and biodegradation for oil sands remediation and demonstrated up to 1.8× improvement in Merichem NA removal and 6.7× for COD removal compared to persulfate oxidation alone. While COD can be used as a general indicator of mineralization, the amount of CO_2 produced can also be examined as an ideal non-harmful end-product.

CO_2 Production

Production of carbon dioxide in the headspace can be used to estimate the mineralization of organics and track microbial growth as a metabolic by-product. After approximately 2 months of persulfate oxidation (68 days for unactivated, 52 days for activated), *P. fluorescens* was inoculated into coupled treatment bottles, lids were added to close the system to air, and CO_2(g) was tracked (Figure 3-4).

Biological treatment bottles containing *P. fluorescens* alone (0CPS) showed a gradual increase in CO_2 to a final concentration of 2.7 mg/L, suggesting some microbial growth and mineralization of organics; however, the increase was not statistically significant ($p>0.05$) compared to negative control bottles without bacteria (0NC). At 30ºC, *P. fluorescens* produced more CO_2, demonstrating a slow increase to day 199, followed by a sharp rise to 7.6 mg/L by day 240. The increase in CO_2 production at 30ºC corresponds with the greater extent of Merichem NA removal (Figure 3-2b).

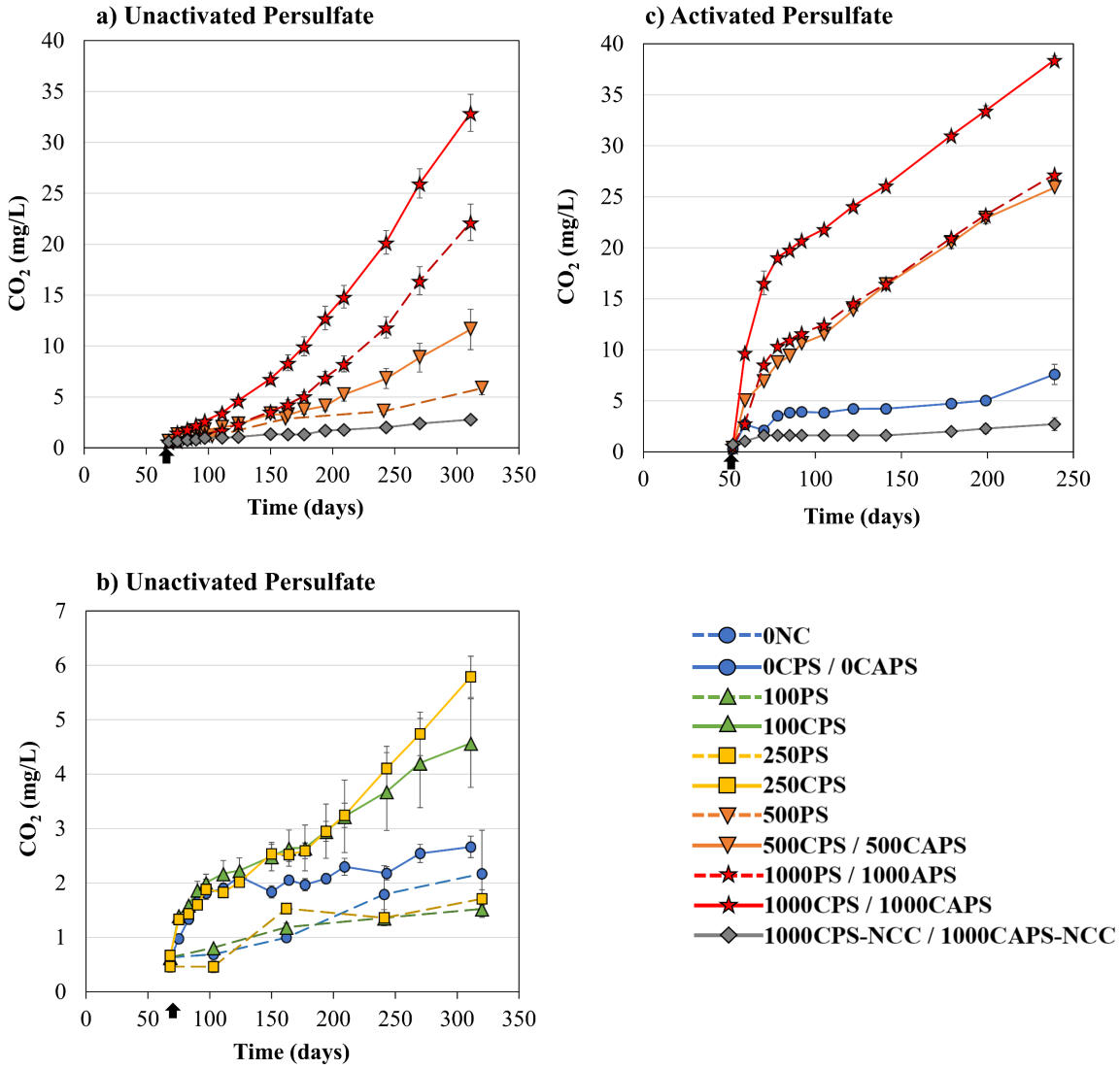

Figure 3-4. Carbon dioxide concentration in the headspace for (a, b) unactivated persulfate bottles at 21°C, and (c) and activated persulfate bottles at 30°C. Note: "PS": unactivated persulfate, "CPS": coupled unactivated persulfate with *P. fluorescens* , "APS": activated persulfate, "CAPS": coupled activated persulfate with *P. fluorescens,* "NC" negative controls, "NCC": no carbon controls, *P. fluorescens* was added after 2 months (⬆), dashed lines represent chemical treatments. All data points are an average of duplicate or triplicate bottles. Error bars represent one standard error of the averaged value.

Chemical treatment bottles at 21°C produced 1.5, 1.7, 5.9, and 22.2 mg/L CO_2 by day 320, for 100PS, 250PS, 500PS and 1000PS, respectively (Figure 3-4). Both 100PS and 250PS did not produce significantly more CO_2 than the negative control bottles (0NC) ($p>0.05$), indicating that very little Merichem NAs were mineralized at this concentration, further

confirmed by the small COD decrease noted above (Figure 3-3a). Conversely, 500PS and 1000PS produced 2.7× and 10.1× more CO_2 than the negative control bottles, suggesting complete mineralization of Merichem NAs by persulfate. In general, ozonation transforms rather than mineralizes NAFCs, causing ozone persistent NAFCs and by-products to accumulate (Martin et al. 2010, Vaiopoulou et al. 2015). Conversely, the results of this study suggests that persulfate does mineralize Merichem NAs. Similarly, Sohrabi et al. (2013) found that persulfate led to more complete mineralization of OSPW NAFCs, seen by 100% and 94% removal of NAFCs and DOC, compared to permanganate which, despite removing 93% of NAFCs, saw only 33% DOC removed.

Coupled treatments with *P. fluorescens* and persulfate at 21ºC (100CPS-1000CPS) all exhibited significantly more ($p<0.05$) CO_2 production compared to their respective chemical treatment bottles. At day 311, there was 4.6, 5.8, 11.6, and 32.9 mg/L of CO_2 produced, for 100CPS, 250CPS, 500CPS and 1000CPS, respectively (Figure 3-4a,b). Similar to results seen for Merichem NA degradation (Figure 3-2a), the lower concentrations of persulfate exhibited a larger difference between chemical and coupled treatments; in particular, 3.4× more CO_2 was produced for 250CPS compared to 250PS. Conversely, as the concentration of persulfate increased, the difference between chemical and coupled bottles declined, with 500CPS producing 2.0× more than 500PS, and 1000CPS producing only 1.5× more CO_2 than 1000PS. Potentially, the persulfate reaction was more aggressive at higher concentrations and preferentially reacted with Merichem NAs and by-products, decreasing the carbon sources available for *P. fluorescens* in addition to higher oxidative stress. Regardless, the overall enhanced CO_2 production and COD removal noted for coupled treatments suggests that there was microbial growth and some increased Merichem NA mineralization with the addition of

P. fluorescens. The most CO_2 was produced at 30ºC for 1000CAPS (38.4 mg/L), in addition to the complete removal of COD noted earlier, this indicates complete mineralization of all Merichem NAs for this condition.

3.3.2 Persulfate Persistence

Unactivated persulfate is known to be a persistent oxidant which is a significant advantage in situ as it allows time for the oxidant to come in contact with the contaminant. Yen et al. (2011) demonstrated that unactivated persulfate could persist for 5 months in diesel contaminated soil, and Li et al. (2017b) found that iron activated persulfate had a longer half-life compared to hydrogen peroxide and permanganate for benzene degradation, decreasing only 35% over 40 days.

Figure 3-5 illustrates the change in persulfate concentration over the experimental timeframe. Regardless of the concentration of persulfate added and the amount of Merichem NAs removed, over 320 days at 21ºC, the persulfate proved to be persistent and had approximately half remaining in the system (45.6-61.7%). Sohrabi et al. (2013) found persulfate was persistent in OSPW with less than 10% of persulfate consumed over 111 days.

Chemical and coupled treatment bottles did not show a statistically significant difference in final persulfate concentrations ($p>0.05$). The no carbon control (1000CPS-NCC) was used to demonstrate the decomposition of persulfate in the absence of Merichem NAs and had 88.0% remaining (982.1 mg/L) by day 320. It is possible that the persulfate was reacting with the small concentration of organics from the inoculated cells and that there was some level of activation even at 21ºC, causing decomposition of the persulfate anion (Petri et al. 2011).

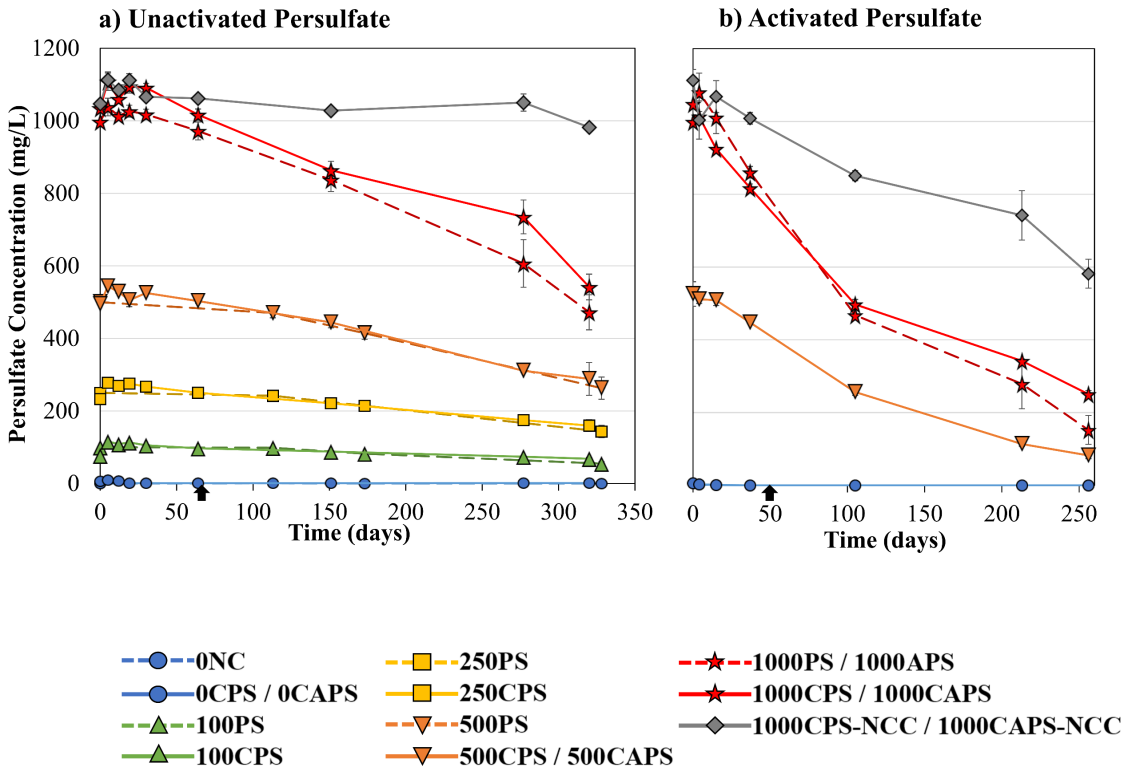

Figure 3-5. Persulfate concentration for (a) unactivated persulfate bottles at 21°C, and (b) and activated persulfate bottles at 30°C. Note: "PS": unactivated persulfate, "CPS": coupled unactivated persulfate with *P. fluorescens*, "APS": activated persulfate, "CAPS": coupled activated persulfate with *P. fluorescens,* "NCC": no carbon control, *P. fluorescens* was added to after 2 months (⬆), dashed lines represent chemical treatments. All data points are an average of duplicate or triplicate bottles. Error bars represent on standard error of the averaged value.

Based on the stoichiometric COD model proposed by Mahour (2016), to remove 260 mg/L of COD (the equivalent of 100 mg/L Merichem NAs) would require a dose of 3.9 g/L of persulfate. Therefore, 100-1000 mg/L of persulfate should theoretically remove 2.6-26% COD. As discussed earlier, at 21°C, 100-1000 mg/L of persulfate alone removed 4.6-71.9% COD, considerably more than predicted, with half the persulfate remaining in solution. Therefore, it is likely that sulfate radicals were created at 21°C, and radical chain reactions enhanced removal. Future work should monitor the presence of radicals to verify the presence and impact of radicals at room temperature.

Raising the temperature to 30ºC activated the persulfate and caused increasing amounts of radicals to be created, which led to considerably faster decomposition of persulfate, with 14.6-25.1% remaining by day 260 (Figure 3-5b). A steep linear decrease was observed until day 105, at which point persulfate removal slowed, likely because there were little organics left to react with, as all Merichem NAs were removed by day 89 and 131 for 1000CAPS and 500CAPS, respectively. The creation of radicals due to heat also led to an increase in the decomposition of persulfate in the absence of Merichem NAs (1000CAPS-NCC), with only 52.3% remaining by day 260.

In OSPW studies combining ozonation with biodegradation, ozonation often does not fully remove the bio-persistent fraction leading to biodegradation activity eventually stalling (Brown et al. 2013, Dong et al. 2015). In addition, increasing the ozone dose does not appear to lead to increased biodegradability (Dong et al. 2015). As ozone reacts quickly, repeated applications may be required to remove the bio-persistent fraction. In this study, Merichem NA degradation did not stall in coupled persulfate and biodegradation treatment bottles (Figure 3-2). The persistence of persulfate allowed the persulfate and *P. fluorescens* to continually act simultaneously throughout the experiment duration, with the persulfate breaking down the Merichem NAs while the bacteria degraded the by-products. Similarly, oxidant persistence has been positively correlated to diesel removal, with enhanced removal seen when using persulfate compared to permanganate and hydrogen peroxide (Chen et al. 2016).

3.3.3 Impact on Bacteria

In addition to examining the impact of the coupled treatment on removal of organics, it is important to understand the impact on the bacteria. A treatment tailored to the microorganisms is not only more cost-effective as it requires a lower quantity of chemical

oxidant, but can also be quicker and lead to more comprehensive overall remediation (Jung et al. 2005, Cassidy et al. 2009, Siegrist et al. 2011, Sutton et al. 2011). This study looked at the viability of *P. fluorescens* as the Merichem NA degrader of interest, and toxicity towards *V. fischeri* as the industry standard used to reflect toxicity towards aquatic microorganisms.

Microbial Viability

Viable cell counts were completed to identify the number of living cells in the bottles at the end of the experiment, shown in Figure 3-6, which can indicate availability of carbon sources along with potential toxic effects from the Merichem NAs and persulfate. Plate counting is known to underestimate the quantity of bacterial cells (Glaze 1987, Paslawski et al. 2009); however, bacterial numbers have demonstrated similar trends when compared to measuring cell concentration via real time polymerase chain reaction (qPCR) (Dong et al. 2015).

Control microcosms without Merichem NAs (1000CPS-NCC) did not show extensive growth, indicating that there were no other sources of carbon in the bottles. Biological treatment bottles containing only *P. fluorescens* (0CPS) yielded 9.9×10^4 CFU/mL at 21ºC and 2.4×10^5 CFU/mL at 30ºC (0CAPS), further verifying that *P. fluorescens* prefers 30ºC as there were 2.4× more viable cells in addition to the improved Merichem NA degradation (Figure 3-2b). Increasing concentrations of persulfate (0-250 mg/L) led to increased bacterial numbers until 500 mg/L, at which point they declined considerably (Figure 3-6). The 100CPS microcosms exhibited the greatest variability in microbial growth due to one triplicate bottle showing higher cell counts. Excluding the outlier bottle, the average bacterial number decreased from 2.7×10^5 to 1.3×10^5 CFU/mL, which is only slightly higher than the biological treatments (0CPS), suggesting that 100 mg/L of persulfate did not enhance microbial viability.

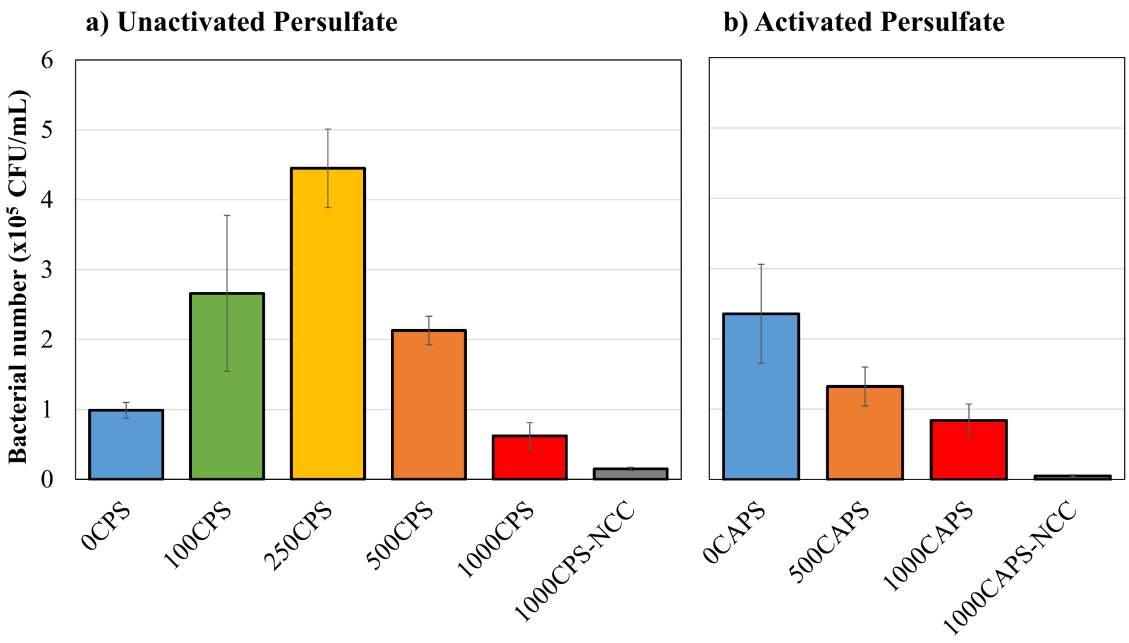

Figure 3-6. Number of colony forming units for (a) unactivated persulfate bottles at 21°C on day 320, and (b) and activated persulfate bottles at 30°C on day 260. Note: "PS": unactivated persulfate, "CPS": coupled unactivated persulfate with *P. fluorescens*, "APS": activated persulfate, "CAPS": coupled activated persulfate with *P. fluorescens*, "NCC": no carbon controls. All data points are an average of triplicate bottles. Error bars represent one standard error of the averaged value.

Microcosms with 250CPS produced the highest number of colony forming units at 4.5×10^5 CFU/mL (Figure 3-6), which is 4.6× the amount generated at 0CPS, indicating that this concentration of persulfate provided the ideal balance between the production of more biodegradable carbon sources without creating significant oxidative stress. Further increasing the concentration of persulfate to 500 mg/L possibly increased stress on the bacteria and thus decreased bacterial number to 2.1×10^5 CFU/mL; however, there were still significantly more viable cells ($p<0.05$) at 500CPS compared to 0CPS, likely due to the increase in bioavailable carbon sources. At 30°C, activated persulfate likely produced a higher concentration of sulfate and hydroxyl radicals which inhibited the bacterial growth and decreased colony forming units to 1.3×10^5 CFU/mL (500CAPS), which was 0.5× less than biological treatments at 30°C (0CAPS).

The highest concentration of persulfate tested (1000 mg/L, 1000CPS) exhibited the lowest bacterial number at 6.2×10^4 CFU/mL (Figure 3-6). Despite the improved Merichem NA and COD removal (Figure 3-2a, 3-3a), the bacteria were subject to more oxidative stress and thus produced 0.3× less cell counts than at 0CPS, implying that this concentration is unfavorable for *P. fluorescens.* At 30ºC there were slightly more colony forming units produced (8.4×10^4 CFU/mL) for 1000CAPS compared to 1000CPS, despite the increased stress from the radicals; however, similar to 500CAPS, there were still 0.4× less bacterial number than at 0CAPS, overall suggesting that microbial viability was not enhanced in coupled systems using activated persulfate.

Currently, only one other study simultaneously coupled chemical oxidation and biodegradation of OSPW to evaluate the impact of the oxidation on the microorganisms. Brown et al. (2013) found that an ozone dose of 50 mg/L did not completely inhibit microbial growth, as ozonated OSPW showed higher *rpoB* gene copy numbers than the sterile control. However, ozonated OSPW did not show clear evidence of improved growth compared to raw OSPW. Conversely, Dong et al. (2015) re-inoculated ozonated OSPW with unstressed indigenous microorganisms which exhibited no lag phase and reached a peak of 10^6 CFU/mL at day 60, compared to indigenous microorganisms in raw OSPW which had a 15-day lag period and reached only 10^5 CFU/mL by day 70.

Persulfate is generally considered less harmful to microorganisms compared to other commonly used chemical oxidants; however, the reason why has not yet been determined and is likely highly dependent on the specific chemistry of the water matrix. Compared to potassium permanganate and Fenton's reagent, iron activated persulfate gave the highest PAH removal and showed the greatest increase in microbial plate counts following oxidation (Liao

et al. 2018). For benzo[a]pyrene removal, a higher concentration of iron activated persulfate (20 mM) was able to be utilized without damaging microbial degradation compared to only 10 mM for permanganate (Xu et al. 2019a). In addition, 10-20 mM (2.7-5.4 g/L) of iron activated persulfate increased the occurrence of PAH degrading bacteria, leading to 12-18% higher degradation efficiency compared to permanganate. Similarly, Cassidy et al. (2009) found that while iron activated persulfate alone removed the least amount of DNT, the persulfate showed a minimal impact on both number of indigenous soil microorganisms and rebound time, leading to overall DNT remediation occurring in 14 days, compared to 30 and 90 days required for Fenton's reagent and ozone, respectively. This demonstrates that designing the treatment based on what is least harmful to the microorganisms leads to more effective overall remediation.

Tsitonaki et al. (2008) studied the effect of heat (40ºC) activated persulfate on both indigenous soil microorganisms and the isolate *Pseudomonas putida* (KT2440) using microscopic enumeration to measure cell density and acetate consumption to measure metabolic activity. Results showed that oxidation with persulfate was less damaging toward microorganisms compared to similar studies using Fenton's reagent, hydrogen peroxide and permanganate. Persulfate concentrations ranging from 0.1-10 g/L did not affect the indigenous site microbial cell density but were detrimental to *P. putida* at 10 g/L. Other studies have also shown that exponentially growing laboratory strains are more vulnerable to oxidative and heat stress compared to stationary phase cultures (Izawa et al. 1996, Díaz-Acosta et al. 2006, Vattanaviboon et al. 2011). However, for both indigenous microorganisms and *P. putida*, acetate consumption was inhibited at 10 g/L, suggesting that membrane integrity does not always relate to metabolic activity. It is important to note that Tsitonaki et al. (2008) did not

adjust for pH, and at 10 g/L of persulfate the pH dropped to 3 which likely played a role in the damaging effects at that concentration.

The reduction of pH is a disadvantage when using persulfate and is likely a primary reason for studies that noted detrimental effects in microbial density following persulfate oxidation (Chen et al. 2016, Liao et al. 2019, Sutton et al. 2015, Sutton et al. 2014a, 2014b). In this study, pH was monitored and controlled to avoid additional microbial stress. The unactivated persulfate bottles did not show a change in pH and did not require adjustment. Conversely, the activated bottles needed to be supplemented with sodium hydroxide 18 days after the addition of *P. fluorescens* as the pH dropped to 6.5, demonstrating an advantage to using unactivated persulfate despite slower reaction rates. However, pH changes in the field are often mitigated due to incoming groundwater and fast rebounds of microbial density to above pre-exposure levels have been observed (Medina et al. 2018, Bartlett et al. 2019, Liao et al. 2019).

Toxicity Reduction

The mechanism of action for NA acute toxicity may be from their surfactant characteristics, which allow them to penetrate and disrupt the cell cytoplasmic membrane, altering membrane properties such as fluidity, thickness and surface tension, leading to cell death (Frank et al. 2008, Kannel and Gan 2012, Klopman et al. 1999, Quagraine et al. 2005b). However, it is important to note that OSPW has many additional organic and inorganic compounds that contribute to toxicity (Li et al. 2017a). Furthermore, the addition of a chemical oxidant can generate more toxic by-products and act as a stressor, creating an increasingly complex system. To date, this is the only study that did not quench persulfate prior to toxicity measurement in order to determine the toxicity of the whole system rather than just the NAFCs.

Table 3-2 outlines the TU towards *V. fischeri* obtained from Microtox for the start and end of the experiment. The toxicity of 100 mg/L of Merichem NAs was found to be 11.30 TU based on the IC_{50} 5 min acute toxicity results. Comparatively, OSPW has much lower toxicity, ranging from 1.49-4.17 TU, based on IC_{50} (Li et al. 2017a). As discussed previously, Merichem NAs consist solely of O_2^- species, which are considered the most acutely toxic fraction, and thus cause the discrepancy in toxicity values compared to OSPW.

Table 3-2. Acute toxicity, measured as toxicity units, at the start (day 0) and end of the experiment for unactivated (21°C; day 320) and activated (30°C; day 260) persulfate bottles. Note: "PS": unactivated persulfate, "CPS": coupled unactivated persulfate with *P. fluorescens*, "APS": activated persulfate, "CAPS": coupled activated persulfate with *P. fluorescens*, "NCC": no carbon controls, "N/A": not applicable. Data points represent a single microcosm for each condition.

Persulfate Concentration	*Day 0* Experiment Start	*Day 320*		*Day 260*	
		PS	CPS	APS	CAPS
0 mg/L	11.30	14.16	7.81	N/A	6.98
100 mg/L	15.01	3.83	1.99	N/A	N/A
250 mg/L	16.13	0.97	0.40	N/A	N/A
500 mg/L	24.81	0.66	0	N/A	0
1000 mg/L	*Too Toxic*	0.02	0	0	0
1000 mg/L - NCC	0	0	0	N/A	0

Negative control microcosms containing only 100 mg/L Merichem NAs with no bacteria or persulfate (0NC) saw an increase to 14.16 TU over 320 days, possibly due to evaporation and subsequent concentration of Merichem NAs. *P. fluorescens* alone in the biological treatments decreased the toxicity by 31.0% and 38.2%, at 21°C and 30°C, respectively, which are relatively similar despite the 2.1× more Merichem NAs removed at 30°C (Figure 3-2). However, at 21°C, the bacteria removed 3.0× more COD (Figure 3-3), which may include any toxic by-products from biodegradation. Further work is required to establish the by-products created during biodegradation.

The addition of persulfate caused a substantial increase in the initial toxicity of the system, to 1.3- 1.4- and 2.2- fold higher than bottles with 100 mg/L Merichem NAs alone (0NC), for 100PS, 250PS and 500PS, respectively (Table 3-2). For 1000 mg/L of persulfate (1000PS), the toxicity increased to above the detection limit, meaning that for all 4 dilutions tested, the bioluminescence of *V. fischeri* was reduced by more than 50%. Interestingly, microcosms containing 1000 mg/L of persulfate without Merichem NAs (1000CPS-NCC) showed no toxicity via Microtox (Table 3-2). Together, these results suggest that acute toxicity effects of persulfate are due to synergistic interactions, where the toxicity is enhanced beyond that of the individual compounds.

Despite the large increase in initial toxicity, chemical treatment bottles at 21°C exhibited a 74.5%, 93.9%, and 97.4% decrease in TU for 100PS, 250PS, and 500PS, respectively, by the end of the experiment (Table 3-2). The initial toxicity of 1000PS could not be determined, however the final TU was the lowest of all the chemical treatments at 0.02 TU. Moreover, as discussed in Section 3.3.1, most of the chemical treatment bottles had considerable COD remaining, therefore the large reduction in toxicity implies that the oxidation by-products produced were less toxic than the parent compound. For example, 250PS saw a substantial toxicity reduction due to the removal of 53.9% of Merichem NAs, yet only 23.1% of COD was removed and an insignificant amount of CO_2 was produced.

Similarly, Sohrabi et al. (2013) found no detectable toxicity of NAFCs after unactivated persulfate treatment, however the authors used extracted NAFCs where by-products may not be extracted by DCM, and persulfate was removed from the system. When comparing UV activated persulfate, hydrogen peroxide and chlorine, Fang et al. (2020) found that UV/persulfate showed the greatest reduction in toxicity (via Microtox). The dissolved organic

matter from the three oxidants had similar elemental compositions despite vastly different toxicity reductions, suggesting toxicity originated from non-degraded organics rather than by-products produced. Another possibility is that the UV/persulfate treatment created by-products with different molecular structure or polarity which had lower permeability though the cell membrane compared to UV/hydrogen peroxide and UV/chlorine (Fang et al. 2020).

Coupled treatments all showed improved toxicity reduction compared to the chemical treatment bottles, with 86.8%, 97.5%, 100% and 100% decrease in TU for 100CPS, 250CPS, 500CPS and 1000CPS, respectively, by the end of the experiment (Table 3-2). This trend has also been observed in studies with combined ozonation and biodegradation for OSPW treatment, where despite similar NAFC removals, there is a significant difference in toxicity removal with the addition of microorganisms (Martin et al. 2010, Vaiopoulou et al. 2015, Wang et al. 2013b). Vaiopoulou et al. (2015) noted ozonation decreased the toxicity of commercial TCI NAs by 3.3-fold, while the addition of microorganisms improved toxicity reduction to a 15-fold decrease. For OSPW, NAFC removals of 50-75% (Martin et al. 2010) and 90% (Wang et al. 2013b) after ozonation did not reduce toxicity towards *V. fischeri*, while the inoculation of microorganisms caused significant acceleration of toxicity removal. The lack of toxicity reduction from ozonation alone in these studies is likely because NAFCs are generally not mineralized after ozonation, leading to an accumulation of potentially toxic by-products. While this study also noted that most conditions had COD remaining (Figure 3-3), there was notable toxicity removed, and the higher persulfate concentrations (500-1000PS) exhibited a large production of CO_2 (Figure 3-3), indicating mineralization was occurring. As CO_2 is a harmless by-product, the greater extent of mineralization with persulfate oxidation compared to ozonation is a significant advantage.

At 30ºC. all persulfate concentrations tested for both chemical and coupled treatments (500CAPS, 1000APS, 1000CAPS) showed a complete removal of toxicity by the end of the experiment (Table 3-2). This is expected since these conditions also showed complete removal of Merichem NAs (Figure 3-2b). As noted above, the decreased acute toxicity is interesting as there was a considerable amount (14.6-25.1%) of persulfate anions remaining in the system (Figure 3-5). In addition, activated persulfate would create sulfate radicals which would have been expected to increase the toxicity. It is possible that sulfate radicals require longer timelines to penetrate the cell membrane due to their relatively large size compared to hydroxyl radicals (Tsitonaki et al. 2008). Another possibility is that the toxic effects of persulfate anions and sulfate radicals comes primarily from physicochemical changes to the environment, such as pH decreases discussed above, or increase salinity from sulfate ions produced during the reaction.

It is interesting to note that despite the complete removal of Microtox acute toxicity noted in activated persulfate coupled treatments, microbial viability of *P. fluorescens* was negatively impacted (Figure 3-6b). This further suggests that toxic effects from persulfate may be due to long term physicochemical changes to the environment, or a lack of available carbon sources if the persulfate reacted with the organics faster than the bacteria could utilize them. Regardless, bacterial growth was enhanced in the lower persulfate concentrations, which should be considered when designing a treatment strategy.

3.4 Conclusions

This study has demonstrated the potential of different doses of unactivated and activated persulfate coupled with biodegradation as an efficient treatment strategy to degrade Merichem NAs and reduce toxicity. The addition of 100 mg/L of unactivated persulfate and *P.*

fluorescens improved Merichem NA degradation by 1.8× compared to persulfate oxidation alone. For unactivated persulfate concentrations of 250-1000 mg/L, the coupled treatment system inoculated with *P. fluorescens* exhibited similar Merichem NA removals compared to the chemical treatment bottles with persulfate alone. However, COD removal was improved 1.2-6.7× and CO_2 production was significantly higher when *P. fluorescens* was added to the coupled system, suggesting that the persulfate was primarily responsible for Merichem NA removal, while the *P. fluorescens* degraded the oxidation by-products. The impact of the bacteria became less pronounced at higher persulfate concentrations (1000 mg/L), likely because there were less carbon sources for the bacteria and increased stressors. Microbial density increased 4.6× with the addition of 250 mg/L of unactivated persulfate, which provided enough increased bioavailable carbon sources to outweigh the oxidative stress effect of the persulfate. At 30ºC, the production of radicals created a more aggressive oxidation reaction, improving the amount and rate of Merichem NA removal; however microbial viability was reduced. The acute toxicity was found to increase considerably due to the addition of persulfate, however persulfate alone did not show toxicity towards *V. fischeri,* suggesting increased toxicity may be due to synergistic interactions.

As Alberta's oil sands industry continues to expand, there is an increasing need for more effective water management and remediation methods. Coupling persulfate oxidation and biodegradation decreases the chemicals required compared to chemical oxidation alone by utilizing microorganisms to degrade the remaining compounds, thereby significantly reducing treatment costs and toxicity of tailings wastewater.

Chapter 4

OSPW NAFC Remediation and Toxicity Reduction by Persulfate Oxidation and Persulfate Oxidation Coupled to Biodegradation

4.1 Introduction

Unconventional oil sands extraction in Alberta is the main contributor to Canadian oil production (CAPP 2022, CER 2022). After bitumen extraction, large volumes of tailings (OSPW, sand, clay, and residual bitumen) are stored in tailings ponds. Wet landscape reclamation strategies such as constructed wetlands and end pit lakes are currently being explored by industry (Brown and Ulrich 2015, Cossey et al. 2021). However, to create a viable self-sustaining ecosystem, the numerous contaminants in OSPW must be addressed. NAFCs in particular are one of the primary causes of OSPW acute toxicity towards aquatic organisms (Li et al. 2017a). Chemical oxidation treatments have been shown to effectively reduce parent NAFC concentrations, but do not lead to complete mineralization and toxicity reduction (Meshref et al. 2017). Therefore, oxidation is commonly paired with biological treatment (Dong et al. 2015, Wang et al. 2013b). Sulfate radical based AOPs such as persulfate (PS) and peroxymonosulfate (PMS) offer an advantage over hydroxyl based AOPs (i.e., catalytic ozonation) in that they generate both sulfate ($SO_4^{\bullet -}$) and hydroxyl ($OH^{\bullet}$) radicals which preferentially react with different compounds, leading to more thorough removals (Lee et al. 2020). Activated persulfate has oxidized >90% of OSPW NAFCs and model NAs using heat, UV, solar and iron as activation methods (Aher et al. 2017, Drzewicz et al. 2012, Fang et al. 2018, Liang et al. 2011, Xu et al. 2016b). Sohrabi et al. (2013) found that 10 g/L of unactivated persulfate could react with OSPW NAFCs, however required months of oxidation compared to only hours or days required for activated persulfate. Similarly, the previous study (Chapter 3) found that much lower concentrations of unactivated persulfate (0.1 – 1 g/L) could oxidize commercial Merichem NAs and led to a considerable reduction in toxicity. Coupling unactivated persulfate oxidation with biodegradation was more effective at lower persulfate

concentrations and led to increased mineralization of organics. OSPW and model NAs pretreated with solar activated PS and PMS have also demonstrated improved mineralization and toxicity reduction by up to 50% and 80%, respectively, when followed with biofiltration (Arslan et al. 2023, Ganiyu et al. 2022a). However, the ability to couple persulfate oxidation with in situ biodegradation processes that already occur in tailings ponds is unknown.

This study aimed to explore the potential for an initial heat activated persulfate treatment followed by a coupled biodegradation and unactivated persulfate stage to remove NAFCs and acute toxicity from OSPW. Unactivated persulfate can reduce NAFC concentrations, however long timelines can be required. Therefore, heat activated persulfate was chosen for this study to create a more aggressive initial oxidation phase, utilizing the high temperatures (40-60ºC) already used during bitumen extraction. The objectives of this study were to: **1)** determine the overall reduction of NAFCs after heat activated persulfate oxidation and the shifts in NAFC distribution; **2)** investigate if residual unactivated persulfate was reactive with remaining organics, and if the addition of bacteria would improve mineralization and toxicity reduction; and, **3)** examine the impact of oxidative stress and OSPW toxicity on the growth of bacteria.

4.2 Materials and Methods

4.2.1 Materials

Commercial NAs were gifted from Merichem Chemicals and Refinery Services LLC (Houston, TX). The OSPW used was surface water (0 m) from an active settling basin collected in 2012, containing 61.5 ± 0.5 mg/L of NAFCs and stored at 4ºC until use. BD Difco™ Bushnell-Haas Broth (BH) was used to provide nutrients for bacteria (per L: 1 g K_2HPO_4; 1 g KH_2PO_4; 1 g NH_4NO_3; 0.2 g $MgSO_4.7H_2O$; 0.02 g $CaCl_2.2H_2O$; 0.05 g $FeCl_3$; pH adjusted to

8.2). Sodium persulfate (>98%) was purchased from Sigma Aldrich (St. Louis, MO). Unless otherwise stated, all materials were purchased from Thermo Fisher Scientific (Waltham, MA).

Pseudomonas fluorescens LP6a was chosen to study biodegradation potential as described in Section 3.2.1. *P. fluorescens* was previously grown in 100 mL of BH mineral media with 0.3 mM acetate and 50 mg/L Merichem NAs for three growth cycles to acclimate the bacteria to the presence of NAs. Cells were grown to exponential phase (OD ~0.9) and washed 3× prior to inoculation into experimental bottles by centrifuging at 4000 rpm for 4 min, discarding the supernatant and resuspending in phosphate buffer solution.

4.2.2 Preliminary Experiments

Preliminary experiments were completed to determine the persulfate activation temperature and reaction time to be used in the more comprehensive experimental microcosm treatments. Trial experiments were completed in 250 mL flasks containing 100 mL of either OSPW or 50 mg/L of Merichem NAs in Milli-Q® Ultrapure water with 250, 500, or 1000 mg/L of sodium persulfate. Flasks were left on an incubator shaker (150 rpm) at 40ºC, 50ºC or 60ºC for up to 24 hours. OSPW trials were completed using single flasks and Merichem trials were done in duplicate.

A second experiment was conducted to determine the impact of inorganic radical scavengers in BH mineral media. Single 250 mL flasks contained 50 mg/L Merichem NAs with 250 and 500 mg/L PS at 60ºC in 100 mL of either 100% BH mineral media, 5% BH mineral media, or Milli-Q® Ultrapure water. In addition, 100 mL of OSPW was supplemented with 0.75 mM P as PO_4^{2-} and 1.24 mM N as NH_4^+/NO_3^- and reacted with 250 mg/L PS at 60ºC to determine any scavenging effects.

4.2.3 Experimental Set-Up

Treatments were created using 500 mL Fisherbrand™ glass media bottles loosely topped with aluminum foil to prevent bacterial contamination and allow for gas exchange. Experiments were conduced with either Merichem NAs (50 mg/L) or OSPW containing 0 (biological treatments), 250, 500, or 1000 mg/L of sodium persulfate. Merichem bottles were filled aseptically with 300 mL of a 5% dilution of BH mineral media. OSPW bottles contained 300 mL of OSPW supplemented with 0.05 g/L K_2HPO_4, 0.05 g/L KH_2PO_4, and 0.05 g/L NH_4NO_3. In the initial activated persulfate stage of the experiment, bottles were placed in a 60ºC shaking incubator (130 rpm) for 8 hours. Bottles were then removed from heat and placed in a water bath to quickly lower temperature to ~20ºC and pH was adjusted (pH ~8) with 1 M NaOH where required. The unactivated persulfate reaction was left for 150 days at room temperature (20ºC; 130 rpm) (Figure 4-1). In this project, unactivated persulfate is defined as having no intentional activation applied.

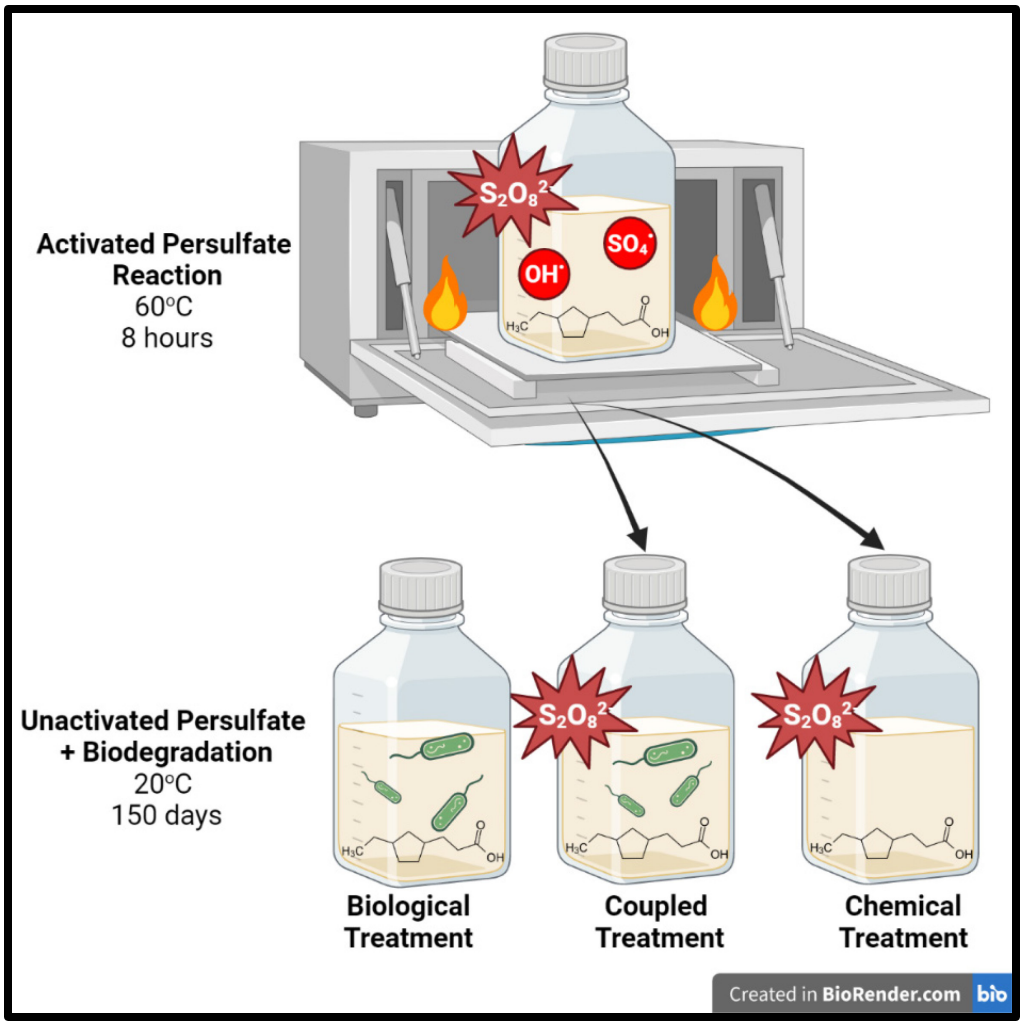

Figure 4-1. Illustration of experimental set-up. Persulfate ($S_2O_8^{2-}$) was activated with heat (60°C) to produce sulfate and hydroxyl radicals. Once removed from heat, *P. fluorescens* was inoculated in select treatment bottles; unactivated persulfate and biodegradation was left to occur at room temperature for 150 days.

Chemical treatment bottles contained only persulfate (250-1000PS), while coupled treatments (250-1000CPS) and biological treatments (0CPS) were inoculated with approximately 10^8 CFU/mL *P. fluorescens* (1% v/v) during the room temperature treatment phase. Killed controls (KC) were set up by inoculating with cells that had been previously autoclaved three times. Negative controls (0NC) contained Merichem NAs and OSPW without persulfate or bacteria and no carbon controls (250-1000NCC) contained persulfate in 5% BH without Merichem NAs (Table 4-1 and 4-2; Figure A-1).

Table 4-1. Summary of experimental bottles for **Merichem NAs**. Treatments were heated (60ºC) for 8 hours and then removed to room temperature for 150 days. *P. fluorescens* was added after removing from heat.

50 mg/L Merichem NAs in 5% BH Mineral Media

	ID	Persulfate (mg/L)	*P. fluorescens*	NA Source	Replicates
No Carbon Control	250NCC	250	No	None	2
	500NCC	500	No	None	2
	1000NCC	1000	No	None	2
Negative Control	0NC	0	No	Merichem	2
Chemical Treatment	250PS	250	No	Merichem	3
	500PS	500	No	Merichem	3
	1000PS	1000	No	Merichem	3
Biological Treatment	0CPS	0	Yes	Merichem	3
Coupled Treatment	250CPS	250	Yes	Merichem	3
	500CPS	500	Yes	Merichem	3
	1000CPS	1000	Yes	Merichem	3
Killed Control	0KC	0	Killed	Merichem	2
	250KC	250	Killed	Merichem	2
	500KC	500	Killed	Merichem	2
	1000KC	1000	Killed	Merichem	2

Table 4-2. Summary of experimental bottles for **OSPW**. Treatments were heated (60ºC) for 8 hours and then removed to room temperature for 150 days. *P. fluorescens* was added after removing from heat.

OSPW with added nitrogen and phosphorous

	ID	Persulfate (mg/L)	*P. fluorescens*	NAFC Source	Replicates
Negative Control	0NC	0	No	OSPW	2
Chemical Treatment	250PS	250	No	OSPW	3
	500PS	500	No	OSPW	3
	1000PS	1000	No	OSPW	3
Biological Treatment	0CPS	0	Yes	OSPW	3
Coupled Treatment	250CPS	250	Yes	OSPW	3
	500CPS	500	Yes	OSPW	3
	1000CPS	1000	Yes	OSPW	3
Killed Control	0KC	0	Killed	OSPW	2
	250KC	250	Killed	OSPW	2
	500KC	500	Killed	OSPW	2
	1000KC	1000	Killed	OSPW	2

4.2.4 Chemical Analyses

Samples were filtered with a 0.22 μm nylon filter and pH, COD, anion and persulfate concentrations were measured immediately. The remaining sample volume was quenched with excess sodium thiosulfate (15 mM) and stored at 4ºC for remaining analyses. The pH was measured using an Accumet AR50 Dual Channel pH/Ion/Conductivity meter. COD was measured using HACH COD Low Range digestion solution vials (LR; limits of 3 - 150 mg/L; product 2125815) for Merichem NA samples, and HACH COD High Range (HR; limits 20 – 1500 mg/L; product 2125915) for OSPW samples, following method 8000, with a HACH digestor reactor and UV-Vis Hach DR/4000 spectrophotometer.

Anions (F^-, Cl^-, NO_2^-, SO_4^{2-}, Br^-, NO_3^-) were analyzed on a Dionex ion chromatography (ICS-2100, Dionex™ IonPac™ AS18 IC columns). Eluent (KOH) was isocratic at 32 mM with a flow rate of 0.25 mL/min for a run time of 15 min. Oven and detector temperature was 30ºC and 35ºC, respectively. Detection occurred using an anion self-regeneration suppressor (ASRS 2 mm) at 20 mA current. System backpressure was 1500 – 2000 psi and background conductance was lower than 2 μS.

Acute toxicity was measured via Microtox with a Model 500 Analyzer (Modern Water, New Castle, DE) and Microtox Omni 4.3 (Modern Water, New Castle, DE) software. The 81.9% screening toxicity method was employed with incubation times of 5 min and 15 min, and only 5 min data was plotted. Samples with a negative inhibition effect indicate the bacteria experienced initial light stimulation, possibly caused by hormesis or the presence of certain nutrients or salts. These were plotted as 0% effect (non-toxic), however full results can be found in Table A-9, A-10. Phenol (100 mg/L) and deionized water were used as positive and negative controls, respectively, according to the manufacturer instructions (data not shown).

Analytical methods for NAFC concentration (via FTIR), persulfate concentration (via spectrophotometer) and viable cell counts were previously described in Section 3.2.3, 3.2.6 and 3.2.7. Unless otherwise stated, statistical analysis was carried out using a Student's t-test (two independent samples, normal distribution, equal variance) comparing chemical treatments to coupled treatments at each persulfate concentration, analyzed in Microsoft Excel with significance set at $p < 0.05$. Paired t-tests were used as noted throughout the text to determine significance over time for individual treatments.

Orbitrap Mass Spectrometer (MS) analysis was completed by Dr. John Headley's lab (National Hydrology Research Centre, SK). Samples were shipped on ice, then stored at 4°C for several days until extractions could proceed. Sample extracts were prepared using a previously reported SPE procedure (Headley et al. 2002) using 200 mg ENV+ cartridges (Biotage, Uppsala, Sweden). The SPE cartridges were initially rinsed with 6 mL each of MilliQ water and LCMS-grade methanol (Fisher Scientific, Hampton, NH), then conditioned with a further 6 mL of MilliQ water (> 18.2 MΩ). Sample aliquots of approximately 100 mL (± 0.5 mL) were acidified to pH <2 with formic acid, then extracted through pre-conditioned SPE cartridges. Cartridges were de-salted post-extraction by rinsing with a further 6 mL of MilliQ water, then dried under vacuum. Once dry, SPE cartridges were eluted with LCMS-grade MeOH, then dried under gentle N_2 flow (5.0 grade) in a 40°C water bath. Sample residues were reconstituted by adding 1.00 mL of 50:50 ACN:H_2O with 0.1% NH_4OH and transferred to 2 mL LCMS vials for analysis. Sample extracts were analyzed via loop injection to an Orbitrap™ Velos Elite MS (ThermoFisher Scientific, Waltham, MA) operating in negative-ion electrospray ionization with resolution set to 240,000 at 400 m/z. Samples were bracketed with external calibration standards every 10-12 samples, where standards were prepared to

between 10 to 100 mg/L total NAFCs using the an OSPW-derived NAFC extract, where details around extract preparation have been previously reported (Rogers et al. 2002a). Spectral data were initially processed in XCalibur software (ver. 2.2, ThermoFisher Scientific, Waltham, MA). Processed data were imported into Composer64 software (ver 1.5.6., Sierra Analytics, Modesto, CA), where formulae were assigned to a level-4 confidence level (Schymanski et al. 2014).

4.3 Preliminary Experiment Results

To determine the persulfate activation temperature and reaction time to be used in the experimental treatments, preliminary trials were conducted using both OSPW and Merichem NAs. The activation temperatures were chosen as 40ºC, 50ºC and 60ºC to reflect the temperatures utilized during bitumen extraction (Foght et al. 2017). The degradation of NAFCs and Merichem NAs were investigated (Figure 4-2 and A-3) along with COD to estimate the extent of mineralization (Figure A-2 and A-3).

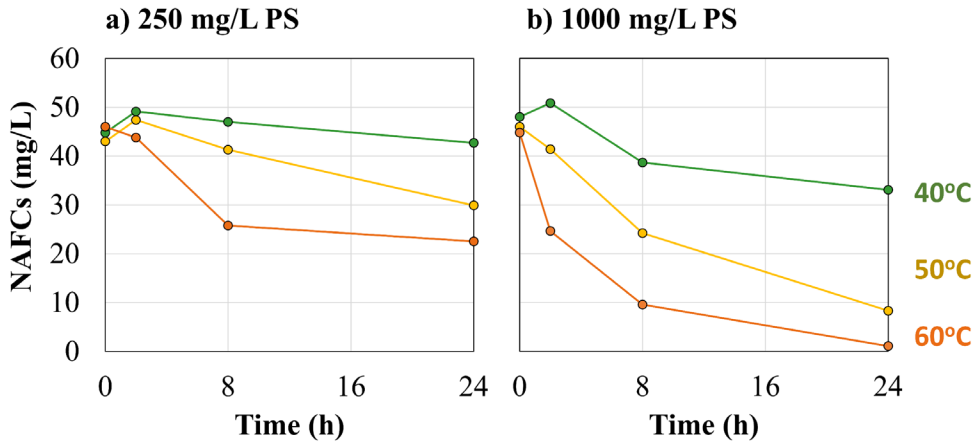

Figure 4-2. Degradation of NAFCs in OSPW with a) 250 mg/L persulfate (PS) and b) 1000 mg/L PS activated at various temperatures. Data represents single treatment bottles.

At lower persulfate doses (250 mg/L), 40ºC did not provide adequate persulfate activation. Increasing the persulfate concentration to 1000 mg/L showed an increase in NAFC degradation at 40ºC, however degradation extent was improved 3.7-fold when the temperature was increased to 60ºC (Table A-1). Conversely, Drzewicz et al. (2012) found that heating OSPW at 40ºC with 2000 mg/L PS for 2 hours led to >80% NAFC removal and there was little change when increasing the temperature to 60ºC. It is likely that the higher persulfate concentration created more rapid radical propagation reactions leading to faster NAFC removal. However, the goal of this research project is to reduce the parent NAFC concentration using limited amounts of persulfate followed with biological treatment, to create a more economical remediation method. After 8 hours of reaction at 60ºC there was 42% and 79% NAFC removal for 250 and 1000 mg/L PS, respectively, and increasing the time to 24 hours did not improve NAFC removal for 250 mg/L PS. Therefore, 8 hours of reaction at 60ºC were chosen as the activation conditions for future experiments.

Preliminary trials at 50ºC and 60ºC were also completed using commercial Merichem NAs in ultrapure water (Figure A-3). There was little change in Merichem NA degradation between 50ºC and 60ºC or when increasing the concentration from 250 to 500 mg/L PS. Merichem NA bottles exhibited 20% removal with 250 mg/L PS, at 60ºC for 8 hours, 2× less than what was found for OSPW. The difference in reactivity might be attributed to the differences in structure between commercial NAs and OSPW NAFCs, such as the higher cyclicity NAFCs in OSPW which are more reactive with oxidants (Chen et al. 2022b, Fang et al. 2018, 2019, Wang et al. 2013b). Differences in the water matrix can also significantly impact the oxidation chemistry as various organics and inorganics can act as either persulfate sinks or activators. Merichem activation temperature experiments were carried out in Milli-Q®

ultrapure water; the impact of inorganic salts was explored comparing 250 and 500 mg/L PS at 60ºC in 100% BH mineral media (15 mM P, 25 mM N), 5% BH mineral media (0.1 mM P, 1.3 mM N), and Milli-Q water (Figure 4-3).

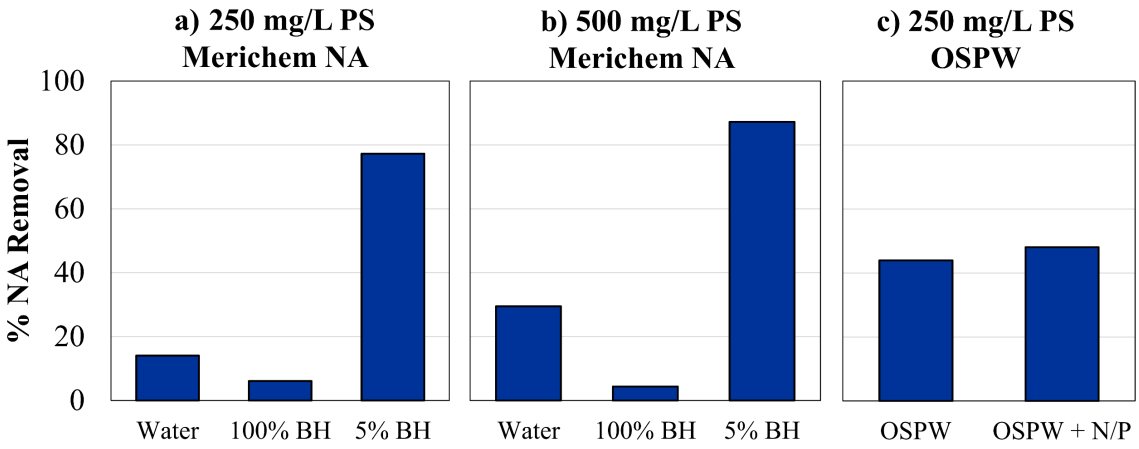

Figure 4-3. Percent decrease of naphthenic acids after 8 hours at 60ºC with 250 or 500 mg/L of persulfate (PS) in different water matrices. "OSPW + N/P" represents OSPW supplemented with nitrogen (N) and phosphorous (P) to the same concentrations present in 5% Bushnell Haas (BH) mineral media (0.75 mM P, 1.25 mM N). Data represents single treatment bottles.

Oxidation reactions occurring in 100% BH mineral media were inhibited and showed almost no Merichem NA removal. Each individual component of BH media was then reacted with heat activated persulfate; visual observations (Figure A-4) showed that only bottles containing the phosphate buffer (~15 mM PO_4) had foaming remaining after the heat activated persulfate reaction, which may indicate the continued presence of surfactants like NAFCs. Oxyanions, in particular phosphate and carbonate, are known to scavenge sulfate radicals by creating weak and highly selective radicals, decreasing treatment efficiency (Lee et al. 2020). Therefore, the use of these anions as pH buffers has the potential to complicate the interpretation of results. Moving forward, a 5% dilution of BH media was chosen as it represented the nitrogen and phosphorus concentrations that are commonly used to supplement OSPW in biodegradation studies (0.7 mM P, 1.3 mM N) (Brown et al. 2013, Scott et al. 2005).

Interestingly, bottles with the diluted mineral media showed improved oxidation of Merichem NAs. Some studies have noted that small concentration of phosphate ions activate persulfate while increasing the concentration further leads to radical scavenging (Lee et al. 2020). The addition of 0.75 mM phosphate did not appear to improve or hinder persulfate oxidation in OSPW.

Based on the results from the preliminary trials, experimental treatments utilizing OSPW and Merichem NAs were set-up containing 250, 500 and 1000 mg/L of persulfate, activated at 60ºC for 8 hours. Bottles were then removed from heat and inoculated with bacteria to simulate OSPW entering tailings ponds containing indigenous microorganisms (Figure 4-1).

4.4 Results and Discussion

The following sections include a discussion on water chemistry, removal of organics, contribution of radical species, NAFC distribution, toxicity reduction and viable cell counts; comparing biodegradation, persulfate oxidation (activated and unactivated stages) and coupled remediation treatments.

4.4.1 Water Chemistry

Benefits to using persulfate for remediation include its powerful oxidizing properties and ability to create sulfate and hydroxyl radicals. Furthermore, persulfate is economical, stable, has a high water solubility, and is effective over a wide range of pH (Tsitonaki et al. 2010, Wacławek et al. 2017). However, persulfate oxidation can also cause acidification, mobilization of metals, and increased electrical conductivity, which can negatively impact the receiving ecosystem (Tsitonaki et al. 2010).

Impact on pH

As described in Section 4.3, a 5% dilution of BH was used in Merichem bottles to avoid radical scavenging effects from the phosphate buffer. Without an adequate pH buffer, heat activated persulfate caused a steep drop in pH to 6.4, 2.6 and 1.8 for 250PS, 500PS and 1000PS, respectively, after 8 hours (Figure A-5). No carbon controls (250-1000NCC) also showed a decrease in pH due to the decomposition of persulfate under heat, however it was much less significant without the increased radical propagation reactions with organics. During the remaining 150 days of unactivated persulfate reaction, the pH was adjusted and maintained to pH > 7 by the addition of 1 M NaOH. While the effect of inorganic radical scavengers was controlled in Merichem bottles, OSPW is well-buffered due to the high concentration of carbonate ions, commonly ranging from 550-820 mg/L $CaCO_3$ (Abdelrahman et al. 2023, Allen 2008a, Drzewicz et al. 2012, Gamal El-Din et al. 2011, Mahaffey and Dube 2016). The OSPW used in these experiments had an alkalinity of 800 mg/L $CaCO_3$, which was adequate to ensure the pH remained consistent over the course of the experiment and did not require any adjustments. Therefore, the natural buffering capabilities of OSPW are well suited to persulfate oxidation treatment.

Impact on Salinity

Electrical conductivity can increase during persulfate oxidation due to the formation of sulfate ions (Equations 1-4, Chapter 2). Sulfate concentrations are provided in Figure 4-4 and Table A-3. Merichem bottles contained a diluted mineral media and therefore initially had minimal sulfate present (6.2 mg/L), however reached a high of 643.3 mg/L by day 150 for 1000PS. Most of the sulfate was produced during heat activation, which is expected as that is the most aggressive reaction stage.

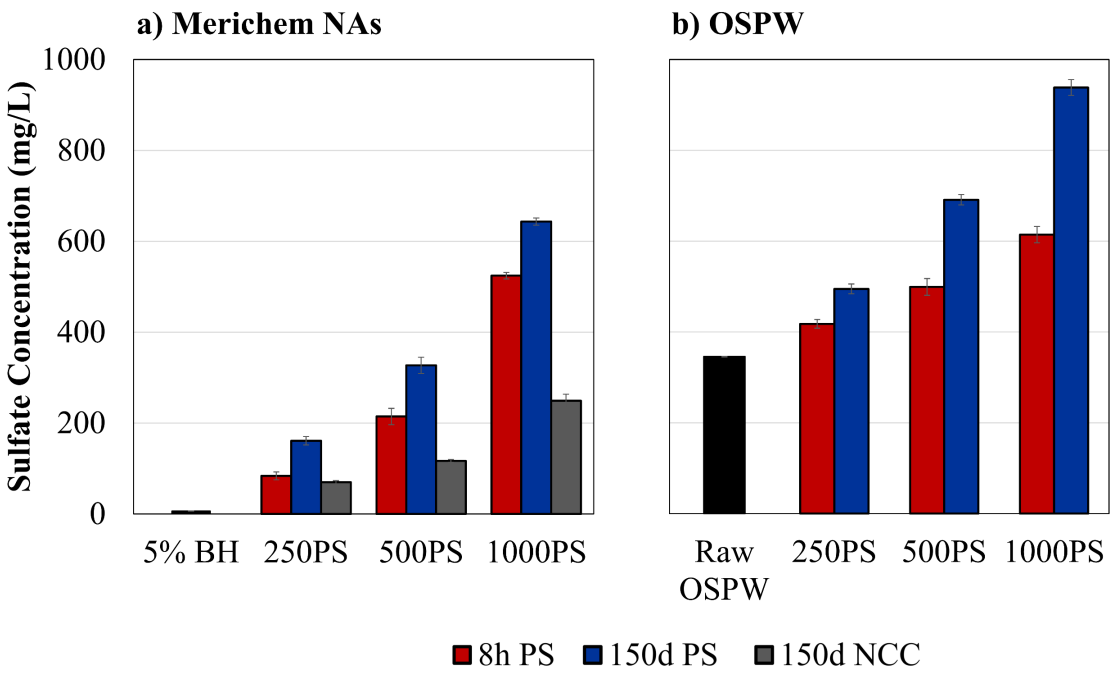

Figure 4-4. Sulfate concentrations (mg/L) for a) Merichem NA and b) OSPW persulfate oxidation treatments (PS) after 8 hours of heat activation (red), followed by 150 days of unactivated persulfate reaction (blue). No carbon controls (NCC) contain persulfate without Merichem NAs (grey). Error bars represent one standard deviation of triplicate bottles.

OSPW has elevated salinity from both naturally occurring saline sediments in the region and additives used during bitumen recovery (NaOH and $CaSO_4$) (Allen 2008a, Chalaturnyk et al. 2002, Kessler et al. 2010). Therefore, the initial sulfate concentration of OSPW (345.7 mg/L) was considerably higher than Merichem NA bottles and reached 938.4 mg/L by day 150 for 1000PS. Regardless of the higher initial concentrations, the net sulfate production by day 150 was similar between Merichem and OSPW bottles (Table A-4). The sulfate guidelines for the protection of aquatic life as laid out in the Environmental Quality Guidelines for Alberta Surface Water (Government of Alberta 2018) range from 128-429 mg/L, depending on the hardness of the water. The salinity of OSPW and tailings is already a challenge when designing reclamation wetlands as native vegetation is sensitive or intolerant to high salinity (Gibson and Peters 2022). Therefore, remediation techniques that increase

salinity should be carefully designed to mitigate impacts. An additional benefit to using lower concentrations of persulfate is the smaller impact on salinity of the water matrix.

Persulfate Utilization

As expected, most persulfate was consumed after the first 8 hours of heat activation, with 42%, 57% and 74% decrease in Merichem bottles, for 250PS, 500PS and 1000PS, respectively (Figure 4-5). Persulfate continued to be utilized at a much slower rate during the unactivated persulfate stage, leading to a total of 82-89% persulfate consumption by day 150. Similarly, no carbon controls had a 17-21% decrease in persulfate concentration during heat activation and then was essentially unchanged over the remaining 150 days. This indicates there was no activation occurring in the Merichem system, and persulfate consumption was due to reaction with organics.

Less persulfate was consumed during heat activation for OSPW, with approximately 40% utilized regardless of the initial concentration. OSPW is a much more complex water matrix, containing numerous inorganics (chloride, bicarbonate) and background organic matter which have the potential to be scavenged by radicals, decreasing treatment efficiency. Generally, sulfate radicals are more selective and thus less impacted by scavengers compared to hydroxyl radicals. However, humic like substances with aromatic and olefinic moieties that may be present in OSPW have been found to scavenge sulfate radicals away from aliphatic acid oxidation (Lee et al. 2020, Romera-Castillo and Jaffé 2015). Additionally, the high pH of OSPW may increase the amount of hydroxyl radicals generated in that system which are non-selective. In general, bicarbonate has not been shown to have an impact on persulfate oxidation of model NAs (Xu et al. 2016b), but chloride concentrations as low as 500 mg/L have negatively impacted the degradation of model NAs (Fang et al. 2018). The OSPW used in this

study had approximately 636 mg/L chloride (Table A-2) which may explain the reduced consumption of persulfate. Ganiyu et al. (2022a) used electron paramagnetic resonance (EPR) spectra to identify radical species during persulfate oxidation and noted that OSPW showed similar peaks to those in the simpler model NA water matrix, however the intensity of peaks was much lower, likely due to inorganic and organic scavengers. Scavenging effects are more prominent with more aggressive activation such as heat (Tsitonaki et al. 2010).

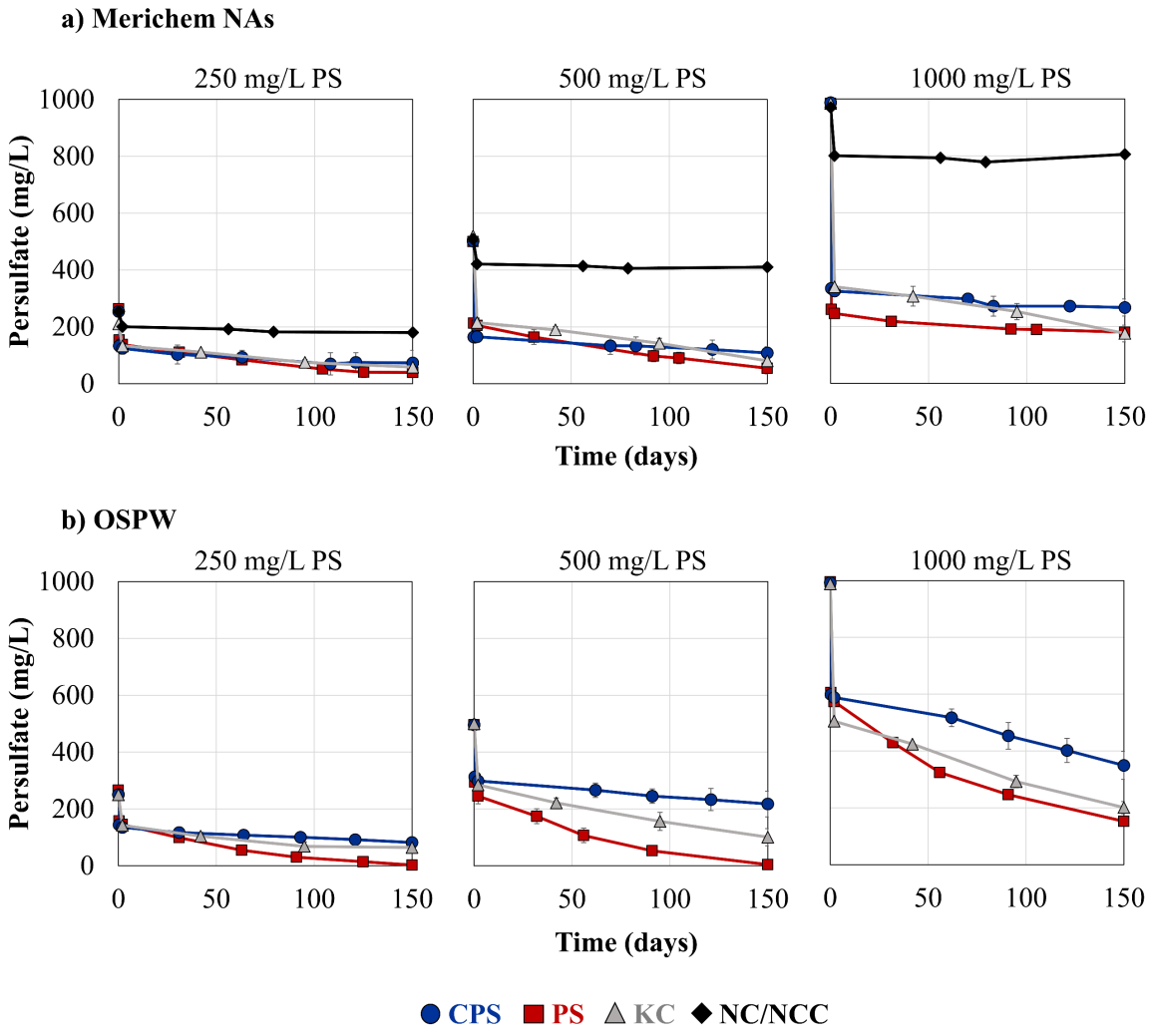

Figure 4-5. Persulfate concentration (mg/L) for a) Merichem NA and b) OSPW after 8 hours of heat activation (60°C) followed by 150 days at room temperature. Treatments include persulfate oxidation (PS; ■), persulfate coupled with *P. fluorescens* (CPS; ●), killed controls (KC; ▲), negative controls without persulfate (0NC; ♦) and no carbon controls without Merichem NAs (250-1000NCC; ♦). Error bars represent one standard deviation of triplicate bottles.

During the unactivated persulfate stage, the persulfate utilization rate was 2.6- to 3.8-fold higher for OSPW compared to Merichem bottles (Table A-5), with 99%, 99% and 85% persulfate consumed by day 150 for 250PS, 500PS and 1000PS. This indicates that there may have been a small degree of activation occurring at room temperature. OSPW contains trace metals such as iron that have been found to cause natural in situ persulfate activation in soil (Liang et al. 2008a, Yen et al. 2011, Mahaffey and Dube 2016). Certain organics (quinone and phenol derivatives) may also be present and can also cause some activation of persulfate depending on their specific pKa and functional groups (Lee et al. 2020). Despite the longer timeframes involved, less aggressive activation can mitigate the impact of scavengers and some activation may occur naturally, providing a balance between the advantages of activated and unactivated persulfate.

The addition of microbes in the OSPW coupled treatments significantly reduced ($p < 0.05$) the overall persulfate utilized (56-67% consumed) and led to a 2.7- to 11.4-fold decrease in rate compared to chemical treatments (Table A-5). Some scavenging impacts may arise from cell biomass, however killed controls (250-1000KC) did not exhibit the same drastic effect, indicating that live cells were primarily responsible. One possibility is that bacterially produced dissolved organic matter (DOM) from metabolism of organics or cell lysis contained electron donating functional groups that can act as oxidant scavengers (Romera-Castillo and Jaffé 2015, Wang et al. 2020). Additionally, *P. fluorescens* may have been producing extracellular polymeric substances (EPS). Bacteria isolated from produced water and oil contaminated soil have shown strong EPS production with antioxidant abilities (Darwish et al. 2019, Mohamed et al. 2019). *Pseudomonas* species are known to be large EPS producers (Costa et al. 2018) and some strains of *P. fluorescens* have been shown to produce EPS with strong antioxidant

properties (Raza et al. 2012, Sirajunnisa et al. 2016). Hydroxyl groups in EPS can donate electrons to reduce radicals to more stable forms, or EPS may be reacting directly with free radicals and terminate the chain reactions (Raza et al. 2012, Wang et al. 2017, Min et al. 2019). Another possibility is that EPS chelated ions (ferrous iron) that were activating persulfate (Wang et al. 2017, Min et al. 2019). Further analyses would be required to determine the cause of scavenging; regardless, the interaction between bacteria and persulfate in OSPW could negatively impact treatment efficiency by scavenging persulfate away from the contaminants of concern. Furthermore, it could increase the persistence of persulfate in the water matrix which could impact water toxicity.

4.4.2 Removal of Organics

NAFCs are principal toxicants in OSPW, however accurate determination of NAFCs can be challenging due to their highly complex nature and will vary depending on the method used. This experiment tracked total NAFC concentrations via FTIR (Figure 4-6) as a reproducible method commonly used by industry that has been found to correlated well with higher resolution techniques such as Orbitrap-MS (Hughes et al. 2017). Liquid-liquid extraction (LLE) of NAFCs was utilized which has been found to provide >80% recovery of total NAFCs, but only 49% recovery of DOC (Qin et al. 2019). Therefore, oxidation by-products may not be captured by LLE and the measurement of carboxyl bonds in FTIR, or may not be part of the acid extractable fraction, thus COD was tracked (Figure 4-7) to determine the extent of mineralization.

Biodegradation

Biodegradation of NAFCs is the most economical remediation strategy but does not lead to complete removal of recalcitrant fractions (Brown and Ulrich 2015). This study used

the bacterial isolate *P. fluorescens*, a common hydrocarbon degrader present in tailings ponds, to determine biodegradation potential (0CPS). *P. fluorescens* degraded 45% of Merichem NAs, mostly occurring in the first 30 days; however, the COD was essentially unchanged, suggesting Merichem NAs were transformed rather than mineralized. The previous study (Chapter 3) found only 16% of Merichem NAs were biodegraded by *P. fluorescens* over 313 days. Notable differences include a lower concentration of Merichem NAs in this study (50 mg/L vs 100 mg/L) and a higher initial cell count (10^8 CFU/mL vs 10^5 CFU/mL). Therefore, the improved biodegradation is likely due to lower NA toxicity and increased biomass.

OSPW did not show any statistically significant biodegradation of NAFCs or COD between 8 hours and 150 days ($p>0.05$; paired t-test). It is well known that commercial NA mixtures such as Merichem are more biodegradable than OSPW NAFCs as they consist of simpler structures with lower molecular weights (Han et al. 2008, Quagraine et al. 2005a, Scott et al. 2005, Whitby 2010, Xu et al. 2017). In addition, OSPW contains other toxic compounds, high salinity and a higher pH which all may cumulatively stress the bacteria, hindering growth.

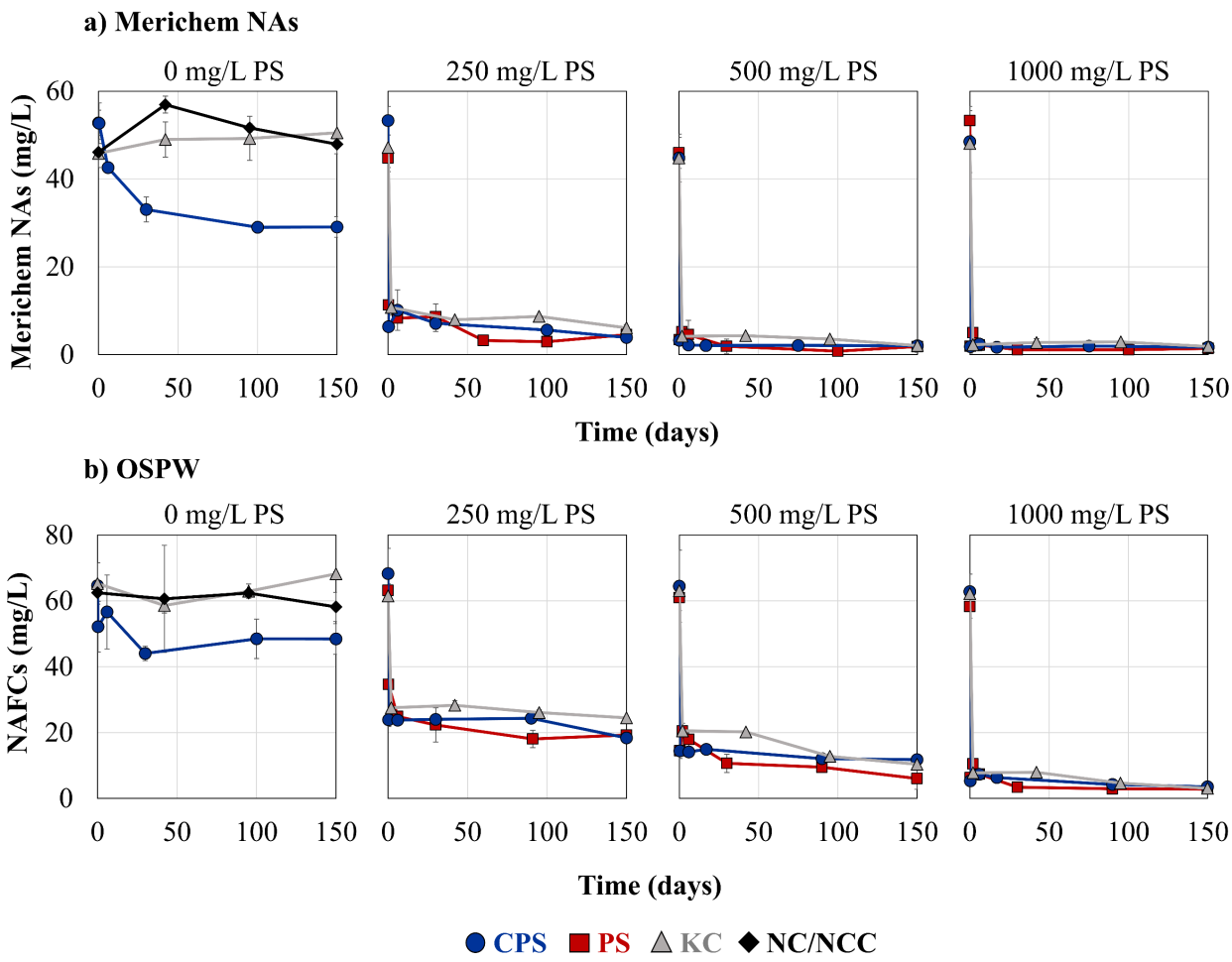

Figure 4-6. a) Merichem NA and b) OSPW NAFC concentrations after 8 hours of heat activation (60°C) followed by 150 days at room temperature. Treatments include persulfate oxidation (PS; ■), persulfate coupled with *P. fluorescens* (CPS; ●), killed controls (KC; ▲), negative controls without persulfate (0NC; ♦) and no carbon controls without Merichem NAs (250-1000NCC; ♦). Error bars represent one standard deviation of triplicate bottles.

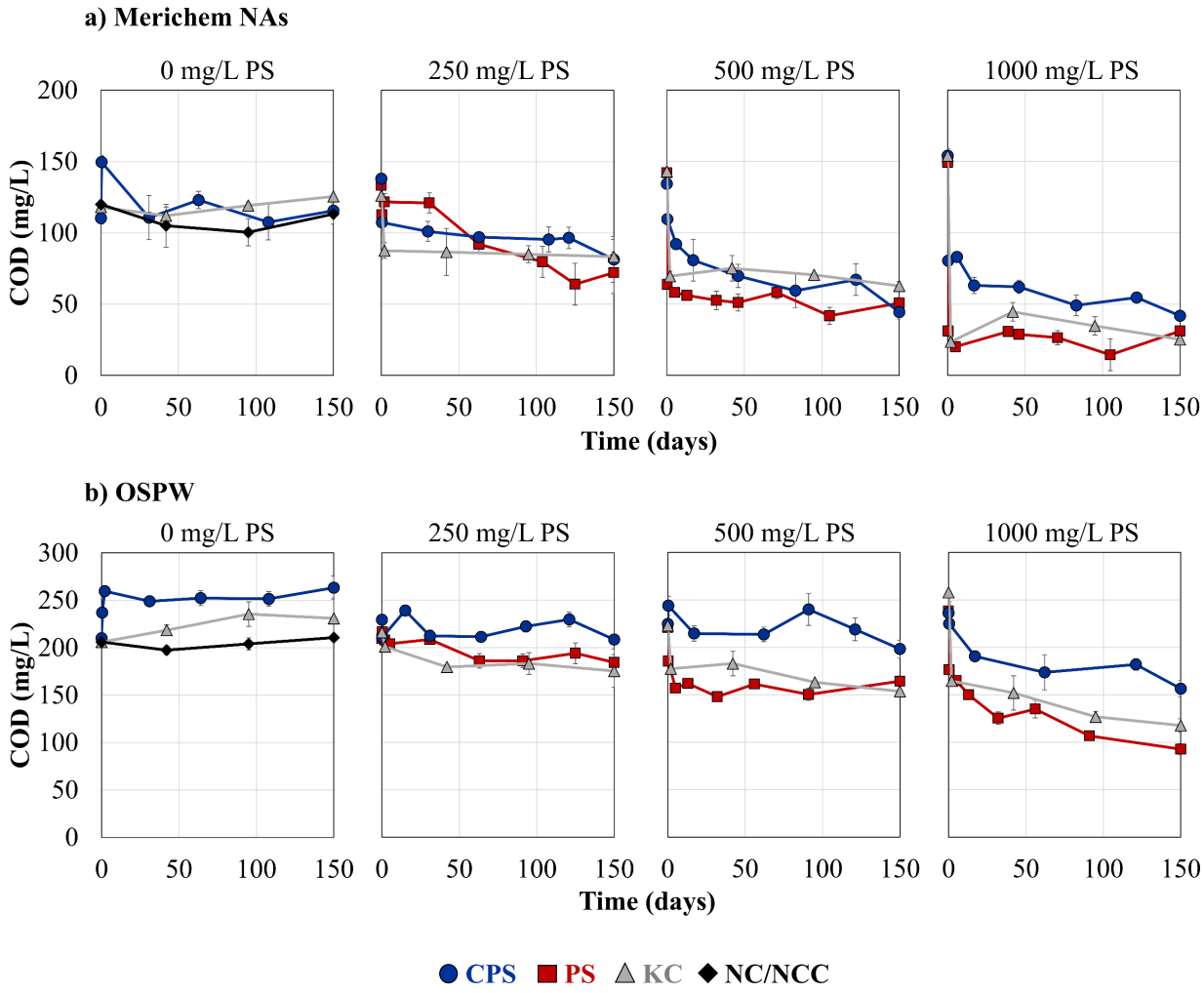

Figure 4-7. Chemical oxygen demand (COD) for a) Merichem NA and b) OSPW after 8 hours of heat activation (60°C) followed by 150 days at room temperature. Treatments include persulfate oxidation (PS; ■), persulfate coupled with *P. fluorescens* (CPS; ●), killed controls (KC; ▲), negative controls without persulfate (0NC; ♦) and no carbon controls without Merichem NAs (250-1000NCC; ♦). Error bars represent one standard deviation of triplicate bottles.

Persulfate Oxidation

Chemical oxidation is an effective treatment for NAFCs but can be expensive for the large volumes of OSPW that require remediation. After 8 hours of heat activated persulfate reaction, Merichem NAs exhibited 74.8%, 92.6%, and 96.4% removal for 250PS, 500PS and 1000PS, respectively, showing a considerable improvement over biodegradation. Furthermore, mineralization increased with persulfate dose, as seen by the 15.5%, 55.2% and 79.3% COD

removal for 250PS, 500PS and 1000PS. After bottles were removed from heat for the unactivated persulfate stage, Merichem NA removal increased to ~90% for 250PS, mostly occurring in the first 30 days. At the higher persulfate concentrations (500PS and 1000PS), almost all Merichem NAs were oxidized during heat activation and no further removal was seen. Additionally, the 1000PS bottles did not show any improved COD removal and little change in persulfate concentration (Figure 4-5) suggesting the remaining by-products may not have been reactive with unactivated persulfate. COD removal increased 3× during the unactivated persulfate stage for 250PS, demonstrating the potential of lower persulfate doses despite longer reaction times.

OSPW similarly had most NAFC removal occurring during heat activation, with 45.2%, 76.3%, and 89.1% removal for 250PS, 500PS and 1000PS, respectively. However, less mineralization occurred with 0%, 18.5% and 26.0% COD removed for 250PS, 500PS and 1000PS. Unactivated persulfate oxidation increased NAFC removals to 69.5%, 89.8% and 95.1% for 250PS, 500PS and 1000PS. Mineralization was also improved for 1000PS (57.2% COD removed), however was relatively minor for 250 and 500PS (11.9% and 25.6% COD removal). Despite large reductions in NAFCs, OSPW exhibited less mineralization of organics compared to Merichem NAs.

Coupled Persulfate Oxidation + Biodegradation

After removing from heat, some bottles were inoculated with *P. fluorescens* to examine the potential for coupling residual unactivated persulfate oxidation with biodegradation (250-1000CPS). Both Merichem and OSPW did not show any significant difference in NAFC removal between chemical (PS) and coupled (CPS) treatments at each persulfate concentration ($p>0.05$). As most NAFCs were removed during heat activated persulfate reaction, it was

expected there would be little differences during the unactivated persulfate and biodegradation stage. The addition of bacteria was hypothesized to improve overall removal of organics in the system, however bottles containing *P. fluorescens* all showed an increase in COD. Soluble microbial products are known to increase BOD and COD during wastewater treatment due to substrate metabolism, biomass decay and cell lysis (Ni et al. 2011). Killed controls similarly saw some increase in COD, suggesting a portion is from cell lysis of dead biomass. The potential role of EPS in coupled treatments was discussed in Section 4.4.1. Solubilization and hydrolysis of EPS is another potential source of soluble microbial products that could increase the COD (Li et al. 2013, Mesquita et al. 2010, Ni et al. 2011).

Combining chemical oxidation and biodegradation has been previously shown to be a successful remediation method for OSPW (Brown et al. 2013, Dong et al. 2015, Martin et al. 2010, Wang et al. 2013b) (see Section 2.1.5). In this study, the addition of microbes did not improve the removal of organics from the system in terms of NAFCs or COD. The previous study (Chapter 3) did demonstrate successful coupling of persulfate activation and biodegradation. However, OSPW or diluted mineral media (BH) used here is a more stressful growth medium for bacteria compared to nutrient rich BH media used in Chapter 3. Furthermore, the higher concentrations of phosphate used as a pH buffer in BH media likely scavenged the persulfate (Section 4.3), possibly increasing the availability of carbon sources for microbes and preventing oxidative stress impacts. Combined treatments for OSPW often use ozone which is short lived and depleted before inoculation of bacteria (Dong et al. 2015, Martin et al. 2010, Vaiopoulou et al. 2015). As persulfate is a persistent oxidant, the activation time could be increased to remove more persulfate from the system, or persulfate could be quenched prior to addition of bacteria. Therefore, the residual simple, low molecular weight

organics that are often not as reactive with oxidants may have been biodegraded by bacteria in the absence of oxidative stress.

4.4.2 Contribution of Radicals

Unlike hydroxyl radical based AOPs such as catalytic ozonation, sulfate radical AOPs can generate both $SO_4^{\bullet-}$ and OH•. Radical quenching tests were performed to identify the contribution of each radical species during heat activation. Tert-Butyl alcohol (TBA) is often chosen to scavenge OH• with a rate constant of 3.8-7.6×10^8 $M^{-1}s^{-1}$, approximately 1000-fold greater than with $SO_4^{\bullet-}$ (4.0-9.1×10^5 $M^{-1}s^{-1}$). Ethanol (EtOH) is commonly used to scavenge both OH• and $SO_4^{\bullet-}$, with rate constants of 1.2-2.8×10^9 and 1.6-7.7×10^7 $M^{-1}s^{-1}$, respectively (Anipsitakis and Dionysiou 2004). While other ROS such as the singlet oxygen ($^1O_2$) and superoxide ion ($O_2^{\bullet-}$) have been identified during persulfate AOPs (Lee et al. 2020, Petri et al. 2011), quenching studies and EPR spectra suggest they play a minimal role so were excluded from this study (Ganiyu et al. 2022a, Lei et al. 2020).

Quenching tests were performed with 50 mg/L of Merichem NAs and 1000 mg/L PS at 60ºC for 8 hours, in either 5% BH or 5% BH supplemented with a carbonate buffer (5 mM). A carbonate buffer was used to mitigate pH drops and determine the impact of carbonate ions as radical scavengers due to their dominance in OSPW. Control bottles without any scavengers degraded 93% of Merichem NAs (Figure 4-8). Carbonate buffer controls had a similar final Merichem NA degradation after 8 hours, however exhibited a 3-fold decrease in degradation rate (Table A-6). The addition of TBA decreased final degradation to 67.5% and 71.1% for unbuffered and carbonate buffered systems, respectively, with a 2- to 4-fold decrease in rate compared to controls. EtOH further suppressed Merichem NA degradation, with only 21.7% and 31.2% degradation for unbuffered and carbonate buffered systems and an 8- to 14-fold

decrease in rate compared to controls. Even with the addition of a carbonate buffer, the pH in the EtOH system dropped (pH 5.5-5.8) and needed to be continuously adjusted with 1 M NaOH (Figure A-6). The reaction of EtOH with $SO_4^{\bullet -}$ produces H^+ ions (Neta et al. 1988) which were not fully mitigated with the carbonate buffer.

Overall, these results suggest that both sulfate and hydroxyl radicals play a role in the oxidation of Merichem NAs using heat activated persulfate, with $SO_4^{\bullet -}$ being the predominant radical species. The contribution of radical species will vary depending on the water chemistry, contaminants, and activation method. Xu et al. (2016b) found a similar trend for heat activated persulfate oxidation of a model NA compound (1,2,3,4-T-2-NA), with TBA inhibiting some degradation and EtOH almost completely inhibiting removal, suggesting the dominance of the sulfate radical. Heat activated persulfate is commonly studied as a treatment for pharmaceutical pollutants where the sulfate radical is similarly the primary ROS (Fan et al. 2015, Gao et al. 2018, Sun et al. 2019).

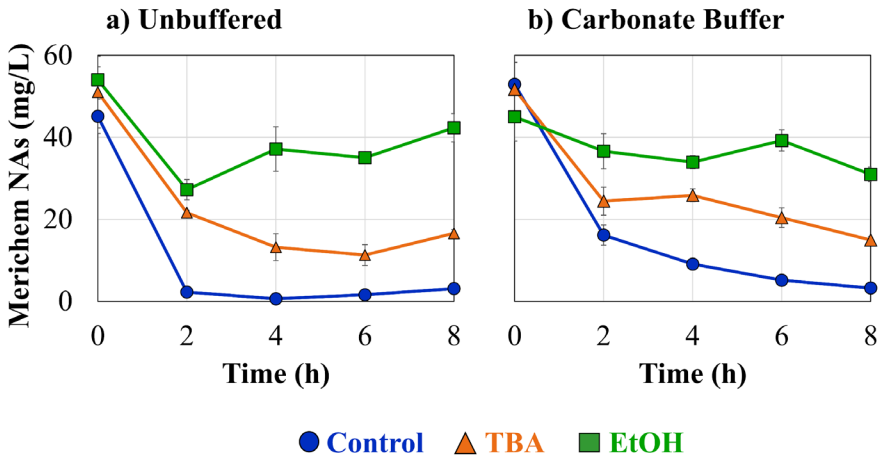

Figure 4-8. The effect of radical scavengers tert-butyl alcohol (TBA) and ethanol (EtOH) (30 mM) on Merichem NA removal with 1000 mg/L PS at 60°C in a) unbuffered 5% BH mineral media, or b) 5 mM carbonate buffer in 5% BH. Error bars represent one standard deviation of duplicate bottles.

Sulfate radicals also dominated in solar activated persulfate oxidation of PVA (Ganiyu et al. 2022a); however, Fang et al. (2018) found that hydroxyl radicals were more significant in the degradation of CHCA under UV activated persulfate. Hydroxyl radicals were also dominant in a system using peroxymonosulfate activated with biochar to oxidize ADA (Song et al. 2022). However, PMS with electro-cocatalytic iron activation found that the relative contribution of sulfate and hydroxyl radicals varied depending on which model NA compound was used (Chen et al. 2022b). Similarly, radical contribution shifted depending on the persulfate activation method for PHC degradation, where hydroxyl radicals dominated for UV activated persulfate, but sulfate radicals dominated with the addition of iron (Li et al. 2020).

Compared to AOPs that only involve hydroxyl radicals, persulfate AOPs have much more complex oxidation pathways that alter depending on water constituents and types of activators (Lee et al. 2020). This can provide a benefit as each radical preferentially oxidizes different types of compounds, potentially leading to more comprehensive removals. Model NAs are commonly used to determine structure reactivity and elucidate degradation pathway. Some studies have found that saturated aliphatic rings are more reactive than aromatic rings with persulfate and peroxymonosulfate (Chen et al. 2022b, Xu et al. 2016b), while others have found that aromatic rings are more reactive (Fang et al. 2018). Contradictory results could be due to differences in model NA structures and dominant radical species. The reactivity of the aromatic rings are strongly impacted by the substituents present, and the aromatic model NA (PVA) used by Fang et al. (2018) had a longer alkyl chain which increases reactivity (Lee et al. 2020). Furthermore, hydroxyl radicals dominated which are generally more reactive with aromatics. Conversely, Xu et al. (2016b) used a bicyclic aromatic (2-NA) in a system where

sulfate radicals dominated, illustrating why they were not as well oxidized since sulfate radicals selectively react with aliphatic carboxylic acids.

The improved oxidation of aliphatic carboxylic acids with $SO_4^{\bullet -}$ is because they react uniquely via decarboxylation, whereas OH• use hydrogen abstraction. For aromatic carboxylic acids, $SO_4^{\bullet -}$ still utilize decarboxylation while OH• more effectively use hydroxylation (Lee et al. 2020). Products identified during heat activated persulfate reaction of model NA compounds verified that decarboxylation was the initial step when sulfate radicals dominated (Xu et al. 2019b). A significant advantage to persulfate AOPs for OSPW is the generation of $SO_4^{\bullet -}$ and OH• which allow for more effective aliphatic acid oxidation.

4.4.3 NAFC Distribution

The distribution of NAFCs is helpful in determining treatment efficiency since different fractions are associated with varying recalcitrance and toxicity (further discussed in Section 4.4.4). Bottles containing 500 mg/L PS (500PS, 500CPS) and biological treatment bottles (0CPS) were analyzed via Orbitrap to determine changes in NAFC distribution over the course of the treatment. Distribution of classical O_2-NAs compared to oxidized (O_{3+}) and heteroatomic (N/S) classes is showed in Figure 4-9. A more in-depth analysis of the toxic O_2-NAs in terms of carbon numbers (n) and hydrogen deficiency as double bond equivalence (DBE) is provided in Figure 4-10, 4-11 and A-8.

Initial Distribution

Merichem NAs consist solely of the O_2 group (>99.9% abundance), predominantly containing more saturated NAs with DBE 1-3 (linear, 1 ring, 2 ring). These less complex structures are generally considered more biodegradable (Scott et al. 2005) and can account for the improved biodegradation noted for Merichem (Figure 4-6). OSPW initially has a wider

range of class distribution than Merichem NAs, consisting primarily of classical O_2-NAs, oxidized O_3 and O_4 NAFCs, along with a smaller abundance of heteroatomic N and S containing species. Within the O_2 group, OSPW contains higher DBE compounds, representing increase in hydrogen deficiency, with DBE 3, 4 and 7 the most abundant. This source of OSPW and Merichem have similar carbon numbers, ranging from n=10-19, with highest proportion being n=15 and 16. However, OSPW commonly has n=5-33 and DBE=1-10, with aged OSPW having a higher proportion of higher molecular weight, cyclic compounds (Bauer et al. 2015, Brown and Ulrich 2015).

Changes to Class Distribution with Different Treatments

Biodegradation of Merichem (0CPS) did not lead to any major changes in class distribution, with the O_2-NAs representing 96.9% abundance. After activated persulfate oxidation (500PS), both Merichem and OSPW bottles had a considerable reduction of the O_2 class, decreasing to 2.2% and 6.9% abundance, respectively, with a shift to more oxidized NAFCs (O_{3+}). Merichem bottles saw a notable increase in O_5 and O_8 class compounds along with nitrogen containing compounds (N_2O_2), while OSPW primarily increased in O_3, O_4 and O_5 compounds. Over the 120 days of residual unactivated persulfate reaction, treatments continued to shift to more oxidized NAFCs. This shift to more oxidized NAFCs (O_3-O_6) after AOPs is commonly seen for persulfate oxidation and ozonation (Abdelrahman et al. 2023, Arslan et al. 2023, Fang et al. 2019, Ganiyu et al. 2022a, Meshref et al. 2017). Often oxidized NAFCs do not change considerably during AOP treatments, possibly because the rate of removal is equal to the rate of formation. Additionally, the increased oxygen atoms can increase resistance to oxidation due to the reduction in electrophilic sites that are most susceptible to attack (Arslan et al. 2023).

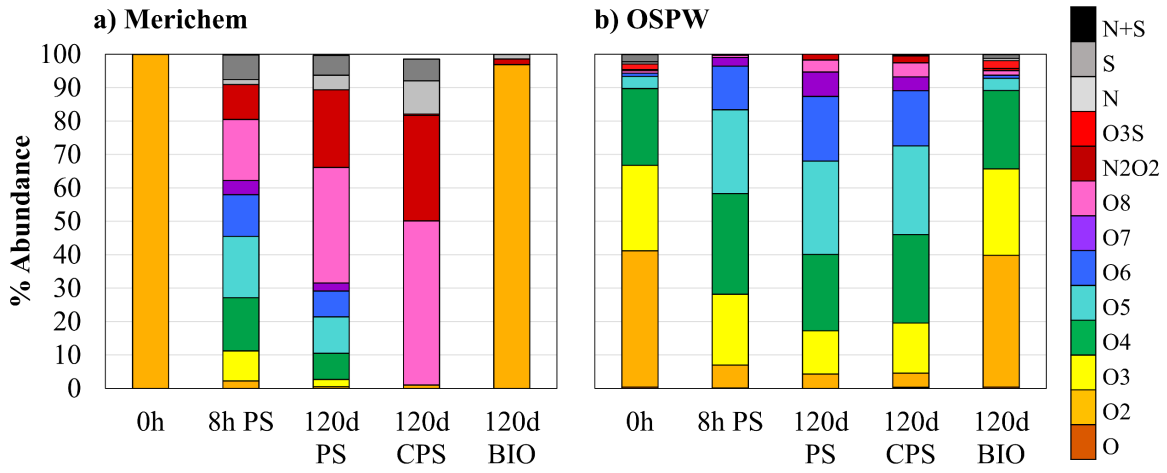

Figure 4-9. NAFC class distribution in a) Merichem NA and b) OSPW after 8 hours of heat activation (60ºC) followed by 120 days at room temperature. Treatments include: 500 mg/L persulfate oxidation after 8 hours of heat activation (8h PS) and 120d at room temperature (120d PS); coupled 500 mg/L PS and *P. fluorescens* after 120d at room temperature (120d CPS); and biological treatments with only *P. fluorescens* after 120d (120d BIO). Data represents single treatment bottles.

P. fluorescens in Merichem coupled treatments (500CPS) completely degraded the O_3-O_7 compounds, leading to a 14.5% and 8.3% increase in O_8 and N_2O_2 compounds. The lack of COD removal in CPS treatments (Figure 4-7) further supports that *P. fluorescens* was transforming NAFCs. Oxidized NAFCs are created as intermediates during biodegradation, and some studies have suggested they are more recalcitrant due to their persistence in aged OSPW and during laboratory biodegradation experiments (Han et al. 2009, Huang et al. 2017, Xue et al. 2016a). Coupling chemical oxidation and biodegradation may be more effective at removing oxidized NAFCs (Wang et al. 2013b, Xue et al. 2016a). Zhang et al. (2018a) found that ozonation and biofiltration alone did not removal any oxy-NAs, but the combined treatment removed 53% O_3-NAs and 43% O_4-NAs. Similar to trends for classical NAs, biodegradation of oxidized NAFCs may depend on cyclicity and carbon number (Zhang et al. 2016d).

O_2-NA Shifts in Carbon Number and DBE with Treatment

The O_2 class was mostly removed during persulfate oxidation, however the remaining NAs with varying carbon number and DBE can still contribute to bio-persistence. Heat activated persulfate preferentially oxidized higher molecular weight NAFCs, removing n>13 for Merichem and n>16 for OSPW, leading to a higher dominance of n=9-12. This is common in AOP treatments where radicals usually attack the C-H bond rather than O-H bond, so higher carbon number compounds have more hydrogen atoms available for radical abstraction (Afzal et al. 2012b). Conversely, higher carbon number NAFCs are considered more resistant towards biological treatment (Clemente et al. 2004, Han et al. 2009, Holowenko et al. 2002, Scott et al. 2005). However, inconsistencies with this correlation have been noted as it appears to be highly dependent on other structural features such as alkyl side chain branching and number of rings (Bataineh et al. 2006, Han et al. 2008).

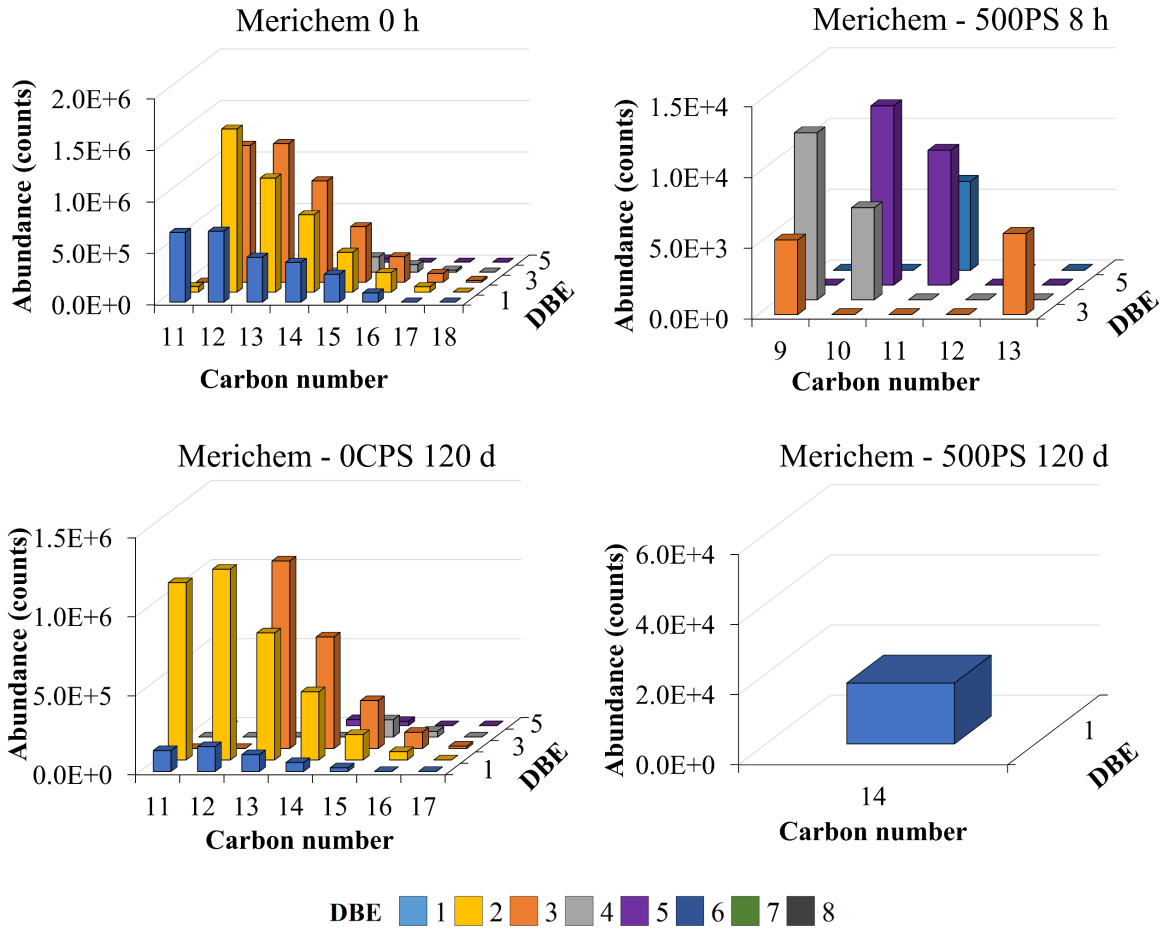

Figure 4-10. Classical O_2-NA distribution in Merichem NA bottles after 8 hours of heat activation (60°C) followed by 120 days at room temperature. Treatments include biological treatments containing only *P. fluorescens* (0CPS) and 500 mg/L persulfate oxidation (500PS). Plots illustrate abundance vs carbon number and double bond equivalence (DBE). Data represents single treatment bottles.

Heat activated persulfate preferentially oxidized higher DBE compounds in OSPW, completely removing highly unsaturated DBE 7 and 8 NAFCs. The higher hydrogen deficiency associated with the formation of rings increases tertiary carbons which increases reactivity with radicals due to the creation of more stable tertiary carbon-centered radicals after hydrogen abstraction (Chen et al. 2022b). Conversely, tertiary carbons hinder β-oxidation, which is thought to be the primary pathway utilized by bacteria during NAFC degradation (Whitby 2010). Therefore, cyclicity has been found to be a greater indicator of biodegradability than

carbon number, with decreasing biodegradation efficiency as DBE increases (Han et al. 2008, Huang et al. 2015, 2017, Wang et al. 2013b, Xue et al. 2016b, 2017). Unactivated persulfate continued to oxidize these cyclic, unsaturated compounds leading to simple and linear DBE 1 compounds remaining for Merichem, while OSPW saw a decrease in abundance of DBE 3-6 with an increase in DBE 1. This removal of highly unsaturated NAFCs is beneficial for future biological treatment which most effectively remove DBE <3 (Han et al. 2009, Huang et al. 2017, Islam et al. 2015).

Similarly, NAFCs with DBE>6 and n>15 have been shown to be preferentially oxidized in OSPW treated with UV activated persulfate and ozone, shifting to a higher abundance of DBE 3-4 compounds with n=10-14 (Meshref et al. 2017, Fang et al. 2019). Therefore, oxidized, lower molecular weight, and more saturated NAFCs are generally leftover after AOPs, regardless of oxidant or activation method. Since NAFC persistence is often tied to higher cyclization and molecular weight, chemical oxidation has the potential to be combined with biological treatments as the composition shifts to simpler, more biodegradable compounds.

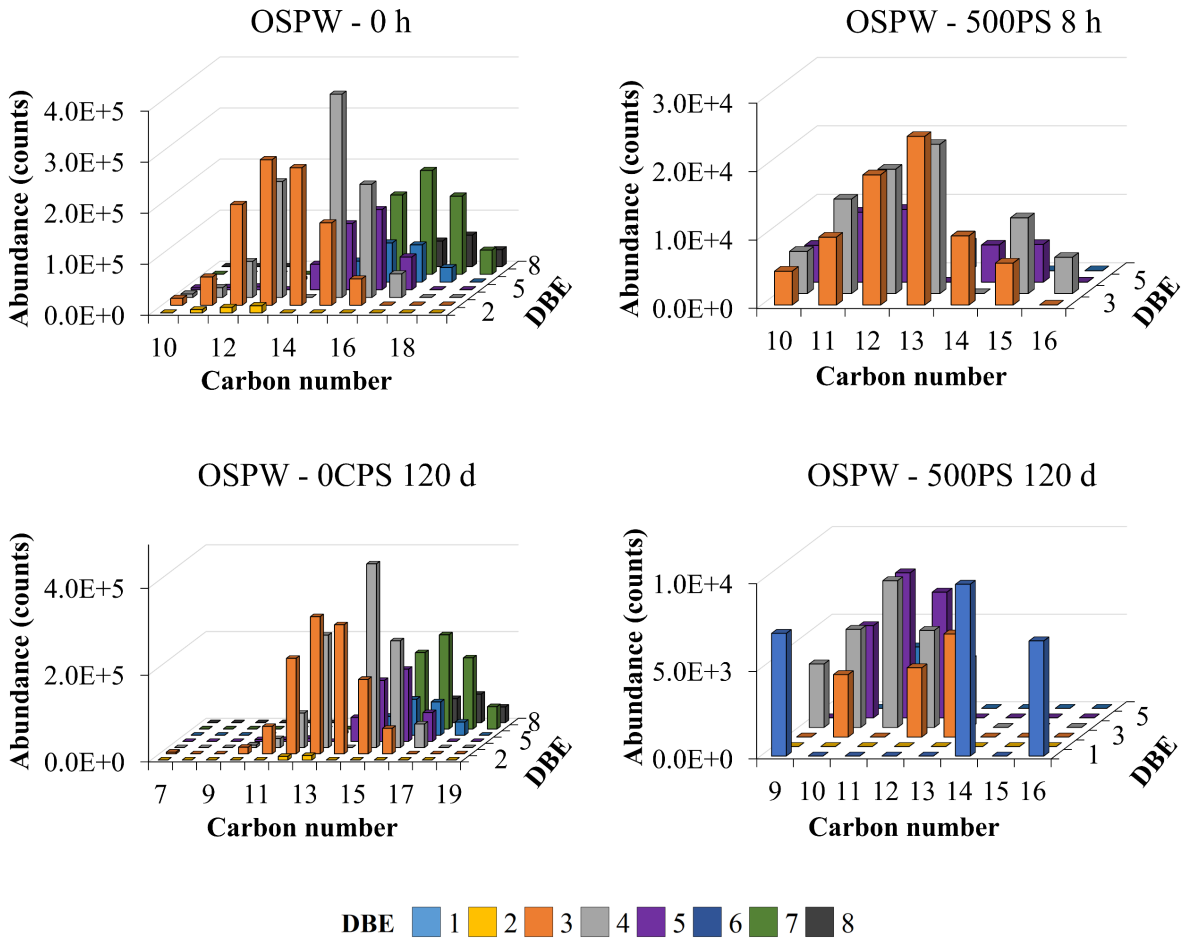

Figure 4-11. Classical O_2-NA distribution in OSPW bottles after 8 hours of heat activation (60°C) followed by 120 days at room temperature. Treatments include biological treatments containing only *P. fluorescens* (0CPS) and 500 mg/L persulfate oxidation (500PS). Plots illustrate abundance vs carbon number and double bond equivalence (DBE). Data represents single treatment bottles.

4.4.4 Acute Toxicity Assessment

OSPW is a complex water matrix, consisting of thousands of polar and nonpolar organics, suspended and dissolved solids, salts and metals, all of which can contribute to toxicity (Vander Meulen et al. 2022). Regardless, NAFCs are consistently found to be main contributors to acute toxicity due to their surfactant characteristics (Frank et al. 2008, Hughes et al. 2017, Li et al. 2017a). The toxicity of NAFCs is driven by molecular weight, aromaticity, and heteroatom content (Bauer et al. 2017); therefore, an overall reduction in NAFC concentration does not always correlate to toxicity reduction (He et al. 2012, Wang et al.

2013b). The Microtox bioassay is a simple, useful method to provide information on the quality of wastewater and is widely used for OSPW toxicity assessment (Clemente and Fedorak 2005, Yue et al. 2015). The inhibition effect towards *V. fischeri* bioluminescence was analyzed at various treatment stages, shown in Figure 4-12. Overall, Merichem and OSPW bottles showed opposite trends; while activated persulfate reduced Merichem toxicity, it increased OSPW toxicity. Further reaction with unactivated persulfate and biodegradation increased Merichem toxicity but reduced OSPW toxicity.

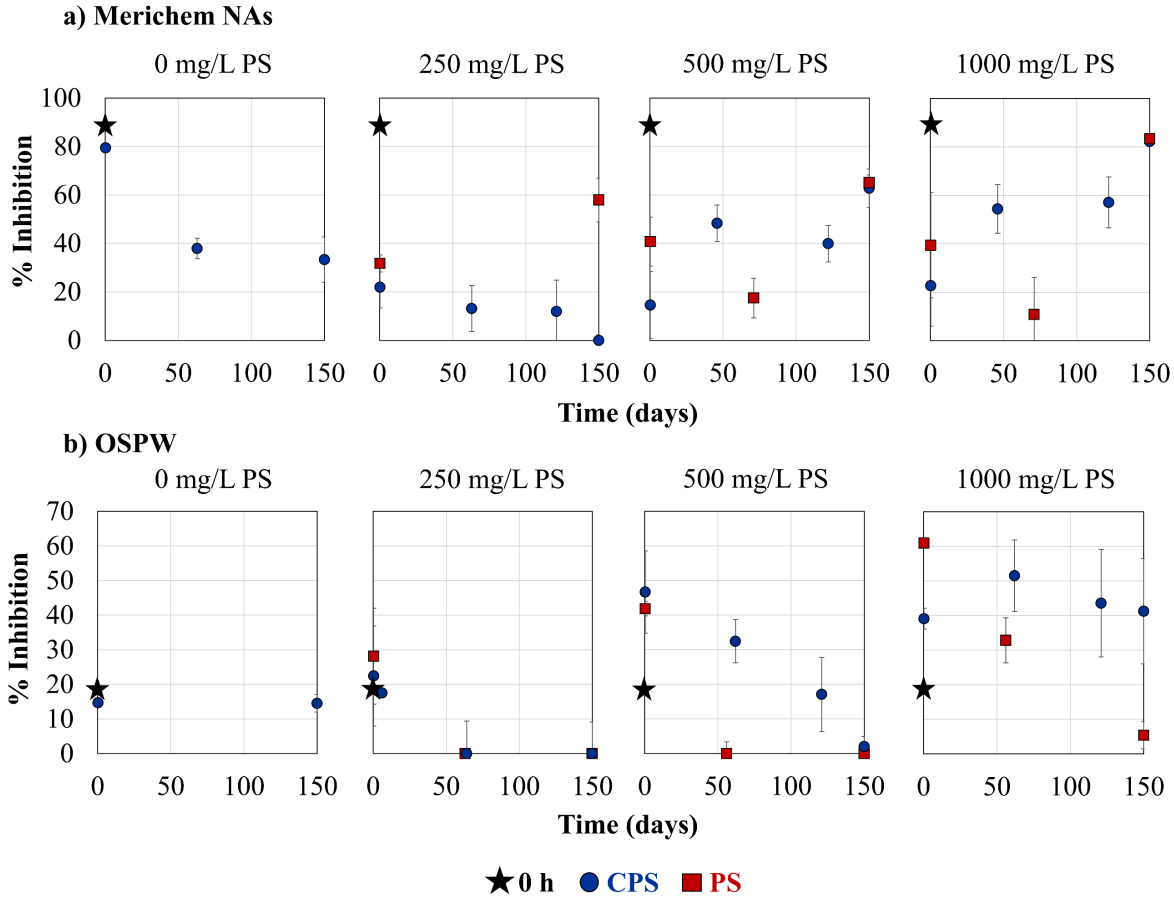

Figure 4-12. Percent inhibition of *V. fischeri* bioluminescence for a) Merichem NA and b) OSPW after 8 hours of heat activation (60°C) followed by 150 days at room temperature. Initial toxicity of Merichem NAs and OSPW represented as the black star. Treatments include persulfate oxidation (PS; ■) and persulfate coupled with *P. fluorescens* (CPS; ●). Error bars represent one standard deviation of triplicate bottles.

Contributions to Merichem NA Toxicity

Commercial NAs contain only the O_2 class which are considered the most acutely toxic fraction. The impact of the O_2 class can be seen by the high initial toxicity, exhibiting an 88.5% inhibition effect towards *V. fischeri.* Biodegradation by *P. fluorescens* reduced the toxicity 2.7-fold (33.3% effect). While the biological treatment did not show a major shift in class composition away from the acutely toxic O_2 group (Figure 4-9), the overall concentration of O_2-NAs was decreased which can account for the reduced toxicity.

In chemical oxidation treatments, the activated persulfate stage led to similar reductions in inhibition effect regardless of the persulfate concentration, showing 31.7%, 40.8%, and 39.4% effect after 8 hours, for 250PS, 500PS and 1000PS, respectively. While the toxicity was similar to that after biodegradation, they likely come from different sources. The biological bottles (0CPS) still contained predominantly O_2-NAs, whereas persulfate treatments (250-1000PS) saw almost complete removal of Merichem NAs (Figure 4-6) and the O_2 class (Figure 4-9). Furthermore, the distribution shifted to more oxidized NAFCs (O_{3+}) which are not generally associated with toxicity, possibly because the increased OH groups reduce hydrophobicity (Wang et al. 2013a, Yue et al. 2015). Therefore, in persulfate treatments, toxicity may be attributed to oxidation by-products or residual species that may not be captured in the acid extractable fraction (Meshref et al. 2017, Morandi et al. 2017). Residual toxicity despite high levels of O_2-NA removals is common in AOP treatments, and often attributed to incomplete mineralization (Dong et al. 2015, He et al. 2012, Martin et al. 2010, Meshref et al. 2017). Wang et al. (2013b) found that there was still 31-34% inhibition towards *V. fischeri* after ozonation of OSPW despite >90% NA degradation. Similarly, 2 mM of UV-activated

persulfate removed 84% of classical O_2-NAs which corresponded to only a 10% reduction in toxicity (Fang et al. 2019).

Over the remaining 150 days of the unactivated persulfate stage, all chemical treatments exhibited an increase in toxicity by day 150, reaching 58.0%, 65.1% and 83.4% for 250PS, 500PS and 1000PS, respectively. For 500PS, the primary difference in NAFC distribution between 8 hours and 120 days was the increase in O_8 and N_2O_2 classes, with the remaining O_2 class consisting of n=14, DBE 1 (Figure 4-9 and 4-10). None of these classes are associated with toxicity (Yue et al. 2015), which further suggests the residual toxicity components may not be represented in the acid extractable compounds. However, the lowest toxicity occurred at day 71, indicating that the transformation of by-products throughout the treatment shifts toxicity.

Merichem coupled treatments with persulfate and *P. fluorescens* (500CPS-1000CPS) exhibited some higher toxicity in the middle of the experiment (day 46-120), however had similar toxicity to their chemical treatment counterparts by day 150. Notably, 250CPS were the only coupled treatment that showed significantly improved toxicity reduction compared to chemical oxidation alone at day 150 ($p<0.05$). While the chemical oxidation bottles increased over time (58.0% effect), the coupled bottles remained significantly lower (<15.0% effect) before showing a complete removal of toxicity by day 150. This demonstrates the potential in a coupled remediation treatment where bacteria can degrade toxic oxidation by-products into non-toxic forms.

Contributions to OSPW Toxicity

The initial toxicity of OSPW was considerably lower than that of Merichem NAs, with a 18.2% inhibition effect towards *V. fischeri*. OSPW inhibition values vary with source and

age, but in general range from 29-53% with older OSPW exhibiting lower toxicity (Fang et al. 2019, Shu et al. 2014, Wang et al. 2016, Wang et al. 2013b, Zhang et al. 2016b).

Unlike Merichem NA bottles, OSPW exhibited a 1.5- to 3.3-fold increase in toxicity after activated persulfate oxidation, reaching 28.1%, 41.8%, and 60.9% inhibition for 250PS, 500PS and 1000PS, respectively. Residual O_2-NAs contained n=14-16 and DBE 3-5 (Figure 4-11) which are considered some of the most toxic compounds within the O_2-NA fraction (Yue et al. 2015). However, the overall abundance of these compounds decreased during the oxidation treatment, suggesting that while they may contribute to toxicity, they are likely not the primary cause. Similar to Merichem NAs, the increase in toxicity could be a cumulative effect of residual NAFCs and oxidation by-products. The production of toxic by-products has also been observed in other studies utilizing sulfate radical AOPs (Arslan et al. 2023, Ganiyu et al. 2022a). For example, the inhibition effect towards *V. fischeri* increased from 58% for raw OSPW to >95% after 3-6 hours of solar activated PMS treatment (Ganiyu et al. 2022a). Chlorinated by-products have been detected during persulfate oxidation of NAFCs, more notably when using higher concentrations of persulfate (Fang et al. 2020), which could explain why 1000PS had the highest toxicity. Despite the initial increased toxicity, all treatments (250-1000PS) exhibited significant toxicity reduction during the unactivated persulfate stage, showing no inhibition effect by day 150 ($p<0.05$; paired t-test between 8 hours and 150 days). Part of the toxicity reduction may be due to a decrease in DBE 3-4 O_2-NA compounds (Figure 4-11), along with continual transformation of by-products to less toxic compounds.

Coupled treatments containing persulfate and *P. fluorescens* (250-1000CPS) showed different trends depending on the persulfate concentration. Unlike Merichem NA bottles, 250CPS bottles for OSPW showed no improvement in toxicity reduction compared to 250PS.

Both 500CPS and 1000CPS exhibited higher toxicity than the chemical treatments, with 1000CPS reaching 41.2% inhibition by day 150, compared to the nontoxic 1000PS. The NAFC distribution shows 500CPS have almost double the abundance of the potentially toxic DBE 3 and 4 fractions in the O_2 group on day 120 (Figure A-8). More specifically, 500CPS contain $C_{15}H_{24}O_2$ (DBE 4, n=15) which has been found to be one of the most abundant compounds within toxic NAFCs (Yue et al. 2015) and was removed in the 500PS treatment (Table A-7, A-8). Furthermore, 500CPS bottles contained O_3S compounds, which have been thought to contribute to toxicity (Quesnel et al. 2015, Yue et al. 2015). While these toxic NAFCs are present in CPS and not PS treatments, their overall abundance is still low and likely contribute to some but not all of the increased toxicity.

Overall, these results suggest that the coupled treatments were not as effective as chemical oxidation alone for OSPW remediation, and in some cases the addition of microbes appears to have hindered detoxification. As discussed in earlier sections, there was less persulfate consumed and more COD in CPS bottles, possibly due to the formation of EPS and soluble microbial products which acted as antioxidants. These may have scavenged the persulfate away from organics, thus hindering the potential for detoxification. Future research should aim to analyze the oxidation by-products produced during persulfate oxidation to help elucidate the toxicity trends. Specialized toxicity assays for genotoxicity and estrogenicity along with in vivo studies can also provide more information.

4.4.5 Bacterial Viability

Viable cell counts were completed to determine the ability of *P. fluorescens* to proliferate by utilizing the remaining carbon sources, along with the impact of persulfate oxidative stress and wastewater toxicity. Biological (0CPS) and coupled treatments (250-

1000CPS) were inoculated with 10^8 CFU/mL after bottles were removed from heat, and viable cell counts were completed during the 150 days of unactivated persulfate reaction and biodegradation at room temperature, shown in Figure 4-13.

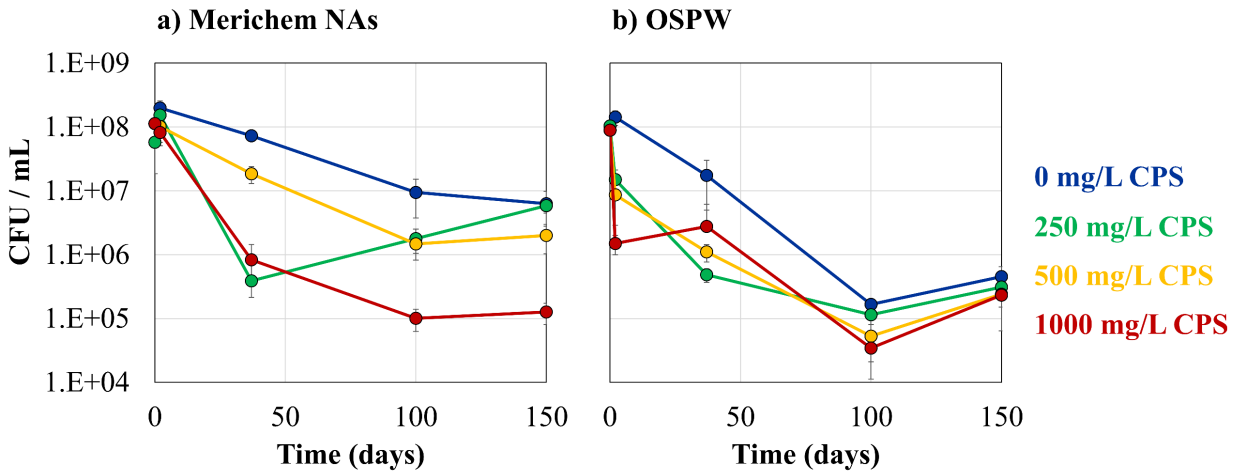

Figure 4-13. Colony forming units (CFU) on a semi-log plot for a) Merichem NA and b) OSPW biological and coupled treatments. Bottles were inoculated with *P. fluorescens* after 8 hours of heat activation once the temperature reached ~20°C. "0CPS" represent biological treatments without persulfate. Error bars represent one standard deviation of triplicate bottles.

Merichem biological treatments (0CPS) exhibited a 1 order of magnitude decrease in viable cells from day 2 to 100, likely due to the high toxicity of Merichem NAs. Regardless, the bacterial numbers at the end of the experiment (6×10^6 CFU/mL) were higher than in the previous study (1×10^5 CFU/mL) which ultimately supported higher degradation extents (Figure 4-6). Viable cell counts in coupled treatments (250-1000CPS) decreased 1.1 – 3.1 and 3.0 – 3.4 orders of magnitude by day 100 for Merichem and OSPW bottles, respectively. 250CPS initially showed the largest decrease, possibly due to the higher concentration of NAFCs compared to 500CPS and 1000CPS (Figure 4-6). 1000CPS maintained the lowest bacterial numbers throughout most of the experiment; these bottles also had higher concentrations of persulfate remaining in the system (2-4× higher than 250CPS and 500CPS) which could create oxidative stress. Microtox also showed the highest acute toxicity in

1000CPS treatments (Figure 4-12), indicating that in addition to oxidative stress, there could be toxic intermediates hindering cell growth. Furthermore, 1000CPS had the lowest COD remaining after activated persulfate treatment, particularly in Merichem bottles (Figure 4-7), limiting bioavailable carbon sources.

All OSPW treatments exhibited a much sharper decrease in viable cell counts compared to Merichem, with less variability between persulfate concentrations. However, Microtox analysis showed Merichem bottles as more acutely toxic than OSPW (Figure 4-12). OSPW has many more compounding factors that can contribute to microbial stress and reduced cell viability. For example, the pH range of OSPW (>8.5) may be too high for the ideal growth of *P. fluorescens* which generally prefers pH 4-8 (Moore et al. 2006). Furthermore, OSPW bottles had higher persulfate and sulfate concentrations (Figure 4-4, 4-5) which may have increased oxidative and osmotic stress. While sulfate anions have been found to be less toxic to microbes than chloride in terms of microbial respiration, the increased ionic strength from sulfate has similar impacts on decreasing bacterial growth as cells move energy away from biomass production and towards maintenance (Rath et al. 2016). These stresses may not be accounted for in Microtox, where the persulfate is quenched, pH is adjusted and the test bacteria is a marine organism that may not be impacted by the increased salinity (Johnson 2005).

For both OSPW and Merichem, the number of viable cells began to recover between day 100 and 150, indicating the lag phase required for the bacteria to acclimate to the stressful environment. Furthermore, this increase in cell viability corresponds with a decrease in COD in the 250-1000CPS bottles between day 120 and 150 (Figure 4-7). The previous study ran for >300 days and showed improved mineralization in coupled treatments (Section 3.3.1); therefore, improved COD removal and biomass growth may have been seen over more time.

The Merichem 250CPS bottles saw a significant increase in viable cell counts from day 37 to 150 ($p<0.05$; paired t-test), reaching the same number of cells as treatments without persulfate (0CPS) which improved detoxification (Figure 4-12). This increase in viable cells may be tied to the decreasing concentration of persulfate in the system (Figure 4-5). Similarly, 250 mg/L PS provided the highest viable cells counts (4×10^5 CFU/mL) in the previous study (Section 3.3.3). These results suggest that lower doses of oxidant are preferred when coupling with biodegradation and the resulting higher biomass may be correlated to improved toxicity reduction.

4.5 Conclusions

Heat activated persulfate was effective in significantly reducing concentrations of NAFCs in OSPW by 45 – 89%. The acutely toxic O_2 group was mostly removed, shifting to more oxidized O_3-O_5 NAFCs. Furthermore, higher molecular weight ($n>16$) and unsaturated (DBE 7 and 8) NAFCs, which are more recalcitrant to biodegradation, were preferentially oxidized. OSPW contains radical scavengers such as chloride and thus activated persulfate oxidation required longer reaction times compared to Merichem NAs bottles. However, unactivated persulfate was utilized at a 2.6 – 3.8× higher rate in OSPW, indicating there may have been some activation occurring from trace iron or reactive functional groups on organics. The toxicity of OSPW initially increased (1.5 – 3.3×) after activated persulfate reaction, likely from oxidation by-products and residual NAFCs ($n=14$-16 and DBE 3-5 in O_2-NAs). However, samples were non-toxic after continued reaction with unactivated persulfate. As COD did not decrease considerably, this indicates the organics were being transformed into less toxic compounds. Future research should focus on identifying the oxidation by-products that may be contributing to toxicity.

The addition of *P. fluorescens* during the unactivated persulfate stage did not improve the treatment and in some cases was detrimental. Merichem bottles showed there was some degradation occurring to more oxidized NAFCs, however there was no change in OSPW NAFC distribution compared to chemical oxidation treatments. Furthermore, OSPW coupled treatments exhibited an increase in COD and decreased the persulfate utilization rate up to 11×. Persulfate may have been less reactive with organics in the presence of bacteria due to the formation of EPS, which can act as antioxidants and can chelate iron that may have been providing some persulfate activation. Over the first 100 days viable cell counts decreased by up to 3 orders of magnitude, which could be due to inadequate growth medium, oxidative stress, toxic intermediates, or a lack of bioavailable carbon sources. Overall, the decreased utilization of persulfate and decreasing viable cells negatively impacted the treatment efficiency, as seen by increased toxicity, up to 40% higher in coupled treatments compared to persulfate oxidation alone. 250CPS for Merichem NAs was the only coupled treatment that saw improved toxicity reduction (58%) compared to chemical treatments and provided the highest number of viable cells. This suggests that cell viability is tied with treatment efficiency and a higher biomass was needed for coupled OSPW bottles to be successful. Quenching the persulfate prior to bacteria inoculation may have decreased stress on the cells and led to improved treatments. However, viable cells began to recover after 100 days, at which point there was a slight decline in COD suggesting there may have been further improvements seen over more time.

NAFCs are a significant contributor towards the acute toxicity of OSPW. This study established that persulfate concentrations as low as 250 mg/L can reduce OSPW NAFC concentrations by 45% after 8 hours of heat activation. Persulfate AOPs are advantageous in

creating both sulfate and hydroxyl radicals which preferentially oxidize aliphatic and aromatics respectively, leading to more comprehensive overall removals. Lower persulfate concentrations are preferred as they lower costs, reduce the amount of sulfate produced and create a better environment for microorganisms when coupling with biodegradation. Coupling persulfate oxidation with biodegradation can potentially be a feasible remediation strategy; however, future research is needed to make coupling persulfate oxidation with biodegradation a viable option for OSPW.

Chapter 5

Impact of Salt on Anaerobic Benzene Biodegradation by a Highly Enriched Methanogenic Consortium

5.1 Introduction

BTEX are widespread contaminants largely due to accidental petroleum spills, leaks and other industrial discharges that can occur at upgrading facilities, refineries, storage facilities and gas plants (Paustenbach et al. 1993, Lovley 2000, NPRI 2023). Benzene is particularly problematic as it is highly mobile, recalcitrant and a known carcinogen, with the allowable concentration in groundwater set at 0.005 mg/L in Alberta (Bennett 1999, Government of Alberta 2022). Remediation methods commonly used to treat benzene contamination include excavation, pump and treat, soil vapour extraction, in situ chemical oxidation and bioremediation (U.S. EPA 2018, FRTR 2023). Bioremediation offers a low cost and non-intrusive option, and benzene is biodegraded relatively easily aerobically, often over days or weeks (CCME 1999, Lovley 2000). However, anaerobically benzene biodegradation is much more challenging as it is often inconsistent and has considerable lag phases up to 200 days (CCME 2004, Foght 2008, Vogt et al. 2011). Bioaugmentation with a well-developed anaerobic benzene degrading culture may be useful for sites with deep contaminated sediments that are otherwise not easily treated. Methanogenic cultures are of particular interest as the microbes are not limited by an exogenous electron acceptor and there is no need to inject nutrients into the subsurface (Luo et al. 2016). Methanogenic benzene degrading bacteria belong to a few clades that are all closely related, primarily in the class *Deltaproteobacteria* (now proposed to be *Desulfobacterota*) (Qiao et al. 2018, Phan et al. 2021, Toth et al. 2021). DGG-B is a highly enriched methanogenic benzene-degrading culture, containing the benzene fermenting bacteria *Deltaproteobacteria* Candidate Sva0485 (ORM2) that was established in 1995 (Nales et al. 1998). Scale up and commercialization of DGG-B has been ongoing and has shown success in bioaugmentation trials (Toth et al. 2021).

During oil and gas extraction, water produced as a byproduct (produced water) contains not only BTEX, but also other contaminants such as PAHs, phenols, organic acids and natural organic matter (NOM), in addition to being brackish with salt concentrations ranging from 10 – 270 g/L (Fathepure 2014, Akbari et al. 2021, Chen et al. 2022a). Most of these salt brines consist primarily of sodium chloride (NaCl), which can cause further complications at oil and gas impacted sites. Salts can impact microbes from osmotic stress or specific ion toxicity. Cells require positive turgor pressure for cell growth, and therefore the osmotic pressure of the cytoplasm must exceed that of the medium, otherwise cells will experience dehydration and lysis (de Souza Silva and Fay 2012, Martin et al. 1999, Yan et al. 2015). Chloride has shown to have higher specific ion toxicity than other salts (Na^+, K^+, SO_4^{2-}), as it can inhibit enzymes (Sindhu and Cornfield 1967, Rath et al. 2016). Most halotolerant microbes use the compatible solute strategy in response to an increase in osmotic pressure of the medium, where they synthesize and accumulate organic solutes (osmolytes). These osmolytes can enhance EPS production and form a protective layer around the cell, in addition to interacting directly with proteins to stabilize them (Hu et al. 2020, Martin et al. 1999, Poli et al. 2010). However, creating osmolytes requires a large amount of energy which reduces the energy available for cell growth, leading to decreased activity of cells (de Souza Silva and Fay 2012).

With salt co-contamination becoming an increasing concern at oil and gas sites, it is vital to understand how salt will impact bioremediation, particularly for microbes that are from naturally non-saline environments. For aerobic hydrocarbon biodegradation, salt has been shown to reduce degradation rates, increase lag times and shift the microbial community composition (Chapter 2, Table 2-7). However, the impact appears to be dependent on factors such as the hydrocarbon of interest, temperature, and nutrients. Few studies have looked at the

impact of salt on anaerobic hydrocarbon biodegradation in naturally non-saline environments; however, anaerobes appear to be more sensitive to salinity than aerobic degraders (Tao and Yu 2013, Xia et al. 2022, Chen et al. 2022b, Jiang et al. 2023). To-date, only two studies have looked at the impact of salt on anaerobic benzene biodegradation. Tao and Yu (2013) compared benzene degradation rates in marsh sediments with different salinity, however the microbes in these sediments were likely already adapted to the salt concentrations. Chen et al. (2022b) explored changes to the microbial community composition in aerobic and anaerobic regions of a BTEX and salt co-contaminated aquifer where benzene biodegradation was not occurring. Therefore, the impact of salt on anaerobic benzene biodegradation is still largely unknown. This study aimed to explore the effect of salt (as NaCl) co-contamination on the anaerobic biodegradation of benzene by a highly enriched methanogenic culture, DGG-B, to help determine the bioaugmentation potential. The objectives of this study were to: **1)** establish the salt concentrations that reduce benzene degradation rate; **2)** determine if the salt tolerance can be improved by a slow acclimation strategy; **3)** identify if benzene fermenting bacteria or methanogenic communities were more sensitive to salinity; and **4)** observe any shifts in the microbial community structure with increased salinity.

5.2 Materials and Methods

5.2.1 Materials

Unless otherwise stated, all materials were purchased from Thermo Fisher Scientific (MA, USA). Mininert valve screw caps (24/400 mm) were purchased from Sigma-Aldrich (ON, Canada) (Product Number 33304).

The benzene-degrading methanogenic DGG-B culture was supplied by SiREM laboratories (Guelph, ON). DGG-B originates from an oil refinery in Oklahoma (OR) and has

been enriched since 1995, previously described in literature (Nales et al. 1998, Burland and Edwards 1999, Ulrich and Edwards 2003, Luo et al. 2016). Large scale (100 L) vessels of DGG-B are currently being maintained at SiREM.

DGG-B is grown in mineral media containing amorphous iron sulfide (FeS) as a reducing agent, resazurin as redox indicator, and amended with 250 – 350 µM of benzene as required. See Appendix A-2 for the full recipe and instructions.

5.2.2 Experimental Set Up

All work was carried out in an anaerobic glovebox (Coy Laboratory Products Inc., MI, USA) with an atmosphere consisting of 85% N_2, 10% CO_2, 5% H_2. Positive controls refer to DGG-B as it is normally maintained, and thus contained only the amount of salt already present in the mineral medium (~0.6 g/L NaCl, 2.7 g/L TDS, 4 dS/m). Salinity experiments were carried out in 40 mL EPA vials with Mininert caps, containing 30 mL of 100% v/v DGG-B. Solid NaCl was added to reduce dilution effects, to final concentrations of 2.5, 5, 10, 15, 25, 50, and 100 g/L. Electrical conductivity values were calculated to be 6, 9, 15, 21, 35, 65 and 127 dS/m, based approximate estimates of the anaerobic mineral media TDS (Appendix A-2). Bottles containing 10 g/L NaCl were set-up 121 days after the other bottles. "No Acclimation" refers to experiments where DGG-B was immediately spiked with NaCl, while "Slow Acclimation" refers to experiments where 1 g/L solid NaCl was added approximately every 2 – 4 degradation cycles. Experiments with live cells were carried out in triplicate. Killed controls were carried out in duplicate using DGG-B that had been autoclaved 3 times, 24 hours apart. After adding DGG-B and NaCl, the headspace of the bottle was purged with a gas mix containing 80% N_2 and 20% CO_2. Neat benzene was added when required to a target concentration of 320 µM aqueous benzene (total 10.3 µmol benzene/bottle). Bottles were

stored in the dark, upside down to reduce potential gas exchange with the anaerobic chamber atmosphere.

In order to determine the impact of salt on the methanogens present in DGG-B, another experiment was conducted where DGG-B was sparged of benzene and fed 40 mM of acetate ("Acetate Fed"), or the headspace was purged with an 80% H_2 and 20% CO_2 gas mix ("H_2 Fed"). Salt was added to final concentration of 5 and 25 g/L, with positive controls at 0.6 g/L NaCl. Mininert caps are not adequate at holding pressure and can allow for some gas exchange, particularly for hydrogen. Therefore, H_2 Fed bottles were refreshed with 1mL of 80/20 H_2/CO_2 gas mix approximately every 2 weeks.

5.2.3 Analytical Methods

Benzene and methane concentrations were determined using an Agilent 7890A gas chromatographer (GC) equipped with a flame ionization detector (FID) with a HP-5 methylsiloxane (30 m x 250 µm x 0.25 µm) column and helium used as a carrier gas. Headspace samples (100 µL) were collected using a 500 µL gas-tight syringe. The oven temperature was held at 50ºC for 4.5 min. The injector was set at 250ºC and 17.45 psi with total flow of 19.5 mL/min, septum purge flow of 3 mL/min and split (10:1) flow 15 mL/min. The column was set at 50ºC, 17.45 psi at 1.5 mL/min. The detector set at 250ºC, with 40 mL/min H_2, 450 mL/min air and 25 mL/min makeup (N_2). Methane eluted at 1.5 min and benzene at 2.4 min. Calibration was carried out using external benzene and methane standards. Headspace benzene concentration was converted to aqueous benzene concentration using Henry's Law (dimensionless H = 0.22), and total benzene in bottles (µmol / bottle) calculated on mass basis of 30 mL liquid and 10 mL headspace. For benzene standards under high salinity (>15 g/L NaCl), the Setschenow equation was used to calculate adjusted Henry's Law

constants and account for reduced benzene solubility in water (Table A-14; Figure A-12). Benzene degradation rates were calculated using zero order kinetics (μmol/L/day) for each degradation cycle, as the model with the best fit for the defined timeline and concentrations of benzene used during refeeding events (320 – 60 μM aqueous benzene; 10.3 – 2.1 μmol total benzene/bottle). When measurements were not able to be taken, initial benzene concentration immediately following feeding events were estimated and are indicated as white circles on graphs and were not used in calculations. Statistical analysis was conduced using one-way analysis of variance (ANOVA) in Microsoft Excel, with significance set at $p < 0.05$. Further, post hoc Turkey's test was used to determine significant differences between conditions (Table A-17).

In methanogen enrichment experiments, 1 mL of sample was taken periodically and filtered with a 0.22 μm nylon filter to measure acetate. Acetate was measured on a Dionex ion chromatography (ICS-2100, Dionex™ IonPac™ AS18 IC columns). Eluent (KOH) conditions were as follows: 10 mM from 0 – 7 min, 10 – 32 mM from 7 – 9 min, 32 mM from 9 – 20 min, 32 – 10 mM from 20 – 22 min, and 10 mM from 22 – 23 min. Eluent flow rate was 0.25 mL/min. Oven and detector temperature was 30°C and 35°C, respectively. Detection occurred using an anion self-regeneration suppressor (ASRS 2 mm) at 20 mA current. System backpressure was 1500 – 2000 psi and background conductance was lower than 2 μS.

5.2.4 DNA Extraction and Analyses

1.5 mL of sample was collected in microcentrifuge tubes and centrifuged at 5000 rpm for 5 min. Genomic DNA was then extracted using FastDNA™ Soil Kit (MP Biomedicals, CA, USA) according to manufactures instructions. Quantitative PCR (qPCR) was conducted using universal 16S rRNA gene primers for bacteria and archaea, as well as specific primers

for Sva0485 class *Deltaproteobacteria* (ORM2) (Table A-15). Enriched methanogen samples were only assayed for total archaea.

qPCR was conducted using a Bio-Rad CFX96 optical reaction module conversion C1000 Touch thermal cycler. A 10 µL qPCR mix contained 1 µL of extracted gDNA template, 5 µL SsoFast EvaGreen SuperMix 2x (Bio-Rad Laboratories, CA, USA), 500 nM of each primer, in HyPure™ Molecular Biology Grade Water (Cytiva, Marlborough, MA). Cycle conditions were as follows: enzyme activation at 98ºC for 2 min, denaturation at 98ºC for 5 sec, annealing at 55ºC for bacteria and 59ºC for ORM2 and archaea for 5 sec, with denaturation and annealing repeated over 40 cycles. Melt curve was completed at 65-95ºC in 0.5ºC increments for 5 seconds each. Samples were completed in technical triplicates. An absolute quantitative standard calibration curve was generated for each run using 6 or 7 ten-fold serial dilutions of a known quantity of appropriate 16S rRNA gene-containing plasmids. E. Coli 16S rRNA sequences cloned into ThermoFisher™ TOPO4 plasmids were used for general bacteria assays (supplied by BioZone, University of Toronto). Synthesized plasmids with gene fragments targeting *Methanoregula* and ORM2 were used for general archaea and ORM2 assays (Twist Bioscience, San Francisco, CA, USA). The coefficient of correlation for all standard curves was greater than 0.99 and efficiencies fell between 97 – 107 % (Figure A-13, A-14, A-15).

The relative abundance of microorganisms in each sample was determined using 16S rRNA gene amplicon sequencing with primers targeting the V6-V8 region. Amplification and Illumina sequencing (MiSeq 300 PE; paired end) was completed by McGill University at Genome Quebec Innovation Centre. Amplicon sequence reads were generated using modified, staggered end primers 926F (AAACTYAAAKGAATWGRCGG) and 1392R

(ACGGGCGGTGWGTRC), where 0 – 3 random bases were inserted between the primer and Illumina adaptor sequences. Read processing and sequencing analyses were performed by C. Toth (BioZone, University of Toronto) using QIIME 2 software (Bolyen et al. 2019) and listed as amplicon sequence variants (ASVs) based on the SSU SILVA 132 database (Quast et al. 2013). *Candidatus* Yanofskubacteria was reclassified as *Candidatus* Nealsonbacteria based on the NCBI and RDP database (Toth et al. 2021). ASVs with relative abundance >3% were used in graphing. Absolute abundance (copies/mL) was calculated multiplying qPCR total bacteria copy numbers by bacteria relative abundance, and qPCR total archaea copy numbers by archaea relative abundance.

5.3 Results and Discussion

The following sections assess the impact of salinity on the methanogenic benzene-degrading culture DGG-B. Differences between sudden salt shock and slowly acclimating the culture to NaCl were evaluated, along with an analysis on the impact to methanogens. Benzene degradation and methane production rates were compared, along with growth of the benzene degrading bacteria ORM2, and shifts in microbial community composition.

5.3.1 Benzene Degradation and Methane Production

Benzene consumption and methane production was monitored over 205 days in microcosms containing DGG-B that had not been previously acclimated to salt ("No Acclimation"; Figure 5-1). Killed controls did not show any reduction in benzene or production of methane, indicating degradation in active microcosms was due to microbial metabolism (Figure A-9). In all active bottles, methane production corresponded to benzene consumption with a measured ratio of 3.4 ± 0.07 (n=21) mole of methane generated per mole benzene consumed (Table A-11), similar to the expected stoichiometric value of 3.6 (Ulrich and

Edwards 2003). Benzene degradation rates in control bottles (0.6 g/L NaCl) increased from 9.0 μM/day initially (Figure 5-2) to >19.9 μM/day by day 52, where it remained until increasing between day 170 and 205 (33.9 – 54.6 μM/day). These rates are consistent with those previously described in literature for DGG-B, which ranges from 1.4–33 μM/day (Nales et al. 1998, Ulrich and Edwards 2003, Luo et al. 2016, Toth et al. 2021). These high benzene degradation rates under methanogenic conditions have been produced consistently over decades while being scaled up to commercial volumes, illustrating the strong potential of DGG-B as a bioaugmentation culture.

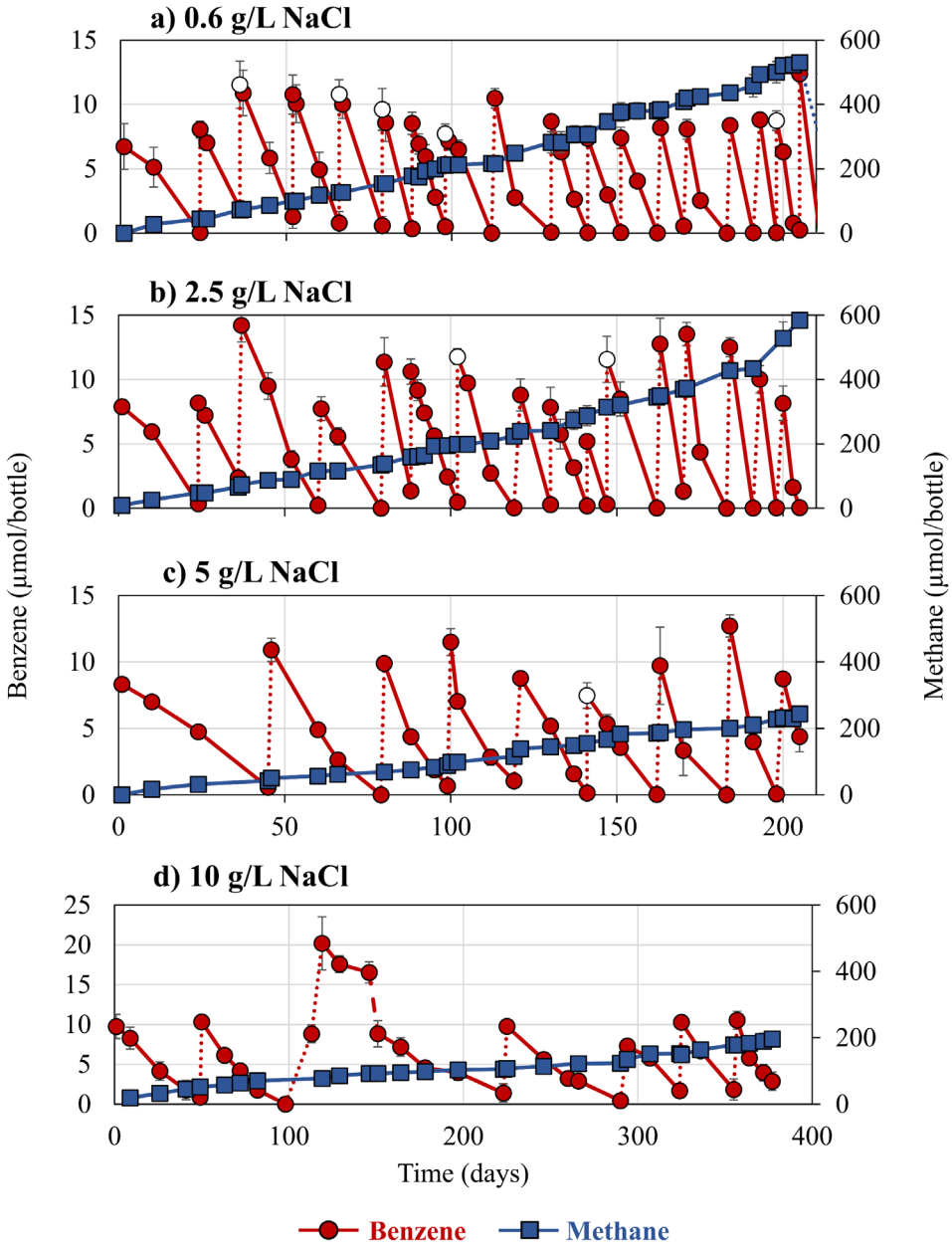

Figure 5-1. Benzene consumption and methane production in DGG-B for a) positive controls (0.6 g/L NaCl), b) 2.5 g/L NaCl, c) 5 g/L NaCl, and d) 10 g/L NaCl for culture not previously acclimated to salt. Dotted lines represent refeeding events. White circles indicate estimated concentrations. Error bars represent ± one standard deviation of triplicate bottles.

Increasing salt concentrations from 0.6 to 10 g/L significantly impacted the initial and final (day 205) benzene degradation rates ($p < 0.05$), with most impacts seen at 5 and 10 g/L. The addition of NaCl to a final concentration of 2.5 g/L did not appear to show any statistically

significant differences in initial or final (day 205) benzene degradation rates compared to the 0.6 g/L positive controls. Further increasing the salt concentration to 5 g/L NaCl led to a 1.6× reduction in benzene degradation rate (5.5 µM/day) compared to controls. However, the microbes appeared to slowly adapt to the increased stress from the salt, reaching 27.0 µM/day by day 205, which was not statistically different from control bottles ($p > 0.05$).

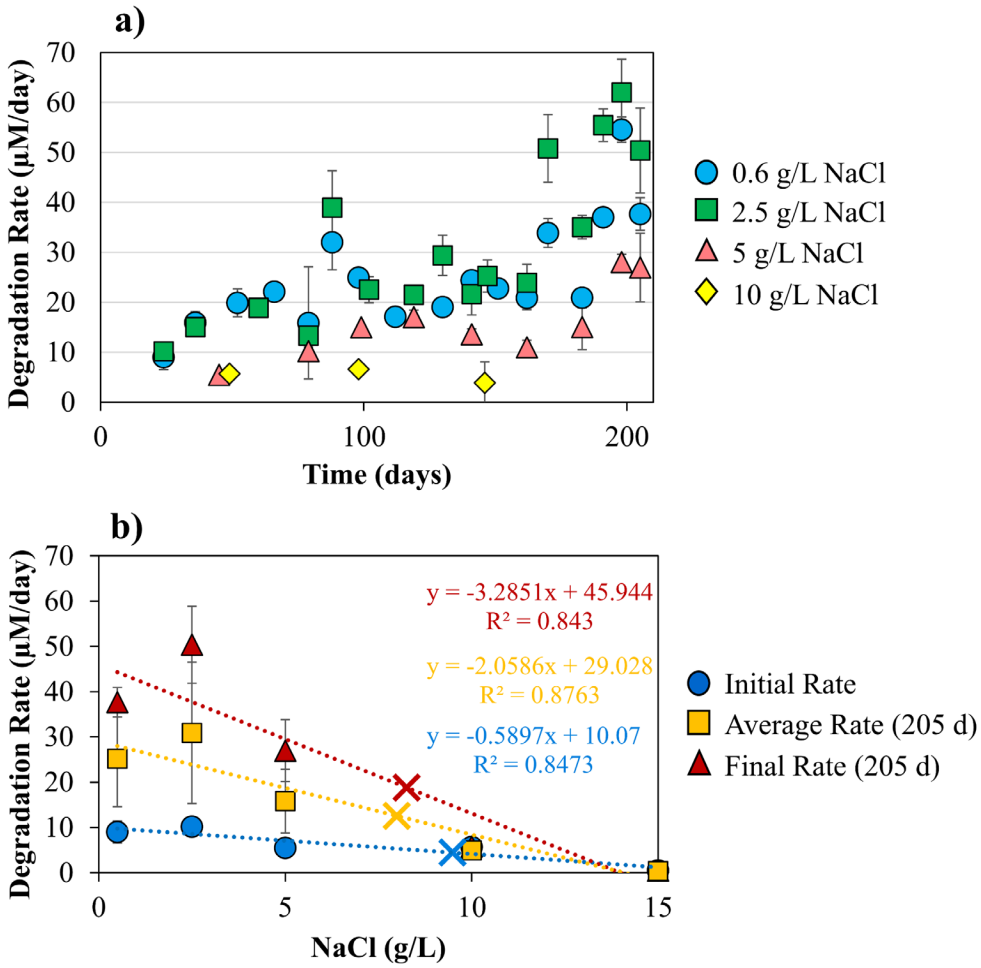

Figure 5-2. a) Benzene degradation rate over time in DGG-B not previously acclimated to salt; b) average benzene degradation rate at various NaCl concentrations. "×" represents the NaCl concentration that causes to a half reduction in rate. Error bars represent ± one standard deviation of triplicate bottles.

Initial degradation rates in microcosms containing 10 g/L NaCl were not statistically different compared to those at 5 g/L NaCl (5.7 μM/day; $p > 0.05$). However, final rates by day 205 were significantly higher at 5 g/L NaCl, while the rate did not start increasing in 10 g/L NaCl microcosms until after 355 days (8.7–11.8 μM/day; Figure A-11). Cells under osmotic stress can show decreased activity due to the metabolic load needed to create stress tolerance mechanisms (de Souza Silva and Fay 2012). A disruption to the microcosms occurred between day 98 and 119, and cultures were fed a higher concentration of benzene than usual (620 μM vs 320 μM). The headspace was sparged (day 146) to reduce benzene concentration to usual levels, and the microcosms were monitored for an extended period (371 days) to determine if degradation rates would eventually increase.

The NaCl concentration that leads to a half reduction in benzene degradation rate was found to range between 8.0 and 9.5 g/L (average 8.4 g/L NaCl) based on the initial rates, average rate over 205 days, or final rate at day 205 (Figure 5-3). Salt concentrations of 15 – 100 g/L NaCl showed minimal to no benzene degradation over 207 days (Figure A-10). Some methane production occurred compared to killed controls (Figure A-9), most notably in 15 g/L NaCl bottles over the first 24 days.

Few studies have examined the impact of salt on benzene biodegradation (as discussed in Section 2.2.4, Table 2.7). Lee and Lin (2006) found that increasing NaCl from 1 g/L to 10 g/L led to decreased benzene degradation rates in an aerobic trickle bed bioreactor, however benzene degradation occurred even at the relatively high concentration of 50 g/L NaCl. Similar to the trends in this study, Rhykerd et al. (1995) found that a lower concentration of 4 g/L NaCl reduced the aerobic mineralization of motor oil. However, other studies have generally found that detrimental impacts are not seen until after 10–20 g/L NaCl, with decreasing hydrocarbon

biodegradation rates and increasing lag times (De Carvalho and Da Fonseca 2005, Hua and Wang 2014, Ulrich et al. 2009). Aerobic biodegradation of model alkane hydrocarbons and diesel oil by soil sediments gave similar removals up to 20 g/L (Hu et al. 2020, Zhang et al. 2021), while further increasing to 30 g/L completely inhibited growth (Zhang et al. 2021). Aerobic biodegradation of crude oil by *Pseudomonas sp.* was improved with 55% biodegradability up to 10 g/L NaCl but reduced significantly to 30–10% biodegradability when salinity increased from 20–50 g/L (Hua and Wang 2014).

The impact of salt on a microbial consortium will vary depending on which hydrocarbon is added as a substrate, possibly due to different salt tolerances of the primary degrading species (Ulrich et al. 2009, Zhang et al. 2021). Aromatic hydrocarbon degrading microbes have been found to be more sensitive to salinity than those for saturated hydrocarbons (Longang et al. 2016). Various other factors can also influence the impact of salinity on biodegradation. Akbari et al. (2021) found that mineralization of hexadecane was enhanced by salinity (0–50 g/L NaCl) in the absence of nutrients, however, was significantly inhibited by salinity when the culture was grown with nutrients. Furthermore, the metabolic respiration process will also play a role in the impact of salt. Most studies on salt co-contamination in naturally non-saline environments are carried out for aerobic cultures which have more energy available and may be better able to withstand osmotic stress effects than anaerobic microbes. An anaerobic toluene degrading culture showed a 1.7 to 4-fold reduction in toluene removal when increasing salinity from 1 g/L NaCl to 10-20 g/L NaCl (Jiang et al. 2023).

Non-halophilic microorganisms are classified as being capable of growth up to 10 g/L NaCl (Fathepure 2014). This indicates that the DGG-B consortium is not halophilic as benzene degradation stalled at 15 g/L NaCl. DGG-B appears to be sensitive to salt, with concentrations

as low as 5 g/L NaCl impacting activity, and 8.4 g/L NaCl the average concentration that reduces benzene degradation rate by half. In contrast, aerobic hydrocarbon biodegradation often appears unimpacted at much higher salt concentrations. Increasing NaCl concentrations up to 10 g/L stimulated aerobic mineralization of hexadecane, phenanthrene, pyrene and crude oil, while further increasing NaCl led to decreased rates of degradation (Hua and Wang 2014, Li et al. 2022, Ulrich et al. 2009). There are many more microorganisms capable of aerobic hydrocarbon degradation that may be present in sediments, and studies have shown that there is a shift in microbial community to more halotolerant organisms with increasing salinity (Akbari et al. 2021, Li et al. 2022, Qin et al. 2012). Conversely, anaerobic benzene biodegradation occurs with very few microbial clades (Toth et al. 2021) which limits adaptability under changing environmental conditions. Furthermore, there is less energy available for these microbes anaerobically compared to aerobically, so they may be more inhibited by salt when they divert energy towards stress adaptation.

DGG-B Salt Tolerance with Slow Acclimation

In order to improve the salt tolerance of DGG-B, bottles were established where 1 g/L NaCl was added every 2-4 degradation cycles ("Slow Acclimation"; Figure 5-3). A disturbance occurred to the bottles between days 218 and 233. Over the first 205 days, benzene degradation continued to increase at the same rate as that of control bottles despite salt levels reaching 6.5 g/L NaCl (Figure 5-4). Furthermore, the average degradation rate was 29.5 µM/day once reaching 10.5 g/L NaCl (Day 339), which is 6.0× higher than the average rate in no acclimation bottles at 10 g/L (4.9 µM/day). Similarly, Chen et al. (2020b) found gradual acclimation improved the salt tolerance of an anaerobic filter treating hypersaline molasses wastewater, in which biogas production was otherwise inhibited. The > 25 µM/day rate was maintained up

to 11.5 g/L NaCl; however, control bottles (0.6 g/L NaCl) showed a continually increasing rate, often > 40 µM/day. This suggests that the proliferation of ORM2 may have been slowed compared to control bottles as cells switched their energy towards maintenance and away from growth. Once salt levels reached 12.5 g/L NaCl, the rate began to decrease to 14.5 – 15.9 µM/day.

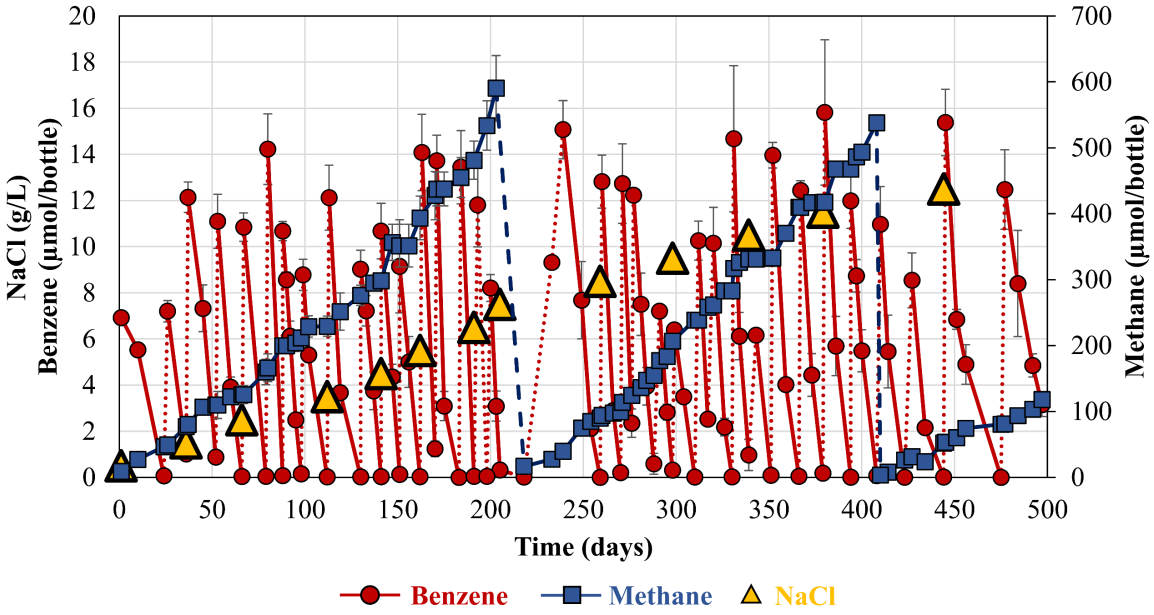

Figure 5-3. Benzene consumption and methane production in Slow Acclimation bottles. 1 g/L NaCl was added every 2 – 4 degradation cycles (▲). Dotted lines represent refeeding events. Dashed lines represent sparging event once methane concentration was >70% of headspace. Error bars represent ± one standard deviation of triplicate bottles.

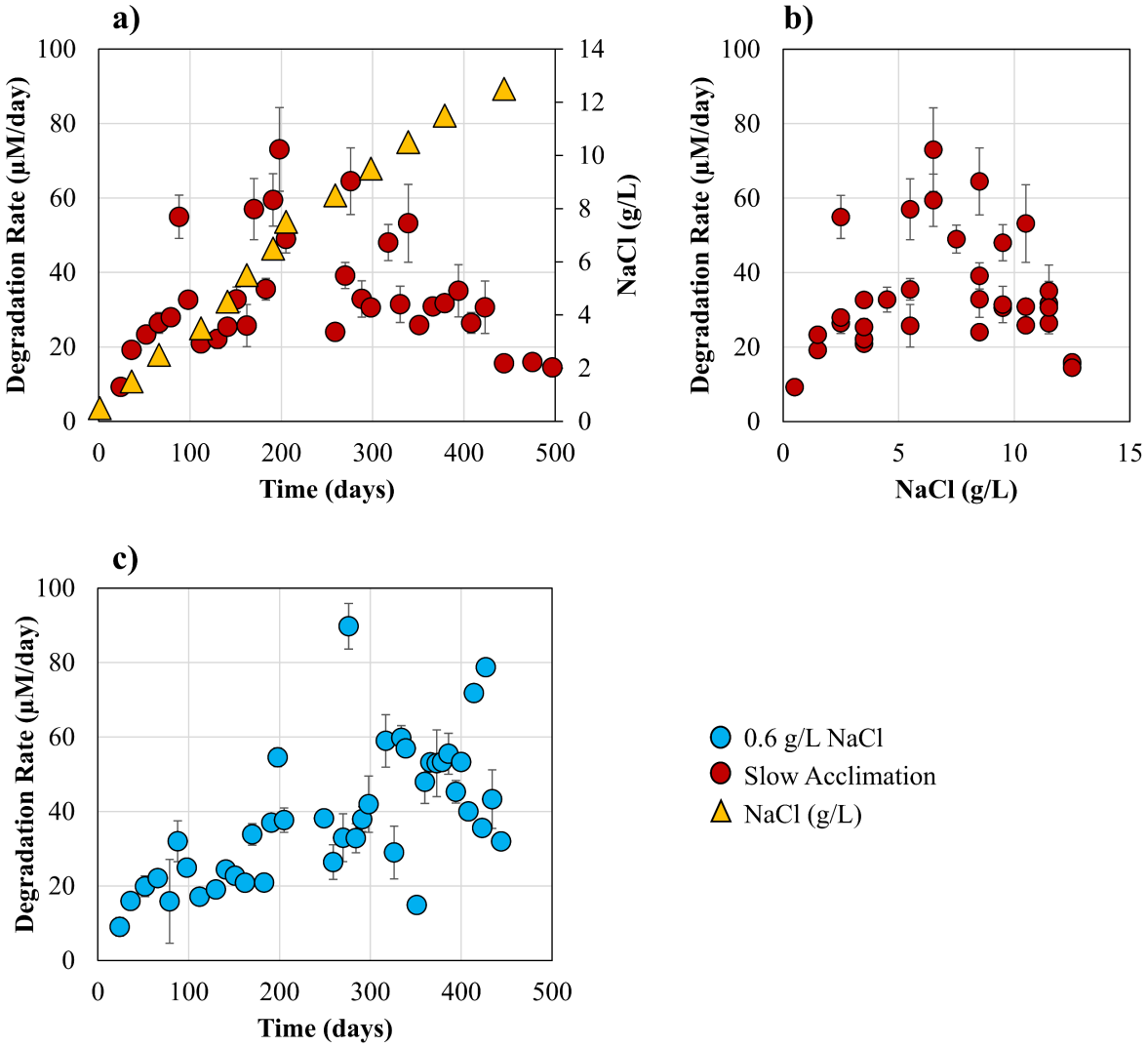

Figure 5-4. a) Benzene degradation rate over time in DGG-B culture slowly acclimated to salt by adding 1 g/L NaCl every 2 – 4 degradation cycles (▲); b) average benzene degradation rate at various NaCl concentrations; c) benzene degradation rate over time in positive control DGG-B (0.6 g/L NaCl). Error bars represent ± one standard deviation of triplicate bottles.

Most halotolerant bacteria use the compatible solute strategy to adapt to osmotic stress, where they produce or accumulate organic osmolytes that act as a barrier against the high salt levels of the water matrix (Oren 2002, Akbari et al. 2021). Production of these osmolytes requires significant and ongoing energy expenditure (Hoehler et al. 2010), and by slowly introducing the microbes to salt allows for time to build up levels of osmolytes. Another strategy to increase salt tolerance is the addition of osmolytes into the water matrix to lessen

the energy needed for cells to produce them and encourage EPS production (Hu et al. 2020). Glycine betaine is most commonly used and has been found to improve methane production in anaerobic digestion of food waste by 29–63% for up to 10 g/L NaCl (Liu et al. 2019). The impact of suppling an exogenous osmolyte to improve DGG-B salt tolerance could be explored in the future. However, osmolytes such as glycine betaine can act as a carbon source which may hinder benzene consumption.

Impact of Salt on Enriched Methanogens

Benzene degradation under methanogenic conditions requires a syntrophic group of microorganisms working in consort to make it energetically favourable. Therefore, salinity (15 g/L NaCl) may have caused benzene degradation to stall due to osmotic stress effects on multiple species or an individual microorganism. To help elucidate if the rate limiting step in benzene degradation was due to the benzene fermenting ORM2 or the methanogens, DGG-B was sparged of benzene and supplemented with either acetate or hydrogen/carbon dioxide to enrich the methanogenic community.

Control bottles (0.6 g/L NaCl) fed acetate produced the most methane in the first 39 days, after which it slowed and plateaued as the acetate had been consumed (Figure 5-5). Increasing the salt to 5 g/L NaCl gave similar final amounts of methane, however significantly reduced the methane production rate by 1.4-fold compared to control bottles ($p < 0.05$) (Table A-12). At 25 g/L NaCl there was a lag phase of over 31 days before methane production began, and the rate was even more significantly reduced by 5.4-fold compared to control bottles ($p < 0.05$). The ratio of acetate consumed to methane produced during exponential growth was found to range from 1.0–1.8, which is close to the theoretical ratio of 1.0 mole acetate/mole methane.

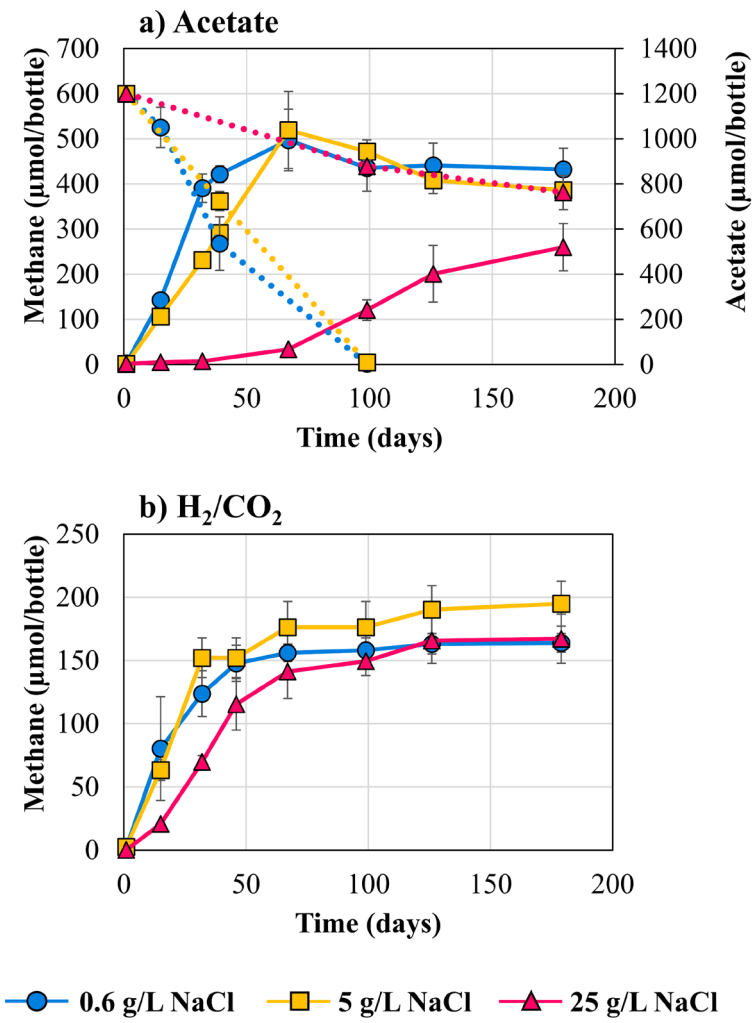

Figure 5-5. Methane production (solid lines) and acetate consumption (dotted lines) in DGG-B culture that was sparged of benzene and fed a) 40 mM acetate, or b) headspace was purged with 80% H_2 and 20% CO_2. Error bars represent ± one standard deviation of triplicate bottles.

Bottles supplemented with hydrogen and carbon dioxide (headspace 80:20, H_2:CO_2) overall produced less methane than those with acetate. Hydrogen is poorly soluble in water (1.6×10^{-6} g H_2 / g H_2O) and bottles were not continuously mixed which may have decreased the amount of hydrogen dissolved in the water. Additionally, Mininert caps are not adept at holding pressure which is generally recommended to encourage hydrogen solubility. Stoichiometrically, 4 moles of H_2 produce 1 mole of CH_4. Theoretically 80% of H_2 in the

headspace (~8 mL) can produce approximately 89 µmol of CH_4; considerably less than what can be produced by the amount of acetate added (1200 µmol CH_4). Methane production plateaued after 46 – 67 days and no statistically significant differences in overall methane production between salt concentrations were observed ($p > 0.05$) with no lag phases. However, methane production rate was 1.5-fold lower at 25 g/L NaCl compared to 0.6 and 5 g/L NaCl ($p < 0.05$). These results suggest that the respiration of hydrogenotrophic methanogens was less impacted by salt than acetoclastic methanogens. Similarly, increasing salinity has been shown to shift the microbial community from acetoclastic towards hydrogenotrophic in anaerobic digestors (Chen et al. 2022a, Gao et al. 2022).

Overall, these results indicate that methanogenesis is not the rate limiting step when benzene degradation stalls at > 10 g/L NaCl. In the presence of an adequate supply of substrate, methanogens were still actively producing methane up to 25 g/L NaCl. Conversely, Chen et al. (2022a) found that the methanogenic archaea were most susceptible to elevated levels of salinity at BTEX and salt co-contaminated oil field site. Similarly, methanogens have been shown to be more sensitive than bacteria to salinity during anaerobic digestion of waste activated sludge (Oliveira et al. 2021, Gao et al. 2022). However, this is likely strongly dependent on the bacteria present.

5.3.2 Growth and Proliferation of ORM2

Salinity and other stressors can impact microbial respiration and microbial growth differently (Rath et al. 2016). Furthermore, benzene degradation rate can be impacted by confounding variables such as the amount of benzene fed and sampling intervals. Therefore, the impact of salinity on microbial proliferation was measured using qPCR with primers specifically designed to target the benzene degrading bacteria ORM2 (Figure 5-6). Control

bottles (0.6 g/L) showed a considerable increase in ORM2 copy numbers over time, reaching 5.6×10^7 and 3.6×10^8 by day 100 and 200, respectively. Increasing the salt to 5 g/L NaCl initially led to a steep decrease in ORM2 concentration to 3.4×10^6 copies/mL, an 8× decrease from initial concentrations and over one order of magnitude lower than control bottles at day 100. By day 200 ORM2 concentration rebounded, which may explain the increase in degradation rate noted by day 198 (Figure 5-2).

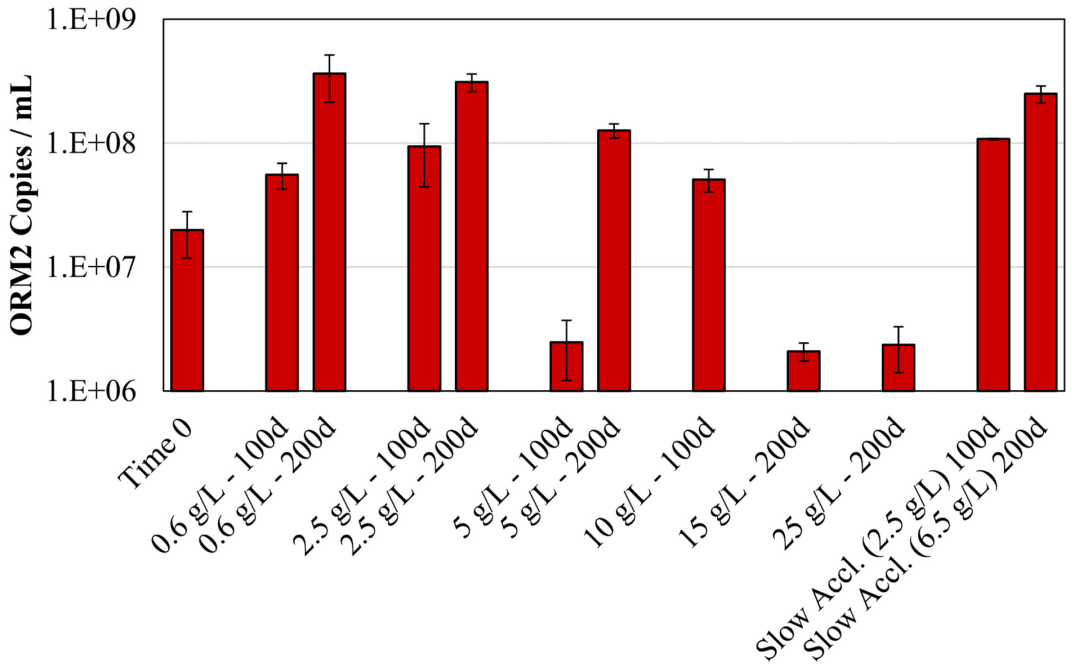

Figure 5-6. ORM2 copy numbers per mL of culture for positive controls (0.6 g/L NaCl), DGG-B not acclimated to salt (2.5 – 25 g/L NaCl) and DGG-B slowly acclimated to salt. Time 0 samples were taken from the original DGG-B bottle before inoculating into experimental bottles. 10 g/L NaCl was set up at a later date and time 0 is assumed to be similar to that of positive controls bottles at 100 d. Error bars represent ± one standard deviation of triplicate bottles.

As stated earlier, 10 g/L NaCl bottles were established from a 0.6 g/L maintenance culture approximately 100 days after the other experimental bottles. Since the maintenance culture was fed and measured at the same time as 0.6 g/L positive control experimental bottles, the initial concentrations of ORM2 in 10 g/L were assumed to be similar to that of 0.6 g/L

control bottles at day 100 (5.6×10^7 copies/mL). At 10 g/L NaCl ORM2 did not appear to exhibit much proliferation as concentrations after 100 days (5.1×10^7 copies/mL) were only slightly lower than the estimated initial concentrations. Interestingly, ORM2 did not exhibit the same steep decrease in copy numbers in the first 100 days that was noted for 5 g/L NaCl (8× decrease). Possibly the higher initial concentrations of a more established culture allowed ORM2 cells to better withstand osmotic shock. Alternatively, the culture may have rebounded more quickly, and initial stress impacts may not have been captured in the first 100 days. Regardless, even with the ORM2 concentration in the same order of magnitude as control bottles, they still exhibited a 3.8× lower benzene degradation rate (Figure 5-2).

Further increasing the salt to 15 – 25 g/L NaCl stalled benzene degradation and ORM2 copies were substantially reduced (~2×10^6 copies/mL), over 2 orders magnitude lower than control bottles at day 200. DGG-B not exposed to any stressors has previously shown active benzene degradation when 10^5 – 10^6 ORM2 copies/mL were present (Luo et al. 2016, Toth et al. 2018). This indicates that under osmotic stress ORM2 may require higher concentrations to achieve benzene degradation, or that ORM2 cannot function at higher salt regardless of the cell concentration. Similarly, Toth et al. (2021) found that a higher concentration of ORM2 was required for adequate benzene degradation in the presence of hydrocarbon co-contaminants.

Over the experiment timeframe, the doubling time of ORM2 in control bottles decreased from 72 to 52 days (average 62 days) (Table 5-1). Furthermore, the yield increased from 1.9×10^4 to 1.2×10^5 copies/nmol benzene at day 100 and 200, respectively, consistent with the increase in degradation rates (Figure 5-2). The doubling time for ORM2 listed in literature are 20 – 34 days with yields of 3×10^5 copies/nmol benzene (Luo et al. 2016, Toth et al. 2021).

The longer doubling times and lower yields noted in this study may be due to culture stress during experiment set-up, or variations in lab techniques. At 2.5 g/L NaCl, ORM2 doubling times had an average of 49 days, similar to that of control bottles.

Table 5-1. Doubling time and yields for DGG-B positive controls (0.6 g/L NaCl), DGG-B not previously acclimated to salt (2.5, 5 g/L NaCl) and slowly acclimated to salt (Slow Accl.). Calculations were completed between day 0 and 100 (100 d) and day 100 and 200 (200 d).

Sample / NaCl (g/L)		***Doubling Time (d)***		***Yield (copies/nmol)***		**n**
		Average	Std. Err.	Average	Std. Err.	
Slow Accl.	2.5 g/L (100 d)	41	0	3.2E+04	1.4E+02	2
	6.5 g/L (200 d)	86	8	4.4E+04	7.8E+03	3
	Overall	68	11	3.9E+04	5.3E+03	5
0.6 g/L	100 d	72	8	2.6E+04	9.7E+03	3
	200 d	52	18	1.7E+05	2.0E+02	3
	Overall	62	11	8.4E+04	3.2E+04	6
2.5 g/L	100 d	37	0	5.5E+04	4.6E+03	2
	200 d	58	12	6.4E+04	3.8E+03	3
	Overall	49	8	6.0E+04	3.6E+03	5
5 g/L	100 d	N/A	N/A	N/A	N/A	N/A
	200 d	17	3	6.9E+04	7.8E+03	3
	Overall	N/A	N/A	N/A	N/A	N/A

At 5g/L NaCl, over the first 100 days ORM2 exhibited faster rates of cell decay than growth, corresponding to the lower degradation rates seen over this period. However, by day 200, ORM2 experienced considerable rebound and between day 100 and 200 gave the shortest doubling time of 17 days, with yields similar to that at 2.5 g/L NaCl. There was also a large increase in the degradation rate between day 183 and 198. These results suggest a halotolerance at 5 g/L NaCl after a lag period. At 10 g/L NaCl the bottles exhibited more variability, which is common when there are greater stressors (Ulrich et al. 2009). Two replicates exhibited only decay over the first 100 days and one replicate had a 198 day doubling time; while 15 and 25 g/L NaCl only exhibited decay over the 200 days studied (Table A-16). Despite benzene

consumption actively occurring at 5 and 10 g/L NaCl, microbial growth was significantly hampered as cells experienced fast decay rates.

Slow acclimation bottles exhibited doubling times of 41 days by day 100 when salt levels were 2.5 g/L NaCl, similar to control bottles. Interestingly, between day 100 and 200 when salt levels increased up to 6.5 g/L NaCl the doubling time increased to 86 days, indicating some stress to cells despite no decrease seen in degradation rates. Furthermore, whereas yields increased in control bottles over time, they remained relatively consistent in slow salt acclimation bottles.

Overall, ORM2 was initially inhibited at 5 g/L NaCl exhibiting only decay but was able to recover. Rebound at 10-25 g/L NaCl was not noted in the timeframe analyzed. As mentioned earlier, ORM2 likely synthesizes compatible solutes (osmolytes) as a protection mechanism against osmotic stress. Osmolytes enhance the production of EPS and cause cells to aggregate (Poli et al. 2010, Hu et al. 2020), which was visually observed in bottles containing high levels of salt (Figure A-22). As cells are stressed, they shift their energy away from cell growth and towards stress adaptation and maintenance (de Souza Silva and Fay 2012). Lee and Lin (2006) showed that salt significantly decreased the biomass in a trickle bed bioreactor and increased the energy spent on cell maintenance from 19-24% at 1 g/L NaCl to 86-91% with >10 g/L NaCl.

5.3.3 Microbial Community Analysis

The relative abundance of microorganisms was determined with 16S rRNA gene amplicon sequencing and, where available, combined with qPCR data for total bacteria and archaea copy numbers to provide the absolute abundances.

Initial DGG-B Microbial Community Structure

Initially, the DGG-B consortium consisted predominantly of bacteria, with total bacterial copies representing 68% of the microbial community. *Deltaproteobacteria* Sva0485 (ORM2), *Pseudopelobacter* ASV1, *Candidatus* Omnitrophus ASV1 and *Acetobacterium* ASV1 represented the dominant bacteria species, representing 33.2%, 14.7%, 6.5% and 6.8%, respectively (Figure 5-7). The dominant archaea consisted of *Methanosaeta* (ASV1, ASV2), *Methanobacterium* ASV1 and *Methanoregula* (ASV1, ASV2), at 57.8%, 20.5% and 11.0%, respectively (Figure 5-8).

Methanogenic benzene degradation depends on syntrophic relationships between fermenting bacteria, acetogenic bacteria and methanogenic archaea (Vogt et al. 2011). DGG-B consistently contains high abundances of OMR2, *Ca*. Nealsonbacteria (OD1), *Ca*. Omnitrophica (OP3), *Methanosaeta* and *Methanoregula* (Luo et al. 2016, Toth et al. 2021, Guo et al. 2022). ORM2 is the benzene fermenting bacteria as its growth has been unequivocally linked to benzene degradation (Luo et al. 2016), and *Acetobacterium* are acetogenic bacteria that partially oxidize organics from benzene degradation into acetate for methanogens to consume. *Ca*. Omnitrophica and *Ca*. Nealsonbacteria likely represent biomass recyclers that appear to preferentially attach to *Methanosaeta* as host cells (Kuroda et al. 2022, Guo et al. 2022, Chen et al. 2023, Seymour et al. 2023). The presence of hydrogenotrophic and acetoclastic methanogens indicates the formation of hydrogen and acetate during benzene fermentation. Similarly, a benzene-degrading methanogenic enrichment culture from Japan consists predominantly of the benzene fermenter *Deltaproteobacterium* Hasda-A, which is nearly identical to ORM2, an OD1 biomass recycling bacterium, along with both

hydrogenotrophic (*Methanoregula* and *Methanolinea*), and acetoclastic (*Methanosaeta*) methanogens (Sakai et al. 2009, Noguchi et al. 2014, Phan et al. 2021).

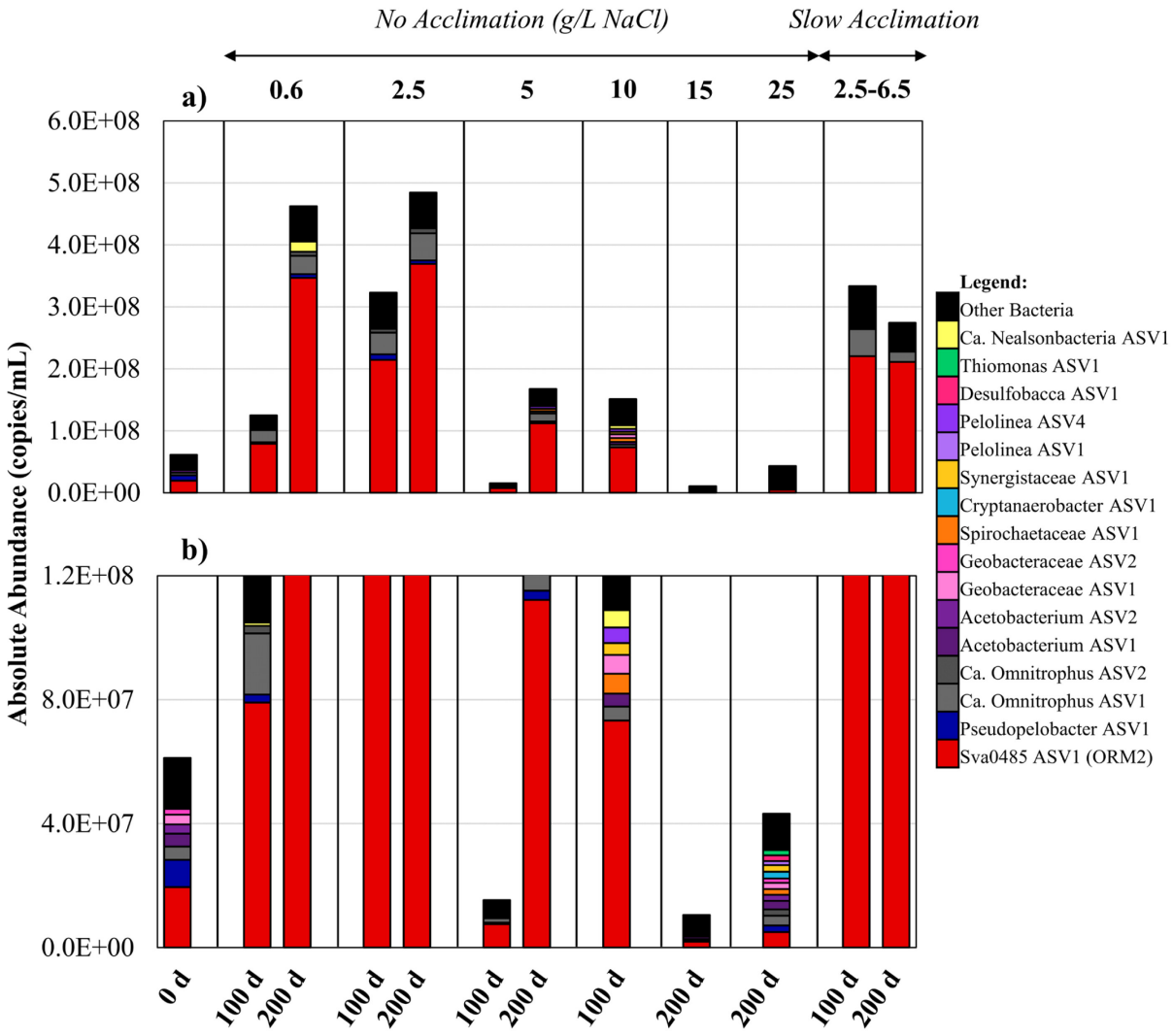

Figure 5-7. Absolute abundance of total bacteria in DGG-B positive controls (0.6 g/L NaCl), DGG-B not acclimated to salt (2.5 – 25 g/L NaCl) and DGG-B slowly acclimated to salt, on a) full scale (6E+08) and b) zoomed in (1.2E+08). Time 0 samples were taken from the original DGG-B bottle before inoculating into experimental bottles. 10 g/L NaCl was set up at a later date and time 0 is assumed to be similar to that of positive controls bottles at 100 d. Data is shown for a single bottle, full replicate data can be seen in Figure A-16 and A-17.

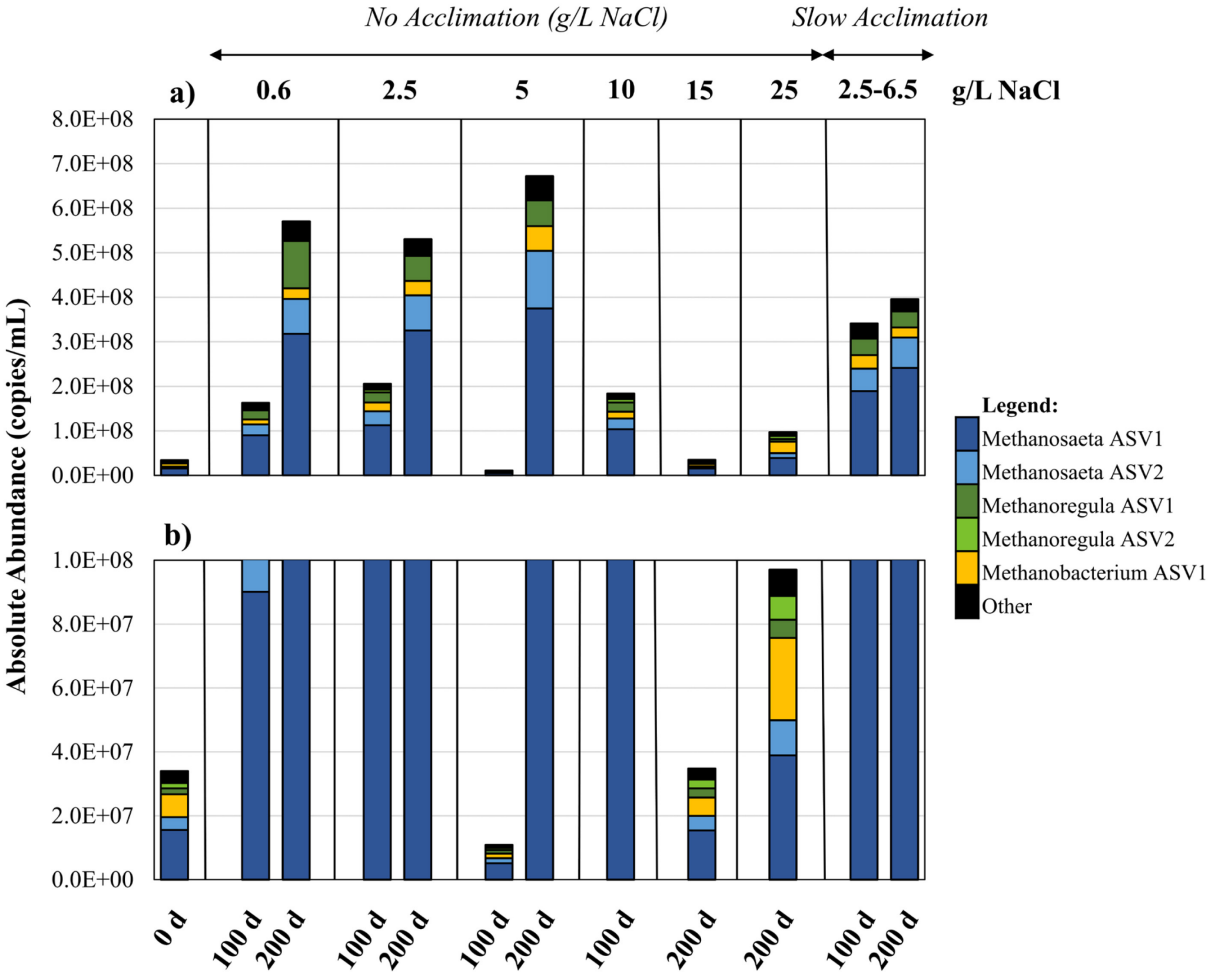

Figure 5-8. Absolute abundance of total archaea in DGG-B positive controls (0.6 g/L NaCl), culture not acclimated to salt (2.5 – 25 g/L NaCl) and culture slowly acclimated to salt, on a) full scale (6E+08) and b) zoomed in (1.2E+08). Time 0 samples were taken from the original DGG-B bottle before inoculating into experimental bottles. 10 g/L NaCl was set up at a later date and time 0 is assumed to be similar to that of positive controls bottles at 100 d. Data is shown for a single bottle at each salt concentration and time, full replicate data can be seen in Figure A-18 and A-19.

DGG-B Community Structure with Increasing Salinity

Control bottles (0.6 g/L) and 2.5 g/L NaCl showed a considerable increase in the total abundance of bacteria and archaea over the course of the experiment. With benzene being the only substrate added, ORM2 was continually enriched and represented an average of 75.7% of the bacterial community by day 200. There was also an increase in abundance of *Ca*. Nealsonbacteria and *Ca*. Omnitrophica. It has been suggested that these biomass recyclers play

a vital role in the proper functioning of DGG-B, and inoculating *Ca*. Nealsonbacteria into culture with slow growth significantly increased degradation rates (Chen et al. 2023). Similar to qPCR trends for ORM2, there was a steep drop in overall abundance of bacteria and archaea at 5 g/L NaCl by day 100. However, ORM2 still represented the dominant bacteria species, and there was not a huge shift in community composition. Bottles that had been slowly acclimated to salt at 2.5 g/L (100 d) and 6.5 g/L (200 d) looked similar to control bottles with ORM2 dominating the bacterial community.

Bottles at 10 g/L NaCl experienced more variability between replicates in terms of bacterial and archaea population size, and exhibited a decrease in ORM2 to 48.7% abundance. 10 g/L NaCl bottles had some of the highest abundances of *Ca*. Nealsonbacteria (3.7-4.5% abundance; 6.9×10^5 – 2.5×10^7 copies/mL), along with an increase in *Spirochaetaceae* ASV1 which may also be a biomass recycler (Dong et al. 2018, Song et al. 2021). This could be due to the higher rates of cell decay than growth, discussed in Section 5.3.2. At 15 – 25 g/L NaCl, there was a further decrease in the overall amount of bacteria and archaea, along with the abundance of ORM2 (~13% abundance). The decrease in ORM2 led to an increased abundance of *Pseudopelobacter* ASV1, *Ca*. Omnitrophus ASV1/ASV2, *Acetobacterium* ASV1/ASV2, *Spirochaetaceaea* ASV1, *Geobacteraceae* ASV1, *Cryptanaerobacter* ASV1, and *Synergistaceae* ASV1; many of which are commonly detected in anaerobic hydrocarbon degrading communities, often with undefined roles (Huang et al. 2021, Wu et al. 2022). There did not appear to be enrichment of any specific bacteria at these higher salt concentrations as they each represented <10% of the total community.

In microcosm studies using hydrocarbon contaminated soils, higher salinity leads to a decrease in total microbial population size and diversity but increases the abundance of salt

tolerant hydrocarbon degrading microbes (Akbari et al. 2021, Li et al. 2022, Qin et al. 2012). This study similarly saw a decrease in overall bacterial population size, but no notable enrichment of halotolerant bacteria. However, benzene was the only substrate added which requires very specialized bacteria under anaerobic conditions. Furthermore, DGG-B has been enriched over 28 years (since 1995) at low salt concentrations, so any halophilic bacterial originally present may have been lost.

The archaea community structure did not change considerably over 200 days regardless of salt concentration, with *Methanosaeta* representing the most dominant methanogen. Archaea shifted to becoming the prevailing microorganisms in the overall microbial community structure, particularly at 25 g/L NaCl, which also saw a slight increase in the abundance of *Methanobacterium* ASV1. *Methanosaeta* is poorly salt tolerant and increasing NaCl allowed for more halotolerant methanogens such as *Methanobacterium* to outcompete *Methanosaeta*, further discussed below.

Enriched Methanogen Microbial Community Structure

The addition of acetate and hydrogen increased the total archaea copy numbers considerably compared to the DGG-B consortium fed benzene. As expected, after benzene was sparged and other substrates were added, the relative abundance of ORM2 decreased considerably (average of 12.2%) and no longer represented the primary bacteria species (Figure 5-9). The abundance of total archaea was highest in acetate control bottles, with 2.4× more copy numbers than hydrogen bottles at day 100; this improved growth was also observed in the higher methane production (Figure 5-5). The acetate utilizing *Methanosaeta* (ASV1, ASV2) represented >90% of archaea at 0.6 g/L and at 5 g/L NaCl (Figure 5-10). However, acetoclastic methanogens exhibited decreasing copies of total archaea with increasing salt,

notably reaching one order of magnitude lower than controls at 25 g/L NaCl, with a shift in community structure to *Methanosarcina* ASV1/ASV2 dominating. In terms of relative abundance of bacteria, biomass recyclers *Ca*. Nealsonbacteria and *Spirochaetaceae* ASV1 were enriched at low salt, possibly due to their close relationships with *Methanosaeta* (Kuroda et al. 2022). As salt increased (25 g/L NaCl), *Ca*. Omnitrophus ASV1/ASV2, *Anaerolineaceae* ASV1 and *Thermovirga* ASV1 also increased in relative abundance.

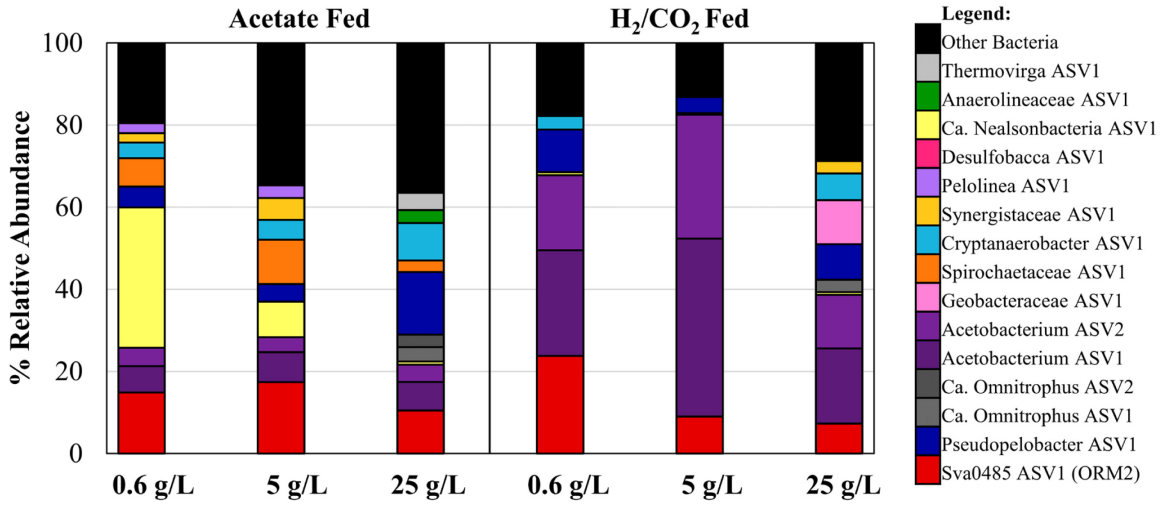

Figure 5-9. Relative abundance of total bacteria after 100 days in DGG-B sparged of benzene and fed acetate or H_2/CO_2 to enrich for methanogens. Data is shown for a single bottle at each salt concentration, full replicate data can be seen in Figure A-20.

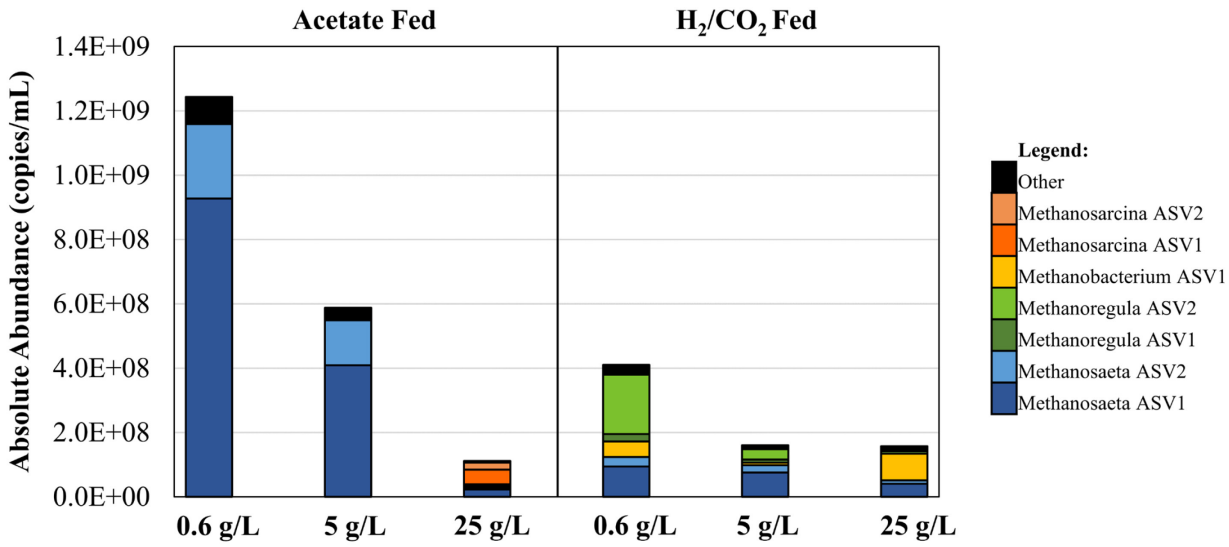

Figure 5-10. Absolute abundance of total archaea after 100 days in DGG-B sparged of benzene and fed acetate or H_2/CO_2 to enrich for methanogens. Data is shown for a single bottle at each salt concentration, full replicate data can be seen in Figure A-21.

In hydrogen supplemented bottles, the bacterial community was dominated by *Acetobacterium* (ASV1, ASV2), which can utilize CO_2 as sole source of carbon, producing acetate. Acetate concentrations ranged from 0.2 – 2.5 mM (Table A-13) and provided a carbon source for *Methanosaeta*. At 0.6 g/L NaCl, the CO_2/H_2 utilizing *Methanoregula* (ASV1, ASV2) and *Methanobacterium* ASV1 were the primary methanogens, at 18.7–51.5% and 2.8–11.9%, respectively. Despite producing similar amounts of methane at all salt concentrations (Figure 5-5), hydrogenotrophic methanogens saw a considerable reduction in total archaea copies at 5 g/L NaCl. *Methanoregula* appears to have low halo-tolerance as abundance decreased considerably at 5 g/L NaCl (26.1–37.8%). These bottles also had the highest abundance of *Acetobacterium* ASV1/ASV2 (62.4–73.5%), suggesting it may be more salt tolerant and outcompeted *Methanoregula*, which led to a relative increase in *Methanosaeta* at 5 g/L NaCl. Future work should include running qPCR assay for total bacteria to determine if bacteria are in greater abundance than methanogens.

Interestingly, at 25 g/L NaCl there was an overall increase in total archaea, possibly due to creating a preferential environment for more halophilic methanogens, as seen by the significant shift in microbial community composition. At 25 g/L NaCl, *Methanobacterium* ASV1 represented 63.2% of methanogens, with a further reduction in *Methanoregula* (<5%). A slight increase in *Methanobacterium* was also noted in 15 – 25 g/L NaCl DGG-B bottles fed benzene. Some species of *Methanobacterium* have been isolated from sea sediments, suggesting halotolerance (Kadam et al. 1989, Chen et al. 2020a).

Overall, acetoclastic methanogens appeared to be more impacted by 25 g/L NaCl than hydrogenotrophic methanogens. The microbial community structure was significantly changed at 25 g/L NaCl with *Methanosaeta* and *Methanoregula* decreasing, and *Methanosarcina* and *Methanobacterium* increasing. Chen et al. (2020b) found the methanogenic community shifted from acetoclastic to hydrogenotrophic as salinity increased in an anaerobic filter for hypersaline molasses wastewater. The authors suggested this may be due to the cell wall in acetoclasts being more easily penetrated by toxic substances. Acetoclastic methanogens have generally been found to have lower tolerance for various stressors during anaerobic digestion, including temperature, ammonia inhibition, salinity, and pH (Liu et al. 2016, Wang et al. 2022, Yan et al. 2020).

Typically, methanogens that grow at higher salinities are methylotrophic, utilizing methylated amines or methanol as energy sources (Oren 2001, McGenity and Sorokin 2019). As salinity increases, *Methanosaeta* often decreases and *Methanosarcina* dominates (Gao et al. 2022, Oren 2008, Sun et al. 2017). *Methanosarcina* has diverse metabolic pathways and can utilize acetate, H_2/CO_2 and methylated compounds. The reason that methylotrophic methanogens dominate at high salinities is not fully understood. One explanation is that the

production of osmolytes in response to increased salt have a high abundance of methyl groups, the breakdown of these osmolytes can thus produce methylotrophic substrates such as methylamine, which have been found to be more abundant in hypersaline settings than other methanogenic substrates (McGenity and Sorokin 2019). Furthermore, methylotrophic methanogens have larger Gibbs Free Energy per mol substrate utilized at -79 to -191 kJ compared to -31 kJ and -34 kJ for acetoclastic and hydrogenotrophic methanogens, respectively. This larger energy yield may be able to balance the higher rates of energy expenditure required under osmotic stress (Hoehler et al. 2010, Oren 2001).

5.4 Conclusions and Implications for Bioremediation

High levels of salt can arise due to both natural and anthropogenic causes. Natural salinity is common in Alberta and mainly consists of sulfate salts, whereas the release of produced water due to oil and gas extraction can cause elevated NaCl (AENV 2001). Few studies have been conducted on the impact of salt co-contamination for anaerobic bioremediation, and even less so for benzene. This study focused on the impact of NaCl on bioremediation as it is generally considered more harmful to microorganisms; however, the impact of sulfate should also be examined in the future due to its prevalence. Oil and gas contaminated sites with salt levels ranging from 0.1 – 10 g/L NaCl are often considered problematic, and concentrations as high as 30 g/L occasionally observed (Stevenson, K. 2020. Personal communication). As 10 g/L NaCl is often the limit for non-halophile growth, it is important to understand how salinity will impact microbes in order to evaluate the potential for bioremediation at a site.

This study demonstrated that anaerobic benzene biodegradation by a highly enriched methanogenic culture, DGG-B, was negatively impacted at 5 g/L NaCl and stalled at 15 g/L

NaCl, suggesting some halotolerance. A half reduction in benzene degradation rate was estimated to occur at 8.4 g/L NaCl, much lower than the concentrations commonly noted in literature as detrimental for aerobic hydrocarbon degrading microbes. Benzene degrading *Deltaproteobacteria* ORM2 abundance decreased as salt increased, and cells initially experienced faster rates of decay than growth at 5 – 25 g/L NaCl. Methanogenesis was able to occur at 25 g/L NaCl when fed acetate or hydrogen, further suggesting osmotic stress effects towards ORM2 is the rate limiting step in benzene degradation at high salinity. ORM2 abundance decreased without any significant enrichment of other possible benzene degrading microbes, however the methanogenic community did exhibit shifts in composition towards methanogens with more versatile metabolic function (*Methanosarcina*). The dominance of methylotrophic methanogens at higher salinities suggests that methanogens may play a different role in halophilic environments, consuming methanol rather than fermentation products (Lowe et al. 1993). For anaerobic benzene degradation, particularly with DGG-B, a specific set of microbes with defined roles acting in syntropy is required, and thus a shift at high salinity to methanogens with different roles could cause benzene degradation to stall. In order to effectively use DGG-B at salt contaminated sites, focus should be placed on ways to improve salt tolerance. Slowly acclimating the culture to salt improved degradation rates up to 6.0× for NaCl concentrations up to 11.5 g/L. However, doubling time increased from 41 days (2.5 g/L NaCl) to 86 days (6.5 g/L NaCl), suggesting there was some stress effects causing slower microbial growth. Future work should include monitoring the efficacy of slowly acclimating DGG-B to salt in terms of microbial community dynamics and at what salt concentration degradation begins to stall. Perhaps an even slower acclimation period (over years) or the addition of exogenous osmolytes may lead to further improvements.

Alternatively, enrichment of a separate benzene-degrading culture from naturally saline materials may be an option.

It is important to note that an undiluted culture with high initial concentrations of ORM2 was used for these experiments. Therefore, impacts may be more pronounced during bioaugmentation in the field when the culture is diluted with groundwater. Furthermore, there are more complex interactions and other stressors at sites that may increase the effect of osmotic stress. Ulrich et al. (2009) found that the combination of environmentally relevant factors such as temperature, nutrients and salinity created a less predictable microbial response during petroleum hydrocarbon degradation which varied depending on the combination of conditions. Benzene contamination rarely exists in isolation, and the presence of co-contaminations such as naphthalene has been previously shown to decrease benzene degradation rate (Toth et al. 2021). Therefore, site specific microcosm treatability studies may be needed to accurately determine the impact of salt in combination with other site-specific factors on the performance of DGG-B.

Chapter 6

Conclusions and Recommendations

6.1 Introduction

The petroleum industry represents a main driver of the Canadian economy, however large volumes of contaminated waste have been generated during the extraction, upgrading, storage and transport of petroleum products, making effective remediation strategies vital. The overall purpose of this research was to address knowledge gaps for NAFC and benzene remediation, two contaminants of concern in the Canadian petroleum industry.

The oil sands contribute to over 70% of upstream crude oil production (CAPP 2022, CER 2022), with large inventories of tailings waste containing toxic contaminants such as NAFCs which are a main focus of remediation efforts (Allen 2008a, Li et al. 2017a, Morandi et al. 2017). Biodegradation provides the cheapest remediation strategy, however, cannot address the portion of NAFCs (cyclic) that are recalcitrant and persistent over decades (Anderson et al. 2012a, Han et al. 2009, Quagraine et al. 2005b). Chemical oxidation, particularly ozonation, appears to be effective for reducing recalcitrant NAFCs, however the residual organics are not as reactive and may be more toxic, and further chemical treatment becomes costly (Brown and Ulrich 2015, Gamal El-Din et al. 2011, Garcia-Garcia et al. 2011, Pérez-Estrada et al. 2011, Wang et al. 2013b). Therefore, a combination of treatments may be required. Ozone pre-treatment followed by biodegradation for NAFCs has shown success in increased rates of NAFC removal and toxicity reduction (Brown et al. 2013, Dong et al. 2015, Martin et al. 2010, Vaiopoulou et al. 2015, Xue et al. 2016b). Persulfate is more recently being studied as a cheaper, more persistent, less aggressive oxidant, that can give more comprehensive removals of aliphatic hydrocarbons than ozone (Liang et al. 2006, Drzewicz et al. 2012, Wacławek et al. 2017). To-date, limited studies have coupled persulfate oxidation with biological treatment via biofiltration (Balaberda and Ulrich 2021, Ganiyu et al. 2022a).

The potential for persulfate oxidation coupled with in situ biodegradation processes that could occur in tailings ponds is not yet known and was the focus of Chapter 3 and 4.

Downstream petroleum processes such as upgrading/refining, transport and storage can cause additional environmental concerns due to accidental spills or releases. Benzene is often a driver for remediation efforts due to its carcinogenicity, recalcitrance and mobility. Excavation and pump and treat are the most commonly used remediation techniques, but may not be viable for low permeability zones, deep aquifers or contamination below infrastructure (Toth et al. 2021). For these more challenging sites, anaerobic biodegradation would be ideal. While anaerobic benzene biodegradation was previously not thought possible (Wilson et al. 1986, CCME 2004, Foght 2008, Vogt et al. 2011), methanogenic enrichment cultures with closely related benzene fermenting bacteria have been described in literature and used in bioaugmentation trials (Phan et al. 2021, Toth et al. 2021). However, petroleum sites, particularly in Alberta, may have the additional challenge of high salinity. Salt (NaCl) has been shown to hinder aerobic hydrocarbon biodegradation (De Carvalho and Da Fonseca 2005, Hu et al. 2020, Hua and Wang 2014, Rhykerd et al. 1995, Ulrich et al. 2009, Zhang et al. 2021), but the impact on anaerobic hydrocarbon degraders, and particularly the highly specialized benzene fermenting bacteria, is still unknown and was the focus of Chapter 5.

6.2 Summary of Findings

A summary of the key research findings from each chapter is provided below.

Chapter 3, Research Question 1: Does coupling unactivated persulfate oxidation and biodegradation using *Pseudomonas fluorescens* decrease Merichem Naphthenic Acid concentration, overall organics (Chemical Oxygen Demand, COD) and toxicity of the water?

Is the rate of removal of Merichem NAs improved by increasing the temperature to 30ºC? Does persulfate effect the number of viable bacteria cells?

1. Unactivated persulfate at 100 – 1000 mg/L removed 30-95% of Merichem NAs and 5-72% of COD over 317 days. The addition of *P. fluorescens* increased removals to 53-99% Merichem NAs and 31-85% COD removal, for 100 – 1000 mg/L persulfate, respectively. 100 mg/L persulfate coupled with *P. fluorescens* was the only condition that led to significantly improved Merichem NA removals compared to chemical bottles (1.8× more). However, COD removal was 1.2 to 6.7× higher for all persulfate concentrations, indicating that the bacteria were primarily degrading oxidation by-products.

2. Unactivated persulfate was highly persistent, with 46-62% remaining after 320 days. There was no difference in persulfate utilization between chemical and coupled treatments. Stoichiometrically, 100-1000 mg/L persulfate should remove 3-26% of COD. However, up to 72% of COD was removed with still half of the persulfate remaining. This indicates that some activation and radical propagation reactions were occurring at room temperature.

3. Microbial viability, measured as viable cell counts, was highest in bottles containing 250 mg/L persulfate, reaching 4.6× more CFUs than bottles without persulfate, suggesting some improved growth conditions. However, further increasing the persulfate decreased the viable cells, particularly at 1000 mg/L persulfate which were one order of magnitude lower than those at 250 mg/L, likely due to increased oxidative stress and decreased carbon sources.

4. The addition of persulfate caused the initial toxicity towards *V. fischeri* to increase 1.3-2.2× for 100-500 mg/L persulfate compared to Merichem NAs alone, and was above detection limit with 1000 mg/L persulfate. However, controls with persulfate alone did not exhibit any toxicity, suggesting the increased toxicity was due to a synergistic effect. Regardless, unactivated persulfate oxidation alone removed 75-97% of toxicity, while coupled treatments slightly improved removals to 87-100%.

5. Increasing temperature to 30ºC increased the persulfate reaction, likely due to the formation of radical species, leading to >99% removal in 89 days for 1000 mg/L persulfate. The addition of *P. fluorescens* improved COD removal to 100%. However, microbial viability was lowest, possibly due to the more aggressive oxidation reactions.

Chapter 4, Research Question 2: Does an initial heat activated persulfate oxidation phase followed by unactivated persulfate oxidation coupled to biodegradation using *P. fluorescens* decrease Merichem NA and OSPW NAFC concentration and reduce toxicity of process water? How does the NAFC distribution shift with each treatment phase? Is the coupled treatment more effective at NAFC and toxicity reduction compared to oxidation or bioremediation alone? How is the growth of bacteria impacted by oxidative stress and OSPW toxicity in the coupled treatment?

6. 250 mg/L of persulfate activated at 60ºC for 8 hours was found ideal to reduce the NAFC concentration in OSPW by half. Lower temperatures (40-50ºC) required longer timeframes or higher doses of persulfate to achieve similar removals. Additionally, the inorganics present (phosphate) were found to play a large role in reaction chemistry, with high concentrations scavenging the persulfate, but a small amount provided some activation.

7. Persulfate activated at 60ºC for 8 hours removed 75-96% of Merichem NAs for 250-1000 mg/L persulfate and decreased toxicity as measured by inhibition effect towards *V. fischeri* from 89% to 32-40% effect. During 150 days of subsequent unactivated persulfate reaction (room temperature), NAFC removals at all persulfate concentration increased to >90%. Mineralization was only improved at the lower persulfate concentrations (250 mg/L), suggesting the remaining organics at higher persulfate doses were not reactive with unactivated persulfate. Toxicity shifted with time likely due to transformation of oxidation by-products, and by day 150 the toxicity had increased to 53-83% inhibition effect.

8. Heat (60ºC) activated persulfate reaction for 8 hours removed 45-89% of NAFCs in OSPW for 250-1000 mg/L persulfate, however little mineralization occurred and toxicity increased from 18% effect to 28-61% effect, possibly due to residual NAFCs (n=14-16 and DBE 3-5) and oxidation by-products. After 150 days of unactivated persulfate reaction, NAFC removals increased to 70-95%, with more mineralization occurring at higher persulfate doses (57% COD removed for 1000 mg/L), and toxicity decreased to no inhibition effect. Unactivated persulfate appeared more effective in OSPW than for Merichem, as seen by a 2.6 to 3.8× higher persulfate utilization rate, possibly due to organic or inorganic species providing some activation.

9. For both OSPW and Merichem NAs, heat activated persulfate removed O_2-NAFCs to <10% abundance shifting to more oxidized O_{3+} NFACs. The recalcitrant higher molecular weight (n>16) and unsaturated (DBE 7 and 8) NAFCs were preferentially removed, leaving behind simpler structure compounds (DBE <3) that are more easily biodegraded.

10. Biodegradation by *P. fluorescens* led to 45% Merichem NA removal, with no notable mineralization occurring; however, was not effective for OSPW NAFCs and did not show any degradation over 150 days.

11. Coupled bottles inoculated with *P. fluorescens* after persulfate heat activation did not improve NAFC removals, but rather increased the COD and decreased the persulfate utilization rate by 2.7 to 11.4×, possibly due to scavenging effects from cell biomass or EPS. Cell viability was significantly decreased by over 3 orders of magnitude and took over 100 days before increasing, indicating cells were experiencing high levels of stress. In Merichem bottles, the coupled treatments showed some shifts in NAFC distribution, creating more oxidized NAFCs (O_8), and one treatment (250 mg/L persulfate) improved toxicity reduction by 28% compared to chemical treatment alone. However, in OSPW bottles, the coupled treatments showed greater toxicity than chemical treatment counterparts.

Chapter 5, Research Question 3: What impact does salt (NaCl) have on anaerobic benzene biodegradation of a highly enriched benzene-degrading methanogenic culture? Is there a difference in benzene degradation rate when microorganisms have been slowly adapted to high salt conditions compared to sudden salt shock? How is the microbial community composition impacted by salt?

12. Benzene degradation rate in positive controls that contain the amount of salt normally present in the growth medium (0.6 g/L NaCl) increased from 9 μM/day to as high as 55 μM/day over 205 days, but in general ranged from 20-30 μM/day. Increasing degradation rate corresponded to increase concentration of ORM2 to $>3\times10^8$

copies/mL by day 200 and decreased doubling time to 52 days. At 2.5 g/L NaCl there was overall little change in benzene degradation rates.

13. Increasing the salt concentration to 5-10 g/L NaCl initially led to a 1.6-fold reduction in benzene degradation rate (6 μM/day). The ORM2 copy numbers at day 100 for 5 g/L NaCl were over one order of magnitude lower than those in control bottles as ORM2 exhibited faster rates of cell decay than growth, indicating ORM2 was poorly tolerant of initial salt stress. At 5 g/L NaCl, the culture recovered from the initial salt stress by day 200, and ORM2 copies rebounded with rates reaching 28 μM/day; however, the rate did not increase in over 300 days at 10 g/L NaCl. Salt concentration of 15-100 g/L NaCl did not show any benzene degradation over 205 days. The salt concentration that will lead to a half reduction in rate was found to be 8.4 g/L NaCl.

14. Slowly acclimating the culture to NaCl significantly improved benzene degradation rates up to 6× at 10 g/L NaCl (30 μM/day). But ORM2 experienced longer doubling times as salt increased from 41 days at 2.5 g/L NaCl to 86 days at 6.5 g/L NaCl, indicating that cells were diverting energy away from growth and towards stress adaptation and maintenance.

15. In DGG-B culture that was enriched for methanogens, acetoclastic methanogens appeared more sensitive to increasing salinity than hydrogenotrophs. In acetate fed bottles, increasing the salt from 0.6 g/L to 5 and 25 g/L NaCl reduced the methane production rate by 1.4 and 5.4×, respectively. In bottles fed hydrogen, methane production rate was only impacted at 25 g/L, decreasing 1.5×.

16. ORM2 represented 33–76% of the bacteria in control bottles and DGG-B exposed to 2.5 g/L NaCl. For a culture that was suddenly exposed to high salt (≥5 g/L NaCl) and a culture that had been slowly acclimated, the microbial community did not appear to enrich for any benzene degrading halophilic bacteria and ORM2 abundance decreased. At 25 g/L NaCl, the methanogen community shifted away from *Methanosaeta* and *Methanoregula*, towards *Methanosarcina* and *Methanobacterium*, which may have different roles by consuming methanol rather than fermentation products, possibly affecting syntrophic relationships and hindering benzene biodegradation.

6.3 Recommendations / Future Research

6.3.1 Oil Sands NAFC Remediation

This research has provided evidence that both unactivated and heat activated persulfate can effectively reduce NAFC concentrations and detoxify OSPW. Unactivated persulfate has not been widely studied as it was assumed unreactive with NAFCs (Liang et al. 2011, Fang et al. 2018). This research has shown that unactivated persulfate is reactive with NAFCs and can provide a more cost-effective option than activated persulfate if time is not a constraint. Heat activated persulfate was chosen to provide faster NAFC removals, at temperatures of 40 – 60ºC which are commonly already utilized during the bitumen extraction process (Foght et al. 2017). Iron and UV activated persulfate have been most commonly studied for OSPW (Liang et al. 2011, Aher et al. 2017, Fang et al. 2018, 2019, 2020), however may provide different results due to different reaction chemistries. This research verified that a significant advantage to heat activated persulfate is the generation of sulfate and hydroxyl radicals which preferentially react with different NAFCs, leading to more comprehensive removals than ozonation (Lee et al. 2020). However, heat activation at 60ºC for 8 hours led to increased toxicity towards *V. fischeri*

and therefore would require additional treatment. Increasing the activation time or temperature may improve toxicity reduction and could be studied in the future. However, oxidized NAFCs have been suggested as being less reactive with oxidants, and increased oxidation does not proportionally increase treatment efficiency (Gamal El-Din et al. 2011, Pérez-Estrada et al. 2011, Wang et al. 2013b). Additional research should aim to analyze the remaining organics after persulfate oxidation in depth, to help elucidate causes of toxicity and potential reactivity with further oxidation or biological treatment. In particular, non-acidic fraction toxicity should be analyzed and more specialized toxicity tests such as for genotoxicity, estrogenicity, and in vivo studies would provide more insight into overall treatment effectiveness.

After heat activated persulfate oxidation, this research utilized a follow-up treatment of continued unactivated persulfate oxidation alone or coupled with biodegradation by a bacterial isolate. Coupling experiments in Chapter 3 were found to be effective at reducing overall system organics (COD) and toxicity for Merichem NAs. Conversely, Chapter 4 experiments for OSPW found coupled treatments increased toxicity and COD and decreased the amount of persulfate consumed. *P. fluorescens* are strong EPS producers which may have antioxidant properties. The antioxidant activity of EPS could be studied through analyzing the functional groups present via FTIR, and by conducting DPPH radical scavenging tests (Wang et al. 2017, Darwish et al. 2019, Shi and Liu 2021, Zhang et al. 2020). Elucidating the composition and radical scavenging ability of the EPS may provide insights into the trends noted in Chapter 4. Unactivated persulfate oxidation in OSPW may have been too aggressive for the cells. The use of an isolate in these experiments may have hindered biodegradation potential, and a mixed microbial community may be better able to withstand oxidative stress. Brown et al. (2013) found that after ozonation, indigenous OSPW microbes were able to provide similar

biodegradation and microbial growth as ozonated-OSPW with unstressed microbes inoculated into the system.

Alternatively, the use of sequential chemical oxidation and biodegradation treatments, rather than combined, may offer an improvement and should be studied. Ozonation is the most commonly studied oxidant for OSPW and is short lived, therefore when used in combination with biodegradation, ozone has generally already left the system (Dong et al. 2015, Hwang et al. 2013, Martin et al. 2010). This research found that the residual NAFCs after heat activated persulfate were those that are generally considered more biodegradation but less reactive with oxidants (linear, lower molecular weight NAFCs). Therefore, in the absence of oxidative stress, the bacteria may have provided quicker removal of organics and toxicity than the unactivated persulfate reaction. In order to remove persulfate prior to the biological treatment stage, the reaction could be quenched or the activation temperature/time can be increased until persulfate is fully removed.

6.3.2 Anaerobic Benzene Biodegradation under Salinity

Anaerobic benzene biodegradation in methanogenic environments appears to occur from very specialized bacteria in the class *Deltaproteobacteria* (Toth et al. 2021). This research had provided valuable insights into the impact of environmentally relevant salt (NaCl) concentrations on anaerobic benzene biodegradation that could occur at petroleum impacted sties. Salt concentrations of 5 g/L NaCl led to a reduction in benzene degradation rate and stalled at 15 g/L, demonstrating the sensitivity of methanogenic benzene degrading microbes to salt. Therefore, for benzene contaminated sites with high salinity, a bioremediation strategy may require adjustments. This research used a gradual acclimation strategy to improve the salt tolerance of the culture, which was successful at the highest concentration tested of 12.5 g/L

NaCl. Future research should continue the gradual acclimation process to determine if there is a salt concentration where microbes no longer function. Due to time constraints, 1 g/L NaCl was added every 2-4 degradation cycles; however, the acclimation process could be increased to months or years, possibly allowing time for cells to increase halotolerance. Microorganisms from naturally non-saline environments utilize the compatible solute strategy to compensate for osmotic stress (Oren 1999). Halophilic microbes that have adapted to environments with high osmotic pressure utilized the salt-in strategy, where they function with a higher concentration of K^+ ions inside the cytoplasm, no longer requiring osmolyte synthesis their energy can be utilized for cell growth (Oren 1999, 2001, Gunde-Cimerman et al. 2018). If through a gradual acclimation process ORM2 could switch from a salt-out to a salt-in strategy, a commercial halophilic benzene degrading culture could be maintained to utilize for sites with high salinity. Other studies have also shown success in adding an exogenous source of osmolytes (glycine betaine), to reduce the energetic load on the cells (Hu et al. 2020, Liu et al. 2019). Future work can determine if this provides increased tolerance of high salinity, or if cells use the osmolytes as a carbon source and thus decrease benzene consumption.

In order to fully elucidate the impact of salinity on bioaugmentation potential, the impact of other environmentally relevant factors should also be explored. This study found that using the more established culture in 10 g/L NaCl bottles may have better resisted initial salt stress effects. Comparing the stress response of cultures with different concentrations of ORM2 may provide insights into target concentrations for field injections. Additionally, multiple stressors that may be present in the field such as lower temperatures and the presence of hydrocarbon co-contaminants has been previously shown to negatively impact hydrocarbon biodegradation and may exacerbate the stress response noted under salinity (Ulrich et al. 2009,

Toth et al. 2021). Lastly, Alberta can naturally have high levels of sulfate salts, up to 6 g/L in the Alberta Basin Formation Water (AENV 2001). Sulfate is generally considered to have less impact in terms of specific ion toxicity, but the increased osmotic pressure can still cause cell dehydration and lysis (Rath et al. 2016). Therefore, future research should compare salinity effects from different ions, including anions (sulfate and chloride) and cations (sodium and potassium).

Bibliography

Abdelrahman, A., Ganiyu, S.O., and Gamal El-Din, M. 2023. Degradation of surrogate and real naphthenic acids from simulated and real oil sands process water using electrochemically activated peroxymonosulfate (EO-PMS) process. Separation and Purification Technology, **306**. Elsevier B.V. doi:10.1016/j.seppur.2022.122462.

Abed, R.M.M., Al-Thukair, A., and de Beer, D. 2006. Bacterial diversity of a cyanobacterial mat degrading petroleum compounds at elevated salinities and temperatures. FEMS Microbiology Ecology, **57**(2): 290–301. doi:10.1111/j.1574-6941.2006.00113.x.

Abu Laban, N., Selesi, D., Jobelius, C., and Meckenstock, R.U. 2009. Anaerobic benzene degradation by Gram-positive sulfate-reducing bacteria. FEMS Microbiology Ecology, **68**(3): 300–311. John Wiley and Sons, Ltd. doi:https://doi.org/10.1111/j.1574-6941.2009.00672.x.

Afzal, A., Drzewicz, P., Martin, J.W., and Gamal El-Din, M. 2012a. Decomposition of cyclohexanoic acid by the UV/H2O2 process under various conditions. Science of The Total Environment, **426**: 387–392. doi:https://doi.org/10.1016/j.scitotenv.2012.03.019.

Afzal, A., Drzewicz, P., Pérez-Estrada, L.A., Chen, Y., Martin, J.W., and Gamal El-Din, M. 2012b. Effect of molecular structure on the relative reactivity of naphthenic acids in the UV/H2O2 advanced oxidation process. Environmental Science and Technology, **46**(19): 10727–10734. doi:10.1021/es302267a.

Agency for Toxic Substances and Disease Registry (ATSDR). 2007. Toxicological Profile for Benzene. Atlanta, GA.

Aher, A., Papp, J., Colburn, A., Wan, H., Hatakeyama, E., Prakash, P., Weaver, B., and Bhattacharyya, D. 2017. Naphthenic acids removal from high TDS produced water by persulfate mediated iron oxide functionalized catalytic membrane, and by nanofiltration. Chem. Eng. J., **327**: 573–583. Elsevier B.V. doi:10.1016/j.cej.2017.06.128.

Ahmadi, M., Jorfi, S., Kujlu, R., Ghafari, S., Darvishi Cheshmeh Soltani, R., and Jaafarzadeh Haghighifard, N. 2017. A novel salt-tolerant bacterial consortium for biodegradation of saline and recalcitrant petrochemical wastewater. Journal of Environmental Management, **191**: 198–208. Academic Press. doi:10.1016/j.jenvman.2017.01.010.

Akbari, A., David, C., Rahim, A.A., and Ghoshal, S. 2021. Salt selected for hydrocarbon-degrading bacteria and enhanced hydrocarbon biodegradation in slurry bioreactors. Water Research, **202**. Elsevier Ltd. doi:10.1016/j.watres.2021.117424.

Alberta Environment (AENV). 2001. Salt contamination assessment & remediation guidelines. Alberta Environment, Environmental Service, Environmental Sciences Division, Edmonton, AB.

Allen, E.W. 2008a. Process water treatment in Canada's oil sands industry: I. Target pollutants and treatment objectives. J. Environ. Eng. Sci., **7**(2): 123–138. doi:10.1139/S07-038.

Allen, E.W. 2008b. Process water treatment in Canada's oil sands industry: II. A review of emerging technologies. J. Environ. Eng. Sci., **7**(5): 499–524. doi:10.1139/S08-020.

Al-Mailem, D.M., Eliyas, M., and Radwan, S.S. 2013. Oil-bioremediation potential of two hydrocarbonoclastic, diazotrophic Marinobacter strains from hypersaline areas along the Arabian Gulf coasts. Extremophiles, **17**(3): 463–470. Springer Japan. doi:10.1007/s00792-013-0530-z.

Al Jibouri, A.K.H., Upreti, S.R., and Wu, J. 2018. Optimal control of continuous ozonation of non-biodegradable pollutants. Journal of Process Control, **66**: 1–11. Elsevier Ltd. doi:10.1016/j.jprocont.2018.02.009.

Amann, R.I., Ludwig, W., and Schleifer, K.H. 1995. Phylogenetic identification and in situ detection of individual microbial cells without cultivation. Microbiological Reviews, **59**(1): 143–169. American Society for Microbiology. doi:10.1128/mr.59.1.143-169.1995.

Amatya, P.L., Hettiaratchi, J.P.A., and Joshi, R.C. 2002. Biotreatment of Fare Pit Waste. Journal of Canadian Petroleum Technology, **41**(09): 30–36.

Anderson, J., Wiseman, S.B., Moustafa, A., Gamal El-Din, M., Liber, K., and Giesy, J.P. 2012a. Effects of exposure to oil sands process-affected water from experimental reclamation ponds on Chironomus dilutus. Water Research, **46**(6): 1662–1672. doi:https://doi.org/10.1016/j.watres.2011.12.007.

Anderson, J.C., Wiseman, S.B., Wang, N., Moustafa, A., Perez-Estrada, L., Gamal El-Din, M., Martin, J.W., Liber, K., and Giesy, J.P. 2012b. Effectiveness of Ozonation Treatment in Eliminating Toxicity of Oil Sands Process-Affected Water to Chironomus dilutus. Environmental Science & Technology, **46**(1): 486–493. American Chemical Society. doi:10.1021/es202415g.

Anderson, R.T., Rooney-Varga, J.N., Gaw, C.V., and Lovley, D.R. 1998. Anaerobic Benzene Oxidation in the Fe(III) Reduction Zone of Petroleum-Contaminated Aquifers. Environ. Sci. Technol., **32**: 1222–1229.

Anipsitakis, G.P., and Dionysiou, D.D. 2004. Radical generation by the interaction of transition metals with common oxidants. Environmental Science and Technology, **38**(13): 3705–3712. doi:10.1021/es035121o.

Aparicio, J.D., Raimondo, E.E., Saez, J.M., Costa-Gutierrez, S.B., Álvarez, A., Benimeli, C.S., and Polti, M.A. 2022. The current approach to soil remediation: A review of physicochemical and biological technologies, and the potential of their strategic combination. Journal of Environmental Chemical Engineering, **10**(2). Elsevier Ltd. doi:10.1016/j.jece.2022.107141.

Arslan, M., Ganiyu, S.O., Lillico, D.M.E., Stafford, J.L., and Gamal El-Din, M. 2023. Fate of dissolved organics and generated sulfate ions during biofiltration of oil sands process water pretreated with sulfate radical advanced oxidation process. Chemical Engineering Journal, **458**. Elsevier B.V. doi:10.1016/j.cej.2023.141390.

Balaberda, A., and Ulrich, A. C. 2021. Persulfate oxidation coupled with biodegradation by pseudomonas Fluorescens enhances naphthenic acid remediation and toxicity reduction. Microorganisms, **9**(7). https://doi.org/10.3390/microorganisms9071502

Bajagain, R., Lee, S., and Jeong, S.W. 2018. Application of persulfate-oxidation foam spraying as a bioremediation pretreatment for diesel oil-contaminated soil. Chemosphere, **207**: 565–572. Elsevier Ltd. doi:10.1016/j.chemosphere.2018.05.081.

Barrow, M.P., Headley, J. V., Peru, K.M., and Derrick, P.J. 2004. Fourier transform ion cyclotron resonance mass spectrometry of principal components in oilsands naphthenic acids. Journal of Chromatography A, **1058**(1–2): 51–59. doi:10.1016/j.chroma.2004.08.082.

Bartlett, A.J., Frank, R.A., Gillis, P.L., Parrott, J.L., Marentette, J.R., Brown, L.R., Hooey, T., Vanderveen, R., McInnis, R., Brunswick, P., Shang, D., Headley, J. V., Peru, K.M., and Hewitt, L.M. 2017. Toxicity of naphthenic acids to invertebrates: Extracts from oil sands process-affected water versus commercial mixtures. Environ. Pollut., **227**: 271–279. Elsevier Ltd. doi:10.1016/j.envpol.2017.04.056.

Bartlett, C.K., Slawson, R.M., and Thomson, N.R. 2019. Response of sulfate-reducing bacteria and supporting microbial community to persulfate exposure in a continuous flow system. Environ. Sci. Process Impacts, **21**(7): 1193–1203. Royal Society of Chemistry. doi:10.1039/c9em00094a.

Bataineh, M., Scott, A.C., Fedorak, P.M., and Martin, J.W. 2006. Capillary HPLC/QTOF-MS for characterizing complex naphthenic acid mixtures and their microbial transformation. Analytical Chemistry, **78**(24): 8354–8361. doi:10.1021/ac061562p.

Bauer, A.E., Frank, R.A., Headley, J. V., Peru, K.M., Farwell, A.J., and Dixon, D.G. 2017. Toxicity of oil sands acid-extractable organic fractions to freshwater fish: Pimephales promelas (fathead minnow) and Oryzias latipes (Japanese medaka). Chemosphere, **171**: 168–176. Elsevier Ltd. doi:10.1016/j.chemosphere.2016.12.059.

Bauer, A.E., Frank, R.A., Headley, J. V., Peru, K.M., Hewitt, L.M., and Dixon, D.G. 2015. Enhanced characterization of oil sands acid-extractable organics fractions using electrospray ionization-high-resolution mass spectrometry and synchronous fluorescence spectroscopy. Environ. Toxicol. Chem., **34**(5): 1001–1008. doi:10.1002/etc.2896.

Bennett, K. 1999. In-Situ Treatment of Soil Contaminated by Benzene (A BTEX Compound). Restoration and Reclamation Review, **5**(2): 1–9.

Berlendis, S., Cayol, J.L., Verhé, F., Laveau, S., Tholozan, J.L., Ollivier, B., and Auria, R. 2010. First Evidence of Aerobic Biodegradation of BTEX Compounds by Pure Cultures of Marinobacter. Applied Biochemistry and Biotechnology, **160**(7): 1992–1999. doi:10.1007/s12010-009-8746-1.

Bolyen, E., Rideout, J.R., Dillon, M.R., Bokulich, N.A., Abnet, C.C., Al-Ghalith, G.A., Alexander, H., Alm, E.J., Arumugam, M., Asnicar, F., Bai, Y., Bisanz, J.E., Bittinger, K., Brejnrod, A., Brislawn, C.J., Brown, C.T., Callahan, B.J., et al. 2019. Reproducible, interactive, scalable and extensible microbiome data science using QIIME 2. Nature Biotechnology, **37**(8): 852–857. doi:10.1038/s41587-019-0209-9.

Bonfá, M.R.L., Grossman, M.J., Mellado, E., and Durrant, L.R. 2011. Biodegradation of aromatic hydrocarbons by Haloarchaea and their use for the reduction of the chemical oxygen demand of hypersaline petroleum produced water. Chemosphere, **84**(11): 1671–1676. Elsevier Ltd. doi:10.1016/j.chemosphere.2011.05.005.

Børresen, M.H., and Rike, A.G. 2007. Effects of nutrient content, moisture content and salinity on mineralization of hexadecane in an Arctic soil. Cold Regions Science and Technology, **48**(2 SPEC. ISS.): 129–138. Elsevier. doi:10.1016/j.coldregions.2006.10.006.

Brient, J.A., Wessner, P.J., and Doyle, M.N. 2000. Naphthenic Acids. *In* Kirk-Othmer Encyclopedia of Chemical Technology.

Brown, L.D., Pérez-Estrada, L., Wang, N., El-Din, M.G., Martin, J.W., Fedorak, P.M., and Ulrich, A.C. 2013. Indigenous microbes survive in situ ozonation improving biodegradation of dissolved organic matter in aged oil sands process-affected waters. Chemosphere, **93**(11): 2748–2755. Elsevier Ltd. doi:10.1016/j.chemosphere.2013.09.026.

Brown, L.D., and Ulrich, A.C. 2015. Oil sands naphthenic acids: A review of properties, measurement, and treatment. Chemosphere, **127**: 276–290. Elsevier Ltd. doi:10.1016/j.chemosphere.2015.02.003.

Bumbac, C., and Diacu, E. 2012. Coupled Chemical and Biological Treatment of Oil Contaminated Soils. REV. CHIM., **63**(11).

Burland, S.M., and Edwards, E.A. 1999. Anaerobic Benzene Biodegradation Linked to Nitrate Reduction. *In* APPLIED AND ENVIRONMENTAL MICROBIOLOGY.

Caldwell, M.E., and Suflita, J.M. 2000. Detection of Phenol and Benzoate as Intermediates of Anaerobic Benzene Biodegradation under Different Terminal Electron-Accepting Conditions. Environmental Science & Technology, **34**(7): 1216–1220. American Chemical Society. doi:10.1021/es990849j.

Canada's Oil & Natural Gas Producers (CAPP). 2013. Crude oil extraction and drilling methods. Calgary, AB. https://www.capp.ca/oil/extraction/ [accessed 4 January 2023]

Canada's Oil & Natural Gas Producers (CAPP). 2022. Canada's Oil Sands. Calgary, AB. https://www.capp.ca/oil [accessed 4 January 2023]

Canadian Council of Ministers of the Environment (CCME). 1999. Canadian Water Quality Guidelines for the Protection of Aquatic Life: Benzene. *In* Canadian Water Quality Guidelines. CCME, Winnipeg.

Canadian Council of Ministers of the Environment (CCME). 2004. Canadian Soil Quality Guidelines for the Protection of Environmental and Human Health: Benzene. Canadian Council of Ministers of the Environment (CCME), Winnipeg.

Canadian Energy Regulator (CER). 2022. Canadian Crude Oil Exports: A 30 Year Review. https://www.cer-rec.gc.ca/en/data-analysis/energy-commodities/crude-oil-petroleum-products/report/canadian-crude-oil-exports-30-year-review/

De Carvalho, C.C.C.R., and Da Fonseca, M.M.R. 2005. Degradation of hydrocarbons and alcohols at different temperatures and salinities by Rhodococcus erythropolis DCL14. FEMS Microbiology Ecology, **51**(3): 389–399. doi:10.1016/j.femsec.2004.09.010.

Cassidy, D., Northup, A., and Hampton, D. 2009. The effect of three chemical oxidants on subsequent biodegradation of 2,4-dinitrotoluene (DNT) in batch slurry reactors. J. Chem. Technol. Biotechnol., **84**(6): 820–826. doi:10.1002/jctb.2140.

Chalaturnyk, R.J., Scott, J.D., and Özüm, B. 2002. Management of oil sands tailings. Petroleum Science and Technology, **20**(9–10): 1025–1046. doi:10.1081/LFT-120003695.

Chang, W., Akbari, A., David, C.A., and Ghoshal, S. 2018. Selective biostimulation of cold- and salt-tolerant hydrocarbon-degrading Dietzia maris in petroleum-contaminated sub-Arctic soils with high salinity. Journal of Chemical Technology and Biotechnology, **93**(1): 294–304. John Wiley and Sons Ltd. doi:10.1002/jctb.5385.

Chen, K.F., Chang, Y.C., and Chiou, W.T. 2016. Remediation of diesel-contaminated soil using in situ chemical oxidation (ISCO) and the effects of common oxidants on the indigenous microbial community: A comparison study. Journal of Chemical Technology and Biotechnology, **91**(6): 1877–1888. doi:10.1002/jctb.4781.

Chen, S., Wang, P., Liu, H., Xie, W., Wan, X.S., Kao, S.-J., Phelps, T.J., and Zhang, C. 2020a. Population dynamics of methanogens and methanotrophs along the salinity gradient in Pearl River Estuary: implications for methane metabolism. Applied Microbiology and Biotechnology, **104**(3): 1331–1346. doi:10.1007/s00253-019-10221-6.

Chen, X., Molenda, O., Brown, C.T., Toth, C.R.A., Guo, S., Luo, F., Howe, J., Nesbø, C.L., He, C., Montabana, E.A., Cate, J.H.D., Banfield, J.F., and Edwards, E.A. 2023. "Candidatus Nealsonbacteria" Are Likely Biomass Recycling Ectosymbionts of Methanogenic Archaea in a Stable Benzene-Degrading Enrichment Culture. doi:10.1128/MRA01342-22.

Chen, X., Sheng, Y., Wang, G., Guo, L., Zhang, H., Zhang, F., Yang, T., Huang, D., Han, X., and Zhou, L. 2022a. Microbial compositional and functional traits of BTEX and salinity co-contaminated shallow groundwater by produced water. Water Research, **215**. Elsevier Ltd. doi:10.1016/j.watres.2022.118277.

Chen, Y., Long, X., Huang, R., Zhang, I.Y., Yao, G., Lai, B., and Xiong, Z. 2022b. Highly efficient electro-cocatalytic Fenton-like reactions for the degradation of recalcitrant naphthenic acids: Exploring reaction mechanisms and environmental implications. Chemical Engineering Journal, **450**. Elsevier B.V. doi:10.1016/j.cej.2022.138331.

Chen, Y.T., Yu, N., Sun, Z.Y., Gou, M., Xia, Z.Y., Tang, Y.Q., and Kida, K. 2020b. Acclimation Improves Methane Production from Molasses Wastewater with High Salinity in an Upflow Anaerobic Filter Reactor: Performance and Microbial Community Dynamics. Applied Biochemistry and Biotechnology, **191**(1): 397–411. Springer. doi:10.1007/s12010-020-03236-7.

Clemente, J.S., and Fedorak, P.M. 2005. A review of the occurrence, analyses, toxicity, and biodegradation of naphthenic acids. Elsevier Ltd.

Clemente, J.S., Mackinnon, M.D., and Fedorak, P.M. 2004. Aerobic Biodegradation of Two Commercial Naphthenic Acids Preparations. Environmental Science and Technology, **38**(4): 1009–1016. American Chemical Society. doi:10.1021/es030543j.

Coates, J.D., Anderson, R.T., and Lovley, D.R. 1996. Oxidation of Polycyclic Aromatic Hydrocarbons under Sulfate-Reducing Conditions. *In* APPLIED AND ENVIRONMENTAL MICROBIOLOGY, 62(3), 1099–1101.

Coates, J.D., Chakraborty, R., Lack, J.G., O'Connor, S.M., Cole, K.A., Bender, K.S., and Achenbach, L.A. 2001. Anaerobic benzene oxidation coupled to nitrate reduction in pure culture by two strains of Dechloromonas. Nature, **411**(6841): 1039–1043. doi:10.1038/35082545.

Cossey, H.L., Batycky, A.E., Kaminsky, H., and Ulrich, A.C. 2021. Geochemical stability of oil sands tailings in mine closure landforms. Minerals, **11**(8). MDPI AG. doi:10.3390/min11080830.

Costa, O.Y.A., Raaijmakers, J.M., and Kuramae, E.E. 2018. Microbial Extracellular Polymeric Substances: Ecological Function and Impact on Soil Aggregation. Frontiers in Microbiology, **9**(2018).

Darwish, A.A., Al-Bar, O.A.M., Yousef, R.H., S.Moselhy, S., Ahmed, Y.M., and Hakeem, K.R. 2019. Production of Antioxidant Exopolysaccharide from Pseudomonas aeruginosa Utilizing Heavy Oil as a Solo Carbon Source. Pharmacognosy Research, **11**(4).

Demeter, M.A., Lemire, J.A., Yue, G., Ceri, H., and Turner, R.J. 2015. Culturing oil sands microbes as mixed species communities enhances ex situ model naphthenic acid degradation. Front. Microbiol., **6**(SEP): 1–13. doi:10.3389/fmicb.2015.00936.

Del Rio, L.F., Hadwin, A.K.M., Pinto, L.J., MacKinnon, M.D., and Moore, M.M. 2006. Degradation of naphthenic acids by sediment micro-organisms. J. Appl. Microbiol., **101**(5): 1049–1061. doi:10.1111/j.1365-2672.2006.03005.x.

De Visscher, A. 2018. Salting out and salting in of benzene in water: a consistency evaluation. Monatshefte fur Chemie, **149**(2): 231–236. Springer-Verlag Wien. doi:10.1007/s00706-017-2122-6.

Díaz-Acosta, A., Sandoval, M.L., Delgado-Olivares, L., and Membrillo-Hernández, J. 2006. Effect of anaerobic and stationary phase growth conditions on the heat shock and oxidative stress responses in Escherichia coli K-12. Archives of microbiology, **185**(6): 429–438. Germany. doi:10.1007/s00203-006-0113-9.

Dong, T., Zhang, Y., Islam, M.S., Liu, Y., and Gamal El-Din, M. 2015. The impact of various ozone pretreatment doses on the performance of endogenous microbial communities for the remediation of oil sands process-affected water. Int. Biodeterior. Biodegrad., **100**: 17–28. Elsevier Ltd. doi:10.1016/j.ibiod.2015.01.014.

Dong, X., Greening, C., Brüls, T., Conrad, R., Guo, K., Blaskowski, S., Kaschani, F., Kaiser, M., Laban, N.A., and Meckenstock, R.U. 2018. Fermentative Spirochaetes mediate necromass recycling in anoxic hydrocarbon-contaminated habitats. The ISME Journal, **12**(8): 2039–2050. doi:10.1038/s41396-018-0148-3.

Dou, J., Ding, A., Liu, X., Du, Y., Deng, D., and Wang, J. 2010. Anaerobic benzene biodegradation by a pure bacterial culture of Bacillus cereus under nitrate reducing conditions. Journal of Environmental Sciences, **22**(5): 709–715. doi:https://doi.org/10.1016/S1001-0742(09)60167-4.

Drzewicz, P., Afzal, A., El-Din, M.G., and Martin, J.W. 2010. Degradation of a Model Naphthenic Acid, Cyclohexanoic Acid, by Vacuum UV (172 nm) and UV (254 nm)/H2O2. The Journal of Physical Chemistry A, **114**(45): 12067–12074. American Chemical Society. doi:10.1021/jp105727s.

Drzewicz, P., Perez-Estrada, L., Alpatova, A., Martin, J.W., and Gamal El-Din, M. 2012. Impact of peroxydisulfate in the presence of zero valent iron on the oxidation of cyclohexanoic acid and naphthenic acids from oil sands process-affected water. Environ. Sci. Technol., **46**(16): 8984–8991. doi:10.1021/es3011546.

D'Souza, L., Sami, Y., Nemati, M., and Headley, J. 2014. Continuous Co-biodegradation of linear and cyclic naphthenic acids in circulating packed-bed bioreactors. Environmental Progress & Sustainable Energy, **33**(3): 835–843. John Wiley & Sons, Ltd. doi:https://doi.org/10.1002/ep.11856.

Edwards, E.A., and Grbic-Galic, D. 1992. Complete Mineralization of Benzene by Aquifer Microorganisms under Strictly Anaerobic Conditions. *In* APPLIED AND ENVIRONMENTAL MICROBIOLOGY.

Environment Climate Change Canada (ECCC). 2022. National Pollutant Release Inventory (NPRI) Sector Overview: Oil Sands Extraction. Accessed 19 December 2022, https://environmental-maps.canada.ca/RAMP-Storylines/index-ca-en.html#/en/410b88da-0ed1-4749-903f-5e76c24e2e5f#story

Fan, Y., Ji, Y., Kong, D., Lu, J., and Zhou, Q. 2015. Kinetic and mechanistic investigations of the degradation of sulfamethazine in heat-activated persulfate oxidation process. Journal of Hazardous Materials, **300**: 39–47. Elsevier B.V. doi:10.1016/j.jhazmat.2015.06.058.

Fang, Z., Chelme-Ayala, P., Shi, Q., Xu, C., and Gamal El-Din, M. 2018. Degradation of naphthenic acid model compounds in aqueous solution by UV activated persulfate: Influencing factors, kinetics and reaction mechanisms. Chemosphere, **211**: 271–277. Elsevier Ltd. doi:10.1016/j.chemosphere.2018.07.132.

Fang, Z., Huang, R., Chelme-Ayala, P., Shi, Q., Xu, C., and Gamal El-Din, M. 2019. Comparison of UV/Persulfate and UV/H2O2 for the removal of naphthenic acids and acute toxicity towards Vibrio fischeri from petroleum production process water. Sci. Total Environ., **694**: 133686. Elsevier B.V. doi:10.1016/j.scitotenv.2019.133686.

Fang, Z., Huang, R., How, Z.T., Jiang, B., Chelme-Ayala, P., Shi, Q., Xu, C., and Gamal El-Din, M. 2020. Molecular transformation of dissolved organic matter in process water from oil and gas operation during UV/H2O2, UV/chlorine, and UV/persulfate processes. Sci. Total Environ., **730**: 139072. Elsevier B.V. doi:10.1016/j.scitotenv.2020.139072.

Fathepure, B.Z. 2014. Recent studies in microbial degradation of petroleum hydrocarbons in hypersaline environments. Frontiers in Microbiology, **5**(173): 1-16, doi: 10.3389/fmicb.2014.00173

Federal Remediation Technologies Roundtable (FRTR). 2023. Technology Screening Matrix. https://www.frtr.gov/matrix/default.cfm [accessed 16 February 2023].

Feizi, R., Jorfi, S., and Takdastan, A. 2020. Bioremediation of phenanthrene-polluted soil using bacillus kochii ahv-kh14 as a halo-tolerant strain isolated from compost. Environmental Health Engineering and Management, **7**(1): 23–30. Kerman University of Medical Sciences. doi:10.34172/EHEM.2020.04.

Ferris, M.J., Muyzer, G., and Ward, D.M. 1996. Denaturing gradient gel electrophoresis profiles of 16S rRNA-defined populations inhabiting a hot spring microbial mat community. Applied and Environmental Microbiology, **62**(2): 340–346. American Society for Microbiology. doi:10.1128/aem.62.2.340-346.1996.

Finkel, M.L. 2018. The impact of oil sands on the environment and health. Curr. Opin. Environ. Sci. Heal., **3**: 52–55. Elsevier Ltd. doi:10.1016/j.coesh.2018.05.002.

Foght, J. 2008. Anaerobic biodegradation of aromatic hydrocarbons: Pathways and prospects. Journal of Molecular Microbiology and Biotechnology, **15**(2–3): 93–120. doi:10.1159/000121324.

Foght, J.M., Gieg, L.M., and Siddique, T. 2017. The microbiology of oil sands tailings: Past, present, future. FEMS Microbiol. Ecol., **93**(5): 1–23. doi:10.1093/femsec/fix034.

Foght, J.M., and Westlake, D.W.S. 1991. Cross hybridization of plasmid and genomic DNA from aromatic and polycyclic aromatic hydrocarbon degrading bacteria. Canadian Journal of Microbiology, **37**(12): 924–932. doi:10.1139/m91-160.

Foght, J.M., and Westlake, D.W.S. 1996. Transposon and spontaneous deletion mutants of plasmid-borne genes encoding polycyclic aromatic hydrocarbon degradation by a strain of Pseudomonas fluorescens. Biodegradation, **7**(4): 353–366. doi:10.1007/BF00115749.

Frank, R.A., Fischer, K., Kavanagh, R., Burnison, B.K., Arsenault, G., Headley, J. V, Peru, K.M., Kraak, G. Van Der, and Solomon, K.R. 2009. Effect of Carboxylic Acid Content on the Acute Toxicity of Oil Sands Naphthenic Acids. Environmental Science & Technology, **43**(2): 266–271. American Chemical Society. doi:10.1021/es8021057.

Frank, R.A., Kavanagh, R., Kent Burnison, B., Arsenault, G., Headley, J. V., Peru, K.M., Van Der Kraak, G., and Solomon, K.R. 2008. Toxicity assessment of collected fractions from an extracted naphthenic acid mixture. Chemosphere, **72**(9): 1309–1314. doi:10.1016/j.chemosphere.2008.04.078.

Gamal El-Din, M., Fu, H., Wang, N., Chelme-Ayala, P., Pérez-Estrada, L., Drzewicz, P., Martin, J.W., Zubot, W., and Smith, D.W. 2011. Naphthenic acids speciation and removal during petroleum-coke adsorption and ozonation of oil sands process-affected water. Sci. Total Environ., **409**(23): 5119–5125. doi:10.1016/j.scitotenv.2011.08.033.

Ganiyu, S.O., Arslan, M., and Gamal El-Din, M. 2022a. Combined solar activated sulfate radical-based advanced oxidation processes (SR-AOPs) and biofiltration for the remediation of dissolved organics in oil sands produced water. Chemical Engineering Journal, **433**(P1): 134579. Elsevier B.V. doi:10.1016/j.cej.2022.134579.

Ganiyu, S.O., Sable, S., and Gamal El-Din, M. 2022b. Advanced oxidation processes for the degradation of dissolved organics in produced water: A review of process performance, degradation kinetics and pathway. Chemical Engineering Journal, **429**. Elsevier B.V. doi:10.1016/j.cej.2021.132492.

Gao, M., Yang, J., Liu, Y., Zhang, J., Li, J., Liu, Y., Wu, B., and Gu, L. 2022. Deep insights into the anaerobic co-digestion of waste activated sludge with concentrated leachate under different salinity stresses. Science of the Total Environment, **838**. Elsevier B.V. doi:10.1016/j.scitotenv.2022.155922.

Gao, Y., Fang, J., Gao, N., Yi, X., Mao, W., and Zhang, J. 2018. Kinetic and mechanistic investigations of the degradation of propranolol in heat activated persulfate process. RSC Advances, **8**(72): 41163–41171. Royal Society of Chemistry. doi:10.1039/c8ra08488b.

Garcia-Garcia, E., Ge, J.Q., Oladiran, A., Montgomery, B., El-Din, M.G., Perez-Estrada, L.C., Stafford, J.L., Martin, J.W., and Belosevic, M. 2011. Ozone treatment ameliorates oil sands process water toxicity to the mammalian immune system. Water Research, **45**(18): 5849–5857. Elsevier Ltd. doi:10.1016/j.watres.2011.08.032.

Gibson, J.J., and Peters, D.L. 2022. Water and environmental management in oil sands regions. Journal of Hydrology: Regional Studies, **44**. Elsevier B.V. doi:10.1016/j.ejrh.2022.101274.

Glaze, W.H. 1987. Drinking-water treatment with ozone. Environmental Science \& Technology, **21**(3): 224–230. doi:10.1021/es00157a001.

Gou, Y., Zhao, Q., Yang, S., Qiao, P., Cheng, Y., Song, Y., Sun, Z., Zhang, T., Wang, L., and Liu, Z. 2020a. Enhanced degradation of polycyclic aromatic hydrocarbons in aged subsurface soil using integrated persulfate oxidation and anoxic biodegradation. Chemical Engineering Journal, **394**. Elsevier B.V. doi:10.1016/j.cej.2020.125040.

Gou, Y., Zhao, Q., Yang, S., Wang, H., Qiao, P., Song, Y., Cheng, Y., and Li, P. 2020b. Removal of polycyclic aromatic hydrocarbons (PAHs) and the response of indigenous bacteria in highly contaminated aged soil after persulfate oxidation. Ecotoxicology and Environmental Safety, **190**. Academic Press. doi:10.1016/j.ecoenv.2019.110092.

Government of Alberta. 2018. Environmental quality guidelines for Alberta surface waters. *In* Environmental Quality Guidelines for Alberta Surface Waters. Water Policy Branch, Alberta Environment and Parks, Edmonton, AB.

Government of Alberta. 2022. Alberta Tier 1 Soil and Groundwater Remediation Guidelines. Alberta Environment and Parks.

Government of Canada. 2020. Benzene in Gasoline Regulations: FAQs. Available fromw.canada.ca/en/environment-climate-change/services/canadian-environmental-protection-act-registry/benzene-gasoline-regulations-frequently-asked-questions.html [accessed 16 February 2023].

Government of Canada, Environment Canada, and Health Canada. 1993. Canadian Environmental Protection Act: Priority Substance List Assessment report: Benzene. Minister of Supply and Services Canada 1993.

Grbić-Galić, D., and Vogel, T.M. 1987. Transformation of toluene and benzene by mixed methanogenic cultures. Applied and Environmental Microbiology, **53**(2): 254–260. American Society for Microbiology. doi:10.1128/aem.53.2.254-260.1987.

Grewer, D.M., Young, R.F., Whittal, R.M., and Fedorak, P.M. 2010. Naphthenic acids and other acid-extractables in water samples from Alberta: What is being measured? Science of the Total Environment, **408**(23): 5997–6010. doi:10.1016/j.scitotenv.2010.08.013.

Gunde-Cimerman, N., Plemenitaš, A., and Oren, A. 2018. Strategies of adaptation of microorganisms of the three domains of life to high salt concentrations. FEMS Microbiology Reviews, **42**(3): 353–375. Oxford University Press. doi:10.1093/femsre/fuy009.

Guo, S., Toth, C.R.A., Luo, F., Chen, X., Xiao, J., and Edwards, E.A. 2022. Transient Oxygen Exposure Causes Profound and Lasting Changes to a Benzene-Degrading Methanogenic Community. Environmental Science and Technology, **56**(18): 13036–13045. American Chemical Society. doi:10.1021/acs.est.2c02624.

Han, X., MacKinnon, M.D., and Martin, J.W. 2009. Estimating the in situ biodegradation of naphthenic acids in oil sands process waters by HPLC/HRMS. Chemosphere, **76**(1): 63–70. Elsevier Ltd. doi:10.1016/j.chemosphere.2009.02.026.

Han, X., Scott, A.C., Fedorak, P.M., Bataineh, M., and Martin, J.W. 2008. Influence of molecular structure on the biodegradability of naphthenic acids. Environ. Sci. Technol., **42**(4): 1290–1295. doi:10.1021/es702220c.

Hassan, H., Rizk, N., 1*, H.A.H., Rizk, N.M., Hefnawy, M.A., and Awad, A.M. 2012. Isolation and Characterization of Halophilic Aromatic and Chloroaromatic Degrader from Wadi El-Natrun Soda lake Environmental Biotechnology View project Prevalence, antibiotic resistance and virulence of Enterococcus spp. View project Isolation and Characterization of Halophilic Aromatic and Chloroaromatic Degrader from Wadi El-Natrun Soda lakes. *In* Life Science Journal.

He, Y., Patterson, S., Wang, N., Hecker, M., Martin, J.W., El-Din, M.G., Giesy, J.P., and Wiseman, S.B. 2012. Toxicity of untreated and ozone-treated oil sands process-affected water (OSPW) to early life stages of the fathead minnow (Pimephales promelas). Water Research, **46**(19): 6359–6368. doi:https://doi.org/10.1016/j.watres.2012.09.004.

Headley, J. V, Barrow, M.P., Peru, K.M., Fahlman, B., Frank, R.A., Bickerton, G., McMaster, M.E., Parrott, J., and Hewitt, L.M. 2011. Preliminary fingerprinting of Athabasca oil sands polar organics in environmental samples using electrospray ionization Fourier transform ion cyclotron resonance mass spectrometry. Rapid Communications in Mass Spectrometry, **25**(13): 1899–1909. John Wiley & Sons, Ltd. doi:https://doi.org/10.1002/rcm.5062.

Headley, J. V., and McMartin, D.W. 2004. A review of the occurrence and fate of naphthenic acids in aquatic environments. Journal of Environmental Science and Health - Part A Toxic/Hazardous Substances and Environmental Engineering, **39**(8), 1989–2010. https://doi.org/10.1081/ESE-120039370

Headley, J. V, Peru, K.M., Adenugba, A.A., Du, J.L., and Mcmartin, D.W. 2010. Dissipation of naphthenic acids mixtures by lake biofilms. Journal of Environmental Science and Health, Part A, **45**(9): 1027–1036. Taylor & Francis. doi:10.1080/10934529.2010.486310.

Headley, J. V, Peru, K.M., Mcmartin, D.W., and Winkler, M. 2002. Determination of Dissolved Naphthenic Acids in Natural Waters by Using Negative-Ion Electrospray Mass Spectrometry. Journal of AOAC INTERNATIONAL, **85**(1): 182–187. doi:10.1093/jaoac/85.1.182.

Health Canada. 2009. Guidelines for Canadian drinking water quality: Guideline technical document: Benzene. Water, Air and Climate Change Bureau, Healthy Environments and Consumer Safety Branch, Health Canada, Ottawa, ON.

Herman, D.C., Fedorak, P.M., and Costerton, J.W. 1993. Biodegradation of cycloalkane carboxylic acids in oil sand tailings. Canadian Journal of Microbiology, **39**(6): 576–580. doi:10.1139/m93-083.

Herman, D.C., Fedorak, P.M., MacKinnon, M.D., and Costerton, J.W. 1994. Biodegradation of naphthenic acids by microbial populations indigenous to oil sands tailings. Can. J. Microbiol., **40**(6): 467–477. doi:10.1139/m94-076.

Hoehler, T., Gunsalus, R.P., and Mcinerney, M.J. 2010. Environmental Constraints that Limit Methanogenesis. *In* Handbook of Hydrocarbon and Lipid Microbiology. pp. 635–654.

Holmes, D., Risso, C., Smith, J., and Lovley, D. 2011. Anaerobic Oxidation of Benzene by the Hyperthermophilic Archaeon Ferroglobus placidus. Applied and Environmental Microbiology, **77**(17): 5926–5933. American Society for Microbiology. doi:10.1128/AEM.05452-11.

Holowenko, F.M., Mackinnon, M.D., and Fedorak, P.M. 2002. Characterization of naphthenic acids in oil sands wastewaters by gas chromatography-mass spectrometry. Water Research, **36**, 2843–2855.

Hu, X., Li, D., Qiao, Y., Song, Q., Guan, Z., Qiu, K., Cao, J., and Huang, L. 2020. Salt tolerance mechanism of a hydrocarbon-degrading strain: Salt tolerance mediated by accumulated betaine in cells. Journal of Hazardous Materials, **392**. Elsevier B.V. doi:10.1016/j.jhazmat.2020.122326.

Hua, F., and Wang, H.Q. 2014. Factors influencing crude oil biodegradation by pseudomonas sp. DG17. Asian Journal of Chemistry, **26**(15): 4637–4642. Chemical Publishing Co. doi:10.14233/ajchem.2014.16149.

Huang, C., Shi, Y., Gamal El-Din, M., and Liu, Y. 2015. Treatment of oil sands process-affected water (OSPW) using ozonation combined with integrated fixed-film activated sludge (IFAS). Water Res., **85**: 167–176. Elsevier Ltd. doi:10.1016/j.watres.2015.08.019.

Huang, C., Shi, Y., Xue, J., Zhang, Y., Gamal El-Din, M., and Liu, Y. 2017. Comparison of biomass from integrated fixed-film activated sludge (IFAS), moving bed biofilm reactor (MBBR) and membrane bioreactor (MBR) treating recalcitrant organics: Importance of attached biomass. Journal of Hazardous Materials, **326**: 120–129. Elsevier B.V. doi:10.1016/j.jhazmat.2016.12.015.

Huang, H., Jiang, Y., Zhao, J., Li, S., Schulz, S., and Deng, L. 2021. BTEX biodegradation is linked to bacterial community assembly patterns in contaminated groundwater ecosystem. Journal of Hazardous Materials, **419**. Elsevier B.V. doi:10.1016/j.jhazmat.2021.126205.

Hughes, S.A., Mahaffey, A., Shore, B., Baker, J., Kilgour, B., Brown, C., Peru, K.M., Headley, J. V., and Bailey, H.C. 2017. Using ultrahigh-resolution mass spectrometry and toxicity identification techniques to characterize the toxicity of oil sands process-affected water: The case for classical naphthenic acids. Environ. Toxicol. Chem., **36**(11): 3148–3157. doi:10.1002/etc.3892.

Hwang, G., Dong, T., Islam, M.S., Sheng, Z., Pérez-Estrada, L.A., Liu, Y., and Gamal El-Din, M. 2013. The impacts of ozonation on oil sands process-affected water biodegradability and biofilm formation characteristics in bioreactors. Bioresourc. Technol., **130**: 269–277. doi:10.1016/j.biortech.2012.12.005.

Imron, M.F., Kurniawan, S.B., Ismail, N. 'Izzati, and Abdullah, S.R.S. 2020. Future challenges in diesel biodegradation by bacteria isolates: A review. Journal of Cleaner Production, **251**. https://doi.org/10.1016/j.jclepro.2019.119716

Islam, M.S., Dong, T., McPhedran, K.N., Sheng, Z., Zhang, Y., Liu, Y., and Gamal El-Din, M. 2014. Impact of ozonation pre-treatment of oil sands process-affected water on the operational performance of a GAC-fluidized bed biofilm reactor. Biodegradation, **25**(6): 811–823. doi:10.1007/s10532-014-9701-6.

Islam, M.S., Zhang, Y., McPhedran, K.N., Liu, Y., and Gamal El-Din, M. 2015. Granular activated carbon for simultaneous adsorption and biodegradation of toxic oil sands process-affected water organic compounds. Journal of Environmental Management, **152**: 49–57. Academic Press. doi:10.1016/j.jenvman.2015.01.020.

Izawa, S., Inoue, Y., and Kimura, A. 1996. Importance of catalase in the adaptive response to hydrogen peroxide: analysis of acatalasaemic Saccharomyces cerevisiae. The Biochemical Journal, **320**(1): 61–67. doi:10.1042/bj3200061.

Jiang, H., Chen, D., Zheng, D., and Xiao, Z. 2023. Anaerobic mineralization of toluene by enriched soil-free consortia with solid-phase humin as a terminal electron acceptor. Environmental Pollution, **317**. Elsevier Ltd. doi:10.1016/j.envpol.2022.120794.

Jivraj, M., Mackinnon, M., and Fung, B. 1995. Naphthenic Acid Extraction and Quantitative Analysis with FT-IR Spectroscopy. Syncrude Analytical Methods Manual, Syncrude Research Department, Edmonton, AB.

Johnson, B.T. 2005. MICROTOX ® ACUTE TOXICITY TEST. *In* Small scale freshwater toxicity investigations. *Edited by* C. Blaise and J.F. Ferards. Springer. pp. 69–105.

Jung, H., Ahn, Y., Choi, H., and Kim, I.S. 2005. Effects of in-situ ozonation on indigenous microorganisms in diesel contaminated soil: Survival and regrowth. Chemosphere, **61**(7): 923–932. doi:10.1016/j.chemosphere.2005.03.038.

Kadam, P.C., Godbole, S.H., and Ranade, D.R. 1989. Isolation of methanogens from Arabian sea sediments and their salt tolerance. FEMS Microbiology Letters, **62**(6): 343–347. doi:https://doi.org/10.1016/0378-1097(89)90002-5.

Kakosová, E., Hrabák, P., Černík, M., Novotný, V., Czinnerová, M., Trögl, J., Popelka, J., Kuráň, P., Zoubková, L., and Vrtoch, Ľ. 2017. Effect of various chemical oxidation agents on soil microbial communities. Chemical Engineering Journal, **314**: 257–265. Elsevier B.V. doi:10.1016/j.cej.2016.12.065.

Kannel, P.R., and Gan, T.Y. 2012. Naphthenic acids degradation and toxicity mitigation in tailings wastewater systems and aquatic environments: A review. Journal of Environmental Science and Health - Part A Toxic/Hazardous Substances and Environmental Engineering, **47**(1): 1–21. doi:10.1080/10934529.2012.629574.

Kasai, Y., Takahata, Y., Manefield, M., and Watanabe, K. 2006. RNA-Based Stable Isotope Probing and Isolation of Anaerobic Benzene-Degrading Bacteria from Gasoline-Contaminated Groundwater. Applied and Environmental Microbiology, **72**(5): 3586–3592. American Society for Microbiology. doi:10.1128/AEM.72.5.3586-3592.2006.

Katyal, A., and Morrison, R.D. 2007. CHAPTER 11 - FORENSIC APPLICATIONS OF CONTAMINANT TRANSPORT MODELS IN THE SUBSURFACE. *In* Introduction to Environmental Forensics (Second Edition). *Edited by* B.L. Murphy and R.D. Morrison. Academic Press, Burlington. pp. 513–575.

Kazumi, J., Caldwell, M.E., Suflita, J.M., Lovley, D.R., and Young, L.Y. 1997. Anaerobic Degradation of Benzene in Diverse Anoxic Environments. Environmental Science & Technology, **31**(3): 813–818. American Chemical Society. doi:10.1021/es960506a.

Kessler, S., Barbour, L., Van Rees, K.C.J., and Dobchuk, B.S. 2010. Salinization of soil over saline-sodic overburden from the oil sands in Alberta. Canadian Journal of Soil Science, **90**(4): 637–647. doi:10.4141/CJSS10019.

Khoshkholgh Sima, N.A., Ebadi, A., Reiahisamani, N., and Rasekh, B. 2019. Bio-based remediation of petroleum-contaminated saline soils: Challenges, the current state-of-the-art and future prospects. Journal of Environmental Management, **250**. https://doi.org/10.1016/j.jenvman.2019.109476

Kinley, C.M., Gaspari, D.P., McQueen, A.D., Rodgers, J.H., Castle, J.W., Friesen, V., and Haakensen, M. 2016. Effects of environmental conditions on aerobic degradation of a commercial naphthenic acid. Chemosphere, **161**: 491–500. Elsevier Ltd. doi:10.1016/j.chemosphere.2016.07.050.

Klamerth, N., Moreira, J., Li, C., Singh, A., McPhedran, K.N., Chelme-Ayala, P., Belosevic, M., and Gamal El-Din, M. 2015. Effect of ozonation on the naphthenic acids' speciation and toxicity of pH-dependent organic extracts of oil sands process-affected water. Science of The Total Environment, **506–507**: 66–75. doi:https://doi.org/10.1016/j.scitotenv.2014.10.103.

Kleinsteuber, S., Riis, V., Fetzer, I., Harms, H., and Müller, S. 2006. Population dynamics within a microbial consortium during growth on diesel fuel in saline environments. Applied and Environmental Microbiology, **72**(5): 3531–3542. doi:10.1128/AEM.72.5.3531-3542.2006.

Kleinsteuber, S., Schleinitz, K.M., Breitfeld, J., Harms, H., Richnow, H.H., and Vogt, C. 2008. Molecular characterization of bacterial communities mineralizing benzene under sulfate-reducing conditions. FEMS Microbiology Ecology, **66**(1): 143–157. John Wiley & Sons, Ltd. doi:https://doi.org/10.1111/j.1574-6941.2008.00536.x.

Klopman, G., Saiakhov, R., Rosenkranz, H.S., and Hermens, J.L.M. 1999. Multiple Computer-Automated structure evaluation program study of aquatic toxicity 1: Guppy. Environmental Toxicology and Chemistry, **18**(11): 2497–2505. doi:https://doi.org/10.1002/etc.5620181116.

Kunapuli, U., Lueders, T., and Meckenstock, R.U. 2007. The use of stable isotope probing to identify key iron-reducing microorganisms involved in anaerobic benzene degradation. The ISME Journal, **1**(7): 643–653. doi:10.1038/ismej.2007.73.

Kuroda, K., Yamamoto, K., Nakai, R., Hirakata, Y., Kubota, K., Nobu, M.K., and Narihiro, T. 2022. Symbiosis between Candidatus Patescibacteria and Archaea Discovered in Wastewater-Treating Bioreactors. mBio, **13**(5). American Society for Microbiology. doi:10.1128/mbio.01711-22.

Kuznetsov, P., Wei, K., Kuznetsova, A., Foght, J., Ulrich, A., and Siddique, T. 2023. Anaerobic Microbial Activity May Affect Development and Sustainability of End-Pit Lakes: A Laboratory Study of Biogeochemical Aspects of Oil Sands Mine Tailings. ACS ES and T Water, **3**(4): 1039–1049. American Chemical Society. doi:10.1021/acsestwater.2c00505.

Lai, J.W.S., Pinto, L.J., Kiehlmann, E., Bendell-Young, L.I., and Moore, M.M. 1996. Factors that affect the degradation of naphthenic acids in oil sands wastewater by indigenous microbial communities. Environ. Toxicol. Chem., **15**(9): 1482–1491. doi:10.1002/etc.5620150909.

Lee, C.Y., and Lin, C.H. 2006. Bacterial growth and substrate degradation by BTX-oxidizing culture in response to salt stress. Journal of Industrial Microbiology and Biotechnology, **33**(1): 37–44. doi:10.1007/s10295-005-0049-0.

Lee, C.Y., and Liu, W. Der. 2006. The effect of salinity conditions on kinetics of trichloroethylene biodegradation by toluene-oxidizing cultures. Journal of Hazardous Materials, **137**(1): 541–549. doi:10.1016/j.jhazmat.2006.02.031.

Lee, J., Von Gunten, U., and Kim, J.H. 2020. Persulfate-Based Advanced Oxidation: Critical Assessment of Opportunities and Roadblocks. Environmental Science and Technology, **54**(6), 3064–3081. https://doi.org/10.1021/acs.est.9b07082

Lee, K., and Ulrich, A. 2021. Indigenous microbial communities in Albertan sediments are capable of anaerobic benzene biodegradation under methanogenic, sulfate-reducing, nitrate-reducing, and iron-reducing redox conditions. Water Environment Research, **93**(4): 524–534. John Wiley and Sons Inc. doi:10.1002/wer.1454.

Lei, Y.J., Zhang, J., Tian, Y., Yao, J., Duan, Q.S., and Zuo, W. 2020. Enhanced degradation of total petroleum hydrocarbons in real soil by dual-frequency ultrasound-activated persulfate. Science of the Total Environment, **748**. Elsevier B.V. doi:10.1016/j.scitotenv.2020.141414.

Lenntech. 2023. Hydrogen Peroxide. Available fromw.lenntech.com/library/oxidation/h2o2/hydrogen-peroxide.htm. [accessed 14 July 2023].

Li, C., Fu, L., Stafford, J., Belosevic, M., and Gamal El-Din, M. 2017a. The toxicity of oil sands process-affected water (OSPW): A critical review. Sci. Total Environ., **601–602**: 1785–1802. doi:10.1016/j.scitotenv.2017.06.024.

Li, W., Orozco, R., Camargos, N., and Liu, H. 2017b. Mechanisms on the Impacts of Alkalinity, pH, and Chloride on Persulfate-Based Groundwater Remediation. Environ. Sci. Technol., **51**(7): 3948–3959. doi:10.1021/acs.est.6b04849.

Li, Y., Li, A.M., Xu, J., Li, W.W., and Yu, H.Q. 2013. Formation of soluble microbial products (SMP) by activated sludge at various salinities. Biodegradation, **24**(1): 69–78. Kluwer Academic Publishers. doi:10.1007/s10532-012-9558-5.

Li, Y., Li, W., Ji, L., Song, F., Li, T., Fu, X., Li, Q., Xing, Y., Zhang, Q., and Wang, J. 2022. Effects of Salinity on the Biodegradation of Polycyclic Aromatic Hydrocarbons in Oilfield Soils Emphasizing Degradation Genes and Soil Enzymes. Frontiers in Microbiology, **12**. Frontiers Media S.A. doi:10.3389/fmicb.2021.824319.

Li, Y.T., Li, D., Lai, L.J., and Li, Y.H. 2020. Remediation of petroleum hydrocarbon contaminated soil by using activated persulfate with ultrasound and ultrasound/Fe. Chemosphere, **238**. Elsevier Ltd. doi:10.1016/j.chemosphere.2019.124657.

Liang, C., Huang, C.F., and Chen, Y.J. 2008a. Potential for activated persulfate degradation of BTEX contamination. Water Res., **42**(15): 4091–4100. doi:10.1016/j.watres.2008.06.022.

Liang, C., Huang, C.F., Mohanty, N., and Kurakalva, R.M. 2008b. A rapid spectrophotometric determination of persulfate anion in ISCO. Chemosphere, **73**(9): 1540–1543. Elsevier Ltd. doi:10.1016/j.chemosphere.2008.08.043.

Liang, C., Wang, Z.S., and Mohanty, N. 2006. Influences of carbonate and chloride ions on persulfate oxidation of trichloroethylene at 20 °C. Sci. Total Environ., **370**(2–3): 271–277. doi:10.1016/j.scitotenv.2006.08.028.

Liang, L., Song, X., Kong, J., Shen, C., Huang, T., and Hu, Z. 2014. Anaerobic biodegradation of high-molecular-weight polycyclic aromatic hydrocarbons by a facultative anaerobe Pseudomonas sp. JP1. Biodegradation, **25**(6): 825–833. doi:10.1007/s10532-014-9702-5.

Liang, X., Zhu, X., and Butler, E.C. 2011. Comparison of four advanced oxidation processes for the removal of naphthenic acids from model oil sands process water. J. Hazard. Mater., **190**(1–3): 168–176. Elsevier B.V. doi:10.1016/j.jhazmat.2011.03.022.

Liao, X., Wu, Z., Li, Y., Cao, H., and Su, C. 2019. Effect of various chemical oxidation reagents on soil indigenous microbial diversity in remediation of soil contaminated by PAHs. Chemosphere, **226**: 483–491. Elsevier Ltd. doi:10.1016/j.chemosphere.2019.03.126.

Liao, X., Wu, Z., Li, Y., Luo, J., and Su, C. 2018. Enhanced degradation of polycyclic aromatic hydrocarbons by indigenous microbes combined with chemical oxidation. Chemosphere, **213**: 551–558. Elsevier Ltd. doi:10.1016/j.chemosphere.2018.09.092.

Liu, C., Li, H., Zhang, Y., Si, D., and Chen, Q. 2016. Evolution of microbial community along with increasing solid concentration during high-solids anaerobic digestion of sewage sludge. Bioresource Technology, **216**: 87–94. doi:https://doi.org/10.1016/j.biortech.2016.05.048.

Liu, Y., Yuan, Y., Wang, W., Wachemo, A.C., and Zou, D. 2019. Effects of adding osmoprotectant on anaerobic digestion of kitchen waste with high level of salinity. Journal of Bioscience and Bioengineering, **128**(6): 723–732. Elsevier B.V. doi:10.1016/j.jbiosc.2019.05.011.

Longang, A., Buck, C., and Kirkwood, K.M. 2016. Halotolerance and effect of salt on hydrophobicity in hydrocarbon-degrading bacteria. Environmental Technology (United Kingdom), **37**(9): 1133–1140. Taylor and Francis Ltd. doi:10.1080/09593330.2015.1102333.

Lovley, D.R. 2000. Anaerobic benzene degradation. Biodegradation, **11**:107-116.

Lovley, D.R., Coates, J.D., Woodward, J.C., and Phillips, E.J.P. 1995. Benzene Oxidation Coupled to Sulfate Reduction. APPLIED AND ENVIRONMENTAL MICROBIOLOGY, **61**(3): 953–958.

Lovley, D.R., Woodward, J.C., and Chapelle, F.H. 1996. Rapid Anaerobic Benzene Oxidation with a Variety of Chelated Fe(III) Forms. Applied and Environmental Microbiology, **62**(1): 288–291. American Society for Microbiology. doi:10.1128/aem.62.1.288-291.1996.

Lowe, S.E., Jain, M.K., and Zeikus, G.J. 1993. Biology of anaerobic bacteria adapted to salt. Microbiological Reviews, **57**(2): 451–509.

Lozupone, C.A., and Knight, R. 2007. Global patterns in bacterial diversity. PNAS, **104**(27): 11436–11440.

Luo, F., Devine, C.E., and Edwards, E.A. 2016. Cultivating microbial dark matter in benzene-degrading methanogenic consortia. Environmental Microbiology, **18**(9): 2923–2936. Blackwell Publishing Ltd. doi:10.1111/1462-2920.13121.

Mahaffey, A., and Dube, M. 2016. Review of the composition and toxicity of oil sands process-affected water. Environmental Reviews, **25**. doi:10.1139/er-2015-0060.

Mahour, R. 2016. Reza Mahour. Master of Science, University of Alberta, Edmonton, AB.

Marsh, W.P. 2006. Sorption of naphthenic acids to soil minerals. Master of Science, University of Alberta, Edmonton, AB.

Martin, D.D., Ciulla, R.A., and Roberts, M.F. 1999. MINIREVIEW Osmoadaptation in Archaea. *In* APPLIED AND ENVIRONMENTAL MICROBIOLOGY.

Martin, J.W., Barri, T., Han, X., Fedorak, P.M., El-Din, M.G., Perez, L., Scott, A.C., and Jiang, J.T. 2010. Ozonation of oil sands process-affected water accelerates microbial bioremediation. Environ. Sci. Technol., **44**(21): 8350–8356. doi:10.1021/es101556z.

Masumoto, H., Kurisu, F., Kasuga, I., Tourlousse, D.M., and Furumai, H. 2012. Complete mineralization of benzene by a methanogenic enrichment culture and effect of putative metabolites on the degradation. Chemosphere, **86**(8): 822–828. Elsevier Ltd. doi:10.1016/j.chemosphere.2011.11.051.

Matzek, L.W., and Carter, K.E. 2016. Activated persulfate for organic chemical degradation: A review. Chemosphere, **151**: 178–188. Elsevier Ltd. doi:10.1016/j.chemosphere.2016.02.055.

McCall, P.J., Swann, R.L., Laskowski, D.A., Unger, S.M., Vrona, S.A., and Dishburger, H.J. 1980. Estimation of chemical mobility in soil from liquid chromatographic retention times. Bulletin of Environmental Contamination and Toxicology, **24**(1): 190–195. doi:10.1007/BF01608096.

McGenity T.J., and Sorokin, D.Y. 2019. Methanogens and Methanogenesis in Hypersaline Environments. *In* Biogenesis of Hydrocarbons. *Edited by* A.J.M. Stams and D.Z. Sousa. Springer Nature Switzerland.

Medina, R., David Gara, P.M., Fernández-González, A.J., Rosso, J.A., and Del Panno, M.T. 2018. Remediation of a soil chronically contaminated with hydrocarbons through persulfate oxidation and bioremediation. Sci. Total Environ., **618**: 518–530. Elsevier B.V. doi:10.1016/j.scitotenv.2017.10.326.

Meshref, M.N.A., Chelme-Ayala, P., and Gamal El-Din, M. 2017. Fate and abundance of classical and heteroatomic naphthenic acid species after advanced oxidation processes: Insights and indicators of transformation and degradation. Water Research, **125**: 62–71. Elsevier Ltd. doi:10.1016/j.watres.2017.08.007.

Mesquita, P.L., Aquino, S.F., Xavier, A.L.P., Silva, J.C.C. da, Afonso, R.C.F., and Silva, S.Q. 2010. Soluble microbial product (SMP) characterization in bench-scale aerobic and anaerobic CSTRs under different operational conditions. Brazilian Journal of Chemical Engineering, **27**(1): 101–111. Brazilian Society of Chemical Engineering. doi:10.1590/S0104-66322010000100009.

Michael-Igolima, U., Abbey, S.J., and Ifelebuegu, A.O. 2022. A systematic review on the effectiveness of remediation methods for oil contaminated soils. Environmental Advances, **9**. https://doi.org/10.1016/j.envadv.2022.100319

Miles, S.M., Asiedu, E., Balaberda, A. lynne, and Ulrich, A.C. 2020. Oil sands process affected water sourced Trichoderma harzianum demonstrates capacity for mycoremediation of naphthenic acid fraction compounds. Chemosphere, **258**: 127281. Elsevier Ltd. doi:10.1016/j.chemosphere.2020.127281.

Min, W.-H., Fang, X.-B., Wu, T., Fang, L., Liu, C.-L., and Wang, J. 2019. Characterization and antioxidant activity of an acidic exopolysaccharide from Lactobacillus plantarum JLAU103. Journal of Bioscience and Bioengineering, **127**(6): 758–766. doi:https://doi.org/10.1016/j.jbiosc.2018.12.004.

Minai-Tehrani, D., Minoui, S., and Herfatmanesh, A. 2009. Effect of salinity on biodegradation of polycyclic aromatic hydrocarbons (PAHs) of heavy crude oil in soil. Bulletin of Environmental Contamination and Toxicology, **82**(2): 179–184. doi:10.1007/s00128-008-9548-9.

Mohamed, S., Selim, M., Mahmoud, M., Ibrahim, A., and Ghazy, E. 2019. Production, characterization, and antioxidant activities of bacterial exopolysaccharides extracted from petroleum oil water. Egyptian Pharmaceutical Journal, **18**(1): 42–52. Wolters Kluwer Medknow Publications. doi:10.4103/epj.epj_36_18.

Moore, E.R.B., Tindall, B.J., Martins Dos Santos, V.A.P., Pieper, D.H., Ramos, J.-L., and Palleroni, N.J. 2006. Nonmedical: Pseudomonas. *In* The Prokaryotes: A Handbook on the Biology of Bacteria Volume 6: Proteobacteria: Gamma Subclass. *Edited by* M. Dworkin, S. Falkow, E. Rosenberg, K.-H. Schleifer, and E. Stackebrandt. Springer New York, New York, NY. pp. 646–703.

Mora, V.C., Madueño, L., Peluffo, M., Rosso, J.A., Del Panno, M.T., and Morelli, I.S. 2014. Remediation of phenanthrene-contaminated soil by simultaneous persulfate chemical oxidation and biodegradation processes. Environ. Sci. Pollut. Res., **21**(12): 7548–7556. doi:10.1007/s11356-014-2687-0.

Morandi, G.D., Wiseman, S.B., Guan, M., Zhang, X.W., Martin, J.W., and Giesy, J.P. 2017. Elucidating mechanisms of toxic action of dissolved organic chemicals in oil sands process-affected water (OSPW). Chemosphere, **186**: 893–900. Elsevier Ltd. doi:10.1016/j.chemosphere.2017.08.025.

Morandi, G.D., Wiseman, S.B., Pereira, A., Mankidy, R., Gault, I.G.M., Martin, J.W., and Giesy, J.P. 2015. Effects-Directed Analysis of Dissolved Organic Compounds in Oil Sands Process-Affected Water. Environmental Science and Technology, **49**(20): 12395–12404. American Chemical Society. doi:10.1021/acs.est.5b02586.

Nales, M., Butler, B.J., and Edwards, E.A. 1998. Anaerobic benzene biodegradation: A microcosm survey. Bioremediation Journal, **2**(2): 125–144. CRC Press. doi:10.1080/10889869891214268.

National Energy Board (NEB). 2018. Canadian Refinery Overview: Energy Market Assessment April 2018. https://www.cer-rec.gc.ca/en/data-analysis/energy-commodities/crude-oil-petroleum-products/report/archive/2018-refinery-report/2018cndnrfnrvrvw-eng.pdf [accessed 16 February 2023].

National Pollutant Release Inventory (NPRI). 2023. National Pollutant Release Inventory Data Search. Environment and Climate Change Canada, Gatineau, Quebec. https://pollution-waste.canada.ca/national-release-inventory/ [accessed 4 January 2023].

National Resources Canada (NRCan). 2019. Energy Fact Book 2019-2020. https://natural-resources.canada.ca/sites/www.nrcan.gc.ca/files/energy/pdf/Energy%20Fact%20Book_2019_2020_web-resolution.pdf [accessed 9 February 2023].

National Resources Canada (NRCan). 2020. Crude Oil Industry Overview. https://natural-resources.canada.ca/our-natural-resources/energy-sources-distribution/fossil-fuels/crude-oil/crude-oil-industry-overview/18078 [accessed 16 December 2022].

Neta, P., Huie, R.E., and Ross, A.B. 1988. Rate Constants for Reactions of Inorganic Radicals in Aqueous Solution. Journal of Physical and Chemical Reference Data, **17**(3): 1027–1284. doi:10.1063/1.555808.

Ni, B.J., Rittmann, B.E., and Yu, H.Q. 2011. Soluble microbial products and their implications in mixed culture biotechnology.

Ni, N., and Yalkowsky, S.H. 2003. Prediction of Setschenow constants. International Journal of Pharmaceutics, **254**(2): 167–172. Elsevier. doi:10.1016/S0378-5173(03)00008-5.

Nicholson, C.A., and Fathepure, B.Z. 2004. Biodegradation of Benzene by Halophilic and Halotolerant Bacteria under Aerobic Conditions. Applied and Environmental Microbiology, **70**(2): 1222–1225. doi:10.1128/AEM.70.2.1222-1225.2004.

Nicholson, C.A., and Fathepure, B.Z. 2005. Aerobic biodegradation of benzene and toluene under hypersaline conditions at the Great Salt Plains, Oklahoma. FEMS Microbiology Letters, **245**(2): 257–262. Elsevier. doi:10.1016/j.femsle.2005.03.014.

Noguchi, M., Kurisu, F., Kasuga, I., and Furumai, H. 2014. Time-resolved DNA stable isotope probing links Desulfobacterales- and Coriobacteriaceae-related bacteria to anaerobic degradation of benzene under methanogenic conditions. Microbes and Environments, **29**(2): 191–199. Japanese Society of Microbial Ecology. doi:10.1264/jsme2.ME13104.

Oil Sands Magazine. 2023. Canadian Refineries. https://www.oilsandsmagazine.com/projects/canadian-refineries [accessed 18 February 2023].

Oliveira, C.A., Fuess, L.T., Soares, L.A., and Damianovic, M.H.R.Z. 2021. Increasing salinity concentrations determine the long-term participation of methanogenesis and sulfidogenesis in the biodigestion of sulfate-rich wastewater. Journal of Environmental Management, **296**. Academic Press. doi:10.1016/j.jenvman.2021.113254.

Oren, A. 1999. Bioenergetic Aspects of Halophilism. MICROBIOLOGY AND MOLECULAR BIOLOGY REVIEWS, **63**(2): 334–348.

Oren, A. 2001. The bioenergetic basis for the decrease in metabolic diversity at increasing salt concentrations: implications for the functioning of salt lake ecosystems. Hydrobiologia, **466**: 61–72.

Oren, A. 2002. Chapter 4: Adaptation of Halophilic Archaea to Life at High Salt Concentrations. *In* Salinity: Environment - Plants - Molecules . *Edited by* A. Lauchli and U. Luttge. Kluwer Academic Publishers, Netherlands. pp. 81–96.

Oren, A. 2008. Microbial life at high salt concentrations: phylogenetic and metabolic diversity. Saline Systems, **4**(1): 2. doi:10.1186/1746-1448-4-2.

Paslawski, J., Nemati, M., Hill, G., and Headley, J. 2009. Biodegradation kinetics of trans-4-methyl-1-cyclohexane carboxylic acid in continuously stirred tank and immobilized cell bioreactors. Journal of Chemical Technology \& Biotechnology, **84**(7): 992–1000. doi:https://doi.org/10.1002/jctb.2122.

Paulssen, J.M., and Gieg, L.M. 2019. Biodegradation of 1-adamantanecarboxylic acid by algal-bacterial microbial communities derived from oil sands tailings ponds. Algal Research, **41**. Elsevier B.V. doi:10.1016/j.algal.2019.101528.

Paustenbach, D.J., Bass, R.D., and Price, P. 1993. Benzene toxicity and risk assessment, 1972-1992: implications for future regulation. Environmental Heath Perspectives Supplements, **101**(6): 1972–1992.

Pereira, A.S., Islam, M.S., Gamal El-Din, M., and Martin, J.W. 2013. Ozonation degrades all detectable organic compound classes in oil sands process-affected water; An application of high-performance liquid chromatography/obitrap mass spectrometry. Rapid Communications in Mass Spectrometry, **27**(21): 2317–2326. John Wiley and Sons Ltd. doi:10.1002/rcm.6688.

Pérez-Estrada, L.A., Han, X., Drzewicz, P., Gamal El-Din, M., Fedorak, P.M., and Martin, J.W. 2011. Structure-reactivity of naphthenic acids in the ozonation process. Environ. Sci. Technol., **45**(17): 7431–7437. doi:10.1021/es201575h.

Petri, B.G., Watts, R.J., Tsitonaki, A., Crimi, M., Thomson, N.R., and Teel, A.L. 2011. Fundamentals of ISCO Using Persulfate. *In* In Situ Chemical Oxidation for Groundwater Remediation. *Edited by* R.L. Siegrist, M. Crimi, and T.J. Simpkin. Springer New York, New York, NY. pp. 147–191.

Phan, H. V., Kurisu, F., Kiba, K., and Furumai, H. 2021. Optimized cultivation and syntrophic relationship of anaerobic benzene-degrading enrichment cultures under methanogenic conditions. Microbes and Environments, **36**(3). Japanese Society of Microbial Ecology. doi:10.1264/jsme2.ME21028.

Phelps, C.D., Kazumi, J., and Young, L.Y. 1996. Anaerobic degradation of benzene in BTX mixtures dependent on sulfate reduction. FEMS Microbiology Letters, **145**(3): 433–437. Oxford University Press (OUP). doi:10.1111/j.1574-6968.1996.tb08612.x.

Phelps, C.D., Kerkhof, L.J., and Young, L.Y. 1998. Molecular characterization of a sulfate-reducing consortium which mineralizes benzene. FEMS Microbiology Ecology, **27**(3): 269–279. John Wiley & Sons, Ltd. doi:https://doi.org/10.1111/j.1574-6941.1998.tb00543.x.

Poli, A., Anzelmo, G., and Nicolaus, B. 2010. Bacterial exopolysaccharides from extreme marine habitats: Production, characterization and biological activities. Marine Drugs, **8**(6), 1779–1802. https://doi.org/10.3390/md8061779

Pourrezaei, P., Drzewicz, P., Wang, Y., Gamal El-Din, M., Perez-Estrada, L.A., Martin, J.W., Anderson, J., Wiseman, S., Liber, K., and Giesy, J.P. 2011. The impact of metallic coagulants on the removal of organic compounds from oil sands process-affected water. Environmental Science and Technology, **45**(19): 8452–8459. doi:10.1021/es201498v.

Prince, R.C., and Prince, V.L. 2022. Hydrocarbon Biodegradation in Utah's Great Salt Lake. Water (Switzerland), **14**(17). MDPI. doi:10.3390/w14172661.

Qiao, W., Luo, F., Lomheim, L., Mack, E.E., Ye, S., Wu, J., and Edwards, E.A. 2018. Natural Attenuation and Anaerobic Benzene Detoxification Processes at a Chlorobenzene-Contaminated Industrial Site Inferred from Field Investigations and Microcosm Studies. Environmental Science and Technology, **52**(1): 22–31. American Chemical Society. doi:10.1021/acs.est.7b04145.

Qin, R., Lillico, D., How, Z. T., Huang, R., Belosevic, M., Stafford, J., and Gamal El-Din, M. 2019. Separation of oil sands process water organics and inorganics and examination of their acute toxicity using standard in-vitro bioassays. Science of the Total Environment, **695**. https://doi.org/10.1016/j.scitotenv.2019.07.338

Qin, X., Tang, J.C., Li, D.S., and Zhang, Q.M. 2012. Effect of salinity on the bioremediation of petroleum hydrocarbons in a saline-alkaline soil. Letters in Applied Microbiology, **55**(3): 210–217. doi:10.1111/j.1472-765X.2012.03280.x.

Quagraine, E.K., Headley, J. V., and Peterson, H.G. 2005a. Is biodegradation of bitumen a source of recalcitrant naphthenic acid mixtures in oil sands tailing pond waters? J. Environ. Sci. Heal. Part A, Toxic/hazardous Subst. Environ. Eng., **40**(3): 671–684. doi:10.1081/ESE-200046637.

Quagraine, E.K., Peterson, H.G., and Headley, J. V. 2005b. In situ bioremediation of naphthenic acids contaminated tailing pond waters in the athabasca oil sands region--demonstrated field studies and plausible options: a review. J. Environ. Sci. Heal. Part A, Toxic/hazardous Subst. Environ. Eng., **40**(3): 685–722. England. doi:10.1081/ese-200046649.

Quast, C., Pruesse, E., Yilmaz, P., Gerken, J., Schweer, T., Yarza, P., Peplies, J., and Glöckner, F.O. 2013. The SILVA ribosomal RNA gene database project: improved data processing and web-based tools. Nucleic Acids Research, **41**(D1): D590–D596. doi:10.1093/nar/gks1219.

Quesnel, D.M., Bhaskar, I.M., Gieg, L.M., and Chua, G. 2011. Naphthenic acid biodegradation by the unicellular alga Dunaliella tertiolecta. Chemosphere, **84**(4): 504–511. doi:https://doi.org/10.1016/j.chemosphere.2011.03.012.

Quesnel, D.M., Oldenburg, T.B.P., Larter, S.R., Gieg, L.M., and Chua, G. 2015. Biostimulation of Oil Sands Process-Affected Water with Phosphate Yields Removal of Sulfur-Containing Organics and Detoxification. Environmental Science and Technology, **49**(21): 13012–13020. American Chemical Society. doi:10.1021/acs.est.5b01391.

Quinlan, P.J., and Tam, K.C. 2015. Water treatment technologies for the remediation of naphthenic acids in oil sands process-affected water. Chem. Eng. J., **279**: 696–714. Elsevier B.V. doi:10.1016/j.cej.2015.05.062.

Rath, K.M., Maheshwari, A., Bengtson, P., and Rousk, J. 2016. Comparative toxicities of salts on microbial processes in soil. Applied and Environmental Microbiology, **82**(7): 2012–2020. American Society for Microbiology. doi:10.1128/AEM.04052-15.

Raza, W., Yang, W., Jun, Y., Shakoor, F., Huang, Q., and Shen, Q. 2012. Optimization and characterization of a polysaccharide produced by Pseudomonas fluorescens WR-1 and its antioxidant activity. Carbohydrate Polymers, **90**(2): 921–929. doi:https://doi.org/10.1016/j.carbpol.2012.06.021.

Rhykerd, R.L., Weaver, R.W., and Mcinnes, K.J. 1995. INFLUENCE OF SALINITY ON BIOREMEDIATION OF OIL IN SOIL. Environmental Pollution, **90**(1): 127–130.

Richardson, S.D., Lebron, B.L., Miller, C.T., and Aitken, M.D. 2011. Recovery of phenanthrene-degrading bacteria after simulated in situ persulfate oxidation in contaminated soil. Environmental Science and Technology, **45**(2): 719–725. doi:10.1021/es102420r.

Riis, V., Kleinsteuber, S., and Babel, W. 2003. Influence of high salinities on the degradation of diesel fuel by bacterial consortia. Canadian Journal of Microbiology, **49**(11): 713–721. doi:10.1139/w03-083.

Ripmeester, M.J., and Duford, D.A. 2019. Method for routine "naphthenic acids fraction compounds" determination in oil sands process-affected water by liquid-liquid extraction in dichloromethane and Fourier-Transform Infrared Spectroscopy. Chemosphere, **233**: 687–696. Elsevier Ltd. doi:10.1016/j.chemosphere.2019.05.222.

Rogers, V. V, Liber, K., and MacKinnon, M.D. 2002a. Isolation and characterization of naphthenic acids from Athabasca oil sands tailings pond water. Chemosphere, **48**(5): 519–527. doi:https://doi.org/10.1016/S0045-6535(02)00133-9.

Rogers, V. V, Wickstrom, M., Liber, K., and MacKinnon, M.D. 2002b. Acute and Subchronic Mammalian Toxicity of Naphthenic Acids from Oil Sands Tailings. Toxicological Sciences, **66**(2): 347–355. doi:10.1093/toxsci/66.2.347.

Romera-Castillo, C., and Jaffé, R. 2015. Free radical scavenging (antioxidant activity) of natural dissolved organic matter. Marine Chemistry, **177**: 668–676. doi:https://doi.org/10.1016/j.marchem.2015.10.008.

Sakai, N., Kurisu, F., Yagi, O., Nakajima, F., and Yamamoto, K. 2009. Identification of putative benzene-degrading bacteria in methanogenic enrichment cultures. Journal of Bioscience and Bioengineering, **108**(6): 501–507. doi:10.1016/j.jbiosc.2009.06.005.

Sander, R. 2015. Compilation of Henry's law constants (version 4.0) for water as solvent. Atmospheric Chemistry and Physics, **15**(8): 4399–4981. Copernicus GmbH. doi:10.5194/acp-15-4399-2015.

Scarlett, A.G., Reinardy, H.C., Henry, T.B., West, C.E., Frank, R.A., Hewitt, L.M., and Rowland, S.J. 2013. Acute toxicity of aromatic and non-aromatic fractions of naphthenic acids extracted from oil sands process-affected water to larval zebrafish. Chemosphere, **93**(2): 415–420. Elsevier Ltd. doi:10.1016/j.chemosphere.2013.05.020.

Schymanski, E.L., Jeon, J., Gulde, R., Fenner, K., Ruff, M., Singer, H.P., and Hollender, J. 2014. Identifying Small Molecules via High Resolution Mass Spectrometry: Communicating Confidence. Environmental Science & Technology, **48**(4): 2097–2098. American Chemical Society. doi:10.1021/es5002105.

Scott, A.C., MacKinnon, M.D., and Fedorak, P.M. 2005. Naphthenic acids in athabasca oil sands tailings waters are less biodegradable than commercial naphthenic acids. Environmental Science and Technology, **39**(21): 8388–8394. doi:10.1021/es051003k.

Scott, A.C., Young, R.F., and Fedorak, P.M. 2008. Comparison of GC-MS and FTIR methods for quantifying naphthenic acids in water samples. Chemosphere, **73**(8): 1258–1264. Elsevier Ltd. doi:10.1016/j.chemosphere.2008.07.024.

Scott, A.C., Zubot, W., Davis, C.W., and Brogly, J. 2020. Bioaccumulation potential of naphthenic acids and other ionizable dissolved organics in oil sands process water (OSPW) – A review. Science of the Total Environment, **712**. https://doi.org/10.1016/j.scitotenv.2019.134558

Sei, A., and Fathepure, B.Z. 2009. Biodegradation of BTEX at high salinity by an enrichment culture from hypersaline sediments of Rozel Point at Great Salt Lake. Journal of Applied Microbiology, **107**(6): 2001–2008. doi:10.1111/j.1365-2672.2009.04385.x.

Seymour, C.O., Palmer, M., Becraft, E.D., Stepanauskas, R., Friel, A.D., Schulz, F., Woyke, T., Eloe-Fadrosh, E., Lai, D., Jiao, J.-Y., Hua, Z.-S., Liu, L., Lian, Z.-H., Li, W.-J., Chuvochina, M., Finley, B.K., Koch, B.J., Schwartz, E., Dijkstra, P., Moser, D.P., Hungate, B.A., and Hedlund, B.P. 2023. Hyperactive nanobacteria with host-dependent traits pervade Omnitrophota. Nature Microbiology, **8**(4): 727–744. doi:10.1038/s41564-022-01319-1.

Shayan, M., Thomson, N.R., Aravena, R., Barker, J.F., Madsen, E.L., Marchesi, M., DeRito, C.M., Bouchard, D., Buscheck, T., Kolhatkar, R., and Daniels, E.J. 2018. Integrated Plume Treatment Using Persulfate Coupled with Microbial Sulfate Reduction. Groundw. Monit. Remediat., **38**(4): 45–61. doi:10.1111/gwmr.12227.

Shetaia, Y.M.H., El khalik, W.A.A., Mohamed, T.M., Farahat, L.A., and ElMekawy, A. 2016. Potential biodegradation of crude petroleum oil by newly isolated halotolerant microbial strains from polluted Red Sea area. Marine Pollution Bulletin, **111**(1–2): 435–442. Elsevier Ltd. doi:10.1016/j.marpolbul.2016.02.035.

Shi, Y., and Liu, Y. 2021. Evolution of extracellular polymeric substances (EPS) in aerobic sludge granulation: Composition, adherence and viscoelastic properties. Chemosphere, 262. https://doi.org/10.1016/j.chemosphere.2020.128033

Shi, Y., Huang, C., Rocha, K.C., El-Din, M.G., and Liu, Y. 2015. Treatment of oil sands process-affected water using moving bed biofilm reactors: With and without ozone pretreatment. Bioresourc. Technol., **192**: 219–227. Elsevier Ltd. doi:10.1016/j.biortech.2015.05.068.

Shu, Z., Li, C., Belosevic, M., Bolton, J.R., and El-Din, M.G. 2014. Application of a solar UV/chlorine advanced oxidation process to oil sands process-affected water remediation. Environmental Science and Technology, **48**(16): 9692–9701. American Chemical Society. doi:10.1021/es5017558.

Siegrist, R.L., Crimi, M., and Simpkin, T.J. 2011. In Situ Chemical Oxidation for Groundwater Remediation. *In* SERDP/ESTCP Environmental Remediation Technology, 1st edition. Springer, New York, NY.

Sindhu, M.A., and Cornfield, A.H. 1967. Comparative Effects of Varying Levels of Chlorides and Sulphates of Sodium, Potassium, Calcium, and Magnesium on Ammonification and Nitrification during Incubation of Soil. Plant and Soil, **XXVII**(3): 468–472.

Singh, K. 2016. Microbial and Enzyme Activities of Saline and Sodic Soils. Land Degradation and Development, **27**(3): 706–718. John Wiley and Sons Ltd. doi:10.1002/ldr.2385.

Sirajunnisa, A.R., Vijayagopal, V., Sivaprakash, B., Viruthagiri, T., and Surendhiran, D. 2016. Optimization, kinetics and antioxidant activity of exopolysaccharide produced from rhizosphere isolate, Pseudomonas fluorescens CrN6. Carbohydrate Polymers, **135**: 35–43. doi:https://doi.org/10.1016/j.carbpol.2015.08.080.

Smith, B.E., Lewis, C.A., Belt, S.T., Whitby, C., and Rowland, S.J. 2008. Effects of Alkyl Chain Branching on the Biotransformation of Naphthenic Acids. Environmental Science & Technology, **42**(24): 9323–9328. American Chemical Society. doi:10.1021/es801922p.

Sohrabi, V., Ross, M.S., Martin, J.W., and Barker, J.F. 2013. Potential for in situ chemical oxidation of acid extractable organics in oil sands process affected groundwater. Chemosphere, **93**(11): 2698–2703. Elsevier Ltd. doi:10.1016/j.chemosphere.2013.08.072.

Song, J., How, Z.T., Huang, Z., and Gamal El-Din, M. 2022. Biochar/iron oxide composite as an efficient peroxymonosulfate catalyst for the degradation of model naphthenic acids compounds. Chemical Engineering Journal, **429**. Elsevier B.V. doi:10.1016/j.cej.2021.132220.

Song, W., Xiong, H., Qi, R., Wang, S., and Yang, Y. 2021. Effect of salinity and algae biomass on mercury cycling genes and bacterial communities in sediments under mercury contamination: Implications of the mercury cycle in arid regions. Environmental Pollution, **269**. Elsevier Ltd. doi:10.1016/j.envpol.2020.116141.

de Souza Silva, C.M.M., and Fay, E.F. 2012. Effect of Salinity on Soil Microorganisms. *In* Soil Health and Land Use Management. InTechOpen.

Sun, M.T., Fan, X.L., Zhao, X.X., Fu, S.F., He, S., Manasa, M.R.K., and Guo, R.B. 2017. Effects of organic loading rate on biogas production from macroalgae: Performance and microbial community structure. Bioresource Technology, **235**: 292–300. doi:https://doi.org/10.1016/j.biortech.2017.03.075.

Sun, Y., Zhao, J., Zhang, B.T., Li, J., Shi, Y., and Zhang, Y. 2019. Oxidative degradation of chloroxylenol in aqueous solution by thermally activated persulfate: Kinetics, mechanisms and toxicities. Chemical Engineering Journal, **368**: 553–563. Elsevier B.V. doi:10.1016/j.cej.2019.02.208.

Sutton, N.B., Atashgahi, S., van der Wal, J., Wijn, G., Grotenhuis, T., Smidt, H., and Rijnaarts, H.H.M. 2015. Microbial dynamics during and after in situ chemical oxidation of chlorinated solvents. Groundwater, **53**(2): 261–270. doi:10.1111/gwat.12209.

Sutton, N.B., Grotenhuis, J.T.C., Langenhoff, A.A.M., and Rijnaarts, H.H.M. 2011. Efforts to improve coupled in situ chemical oxidation with bioremediation: A review of optimization strategies. J. Soils Sediments, **11**(1): 129–140. doi:10.1007/s11368-010-0272-9.

Sutton, N.B., Kalisz, M., Krupanek, J., Marek, J., Grotenhuis, T., Smidt, H., de Weert, J., Rijnaarts, H.H.M., van Gaans, P., and Keijzer, T. 2014a. Geochemical and microbiological characteristics during in situ chemical oxidation and in situ bioremediation at a diesel contaminated site. Environmental Science and Technology, **48**(4): 2352–2360. doi:10.1021/es404512a.

Sutton, N.B., Langenhoff, A.A.M., Lasso, D.H., Van Der Zaan, B., Van Gaans, P., Maphosa, F., Smidt, H., Grotenhuis, T., and Rijnaarts, H.H.M. 2014b. Recovery of microbial diversity and activity during bioremediation following chemical oxidation of diesel contaminated soils. Appl. Microbiol. Biotech., **98**(6): 2751–2764. doi:10.1007/s00253-013-5256-4.

Tan, Y.S., Zhang, R.K., Liu, Z.H., Li, B.Z., and Yuan, Y.J. 2022. Microbial Adaptation to Enhance Stress Tolerance. Frontiers in Microbiology, **13.** https://doi.org/10.3389/fmicb.2022.888746

Tao, R., and Yu, K. 2013. Nitrate addition has minimal effect on anaerobic biodegradation of benzene in coastal saline (salt), brackish and freshwater marsh sediments. Wetlands, **33**(4): 759–767. doi:10.1007/s13157-013-0435-8.

Thiessen, R.J., and Achari, G. 2017. Abandoned oil and gas well site environmental risk estimation. Toxicological and Environmental Chemistry, **99**(7–8): 1170–1192. Taylor and Francis Ltd. doi:10.1080/02772248.2016.1260132.

Toor, N.S., Franz, E.D., Fedorak, P.M., MacKinnon, M.D., and Liber, K. 2013. Degradation and aquatic toxicity of naphthenic acids in oil sands process-affected waters using simulated wetlands. Chemosphere, **90**(2): 449–458. doi:https://doi.org/10.1016/j.chemosphere.2012.07.059.

Toth, C.R.A., Luo, F., Bawa, N., Webb, J., Guo, S., Dworatzek, S., and Edwards, E.A. 2021. Anaerobic benzene biodegradation linked to the growth of highly specific bacterial clades. Environmental Science and Technology, **55**(12): 7970–7980. American Chemical Society. doi:10.1021/acs.est.1c00508.

Toth, C.R.A., Luo, F., Guo, S., Bawa, N., Dworatzek, S., Webb, J., Chen, C., Shyi, C., and Edwards, E.A. 2018. Anaerobic Benzene Degradation: Pathways and Prospects for Field Bioremediation Technologies. Toronto, ON.

Tsitonaki, A., Petri, B., Crimi, M., Mosbk, H., Siegrist, R.L., and Bjerg, P.L. 2010. In situ chemical oxidation of contaminated soil and groundwater using persulfate: A review. Crit. Rev. Environ. Sci. Technol., **40**(1): 55–91. doi:10.1080/10643380802039303.

Tsitonaki, A., Smets, B.F., and Bjerg, P.L. 2008. Effects of heat-activated persulfate oxidation on soil microorganisms. Water Res., **42**(4–5): 1013–1022. doi:10.1016/j.watres.2007.09.018.

Ulrich, A.C., Beller, H.R., and Edwards, E.A. 2005. Metabolites detected during biodegradation of 13C 6-benzene in nitrate-reducing and methanogenic enrichment cultures. Environmental Science and Technology, **39**(17): 6681–6691. doi:10.1021/es050294u.

Ulrich, A.C., and Edwards, E.A. 2003. Physiological and molecular characterization of anaerobic benzene-degrading mixed cultures. Environmental Microbiology, **5**(2): 92–102. doi:10.1046/j.1462-2920.2003.00390.x.

Ulrich, A.C., Guigard, S.E., Foght, J.M., Semple, K.M., Pooley, K., Armstrong, J.E., and Biggar, K.W. 2009. Effect of salt on aerobic biodegradation of petroleum hydrocarbons in contaminated groundwater. Biodegradation, **20**(1): 27–38. doi:10.1007/s10532-008-9196-0.

United Stated Environmental Protection Agency (U.S. EPA). 2018. Examples of Groundwater Remediation at NPL Sites. EPA 542-R-18-002.

U.S. EPA. 2008. EPA's Report on the Environment (ROE) (2008 Final Report). Washington, D.C. EPA/600/R-07/045F (NTIS PB2008-112484).

Vander Meulen, I.J., Downham, R.P., Alostad, L., Peru, K.M., McMartin, D.W., Barrow, M.P., and Headley, J. V. 2022. Advances in Fourier transform mass spectrometry forensic tools for naphthenic acid fraction compounds in oil sand environmental samples and crude oil. *In* The Chemistry of Oil and Petroleum Products. De Gruyter. pp. 127–175.

Vander Meulen, I.J., Klemish, J.L., Peru, K.M., Chen, D.D.Y., Pyle, G.G., and Headley, J. V. 2021. Molecular profiles of naphthenic acid fraction compounds from mine lease wetlands in the Athabasca Oil Sands Region. Chemosphere, **272**. Elsevier Ltd. doi:10.1016/j.chemosphere.2021.129892.

van der Zaan, B.M., Saia, F.T., Stams, A.J.M., Plugge, C.M., de Vos, W.M., Smidt, H., Langenhoff, A.A.M., and Gerritse, J. 2012. Anaerobic benzene degradation under denitrifying conditions: Peptococcaceae as dominant benzene degraders and evidence for a syntrophic process. Environmental Microbiology, **14**(5): 1171–1181. John Wiley & Sons, Ltd. doi:https://doi.org/10.1111/j.1462-2920.2012.02697.x.

Vaiopoulou, E., Misiti, T.M., and Pavlostathis, S.G. 2015. Removal and toxicity reduction of naphthenic acids by ozonation and combined ozonation-aerobic biodegradation. Bioresourc. Technol., **179**: 339–347. Elsevier Ltd. doi:10.1016/j.biortech.2014.12.058.

Valderrama, C., Alessandri, R., Aunola, T., Cortina, J.L., Gamisans, X., and Tuhkanen, T. 2009. Oxidation by Fenton's reagent combined with biological treatment applied to a creosote-comtaminated soil. J. Hazard. Mater., **166**(2–3): 594–602. doi:10.1016/j.jhazmat.2008.11.108.

Vattanaviboon, P., Praituan, W., and Mongkolsuk, S. 2011. Growth phase dependent resistance to oxidative stress in a phytopathogen Xanthomonas oryzae pv. oryzae. Canadian Journal of Microbiology, **41**: 1043–1047. doi:10.1139/m95-145.

Vogt, C., Kleinsteuber, S., and Richnow, H.H. 2011. Anaerobic benzene degradation by bacteria. Microbial Biotechnology, **4**(6), 710–724. https://doi.org/10.1111/j.1751-7915.2011.00260.x

Wacławek, S., Lutze, H. V., Grübel, K., Padil, V.V.T., Černík, M., and Dionysiou, D.D. 2017. Chemistry of persulfates in water and wastewater treatment: A review. Chem. Eng. J., **330**(July): 44–62. doi:10.1016/j.cej.2017.07.132.

Wang, B., Wan, Y., Gao, Y., Yang, M., and Hu, J. 2013a. Determination and Characterization of Oxy-Naphthenic Acids in Oilfield Wastewater. Environmental Science & Technology, **47**(16): 9545–9554. American Chemical Society. doi:10.1021/es401850h.

Wang, C., Klamerth, N., Messele, S.A., Singh, A., Belosevic, M., and Gamal El-Din, M. 2016. Comparison of UV/hydrogen peroxide, potassium ferrate(VI), and ozone in oxidizing the organic fraction of oil sands process-affected water (OSPW). Water Research, **100**: 476–485. Elsevier Ltd. doi:10.1016/j.watres.2016.05.037.

Wang, N., Chelme-Ayala, P., Perez-Estrada, L., Garcia-Garcia, E., Pun, J., Martin, J.W., Belosevic, M., and Gamal El-Din, M. 2013b. Impact of ozonation on naphthenic acids speciation and toxicity of oil sands process-affected water to vibrio fischeri and mammalian immune system. Environ. Sci. Technol., **47**(12): 6518–6526. doi:10.1021/es4008195.

Wang, X., Shao, C., Liu, L., Guo, X., Xu, Y., and Lü, X. 2017. Optimization, partial characterization and antioxidant activity of an exopolysaccharide from Lactobacillus plantarum KX041. International Journal of Biological Macromolecules, **103**: 1173–1184. Elsevier B.V. doi:10.1016/j.ijbiomac.2017.05.118.

Wang, Y., Couet, M., Gutierrez, L., Allard, S., and Croué, J.-P. 2020. Impact of DOM source and character on the degradation of primidone by UV/chlorine: Reaction kinetics and disinfection by-product formation. Water Research, **172**: 115463. doi:https://doi.org/10.1016/j.watres.2019.115463.

Wang, Z., Wang, S., Hu, Y., Du, B., Meng, J., Wu, G., Liu, H., and Zhan, X. 2022. Distinguishing responses of acetoclastic and hydrogenotrophic methanogens to ammonia stress in mesophilic mixed cultures. Water Research, **224**. Elsevier Ltd. doi:10.1016/j.watres.2022.119029.

Weiner, J., and Lovley, D. 1998. Anaerobic Benzene Degradation in Petroleum-Contaminated Aquifer Sediments after Inoculation with a Benzene-Oxidizing Enrichment. Applied and Environmental Microbiology, **64**(2): 775–778. American Society for Microbiology. doi:10.1128/AEM.64.2.775-778.1998.

Whitby, C. 2010. Microbial Naphthenic Acid Degradation. *In* Advances in Applied Microbiology, 1st edition. Elsevier Inc. pp. 93–125.

White, K.B., and Liber, K. 2020. Chronic Toxicity of Surface Water from a Canadian Oil Sands End Pit Lake to the Freshwater Invertebrates Chironomus dilutus and Ceriodaphnia dubia. Archives of Environmental Contamination and Toxicology, **78**(3): 439–450. Springer. doi:10.1007/s00244-020-00720-3.

Wilson, B.H., Smith, G.B., and Rees, J.F. 1986. Biotransformations of selected alkylbenzenes and halogenated aliphatic hydrocarbons in methanogenic aquifer material: a microcosm study. Environmental Science & Technology, **20**(10): 997–1002. American Chemical Society. doi:10.1021/es00152a005.

Wu, Z., Liu, G., Ji, Y., Li, P., Yu, X., Qiao, W., Wang, B., Shi, K., Liu, W., Liang, B., Wang, D., Yanuka-Golub, K., Freilich, S., and Jiang, J. 2022. Electron acceptors determine the BTEX degradation capacity of anaerobic microbiota via regulating the microbial community. Environmental Research, **215**. Academic Press Inc. doi:10.1016/j.envres.2022.114420.

Xia, Y., Cheng, Y., Li, L., Chen, Y., and Jiang, Y. 2020. A microcosm study on persulfate oxidation combined with enhanced bioremediation to remove dissolved BTEX in gasoline-contaminated groundwater. Biodegradation, **31**(3): 213–222. Springer. doi:10.1007/s10532-020-09904-z.

Xia, Y., Jiang, X., Wang, Y., Huang, Q., Chen, D., Hou, C., Mu, Y., and Shen, J. 2022. Enhanced anaerobic reduction of nitrobenzene at high salinity by betaine acting as osmoprotectant and regulator of metabolism. Water Research, **223**. Elsevier Ltd. doi:10.1016/j.watres.2022.118982.

Xie, G., and Barcelona, M.J. 2003. Sequential chemical oxidation and aerobic biodegradation of equivalent carbon number-based hydrocarbon fractions in jet fuel. Environ. Sci. Technol., **37**(20): 4751–4760. doi:10.1021/es026260t.

Xiong, W., Mathies, C., Bradshaw, K., Carlson, T., Tang, K., and Wang, Y. 2012. Benzene removal by a novel modification of enhanced anaerobic biostimulation. Water Res., **46**(15): 4721–4731. Elsevier Ltd. doi:10.1016/j.watres.2012.06.036.

Xu, J., Deng, X., Cui, Y., and Kong, F. 2016a. Impact of chemical oxidation on indigenous bacteria and mobilization of nutrients and subsequent bioremediation of crude oil-contaminated soil. J. Hazard. Mater., **320**: 160–168. Elsevier B.V. doi:10.1016/j.jhazmat.2016.08.028.

Xu, S., Wang, W., and Zhu, L. 2019a. Enhanced microbial degradation of benzo[a]pyrene by chemical oxidation. Sci. Total Environ., **653**: 1293–1300. Elsevier B.V. doi:10.1016/j.scitotenv.2018.10.444.

Xu, X., Pliego, G., Alonso, C., Liu, S., Nozal, L., and Rodriguez, J.J. 2019b. Reaction pathways of heat-activated persulfate oxidation of naphthenic acids in the presence and absence of dissolved oxygen in water. Chem. Eng. J., **370**(March): 695–705. Elsevier. doi:10.1016/j.cej.2019.03.213.

Xu, X., Pliego, G., Garcia-Costa, A.L., Zazo, J.A., Liu, S., Casas, J.A., and Rodriguez, J.J. 2018a. Cyclohexanoic acid breakdown by two-step persulfate and heterogeneous Fenton-like oxidation. Appl. Catal. B: Environ., **232**(January): 429–435. Elsevier. doi:10.1016/j.apcatb.2018.03.092.

Xu, X., Pliego, G., Zazo, J.A., Casas, J.A., and Rodriguez, J.J. 2016b. Mineralization of naphtenic acids with thermally-activated persulfate: The important role of oxygen. J. Hazard. Mater., **318**: 355–362. Elsevier B.V. doi:10.1016/j.jhazmat.2016.07.009.

Xu, X., Pliego, G., Zazo, J.A., Liu, S., Casas, J.A., and Rodriguez, J.J. 2018b. Two-step persulfate and Fenton oxidation of naphthenic acids in water. J. Chem. Technol. Biotechnol., **93**(8): 2262–2270. doi:10.1002/jctb.5569.

Xu, X., Pliego, G., Zazo, J.A., Sun, S., García-Muñoz, P., He, L., Casas, J.A., and Rodriguez, J.J. 2017. An overview on the application of advanced oxidation processes for the removal of naphthenic acids from water. Critical Reviews in Environmental Science and Technology, **47**(15): 1337–1370. Taylor and Francis Inc. doi:10.1080/10643389.2017.1348113.

Xue, J., Huang, C., Zhang, Y., Liu, Y., and Gamal El-Din, M. 2018. Bioreactors for oil sands process-affected water (OSPW) treatment: A critical review. Science of the Total Environment, **627**, 916–933. https://doi.org/10.1016/j.scitotenv.2018.01.292

Xue, J., Zhang, Y., Liu, Y., and Gamal El-Din, M. 2016a. Treatment of raw and ozonated oil sands process-affected water under decoupled denitrifying anoxic and nitrifying aerobic conditions: a comparative study. Biodegradation, **27**(4–6): 247–264. Springer Netherlands. doi:10.1007/s10532-016-9770-9.

Xue, J., Zhang, Y., Liu, Y., and Gamal El-Din, M. 2016b. Treatment of oil sands process-affected water (OSPW) using a membrane bioreactor with a submerged flat-sheet ceramic microfiltration membrane. Water Research, **88**: 1–11. Elsevier Ltd. doi:10.1016/j.watres.2015.09.051.

Xue, J., Zhang, Y., Liu, Y., and Gamal El-Din, M. 2017. Dynamics of naphthenic acids and microbial community structures in a membrane bioreactor treating oil sands process-affected water: impacts of supplemented inorganic nitrogen and hydraulic retention time. RSC Advances, **7**(29): 17670–17681. The Royal Society of Chemistry. doi:10.1039/C7RA01836C.

Yan, M., Treu, L., Zhu, X., Tian, H., Basile, A., Fotidis, I.A., Campanaro, S., and Angelidaki, I. 2020. Insights into Ammonia Adaptation and Methanogenic Precursor Oxidation by Genome-Centric Analysis. Environmental Science & Technology, **54**(19): 12568–12582. American Chemical Society. doi:10.1021/acs.est.0c01945.

Yan, N., Marschner, P., Cao, W., Zuo, C., and Qin, W. 2015. Influence of salinity and water content on soil microorganisms. International Soil and Water Conservation Research, **3**(4): 316–323. International Research and Training Center on Erosion and Sedimentation and China Water and Power Press. doi:10.1016/j.iswcr.2015.11.003.

Yen, C.H., Chen, K.F., Kao, C.M., Liang, S.H., and Chen, T.Y. 2011. Application of persulfate to remediate petroleum hydrocarbon-contaminated soil: Feasibility and comparison with common oxidants. J. Hazard. Mater., **186**(2–3): 2097–2102. Elsevier B.V. doi:10.1016/j.jhazmat.2010.12.129.

Yu, J., Tao, R., and Yu, K. 2012. Anaerobic biodegradation of benzene in salt marsh sediment of the Louisiana Gulf coast. Ecological Engineering, **40**: 6–10. doi:10.1016/j.ecoleng.2011.12.025.

Yu, Y., Lee, C., Kim, J., and Hwang, S. 2005. Group-specific primer and probe sets to detect methanogenic communities using quantitative real-time polymerase chain reaction. Biotechnology and Bioengineering, **89**(6): 670–679. John Wiley & Sons, Ltd. doi:https://doi.org/10.1002/bit.20347.

Yue, S., Ramsay, B.A., Wang, J., and Ramsay, J. 2015. Toxicity and composition profiles of solid phase extracts of oil sands process-affected water. Science of the Total Environment, **538**: 573–582. Elsevier. doi:10.1016/j.scitotenv.2015.08.079.

Yue, S., Ramsay, B.A., Wang, J., and Ramsay, J.A. 2016. Biodegradation and detoxification of naphthenic acids in oil sands process affected waters. Science of the Total Environment, **572**: 273–279. Elsevier B.V. doi:10.1016/j.scitotenv.2016.07.163.

Zelver, N., Hamilton, M., Putts, B., Goeres, D., Walker, D., Struman, P., and Heersink, J. 1999. Measuring antimicrobial effects on biofilm bacteria: From laboratory to field. *In* Methods in Enzymology. Academic Press. pp. 608–628.

Zhang, L., Zhang, Y., and Gamal El-Din, M. 2018a. Degradation of recalcitrant naphthenic acids from raw and ozonated oil sands process-affected waters by a semi-passive biofiltration process. Water Res., **133**: 310–318. Elsevier Ltd. doi:10.1016/j.watres.2018.01.001.

Zhang, L., Zhang, Y., and Gamal El-Din, M. 2019. Integrated mild ozonation with biofiltration can effectively enhance the removal of naphthenic acids from hydrocarbon-contaminated water. Sci. Total Environ., **678**: 197–206. Elsevier B.V. doi:10.1016/j.scitotenv.2019.04.302.

Zhang, L., Zhao, B., Liu, C. J., and Yang, E. 2020. Optimization of Biosynthesis Conditions for the Production of Exopolysaccharides by Lactobacillus plantarum SP8 and the Exopolysaccharides Antioxidant Activity Test. Indian Journal of Microbiology, **60**(3), 334–345. https://doi.org/10.1007/s12088-020-00865-8

Zhang, T., Bain, T., Nevin, K., Barlett, M., and Lovley, D. 2012. Anaerobic Benzene Oxidation by Geobacter Species. Applied and Environmental Microbiology, **78**(23): 8304–8310. American Society for Microbiology. doi:10.1128/AEM.02469-12.

Zhang, X., Bao, D., Li, M., Tang, Q., Wu, M., Zhou, H., Liu, L., and Qu, Y. 2021. Bioremediation of petroleum hydrocarbons by alkali–salt-tolerant microbial consortia and their community profiles. Journal of Chemical Technology and Biotechnology, **96**(3): 809–817. John Wiley and Sons Ltd. doi:10.1002/jctb.6594.

Zhang, Y., Klamerth, N., Chelme-Ayala, P., and Gamal El-Din, M. 2016a. Comparison of Nitrilotriacetic Acid and [S,S]-Ethylenediamine-N,N′-disuccinic Acid in UV–Fenton for the Treatment of Oil Sands Process-Affected Water at Natural pH. Environmental Science & Technology, **50**(19): 10535–10544. American Chemical Society. doi:10.1021/acs.est.6b03050.

Zhang, Y., Klamerth, N., and Gamal El-Din, M. 2016b. Degradation of a model naphthenic acid by nitrilotriacetic acid – modified Fenton process. Chemical Engineering Journal, **292**: 340–347. doi:https://doi.org/10.1016/j.cej.2016.02.045.

Zhang, Y., Klamerth, N., Messele, S.A., Chelme-Ayala, P., and Gamal El-Din, M. 2016c. Kinetics study on the degradation of a model naphthenic acid by ethylenediamine-N,N'-disuccinic acid-modified Fenton process. Journal of Hazardous Materials, **318**: 371–378. doi:https://doi.org/10.1016/j.jhazmat.2016.06.063.

Zhang, Y., Xue, J., Liu, Y., and Gamal El-Din, M. 2016d. Treatment of oil sands process-affected water using membrane bioreactor coupled with ozonation: A comparative study. Chem. Eng. J., **302**: 485–497. Elsevier B.V. doi:10.1016/j.cej.2016.05.082.

Zhang, Y., Xue, J., Liu, Y., and Gamal El-Din, M. 2018b. The role of ozone pretreatment on optimization of membrane bioreactor for treatment of oil sands process-affected water. J. Hazard. Mater., **347**: 470–477. Elsevier B.V. doi:10.1016/j.jhazmat.2017.12.013.

Zheng, Z., Fu, Y., Liu, K., Xiao, R., Wang, X., and Shi, H. 2018. Three-stage vertical distribution of seawater conductivity. Scientific Reports, **8**(1): 9916. doi:10.1038/s41598-018-27931-y.

Appendix A-1: Additional Data for Chapter 4

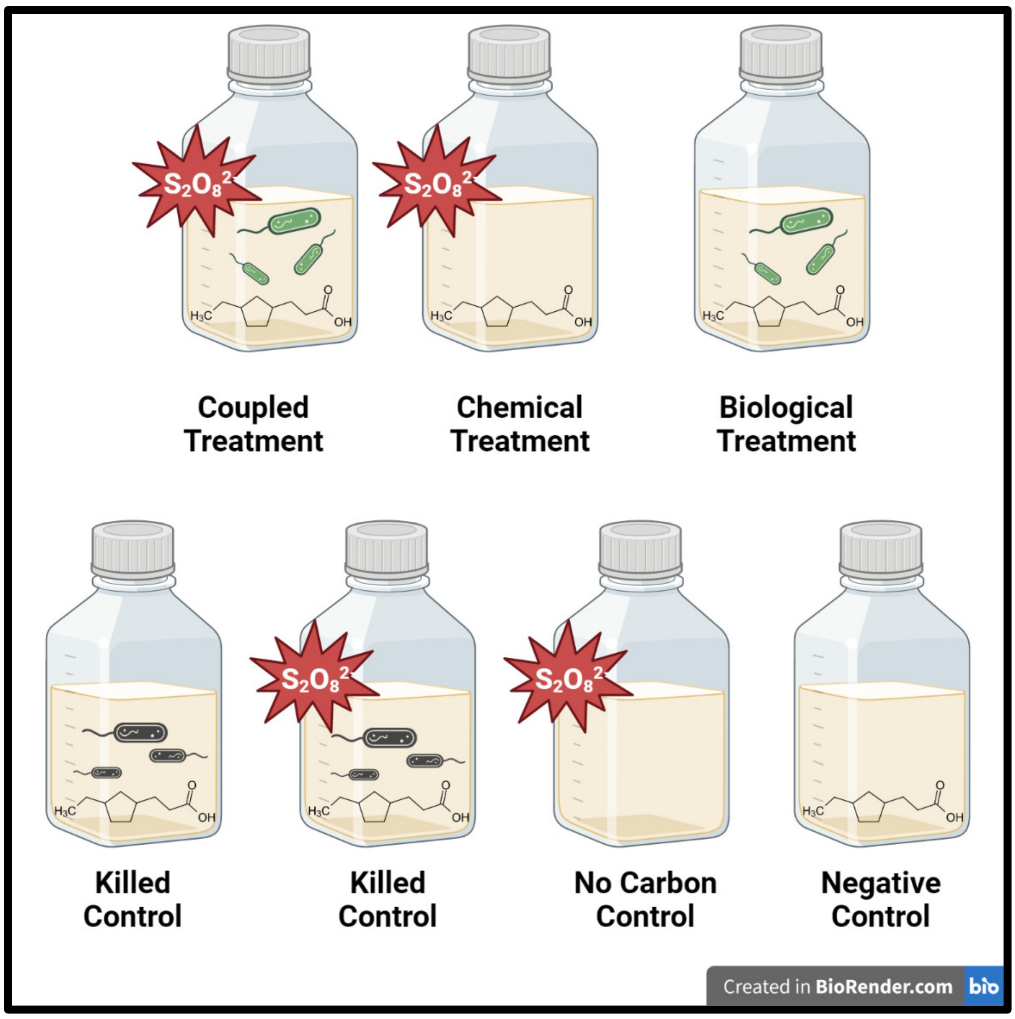

Figure A-1. Illustration of treatments and control bottles for Chapter 4 experiment.

Table A-1. Percent decrease of NAFCs in OSPW after 24 h of reaction with heat activated persulfate in preliminary trial experiments. Data represents single treatment bottles.

Temperature (°C)	% Decrease of NAFCs	
	250 mg/L PS	1000 mg/L PS
40	4.7	26.2
50	33.2	81.5
60	49.7	97.6

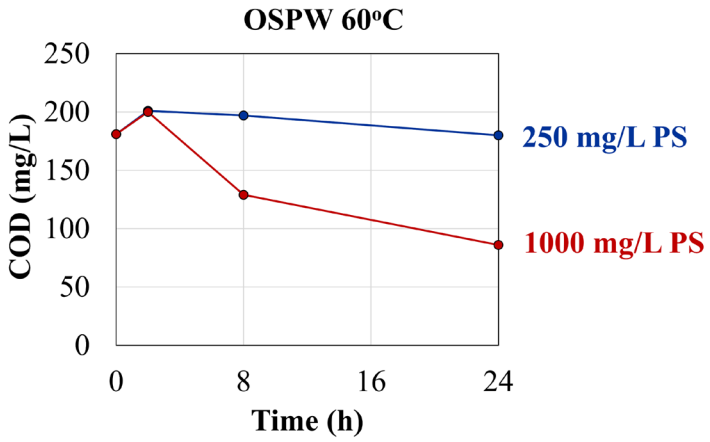

Figure A-2. Chemical oxygen demand (COD) of OSPW with 250 and 1000 mg/L persulfate (PS) activated at 60°C in preliminary trial experiments. Data represents single treatment bottles.

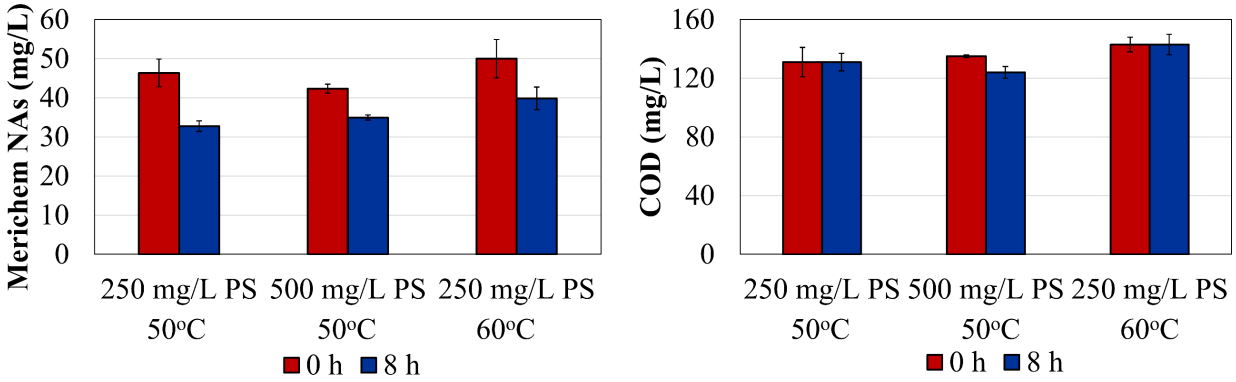

Figure A-3. Degradation of Merichem NAs and COD using 250 mg/L and 500 mg/L of activated persulfate (PS) at 50°C and 60°C in preliminary trial experiments. Error bars represent one standard deviation of duplicate bottles.

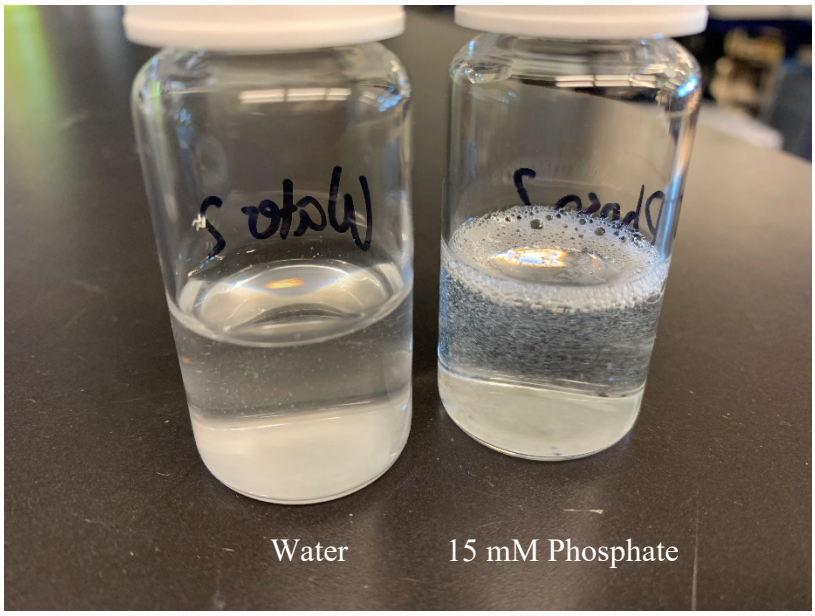

Figure A-4. Samples taken after inorganic ion scavenging test in preliminary experiments. Individual components of Bushnell Haas mineral media with 50 mg/L Merichem NAs were reacted with 1000 mg/L persulfate at 60°C for 8 hours. Only phosphate samples still produced bubbles after reaction, indicating the presence of NAs as they are surfactants. Phosphate bottles: 1 g/L K_2HPO_4 + 1 g/L KH_2PO_4 (15 mM PO_4^{2-}). Nitrate bottles: 1 g/L KNO_3 (10 mM NO_3^-); Chloride bottles: 20 mg/L $CaCl_2$ (0.4 mM Cl^-).

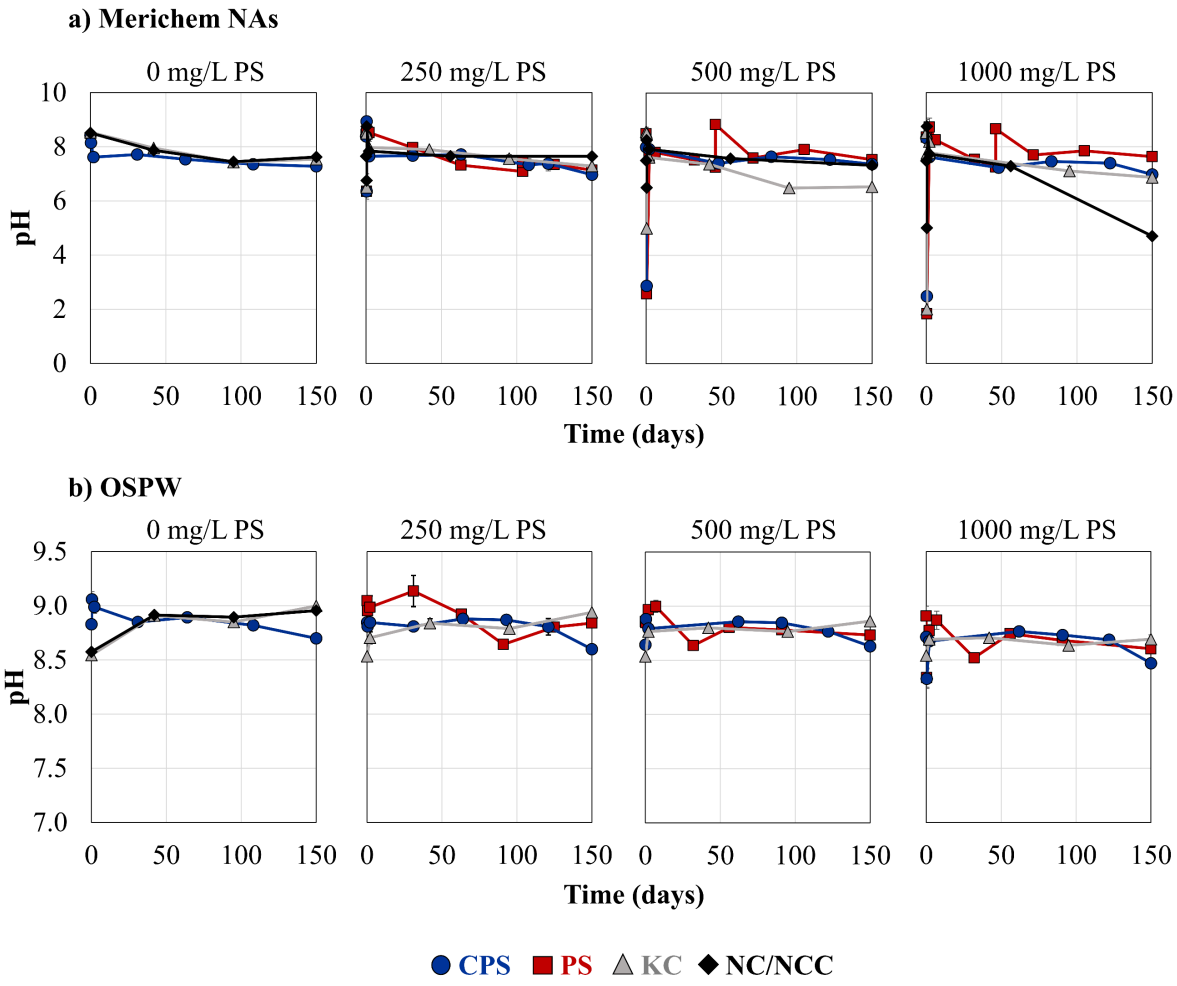

Figure A-5. pH levels for a) Merichem NA and b) OSPW after 8 hours of heat activation (60°C) followed by 150 days at room temperature. Merichem bottles were adjusted after 8 hours and then adjusted continuously over 150 days to maintain pH ~8. Different treatments include persulfate oxidation (PS; ■), persulfate coupled with *P. fluorescens* (CPS; ●), killed controls (KC; △), negative controls without persulfate (NC; ◆) and no carbon controls without Merichem NAs (NCC; ◆). Error Bars represent one standard deviation of triplicate bottles.

Table A-2. Initial concentration of anions. "OSPW + N/P" represents OSPW supplemented with per L: 0.05 g K_2HPO_4, 0.05 g KH_2PO_4, 0.05 g NH_4NO_3. Data represents the average of triplicate samples.

	Chloride (mg/L)	Nitrite (mg/L)	Nitrate mg/L)	Sulfate (mg/L)	Phosphate (mg/L)
BH Mineral Media	27.3	2.8	499.1	134.2	1298.9
5% BH Mineral Media	3.0	2.2	23.4	6.2	69.5
OSPW + N/P	635.9	38.7	61.9	345.7	57.9

Table A-3. Sulfate concentrations (mg/L) after 8 hours of heat activation (60°C) followed by 150 days at room temperature. Treatments include persulfate oxidation (PS); persulfate coupled with *P. fluorescens* (CPS); killed controls of persulfate with autoclaved bacteria (KC); and negative controls without persulfate or bacteria (NC). Note: 8 h samples for KC and NC bottles were not analyzed due to equipment errors. Data represents averaged triplicate bottles.

Merichem

SO_4^{2-} Concentration (mg/L)

Treatment	8 h	150 d
0NC	9.9	7.9
0CPS	6.9	7.8
0KC		7.7
250NC		69.9
250PS	83.6	161.0
250CPS	96.6	152.9
250KC		153.1
500NC		116.8
500PS	214.4	326.9
500CPS	242.9	305.3
500KC		349.1
1000NC		249.1
1000PS	524.3	643.3
1000CPS	451.1	553.9
1000KC		635.9

OSPW

SO_4^{2-} Concentration (mg/L)

Treatment	8 h	150 d
0NC		376.4
0CPS	329.1	375.5
0KC		401.5
250PS	417.8	494.7
250CPS	410.3	505.6
250KC		507.3
500PS	499.1	691.0
500CPS	459.9	620.7
500KC		677.4
1000PS	614.2	938.4
1000CPS	615.1	910.3
1000KC		927.4

Table A-4. Net persulfate (PS) consumption and net sulfate (SO_4^{2-}) production after 8 hours of heat activation (60°C) followed by 150 days at room temperature. Treatments include persulfate oxidation (PS); persulfate coupled with *P. fluorescens* (CPS); and negative controls without persulfate or bacteria (NC).

Merichem

Treatment	Time	PS Consumption (mM)	SO_4^{2-} Production (mM)	Molar Ratio
250PS	8 h	0.46	0.81	1.75
	150 d	0.94	1.61	1.71
500PS	8 h	1.20	2.17	1.80
	150 d	1.87	3.34	1.78
1000PS	8 h	3.04	5.39	1.77
	150 d	3.38	6.63	1.96
250CPS	8 h	0.51	0.94	1.85
	150 d	0.76	1.53	2.01
500CPS	8 h	1.42	2.46	1.74
	150 d	1.65	3.11	1.88
1000CPS	8 h	2.75	4.63	1.69
	150 d	3.03	5.70	1.88
250NC	150 d	0.31	0.66	2.14
500NC	150 d	0.41	1.15	2.79
1000NC	150 d	0.69	2.53	3.66

OSPW

Treatment	Time	PS Consumption (mM)	SO_4^{2-} Production (mM)	Molar Ratio
250PS	8 h	0.45	0.75	1.65
	150 d	1.11	1.55	1.40
500PS	8 h	0.84	1.60	1.89
	150 d	2.06	3.59	1.74
1000PS	8 h	1.64	2.80	1.71
	150 d	3.54	6.17	1.74
250CPS	8 h	0.45	0.67	1.50
	150 d	0.71	1.66	2.35
500CPS	8 h	0.77	1.19	1.54
	150 d	1.17	2.86	2.45
1000CPS	8 h	1.66	2.80	1.69
	150 d	2.70	5.88	2.17

Table A-5. First-order kinetic rate constants for the unactivated persulfate reaction calculated from 8 hours to 150 days. Treatments include persulfate oxidation (PS); and persulfate coupled with *P. fluorescens* (CPS).

Merichem		
Treatment	**-k (/d)**	**R^2**
250PS	0.010	0.984
250CPS	0.004	0.913
500PS	0.009	0.995
500CPS	0.003	0.993
1000PS	0.002	0.924
1000CPS	0.002	0.901

OSPW		
Treatment	**-k (/d)**	**R^2**
250PS	0.024	0.926
250CPS	0.003	0.975
500PS	0.026	0.947
500CPS	0.002	0.989
1000PS	0.009	0.994
1000CPS	0.003	0.977

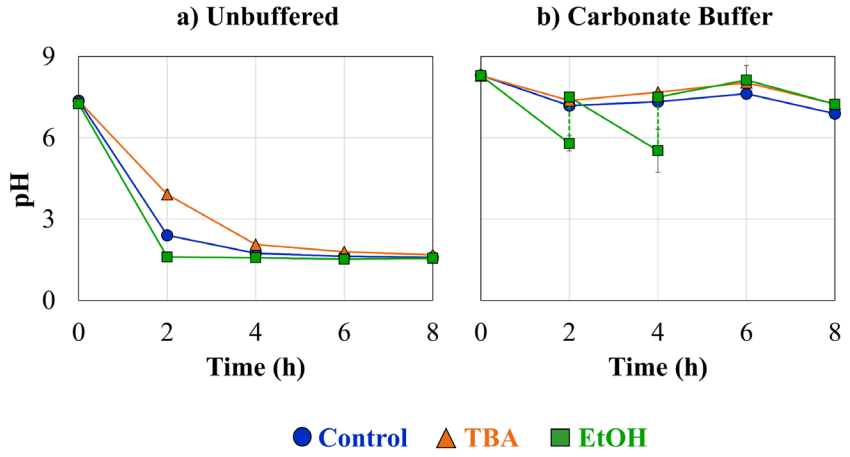

Figure A-6. pH levels during radical quenching tests using tert-butyl alcohol (TBA) and ethanol (EtOH) (30 mM) on Merichem NA removal with 1000 mg/L PS at 60°C in a) Unbuffered 5% BH mineral media, b) 5 mM carbonate buffer in 5% BH. EtOH Carbonate Buffered bottles had pH adjusted (dashed line). Error bars represent one standard deviation of duplicate bottles.

Table A-6. First-order kinetic rate constants of Merichem NA degradation for radical quenching tests using tert-butyl alcohol (TBA) and ethanol (EtOH) (30 mM) with 1000 mg/L PS at 60°C in unbuffered 5% BH mineral media or 5 mM carbonate buffer in 5% BH.

Treatment		**-k (/h)**	**R^2**
Control	Unbuffered	1.07	0.950
	Carbonate Buffered	0.34	0.961
TBA	Unbuffered	0.25	0.911
	Carbonate Buffered	0.15	0.995
EtOH	Unbuffered	0.08	0.957
	Carbonate Buffered	0.04	0.862

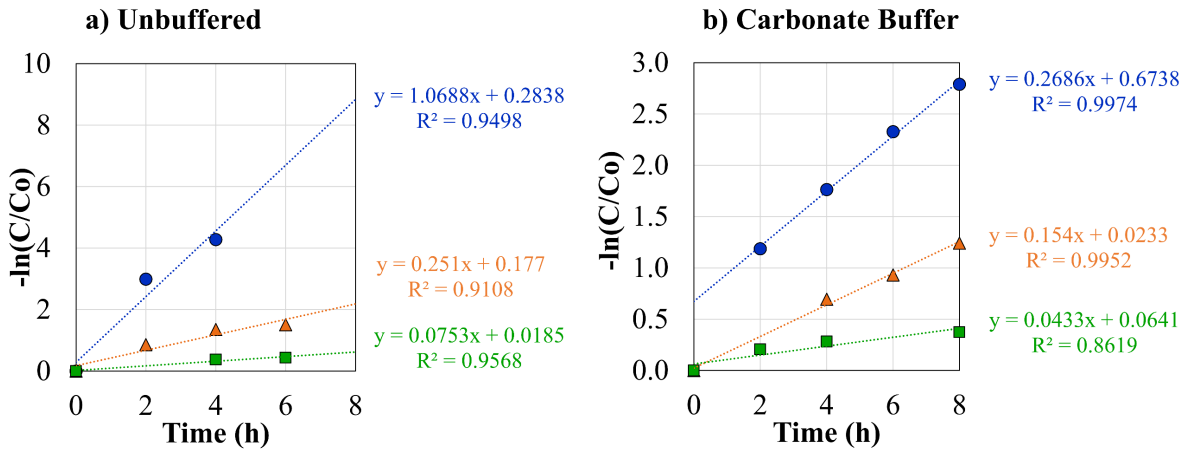

Figure A-7. First-order kinetic plots of Merichem NA degradation for radical quenching tests for controls (blue), tert-butyl alcohol (orange) and ethanol (green) (30 mM) with 1000 mg/L PS at 60ºC in a) unbuffered 5% BH mineral media or b) 5 mM carbonate buffer in 5% BH.

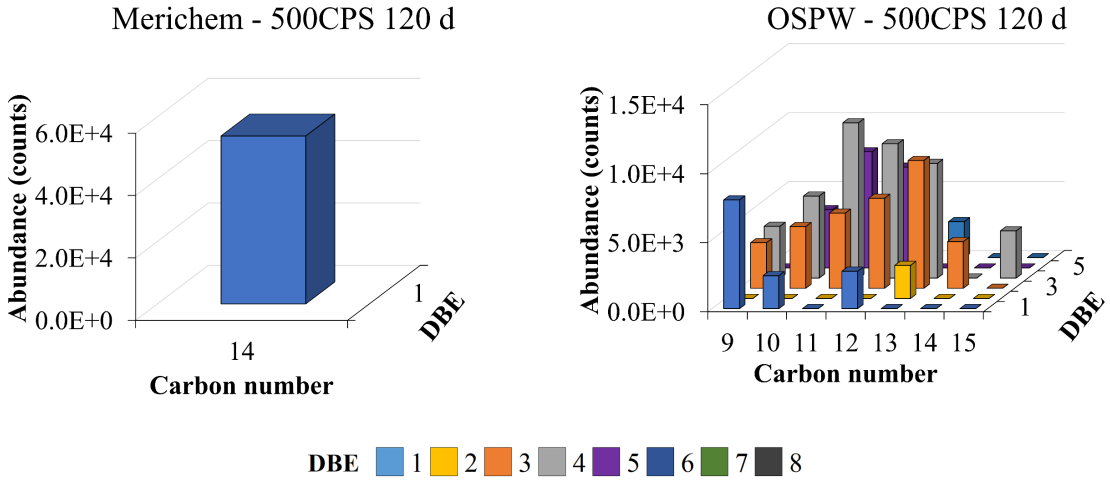

Figure A-8. Classical O2-NA distribution of Merichem and OSPW 500 mg/L persulfate oxidation coupled to *P. fluorescens* biodegradation (500CPS) after 120 days. Plots illustrate abundance vs carbon number and double bond equivalence (DBE). Data represents single treatment bottles.

Table A-7. Detailed Orbitrap results of NAFC class, double bond equivalence (DBE), chemical formula and abundance for OSPW bottles with 500 mg/L persulfate (500PS) after 120 days.

OSPW - 500PS - 120d			
Class	Neutral DBE	Formula	Total Abund
O8	0	C23H48O8	76641.13
O2	1	C9H18O2	7003.61
O2	1	C14H28O2	9810.65
O2	1	C16H32O2	6575.4
O4	2	C7H12O4	3966.78
N2O2	3	C12H22N2O2	36506.8
O2	3	C10H16O2	3563.74
O2	3	C12H20O2	3949.52
O2	3	C13H22O2	5882.36
O3	3	C8H12O3	6427.06
O3	3	C9H14O3	11174.74
O3	3	C10H16O3	14973.08
O3	3	C11H18O3	10462
O3	3	C12H20O3	5446.07
O4	3	C7H10O4	3715.56
O4	3	C8H12O4	9934.75
O4	3	C9H14O4	16680.36
O4	3	C10H16O4	10198.13
O4	3	C11H18O4	6938.3
O5	3	C7H10O5	4982.9
O5	3	C8H12O5	14249.21
O5	3	C9H14O5	13857.78
O5	3	C10H16O5	8522.76
O5	3	C11H18O5	4226.34
O6	3	C8H12O6	3626.35
O6	3	C9H14O6	3875.96
O	4	C14H22O	5974.42
O2	4	C9H12O2	3621.13
O2	4	C10H14O2	5606.78
O2	4	C11H16O2	8384.41
O2	4	C12H18O2	5544.16
O2	4	C13H20O2	3865.87
O3	4	C8H10O3	5566.11
O3	4	C9H12O3	15737.24
O3	4	C10H14O3	28937.99
O3	4	C11H16O3	31090.09
O3	4	C12H18O3	28314.7
O3	4	C13H20O3	15356.44
O3	4	C14H22O3	9348.14
O4	4	C8H10O4	10385.65
O4	4	C9H12O4	21575.37
O4	4	C10H14O4	34191.51
O4	4	C11H16O4	37454.14
O4	4	C12H18O4	37303.99
O4	4	C13H20O4	31558.88
O4	4	C14H22O4	17337.97
O5	4	C8H10O5	10060.09
O5	4	C9H12O5	23062.35
O5	4	C11H16O5	43469.94
O5	4	C12H18O5	44038.36
O5	4	C13H20O5	31661.15
O5	4	C14H22O5	12219.12
O6	4	C9H12O6	6307.33
O6	4	C10H14O6	18766.85
O6	4	C11H16O6	26869.41
O6	4	C12H18O6	24426.61
O6	4	C13H20O6	11090.95
O7	4	C11H16O7	5816.65

OSPW - 500PS - 120d			
Class	Neutral DBE	Formula	Total Abund
O2	5	C10H12O2	5267.24
O2	5	C11H14O2	8284.97
O2	5	C12H16O2	7183.22
O3	5	C9H10O3	3815.18
O3	5	C10H12O3	11408.92
O3	5	C11H14O3	18884.96
O3	5	C12H16O3	20342.03
O3	5	C13H18O3	17341.8
O3	5	C14H20O3	14466.38
O3	5	C15H22O3	8855.72
O4	5	C9H10O4	3851.4
O4	5	C10H12O4	12467.61
O4	5	C11H14O4	25627.66
O4	5	C12H16O4	35595.51
O4	5	C13H18O4	46258.01
O4	5	C14H20O4	37576.09
O4	5	C15H22O4	16956.57
O5	5	C10H12O5	9665.32
O5	5	C11H14O5	35591.62
O5	5	C12H16O5	57828.12
O5	5	C13H18O5	68130.21
O5	5	C14H20O5	50573.27
O5	5	C15H22O5	21612.05
O6	5	C10H12O6	7365.08
O6	5	C11H14O6	31568.11
O6	5	C12H16O6	52116.79
O6	5	C13H18O6	54549.09
O6	5	C14H20O6	36706.56
O6	5	C15H22O6	12362.97
O7	5	C11H14O7	11906.2
O7	5	C12H16O7	26825.86
O7	5	C13H18O7	27033.93
O7	5	C14H20O7	13930.35
O2	6	C11H12O2	3503.09
O2	6	C12H14O2	3524.98
O3	6	C11H12O3	4220.99
O3	6	C12H14O3	4524.44
O3	6	C13H16O3	4397.64
O3	6	C14H18O3	4496.92
O4	6	C11H12O4	3570.38
O4	6	C12H14O4	7921.87
O4	6	C13H16O4	18120.1
O4	6	C14H18O4	22596.52
O4	6	C15H20O4	16590.52
O5	6	C12H14O5	16535.11
O5	6	C13H16O5	35740.37
O5	6	C14H18O5	37746.95
O5	6	C15H20O5	29241.54
O5	6	C16H22O5	8235.87
O6	6	C12H14O6	17543.14
O6	6	C13H16O6	35745.44
O6	6	C14H18O6	39498.38
O6	6	C15H20O6	25006.03
O7	6	C12H14O7	9530.32
O7	6	C13H16O7	23442
O7	6	C14H18O7	23870.28
O7	6	C15H20O7	11556.44
O4	7	C15H18O4	3617
O5	7	C14H16O5	7242.38
O5	7	C15H18O5	8691.97
O6	7	C13H14O6	3611.54
O6	7	C14H16O6	8629.23
O6	7	C15H18O6	9136.99

Table A-8. Detailed Orbitrap results of NAFC class, double bond equivalence (DBE), chemical formula and abundance for OSPW bottles with 500 mg/L persulfate and *P. fluorescens* (500CPS) after 120 days.

OSPW - 500CPS - 120d			
Class	Neutral DBE	Formula	Total Abund
O8	0	C23H48O8	118837.49
O2	1	C9H18O2	7880.58
O2	1	C10H20O2	2390.01
O2	1	C12H24O2	2709.58
O2	2	C13H24O2	2390.59
O3	2	C8H14O3	2710.14
O3	2	C9H16O3	3019.54
O4	2	C7H12O4	3986.16
O4	2	C8H14O4	4309.56
O4	2	C9H16O4	3469.68
N2O2	3	C12H22N2O2	58878.5
O2	3	C9H14O2	3300.76
O2	3	C10H16O2	4475.75
O2	3	C11H18O2	5444.05
O2	3	C12H20O2	6526.83
O2	3	C13H22O2	9266.14
O2	3	C14H24O2	3376.21
O3	3	C8H12O3	7607.8
O3	3	C9H14O3	15103.86
O3	3	C10H16O3	20749.93
O3	3	C11H18O3	19278.34
O3	3	C12H20O3	13465.98
O3	3	C13H22O3	3234.59
O4	3	C7H10O4	4034.45
O4	3	C8H12O4	11145.86
O4	3	C9H14O4	19727.37
O4	3	C10H16O4	18123.04
O4	3	C11H18O4	13629.47
O4	3	C12H20O4	9754.26
O4	3	C13H22O4	6955.17
O5	3	C7H10O5	5153.72
O5	3	C8H12O5	14560.63
O5	3	C9H14O5	15753.11
O5	3	C10H16O5	11825.19
O5	3	C11H18O5	6748.43
O5	3	C12H20O5	4507.6
O6	3	C8H12O6	2716.61
O6	3	C9H14O6	3596.84
O6	3	C10H16O6	2893.27
O6	3	C11H18O6	2416.7
OS	3	C8H12OS	2563.37
OS2	3	C13H22OS2	2612.82
O	4	C10H14O	3244.07
O	4	C11H16O	2936.02
O	4	C12H18O	2519.57
O	4	C14H22O	8163.98
O2	4	C9H12O2	3749.75
O2	4	C10H14O2	5947.13
O2	4	C11H16O2	11259.27
O2	4	C12H18O2	9746.38
O2	4	C13H20O2	8309.93
O2	4	C14H22O2	3067.82
O2	4	C15H24O2	3419.39
O3	4	C8H10O3	5698.59
O3	4	C9H12O3	16832.51
O3	4	C10H14O3	33485.68
O3	4	C11H16O3	44797.28
O3	4	C12H18O3	45889.53
O3	4	C13H20O3	34479.15
O3	4	C14H22O3	26215.21
O3	4	C15H24O3	10327.78

OSPW - 500CPS - 120d			
Class	Neutral DBE	Formula	Total Abund
O4	4	C7H8O4	2383.26
O4	4	C8H10O4	9053.82
O4	4	C9H12O4	21686.27
O4	4	C10H14O4	38932.26
O4	4	C11H16O4	51330.41
O4	4	C12H18O4	59024.56
O4	4	C13H20O4	57375.07
O4	4	C14H22O4	39829.93
O4	4	C15H24O4	12159.78
O5	4	C8H10O5	8163.73
O5	4	C9H12O5	22955.64
O5	4	C11H16O5	54737.32
O5	4	C12H18O5	60268.65
O5	4	C13H20O5	49068.02
O5	4	C14H22O5	24990.66
O6	4	C9H12O6	5687.5
O6	4	C10H14O6	18523.96
O6	4	C11H16O6	30775.62
O6	4	C12H18O6	30883.02
O6	4	C13H20O6	18488.37
O6	4	C14H22O6	12274.05
O7	4	C10H14O7	3441.89
O7	4	C11H16O7	6154.29
N2O3	5	C18H30N2O3	2119.01
O	5	C11H14O	2367.28
O	5	C12H16O	2461.4
O2	5	C10H12O2	4221.49
O2	5	C11H14O2	8419.18
O2	5	C12H16O2	7302
O2	5	C13H18O2	5418.25
O3	5	C9H10O3	3344.52
O3	5	C10H12O3	10570.68
O3	5	C11H14O3	18767.86
O3	5	C12H16O3	24052.57
O3	5	C13H18O3	26674.42
O3	5	C14H20O3	27051.04
O3	5	C15H22O3	18620.95
O4	5	C9H10O4	3295.5
O4	5	C10H12O4	13490.54
O4	5	C11H14O4	29561.33
O4	5	C12H16O4	45829.06
O4	5	C13H18O4	64412.2
O4	5	C14H20O4	63058.05
O4	5	C15H22O4	37221.46
O4	5	C16H24O4	10506.44
O5	5	C9H10O5	2948.56
O5	5	C10H12O5	6901.51
O5	5	C11H14O5	35772.92
O5	5	C12H16O5	66621.39
O5	5	C13H18O5	85090.13
O5	5	C14H20O5	71388.43
O5	5	C15H22O5	37276.45
O6	5	C10H12O6	6266.76
O6	5	C11H14O6	29614.54
O6	5	C12H16O6	54464.3
O6	5	C13H18O6	61735.52
O6	5	C14H20O6	43067.44
O6	5	C15H22O6	18627.11
O7	5	C11H14O7	11945.95
O7	5	C12H16O7	23540.12
O7	5	C13H18O7	25004.97

OSPW - 500CPS - 120d			
Class	Neutral DBE	Formula	Total Abund
O2	6	C11H12O2	3346.36
O2	6	C12H14O2	3671.57
O2	6	C13H16O2	2611.56
O3	6	C10H10O3	2136.97
O3	6	C11H12O3	3443.66
O3	6	C12H14O3	4042.34
O3	6	C13H16O3	4934.45
O3	6	C14H18O3	5496.39
O3	6	C15H20O3	5083.7
O4	6	C11H12O4	3275.21
O4	6	C12H14O4	9334.32
O4	6	C13H16O4	19962.58
O4	6	C14H18O4	30471.17
O4	6	C15H20O4	25770.83
O4	6	C16H22O4	11488.15
O5	6	C11H12O5	3210.85
O5	6	C12H14O5	15842.37
O5	6	C13H16O5	36820.64
O5	6	C14H18O5	48918.6
O5	6	C15H20O5	37250.6
O5	6	C16H22O5	15779.41
O6	6	C11H12O6	2463.04
O6	6	C12H14O6	16104.28
O6	6	C13H16O6	36492.28
O6	6	C14H18O6	41350.61
O6	6	C15H20O6	29063.71
O7	6	C12H14O7	8090.22
O7	6	C13H16O7	18408.61
O7	6	C14H18O7	21123.37
O4	7	C14H16O4	3297.39
O4	7	C15H18O4	4733.3
O5	7	C13H14O5	3258.77
O5	7	C14H16O5	7944.75
O5	7	C15H18O5	10211.61
O6	7	C13H14O6	2748.03
O6	7	C14H16O6	8301.31
O6	7	C15H18O6	10055.87
N2OS	8	C23H34N2OS	3877.02
O2S	10	C20H22O2S	3106.06
O3S	10	C19H20O3S	2352.21

Table A-9. Microtox acute toxicity as inhibition effect (%) towards Vibrio fischeri at 81.9% concentration for **Merichem NAs** with persulfate oxidation alone (250-1000PS) or coupled with *P. fluorescens* biodegradation (0-1000CPS). Negative inhibition effects were inputted as "0.0" when calculating averages.

	Time	5 min						15 min					
	(d)	1	2	3	4	Average	Std Dev	1	2	3	4	Average	Std Dev
50 mg/L Merichem NA	0	88.35	88.87	88.75	88.02	88.5	0.3	89.51	89.19	90.38	88.77	89.5	0.6

Treatment	Time	5 min					15 min				
	(d)	1	2	3	Average	Std Dev	1	2	3	Average	Std Dev
250PS	0.3	30.4	36.6	28.2	31.7	3.5	22.5	24.8	28.5	25.3	2.5
	2		68.1					51.9			
	150	66.8	61.4	45.6	57.9	9.0	52.9	49.8	36.6	46.4	7.1
500PS	0.3	55.0	34.1	33.3	40.8	10.1	44.2	27.5	28.9	33.5	7.6
	2		88.3					84.3			
	71	17.7	7.3	27.4	17.5	8.2	16.1	4.9	18.2	13.1	5.8
	150	68.3	61.8		65.1	3.3	51.6	39.3		45.5	6.2
1000PS	0.3	67.2	14.1	37.0	39.4	21.8	52.6	5.0	32.0	29.9	19.5
	2		72.9					51.2			
	71	32.6	-25.5	-14.5	10.9	15.4	19.0	-26.9	-16.2	6.4	9.0
	150	83.8	81.5	84.8	83.4	1.4	73.5	71.2	76.3	73.7	2.1
0CPS	0.3	80.3	78.5		79.4	0.9	81.2	80.1		80.6	0.6
	63	42.8	38.3	32.5	37.9	4.2	39.7	39.0	36.5	38.4	1.4
	150	21.3	44.2	34.4	33.3	9.4	18.2	38.1	30.8	29.0	8.2
250CPS	0.3	33.7	18.2	13.8	21.9	8.5	24.4	10.4	5.2	13.3	8.1
	63	17.4	22.0	-19.2	13.1	9.5	15.5	15.8	-24.8	10.4	7.4
	121	30.0	-10.2	5.8	11.9	12.9	26.7	-3.7	6.0	10.9	11.4
	150	-18.0	-13.3	-18.7	0.0	2.4	-18.1	-20.3	-24.1	-20.8	2.5
500CPS	0.3	8.9	1.2	33.6	14.6	13.8	-3.9	-10.5	22.0	7.4	10.4
	46	38.2	50.5	56.3	48.3	7.5	28.5	38.0	41.2	35.9	5.4
	83										
	122	31.1	49.5	39.3	40.0	7.5	28.6	40.5	32.5	33.9	5.0
	150	-28.0	70.7	54.8	62.8	7.9	-28.8	57.1	39.7	48.4	8.7
1000CPS	0.3	37.2	31.7	-0.7	22.7	16.7	22.3	22.3	-9.5	11.7	15.0
	46	44.8	50.3	68.2	54.4	10.0	27.6	32.4	53.2	37.7	11.1
	122	51.2	48.2	71.9	57.1	10.5	44.4	39.5	58.2	47.3	7.9
	150	79.3	83.5	83.9	82.2	2.1	62.4	67.5	67.9	65.9	2.5

Red text indicates the sample wasn't included to calculate the average

Table A-10. Microtox acute toxicity as inhibition effect (%) towards Vibrio fischeri at 81.9% concentration for **OSPW** with persulfate oxidation alone (250-1000PS) or coupled with *P. fluorescens* biodegradation (0-1000CPS). Negative inhibition effects were inputted as "0.0" when calculating averages.

	Time (d)	5 min						15 min					
		1	2	3	4	Average	Std Dev	1	2	3	4	Average	Std Dev
OSPW	0	19.27	17.94	16.67	18.79	18.2	1.0	16.94	18.17	12.17	14.26	15.4	2.3

Treatment	Time (d)	5 min					15 min				
		1	2	3	Average	Std Dev	1	2	3	Average	Std Dev
250PS			46.5	12.9	28.1	13.9		36.7	10.9	23.3	10.6
	0.3	25.0					22.5				
	6	8.4	-8.2				-4.1	-0.1			
	63	-5.2		-4.1	0.0	0.6	-15.4		-8.4	0.0	3.5
	150	-29.5	-9.3	-10.8	0.0	9.2	-29.3	-15.1	-18.4	0.0	6.1
500PS	0.3	41.6	44.4	39.5	41.8	2.0	30.5	33.7	28.5	30.9	2.1
	56	-14.8	-22.5	-16.0	0.0	3.4	-21.5	-32.9	-29.6	-28.0	4.8
	150	-26.6	-20.3	-19.0	0.0	3.3	-30.7	-26.1	-34.2	-30.3	3.3
1000PS	0.3	60.7	62.2	59.8	60.9	1.0	55.6	54.2	52.0	54.0	1.5
	56	26.1	41.7	30.7	32.8	6.5	14.4	22.8	9.0	15.4	5.7
	150	-0.1	7.4	-4.8	5.4	3.9	-7.1	-1.8	-12.2	0.0	4.2
0CPS	0.3	13.9	15.5		14.7	0.8	13.2	17.0		15.1	1.9
	150	17.1	15.3	11.1	14.5	2.5	4.5	3.5	-1.5	2.1	2.6
250CPS	0.3	39.2	24.2	3.9	22.4	14.5	25.1	16.8	-2.4	13.2	11.5
	6			17.5	17.5	0.0			4.7	4.7	0.0
	64	-22.8		-3.9	0.0	9.5	-30.8		-10.9	0.0	10.0
	150	-11.4	-11.1	-12.2	0.0	0.5	-21.5	-31.4	-37.3	0.0	6.5
500CPS	0.3	60.3	48.3	31.4	46.6	11.9	47.2	35.0	10.6	30.9	15.2
	62	40.7	31.1	25.5	32.4	6.3	20.4	12.9	5.9	13.1	5.9
	121	14.9	5.2	31.2	17.1	10.7	1.7	-5.8	15.9	5.9	7.1
	150	-4.7	-22.5	6.1	2.0	2.9	-31.4	-40.4	-11.8	0.0	11.9
1000CPS	0.3	42.4	35.1	39.7	39.1	3.0	30.6	23.3	27.8	27.2	3.0
	62	65.2	40.3	49.0	51.5	10.3	51.2	23.1	27.2	33.8	12.4
	121	60.9	46.5	23.2	43.6	15.5	55.6	34.1	14.3	34.6	16.8
	150	20.0	49.0	54.7	41.2	15.2	4.1	25.7	31.9	20.6	11.9

Appendix A-2: Additional Data for Chapter 5

For preparing 1 L of mineral medium, first add:

- 10 mL phosphate buffer solution
    - 27.2 g KH_2PO_4 and 34.8 g K_2HPO_4 per liter
- 10 mL salt solution
    - 53.5 g NH_4Cl, 7.0 g $CaCl_2 \cdot 6H_2O$, and 2.0 g $FeCl_2 \cdot 4H2O$ per liter
- 2 mL trace mineral solution
    - 0.3 g H_3BO_3, 0.1 g $ZnCl_2$, 0.75 g of $NiCl_2 \cdot 6H_2O$, 1.0 g $MnCl_2 \cdot 4H_2O$, 0.1 g $CuCl_2 \cdot 2H_2O$, 1.5 goCoC$l_2 \cdot$ $6H_2O$, 0.02 g Na_2SeO_3, 0.1 g A$l_2(SO_4)_3 \cdot 16$ H_2O
- 1 mL concentrated H_2SO_4 per liter
- 2 mL magnesium chloride solution
    - 50.8 g $MgCl_2.6H_2O$ per liter
- 1 mL redox indicator
    - 1g resazurin per liter
- 945 ml deionized water

Autoclave this mixture, purge with 80% N_2 / 20% CO_2 and transfer to glove box.

Add 10mL of sterilized anaerobic vitamin solution (per liter: 0.02 g biotin, 0.02 g folic acid, 0.1 g pyridoxine hydrochloride, 0.05 g riboflavin, 0.05 g thiamine, 0.05 g nicotinic acid, 0.05 g pantothenic acid, 0.05 g 4-aminobenzoate (PABA), 0.05 g cyanocobalamin, and 0.05 g thioctic acid); 10 mL of anaerobic amorphous ferrous sulfide solution (13.9 g $FeSO_4 \cdot 7H_2O$ per 500 mL and 12.0 g $Na_2S \cdot 9H_2O$ per 500 mL) and 10 mL of saturated bicarbonate buffer (20 g sodium bicarbonate / 100 mL deionized water).

Table A-11. Molar ratios of benzene consumed to methane produced for DGG-B positive controls (0.6 g/L NaCl), bottles not acclimated to salt (2.5 – 10 g/L) and culture slowly acclimated to salt.

NaCl (g/L)	Benzene Consumed (µmol)	Methane Produced (µmol)	Methane / Benzene	Timeframe
0.6 g/L - 1	148.57	550.38	3.70	0 - 205 d
	258.80	965.63	3.73	205 - 408 d
0.6 g/L - 2	134.23	495.87	3.69	0 - 205 d
	229.32	777.79	3.39	205 - 408 d
0.6 g/L - 3	156.01	544.42	3.49	0 - 205 d
	220.68	725.20	3.29	205 - 408 d
2.5 g/L - 1	169.69	589.15	3.47	0 - 205 d
2.5 g/L - 2	160.51	608.33	3.79	0 - 205 d
2.5 g/L - 3	156.43	556.63	3.56	0 - 205 d
5 g/L - 1	88.95	237.06	2.67	0 - 205 d
5 g/L - 2	87.38	240.06	2.75	0 - 205 d
5 g/L - 3	86.42	253.71	2.94	0 - 205 d
10 g/L - 1	56.35	166.05	2.95	0 - 364 d
10 g/L - 2	52.47	189.72	3.62	0 - 364 d
10 g/L - 3	59.90	196.33	3.28	0 - 364 d
Slow Accl (0.5 - 6.5 g/L) - 1	197.29	640.02	3.24	0 - 205 d
Slow Accl (6.5 - 11.5 g/L) - 1	174.77	562.93	3.22	205 - 408 d
Slow Accl (0.5 - 6.5 g/L) - 2	179.69	560.23	3.12	0 - 205 d
Slow Accl (6.5 - 11.5 g/L) - 2	165.05	551.51	3.34	205 - 408 d
Slow Accl (0.5 - 6.5 g/L) - 3	175.44	682.60	3.89	0 - 205 d
Slow Accl (6.5 - 11.5 g/L) - 3	140.15	499.84	3.57	205 - 408 d
		Average	***3.37***	
		Std Err	**0.07**	
		n	**21**	

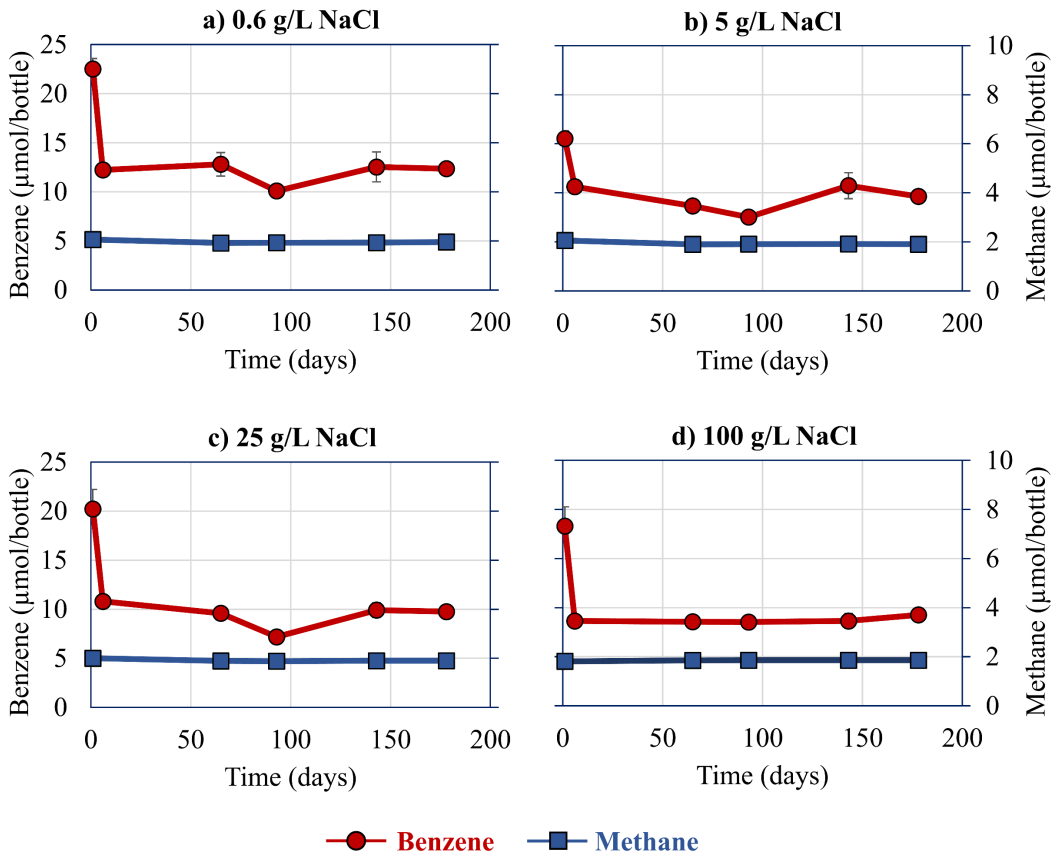

Figure A-9. Benzene consumption and methane production for autoclaved DGG-B (Killed Controls) at various salt concentrations. Error bars represent ± one standard deviation of duplicate bottles.

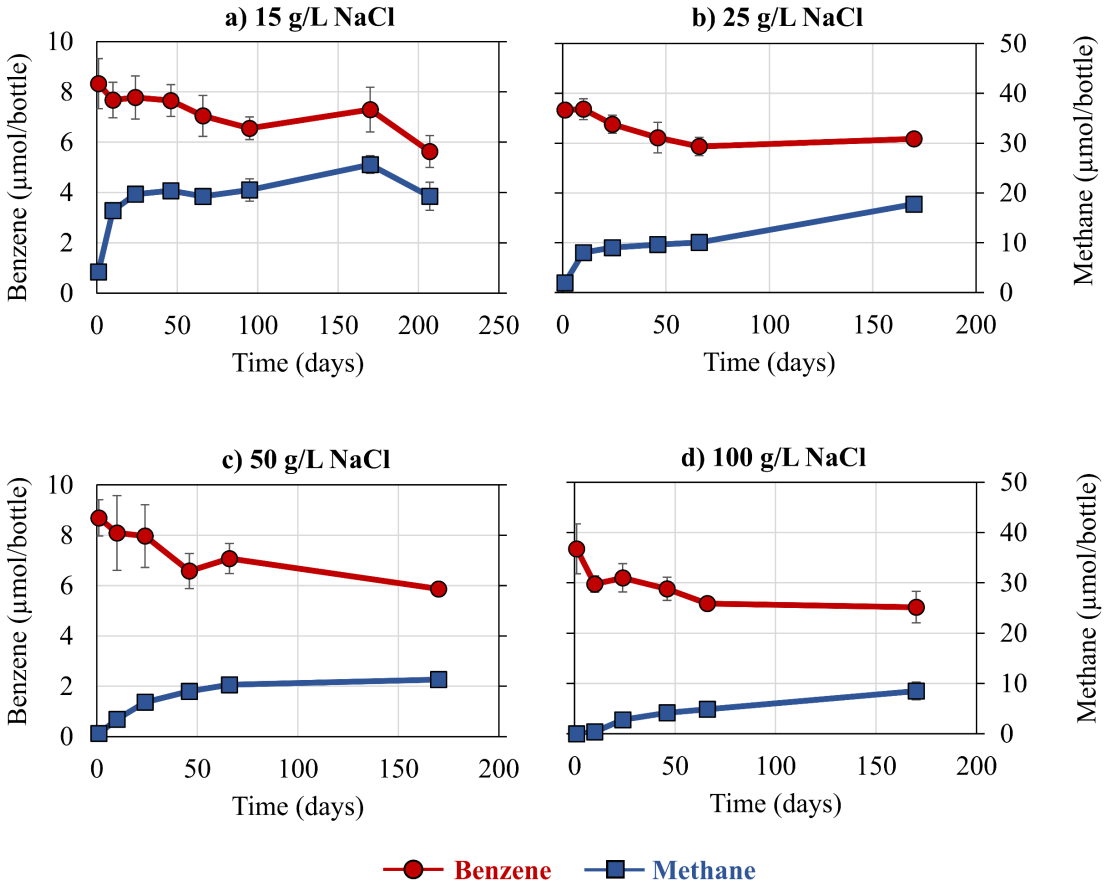

Figure A-10. Benzene consumption and methane production for DGG-B not previously acclimated to high salt at a) 15 g/L NaCl, b) 25 g/L NaCl, c) 50 g/L NaCl and d) 100 g/L NaCl. Error bars represent ± one standard deviation of triplicate bottles.

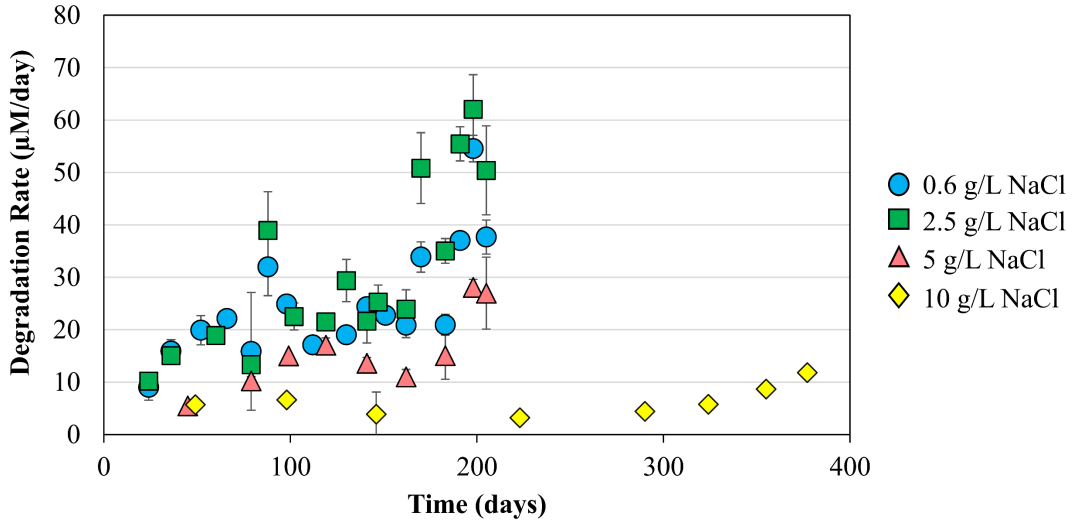

Figure A-11. Benzene degradation rate over time in DGG-B not previously acclimated to salt. Error bars represent ± one standard deviation of triplicate bottles.

Table A-12. Methane production rates in DGG-B sparged of benzene and fed acetate or H2/CO2, for each replicate along with averaged values.

NaCl	Methane Production Rate (µmol / day)			
	Acetate		H2/CO2	
0.6 g/L	10.15 11.21 11.07	0 - 39 d	2.84 3.60 3.20	0 - 46 d
5 g/L	7.97 7.00 7.40	0 - 39 d	3.79 3.05 3.09	0 - 46 d
25 g/L	2.55 1.47 2.03	67 - 179 d	2.46 2.17 1.70	0 - 67 d

NaCl	Acetate	H2/CO2
	Average (µmol/d)	Average (µmol/d)
0.6 g/L	10.81	3.21
5 g/L	7.46	3.31
25 g/L	2.02	2.11

Table A-13: Acetate concentrations in H_2/CO_2 Fed Bottles for duplicate bottles.

NaCl (g/L)	Time (d)	Acetate (mM)
0.6 g/L - 1	100	0.22
0.6 g/L - 2	100	0.22
5 g/L - 1	100	0.18
5 g/L - 2	100	0.23
25 g/L - 1	100	1.70
25 g/L - 2	100	2.49
0.6 g/L - 1	200	0.25
0.6 g/L - 2	200	0.23
5 g/L - 1	200	0.16
5 g/L - 2	200	0.18
25 g/L - 1	200	0.25
25 g/L - 2	200	0.20

Table A-14. Dimensionless Henry's Law Constants (H) for benzene and methane adjusted for salting out effect with Setschenow constant (K_s).

NaCl (g/L)	H (benzene)	H (methane)
0.6	0.22	28.07
2.5	0.22	28.36
5	0.23	28.72
10	0.24	29.46
15	0.25	30.22
25	0.27	31.79
50	0.32	36.10
100	0.47	46.55

$$H = H_o \times 10^{Ks \times NaCl(mol/L)}$$

	Benzene	Methane
H_o	0.22	28
K_s (L/mol)	0.195*	0.129**

*(Sander 2015), **(Ni and Yalkowsky 2003)

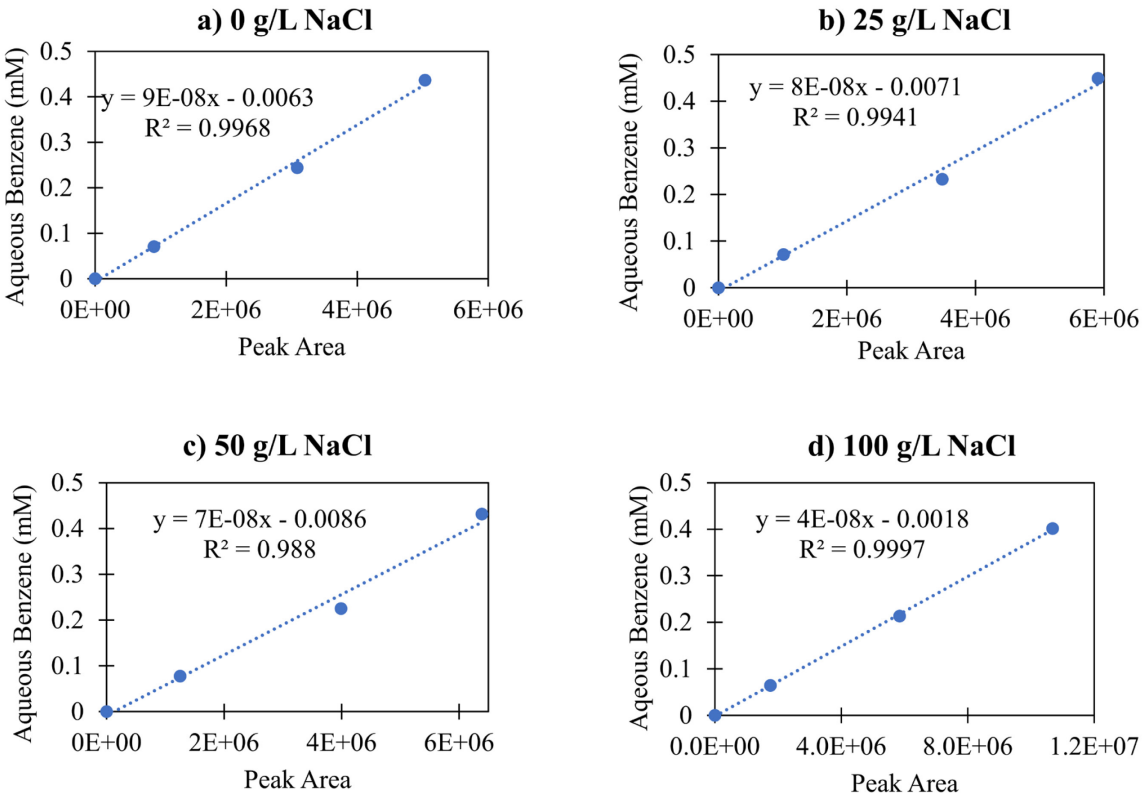

Figure A-12. Standard curves for aqueous benzene concentration versus peak area on GC-FID for various salt concentrations.

Table A-15. Primer sequences for general bacteria, general archaea and ORM2.

Primer Name	Target Organism/Gene	Primer Sequence (5' – 3')	Expected Amplicon Length (bp)	Annealing Temp	References
Bac_1055f Bac_1392r	General Bacteria	ATGGCTGTCGTCAGCT ACGGGCGGTGTGTAC	338	55	(Amann et al. 1995, Ferris et al. 1996)
Arch_787f Arch_1059r	General Archaea	ATTAGATACCCGBGTAGTCC GCCATGCACCWCCTCT	273	59	(Yu et al. 2005)
ORM2_168f ORM2_422r	*Deltaproteobacteria ORM2*	GAGGGAATAGCCAAAGGTGA GAGCTTTACGACCCGAAGAC	255	59	(Qiao et al. 2018, Toth et al. 2021)

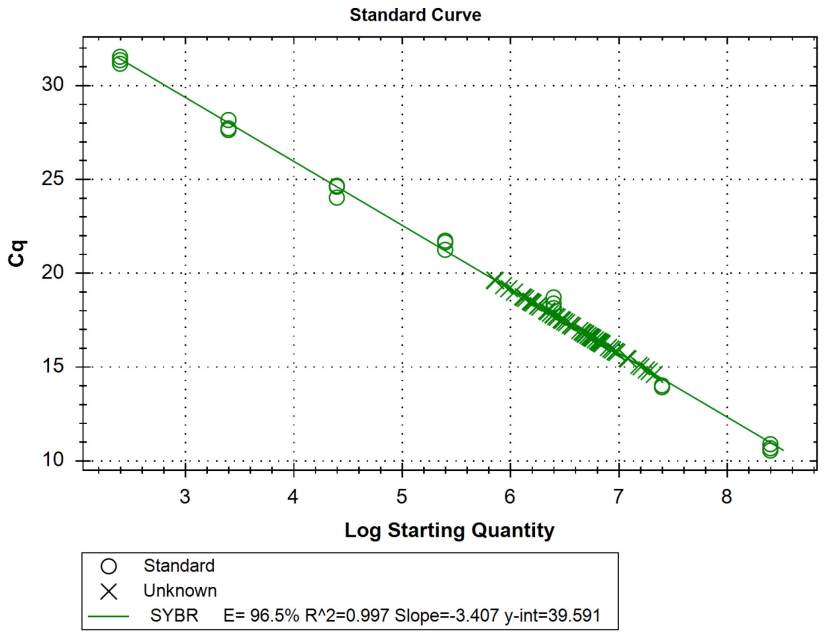

Figure A-13. Standard calibration curve for qPCR of general archaea, using 10-fold serial dilutions of Methanoregula plasmids.

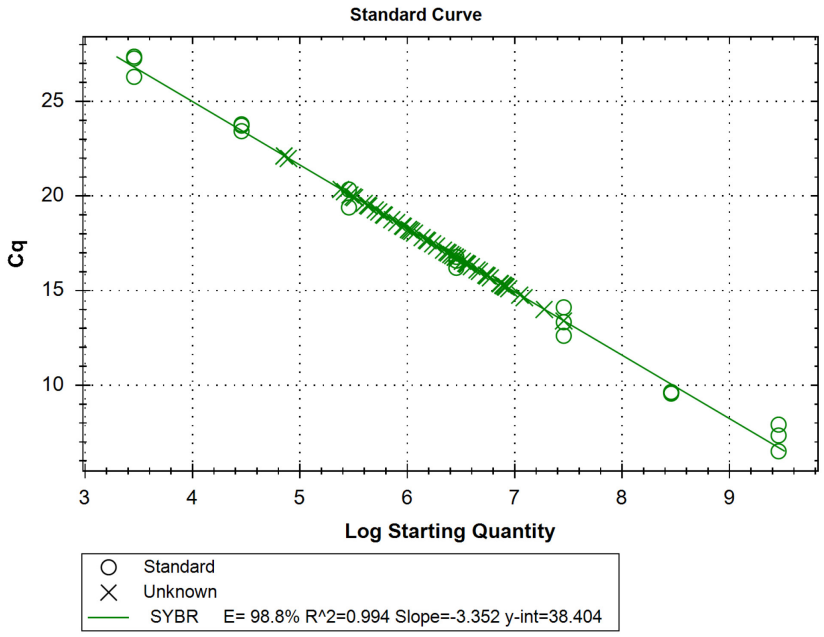

Figure A-14. Standard calibration curve for qPCR of general bacteria, using 10-fold serial dilutions of e. Coli plasmids.

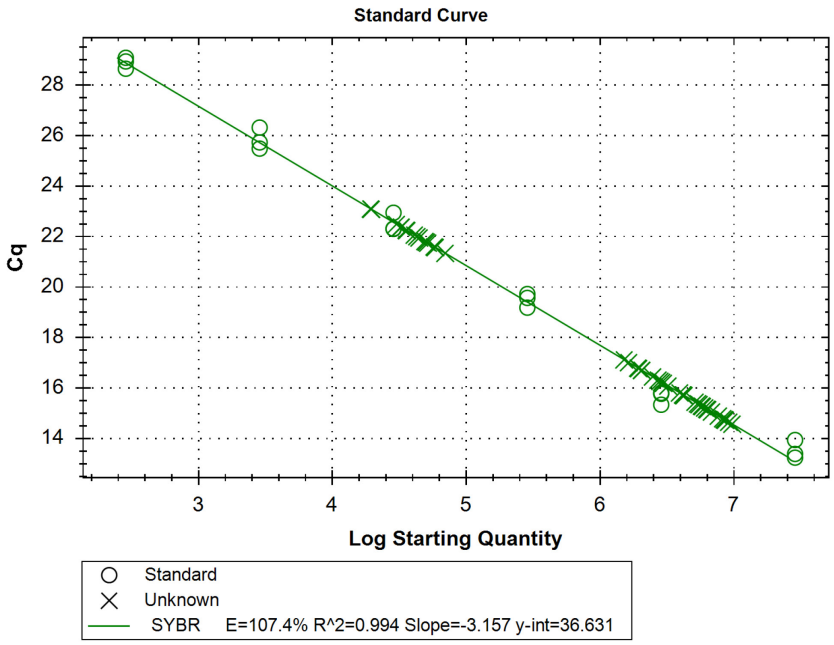

Figure A-15. Standard calibration curve for qPCR of OMR2, using 10-fold serial dilutions of ORM2 plasmids.

Table A-16. Doubling times and yields for ORM2.

Sample	Replicate	ORM2 copies / mL	Average (copies/mL)	µmol Benzene Consumed	Time (days)	Yield (copies/nmol)	Doubling Time (t1: 0 d)	Doubling Time (t1: 100 d)
Time 0	1	2.74E+07	1.99E+07		0			
	2	1.81E+07			0			
	3	2.66E+07			0			
	4	7.40E+06			0			
Slow - 100d	2	1.09E+08	1.08E+08	82.38	100	3.25E+04	41	
	3	1.07E+08		81.12	100	3.21E+04	41	
Slow - 200d	1	2.19E+08	2.50E+08	101.05	200	3.30E+04	58	98
	2	2.27E+08		97.31	200	3.62E+04	57	95
	3	3.05E+08		94.34	200	6.30E+04	51	66
0g/L - 100d	1	7.40E+07	5.56E+07	57.20	100	2.84E+04	53	
	2	4.80E+07		52.36	100	1.61E+04	79	
	3	4.48E+07		66.24	100	1.13E+04	85	
0g/L - 200d	1	1.51E+08	3.64E+08	79.52	200	2.92E+04	68	97
	2	4.62E+08		72.73	200	1.71E+05	44	31
	3	4.77E+08		76.16	200	1.70E+05	44	29
2.5g/L - 100d	1	1.27E+08	9.39E+07	66.61	100	4.82E+04	37	
	2	1.31E+08		54.56	100	6.12E+04	37	
	3	2.38E+07		58.92	100	2.01E+03	383	
2.5g/L - 200d	1	3.14E+08	3.11E+08	103.09	200	5.44E+04	50	77
	2	3.71E+08		105.95	200	6.80E+04	47	67
	3	2.48E+08		97.51	200	6.90E+04	55	30
5g/L - 100d	1	3.25E+06	3.36E+06	29.28	100	-1.70E+04	-38	
	2	3.46E+06		27.40	100	-1.80E+04	-40	
	3	7.04E+05		30.71	100	-1.87E+04	-21	
5g/L - 200d	1	1.50E+08	1.26E+08	56.15	200	7.83E+04	69	18
	2	1.15E+08		56.37	200	5.92E+04	79	20
	3	1.15E+08		49.67	200	6.88E+04	79	14
10g/L - 100d	1	2.49E+07	5.08E+07	21.86	100	-6.02E+04	-68	
	2	4.08E+06		18.32	100	-1.06E+05	-25	
	3	9.76E+07		20.01	100	4.32E+04	198	
15g/L - 200d	1	1.95E+06	2.09E+06	2.03	200	-2.65E+05	-60	
	2	1.75E+06		2.47	200	-2.20E+05	-57	
	3	2.57E+06		3.59	200	-1.45E+05	-68	
25g/L - 200d	1	2.85E+06	2.36E+06	2.42	200	-2.11E+05	-71	
	2	1.03E+06		3.08	200	-1.84E+05	-47	
	3	3.18E+06		1.88	200	-2.67E+05	-76	

Note: 10 g/L used 0 g/L 100d as time 0;
red text indicates outliers

*Td = (t2-t1)*ln2/ln[N2/N1]*

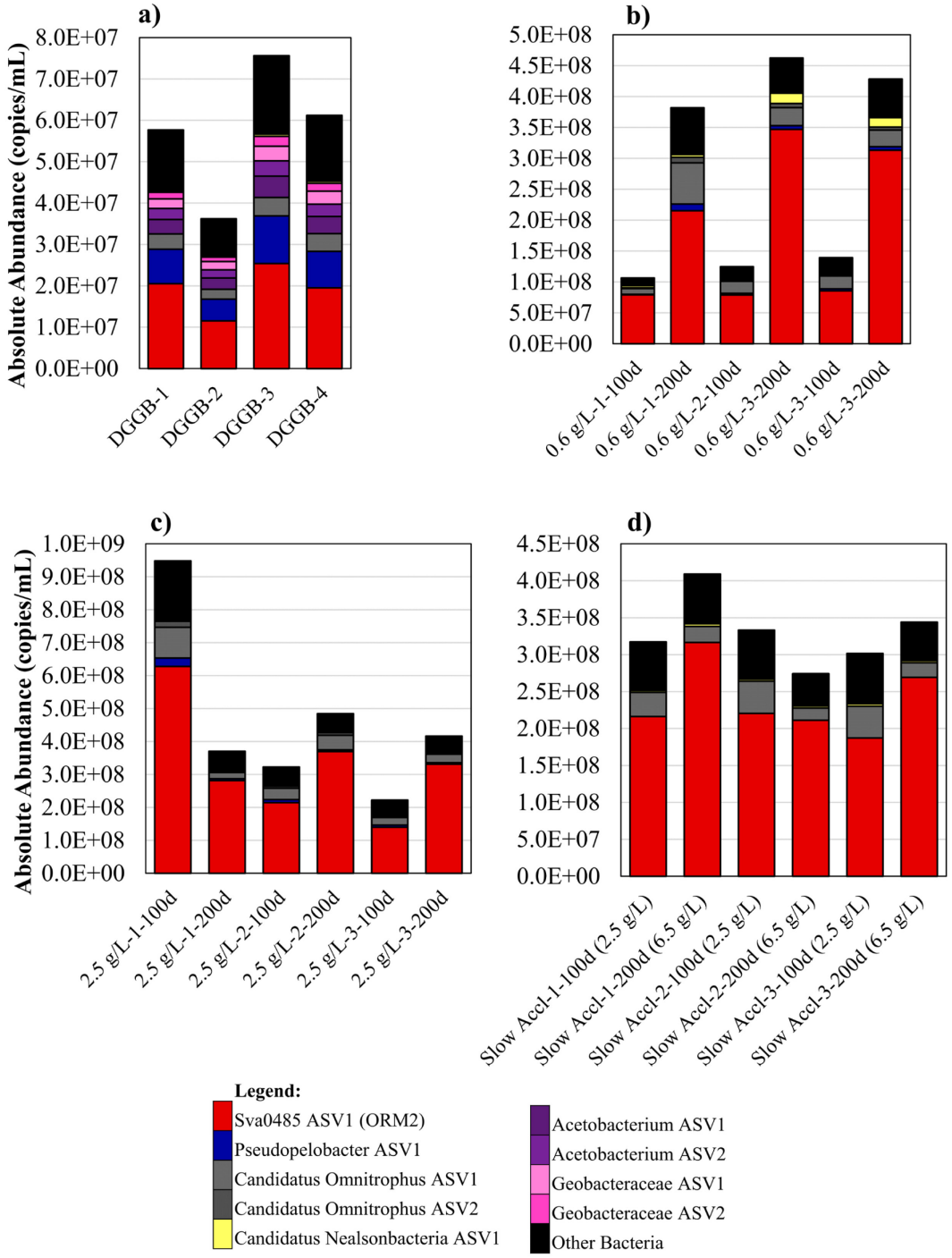

Figure A-16. Absolute abundance of total bacteria in DGG-B, a) original (time 0) DGG-B inoculum, b) positive controls (0.6 g/L NaCl) after 100 and 200 d, c) at 2.5 g/L NaCl after 100 and 200 d and d) DGG-B slowly acclimated to salt at 100 d (2.5 g/L) and 200 d (6.5 g/L).

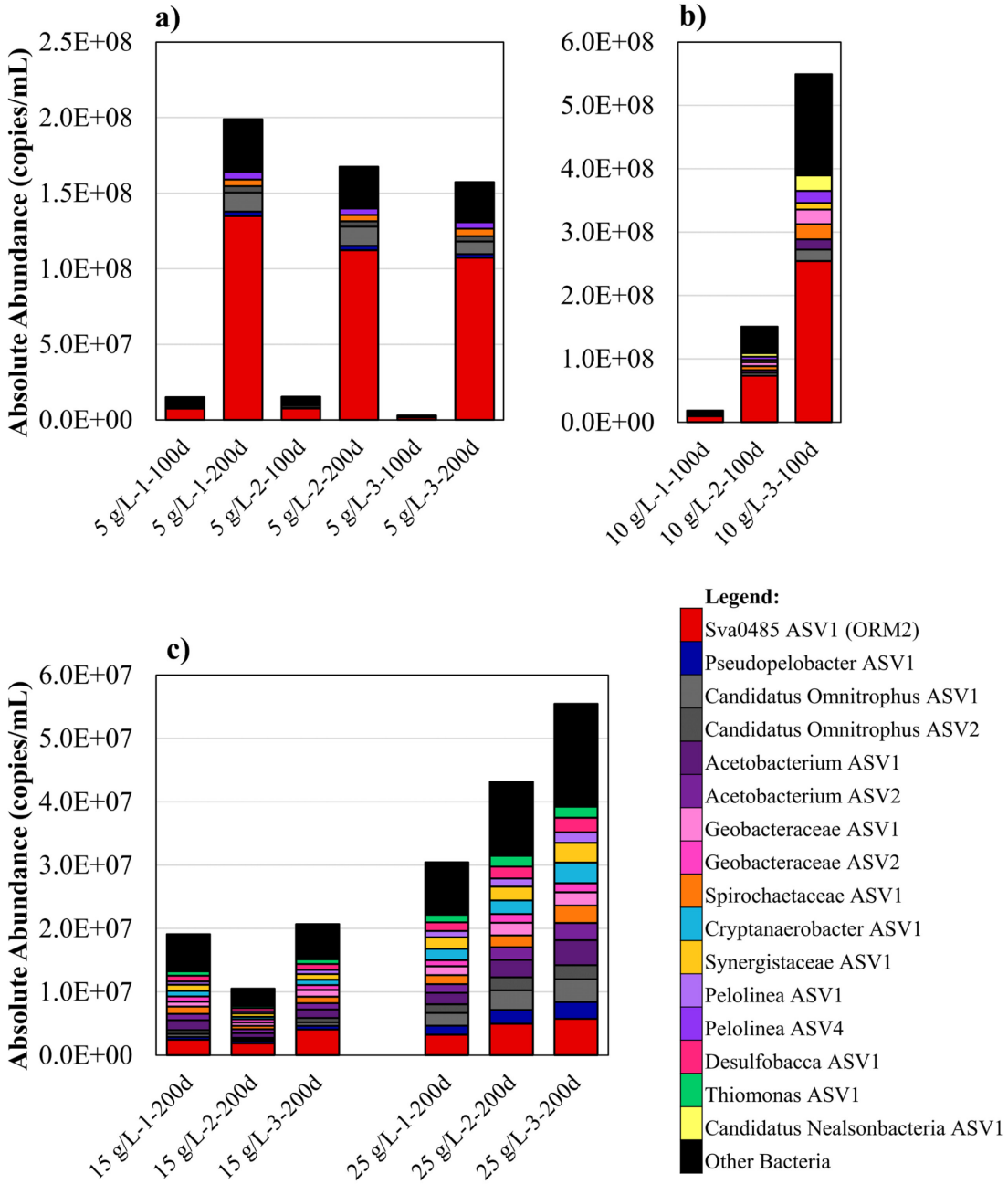

Figure A-17. Absolute abundance of total bacteria in DGG-B, a) at 5 g/L NaCl after 100 and 200d, b) 10 g/L NaCl after 100 d, and c), 15 and 25 g/L NaCl after 200 d. Note: 10 g/L NaCl were set up ~100 d after other bottles.

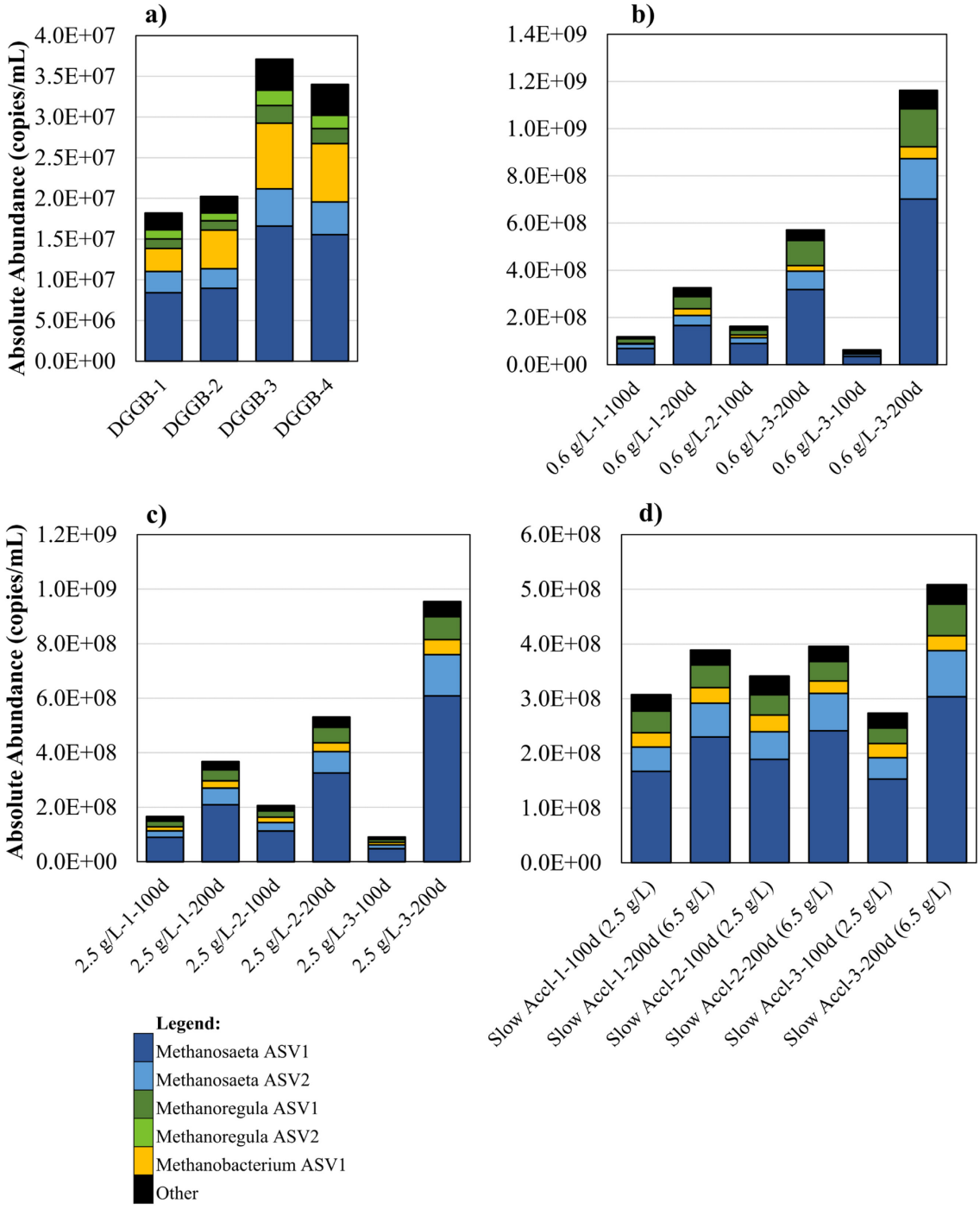

Figure A-18. Absolute abundance of total archaea in DGG-B, a) original (time 0) DGG-B inoculum, b) positive controls (0.6 g/L NaCl) after 100 and 200 d, c) at 2.5 g/L NaCl after 100 and 200 d and d) DGG-B slowly acclimated to salt at 100 d (2.5 g/L) and 200 d (6.5 g/L).

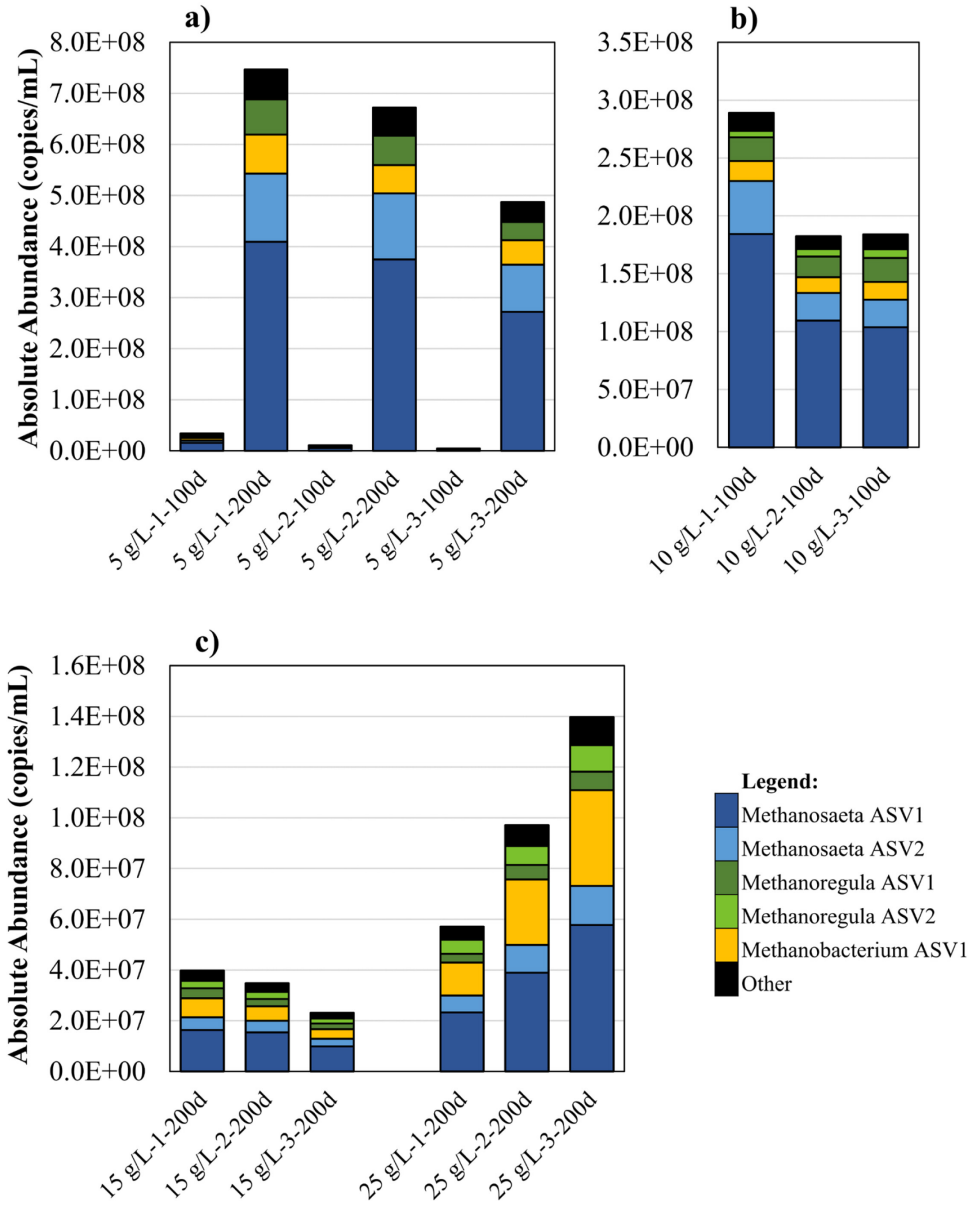

Figure A-19. Absolute abundance of total archaea in DGG-B, a) at 5 g/L NaCl after 100 and 200d, b) 10 g/L NaCl after 100 d, and c), 15 and 25 g/L NaCl after 200 d. Note: 10 g/L NaCl were set up ~100 d after other bottles.

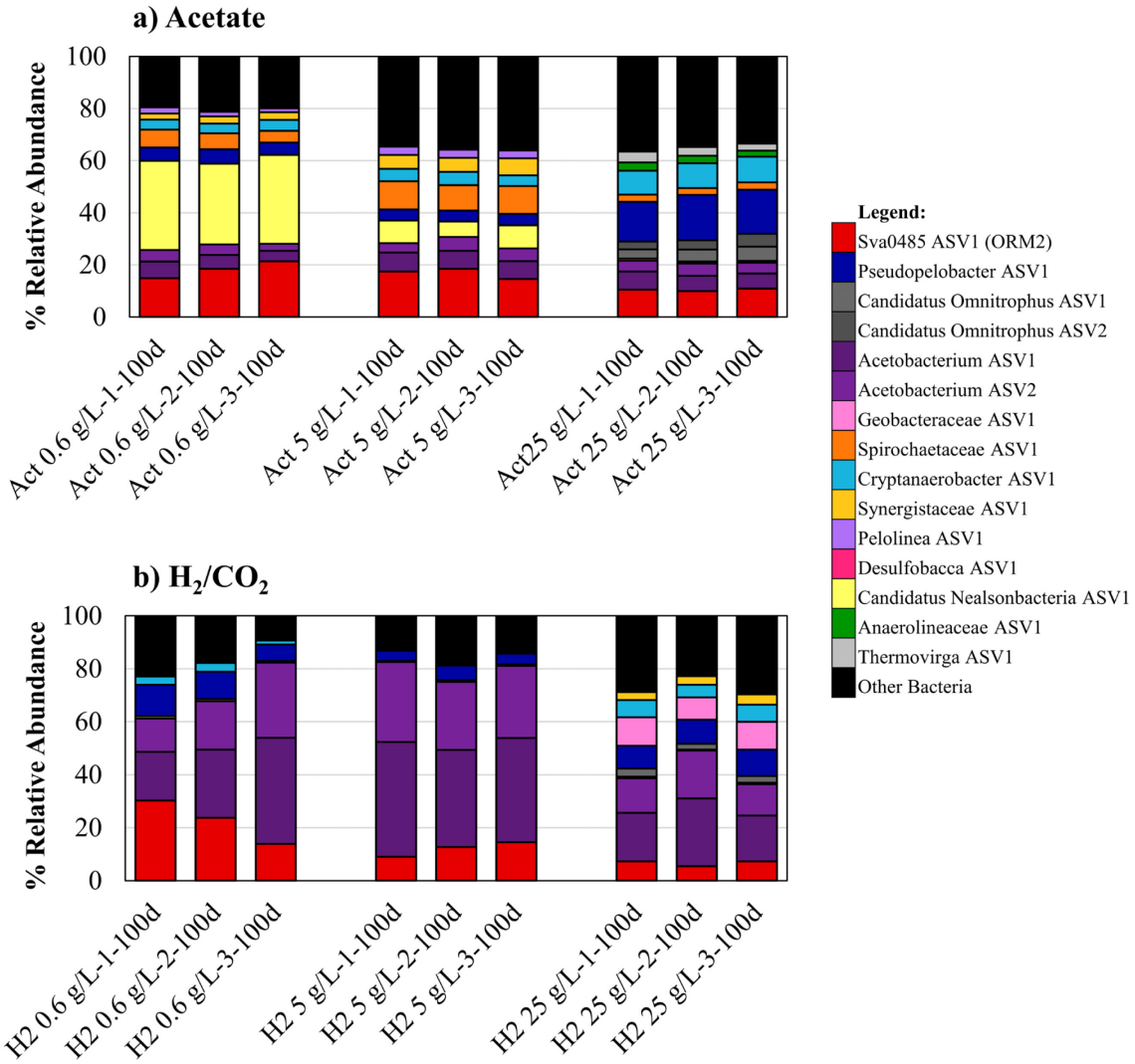

Figure A-20. Relative abundance of total bacteria after 100 days in DGG-B sparged of benzene and fed acetate or H_2/CO_2 to enrich for methanogens.

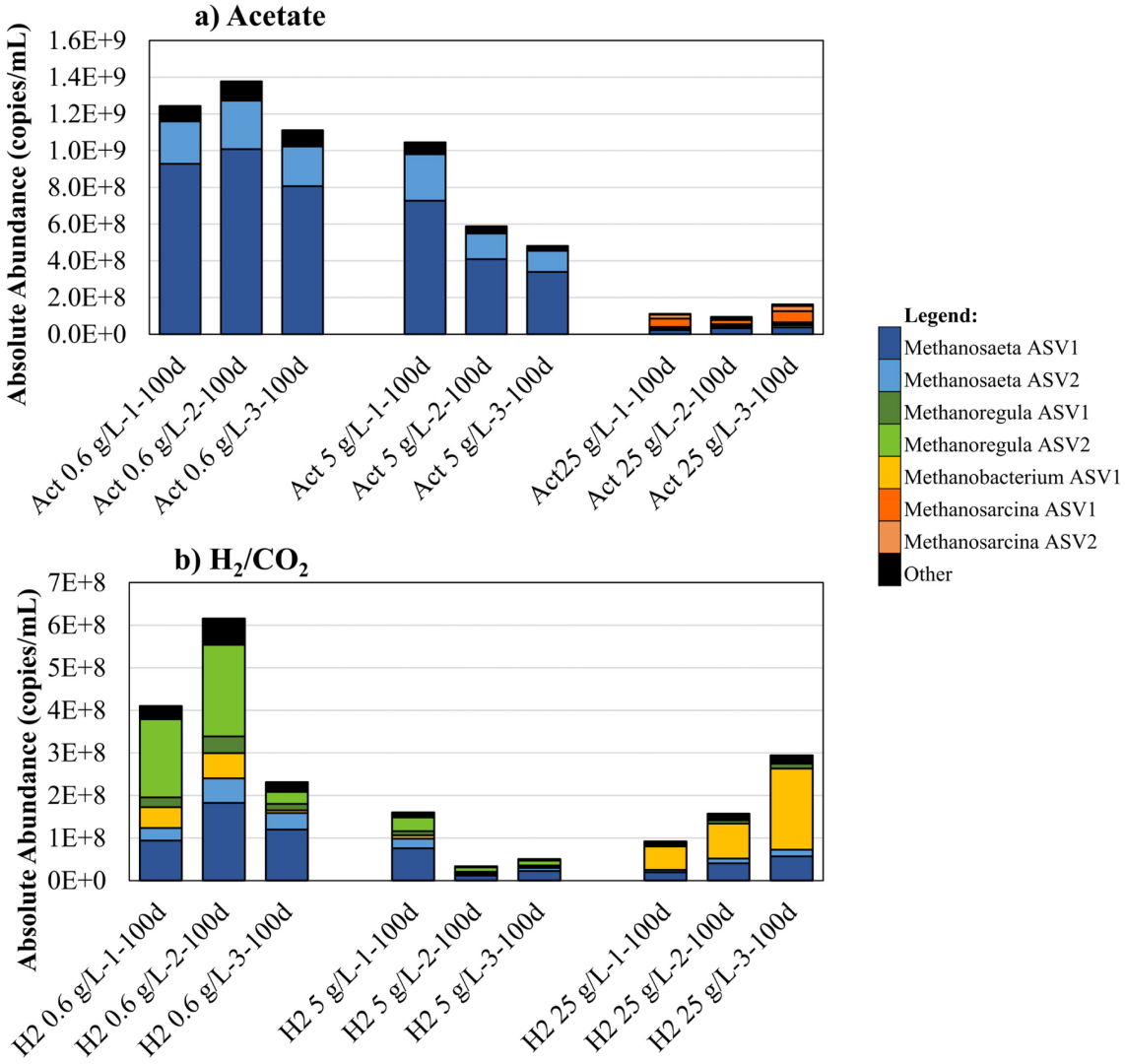

Figure A-21. Absolute abundance of total archaea after 100 days in DGG-B sparged of benzene and fed acetate or H_2/CO_2 to enrich for methanogens.

a) DGG-B Positive Control (0.6 g/L NaCl)

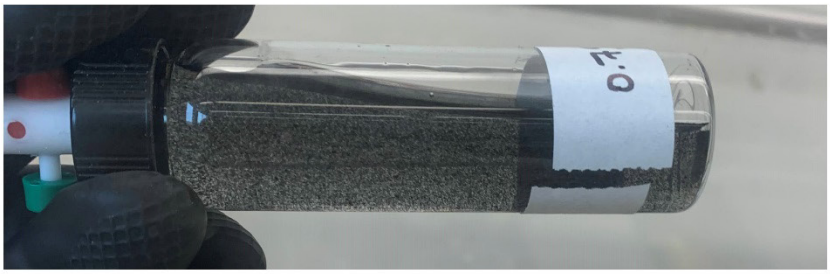

b) DGG-B at 25 g/L NaCl

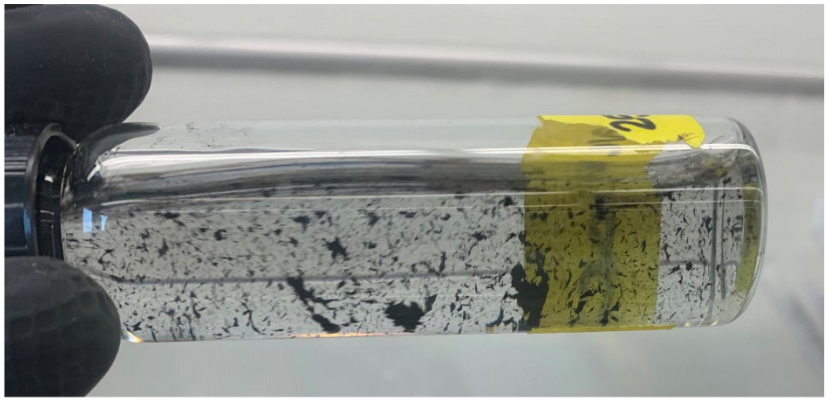

c) Killed Control DGG-B at 25 g/L NaCl

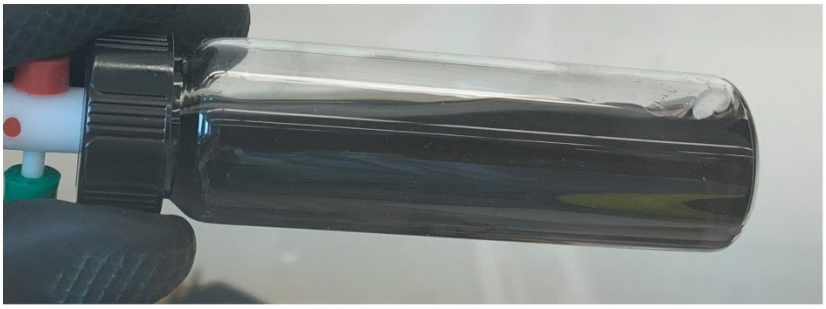

Figure A-22. DGG-B comparison at different salt concentrations for active and killed controls. At 25 g/L NaCl, DGG-B exhibits clumping due to EPS production (b). Killed controls show no clumping with added salt (c), indicating clumping is due to microbial stress response.

Table A-17. ANOVA and Turkey post hoc analysis for initial and final benzene degradation rates in DGG-B and methane production rates in acetate and H2/CO2 fed bottles. p values less than 0.05 are considered statistically significant.

Initial Benzene Degradation Rates (umol/d)			
0.6 g/L	**2.5 g/L**	**5 g/L**	**10 g/L**
8.69	11.09	5.38	6.65
12.20	9.36	5.33	4.89
6.18	10.08	5.68	5.60

Initial Benzene Degradation Rates (umol/d)

ANOVA: Single Factor

DESCRIPTION — Alpha 0.05

Group	*Count*	*Sum*	*Mean*	*Variance*	*SS*	*Std Err*	*Lower*	*Upper*
0.6 g/L	3	27.07	9.02	9.17	18.34	0.95	6.84	11.21
2.5 g/L	3	30.54	10.18	0.75	1.50	0.95	8.00	12.36
5 g/L	3	16.39	5.46	0.04	0.07	0.95	3.28	7.64
10 g/L	3	17.14	5.71	0.78	1.56	0.95	3.53	7.89

ANOVA

Sources	*SS*	*df*	*MS*	*F*	*P value*	*Eta-sq*	*RMSSE*	*Omega Sq*
Between Groups	50.42	3	16.81	6.26	**0.02**	0.70	1.44	0.57
Within Groups	21.47	8	2.68					
Total	71.89	11	6.54					

TUKEY HSD/KRAMER — alpha 0.05

group	*mean*	*n*	*ss*	*df*	*q-crit*
0.6 g/L	9.02	3	18.34		
2.5 g/L	10.18	3	1.50		
5 g/L	5.46	3	0.07		
10 g/L	5.71	3	1.56		
		12	21.47	8	4.53

Q TEST

group 1	*group 2*	*mean*	*std err*	*q-stat*	*lower*	*upper*	*p-value*	*mean-crit*	*Cohen d*
0.6 g/L	2.5 g/L	1.15	0.95	1.22	-3.13	5.44	0.82	4.28	0.70
0.6 g/L	5 g/L	3.56	0.95	3.77	-0.72	7.84	0.11	4.28	2.17
0.6 g/L	10 g/L	3.31	0.95	3.50	-0.97	7.60	0.14	4.28	2.02
2.5 g/L	**5 g/L**	4.72	0.95	4.99	0.43	9.00	**0.03**	4.28	2.88
2.5 g/L	**10 g/L**	4.47	0.95	4.72	0.18	8.75	**0.04**	4.28	2.73
5 g/L	10 g/L	0.25	0.95	0.26	-4.03	4.53	1.00	4.28	0.15

Table A-17 (cont'd): ANOVA and Turkey post hoc analysis.

Final Benzene Degradation Rates (day 205) (umol/d)			
0.6 g/L	**2.5 g/L**	**5 g/L**	**10 g/L**
39.10	49.05	30.54	4.67
33.18	61.37	33.00	4.70
40.76	40.71	17.37	3.92

Final Benzene Degradation Rates (day 205) (umol/d)

ANOVA: Single Factor

DESCRIPTION — Alpha 0.05

Group	*Count*	*Sum*	*Mean*	*Variance*	*SS*	*Std Err*	*Lower*	*Upper*
0.6 g/L	3	113.04	37.68	15.88	31.76	4.03	28.39	46.97
2.5 g/L	3	151.13	50.38	108.01	216.01	4.03	41.09	59.67
5 g/L	3	80.92	26.97	70.58	141.16	4.03	17.68	36.26
10 g/L	3	13.30	4.43	0.20	0.39	4.03	-4.85	13.72

ANOVA

Sources	*SS*	*df*	*MS*	*F*	*P value*	*Eta-sq*	*RMSSE*	*Omega Sq*
Between Groups	3410.91	3	1136.97	23.36	**0.0003**	0.90	2.79	0.85
Within Groups	389.32	8	48.67					
Total	3800.23	11	345.48					

TUKEY HSD/KRAMER — alpha 0.05

group	*mean*	*n*	*ss*	*df*	*q-crit*
0.6 g/L	37.68	3	31.76		
2.5 g/L	50.38	3	216.01		
5 g/L	26.97	3	141.16		
10 g/L	4.43	3	0.39		
		12	389.32	8	4.53

Q TEST

group 1	*group 2*	*mean*	*std err*	*q-stat*	*lower*	*upper*	*p-value*	*mean-crit*	*Cohen d*
0.6 g/L	2.5 g/L	12.70	4.03	3.15	-5.54	30.94	0.19	18.24	1.82
0.6 g/L	5 g/L	10.71	4.03	2.66	-7.53	28.95	0.31	18.24	1.54
0.6 g/L	**10 g/L**	33.25	4.03	8.25	15.01	51.49	**0.002**	18.24	4.77
2.5 g/L	**5 g/L**	23.41	4.03	5.81	5.16	41.65	**0.01**	18.24	3.36
2.5 g/L	**10 g/L**	45.94	4.03	11.41	27.70	64.19	**0.0002**	18.24	6.59
5 g/L	**10 g/L**	22.54	4.03	5.60	4.30	40.78	**0.02**	18.24	3.23

Acetate Fed Methane Produce Rate (uM/d)			
NaCl	**0.6 g/L**	**5 g/L**	**25 g/L**
1	10.15	7.97	2.55
2	11.21	7.00	1.47
3	11.07	7.40	2.03
Average	**10.81**	**7.46**	**2.02**

Acetate Fed

ANOVA: Single Factor

DESCRIPTION — Alpha 0.05

Group	*Count*	*Sum*	*Mean*	*Variance*	*SS*	*Std Err*	*Lower*	*Upper*
0.6 g/L	3	32.42	10.81	0.33	0.67	0.31	10.05	11.56
5 g/L	3	22.38	7.46	0.24	0.48	0.31	6.70	8.22
25 g/L	3	6.05	2.02	0.29	0.58	0.31	1.26	2.77

ANOVA

Sources	*SS*	*df*	*MS*	*F*	*P value*	*Eta-sq*	*RMSSE*	*Omega Sq*
Between Groups	118.08	2	59.04	205.87	**2.96E-06**	0.99	8.28	0.98
Within Groups	1.72	6	0.29					
Total	119.80	8	14.98					

TUKEY HSD/KRAMER — alpha 0.05

group	*mean*	*n*	*ss*	*df*	*q-crit*
0.6 g/L	10.81	3	0.67		
5 g/L	7.46	3	0.48		
25 g/L	2.02	3	0.58		
		9	1.72	6	4.34

Q TEST

group 1	*group 2*	*mean*	*std err*	*q-stat*	*lower*	*upper*	*p-value*	*mean-crit*	*Cohen d*
0.6 g/L	5 g/L	3.35	0.31	10.83	2.01	4.69	**0.000635**	1.34	6.25
0.6 g/L	25 g/L	8.79	0.31	28.43	7.45	10.13	**0.000002**	1.34	16.41
5 g/L	25 g/L	5.44	0.31	17.60	4.10	6.78	**0.000041**	1.34	10.16

Table A-17 (cont'd): ANOVA and Turkey post hoc analysis.

H2/CO2 Fed

Methane Produce Rate (uM/d)

NaCl	0.6 g/L	5 g/L	25 g/L
1	2.84	3.79	2.46
2	3.60	3.05	2.17
3	3.20	3.09	1.70
Average	**3.21**	**3.31**	**2.11**

H2/CO2 Fed

ANOVA: Single Factor

DESCRIPTION — Alpha 0.05

Group	*Count*	*Sum*	*Mean*	*Variance*	*SS*	*Std Err*	*Lower*	*Upper*
0.6 g/L	3	9.64	3.21	0.15	0.29	0.23	2.65	3.77
5 g/L	3	9.93	3.31	0.18	0.35	0.23	2.75	3.87
25 g/L	3	6.33	2.11	0.15	0.30	0.23	1.55	2.67

ANOVA

Sources	*SS*	*df*	*MS*	*F*	*P value*	*Eta-sq*	*RMSSE*	*Omega Sq*
Between Groups	2.67	2	1.34	8.51	**0.02**	0.74	1.68	0.63
Within Groups	0.94	6	0.16					
Total	3.62	8	0.45					

TUKEY HSD/KRAMER — alpha 0.05

group	*mean*	*n*	*ss*	*df*	*q-crit*
0.6 g/L	3.21	3	0.29		
5 g/L	3.31	3	0.35		
25 g/L	2.11	3	0.30		
		9	0.94	6	4.34

Q TEST

group 1	*group 2*	*mean*	*std err*	*q-stat*	*lower*	*upper*	*p-value*	*mean-crit*	*Cohen d*
0.6 g/L	5 g/L	0.10	0.23	0.42	-0.90	1.09	0.95	0.99	0.24
0.6 g/L	25 g/L	1.11	0.23	4.83	0.11	2.10	**0.03**	0.99	2.79
5 g/L	25 g/L	1.20	0.23	5.25	0.21	2.19	**0.02**	0.99	3.03